11-2017

Calibrating and Evaluating Dynamic Rule-Based Transit-Signal-Priority Control Systems in Urban Traffic Networks

MD Didarul Alam

UAEU

جامعة الإمارات العربيــة المتحدة
United Arab Emirates University

United Arab Emirates University

College of Engineering

Department of Civil and Environmental Engineering

CALIBRATING AND EVALUATING DYNAMIC RULE-BASED TRANSIT-SIGNAL-PRIORITY CONTROL SYSTEMS IN URBAN TRAFFIC NETWORKS

MD Didarul Alam

This thesis is submitted in partial fulfilment of the requirements for the degree of Master of Science in Civil Engineering

Under the Supervision of Professor Yaser E. Hawas

November 2017

Declaration of Original Work

I, Md. Didarul Alam, the undersigned, a graduate student at the United Arab Emirates University (UAEU), and the author of this thesis entitled "*Calibrating and Evaluating Dynamic Rule-Based Transit-Signal-Priority Control Systems in Urban Traffic Networks*", hereby, solemnly declare that this thesis is my own original research work that has been done and prepared by me under the supervision of Professor Yaser E. Hawas, in the College of Engineering at UAEU. This work has not previously been presented or published, or formed the basis for the award of any academic degree, diploma or a similar title at this or any other university. Any materials borrowed from other sources (whether published or unpublished) and relied upon or included in my thesis have been properly cited and acknowledged in accordance with appropriate academic conventions. I further declare that there is no potential conflict of interest with respect to the research, data collection, authorship, presentation and/or publication of this thesis.

Student's Signature: ______________ Date: 19/11/2017

Approval of the Master Thesis

This Master Thesis is approved by the following Examining Committee Members:

1) Advisor (Committee Chair): Yaser Hawas
   Title: Professor
   Department of Civil and Environmental Engineering
   College of Engineering
   Signature ______________ Date 19/11/2017

2) Member: Younes Hamdouch
   Title: Associate Professor
   Department of Business Administration
   College of Business and Economics
   Signature ______________ Date 19/11/2017

3) Member (External Examiner): For Bruce Hellinga
   Title: Professor and Associate Dean of Graduate Studies
   Department of Civil and Environmental Engineering
   Institution: University of Waterloo, Canada
   Signature ______________ Date 19/11/2017

This Master Thesis is accepted by:

Dean of the College of Engineering: Professor Sabah Alkass

Signature ______________________ Date 18/12/2017

Dean of the College of Graduate Studies: Professor Nagi T. Wakim

Signature ______________________ Date 19/12/2017

Copy 7 of 10

Abstract

Setting the traffic controller parameters to perform effectively in real-time is a challenging task, and it entails setting several parameters to best suit some predicted traffic conditions. This study presents the framework and method that entail the application of the Response Surface Methodology (RSM) to calibrate the parameters of any control system incorporating advanced traffic management strategies (e.g., the complex integrated traffic control system developed by Ahmed and Hawas). The integrated system is a rule-based heuristic controller that reacts to specific triggering conditions, such as identification of priority transit vehicle, downstream signal congestion, and incidents by penalizing the predefined objective function with a set of parameters corresponding to these conditions. The integrated system provides real time control of actuated signalized intersections with different phase arrangements (split, protected and dual).

The premise of the RSM is its ability to handle either single or multiple objective functions; some of which may be contradicting to each other. For instance, maximizing transit trips in a typical transit priority system may affect the overall network travel time. The challenging task is to satisfy the requirements of transit and non-transit vehicles simultaneously.

The RSM calibrates the parameters of the integrated system by selecting the values that can produce optimal measures of effectiveness. The control system was calibrated using extensive simulation-based analyses under high and very high traffic demand scenario for the split, protected, and dual control types.

A simulation-based approach that entailed the use of the popular TSIS software with code scripts representing the logic of the integrated control system was used. The simulation environment was utilized to generate the data needed to carry on the RSM analysis and calibrate the models.

The RSM was used to identify the optimal parameter settings for each control type and traffic demand level. It was also used to determine the most influential parameters on

the objective function(s) and to develop models of the significant parameters as well as their interactions on the overall network performance measures.

RSM uses the so-called composite desirability value as well as the simultaneous multi-objective desirabilities (e.g., the desirability of maximizing the transit vehicles throughput and minimizing the average vehicular travel time) estimates of the responses to identify the best parameters. This study also demonstrated how to develop "mathematical" models for rough estimation of the performance measures vis-à-vis the various parameter values, including how to validate the optimal settings. The calibrated models are proven to be significant.

The optimal parameters of each control type and demand level were also checked for robustness, and whether a universal set of relative parameter values can be used for each control type. For the high traffic demand level, the optimal set of parameters is more robust than those of the very high traffic demand. Besides, the dual actuated controller optimal setting under the very high traffic demand scenario is more robust (than other control types settings) and shows the best performance.

Keywords: Integrated traffic control system, transit signal priority, TSP, TSIS-CORSIM, calibration, robust, optimization, response surface methodology, RSM, multi-objective desirability, micro-simulation.

Title and Abstract (in Arabic)

معايرة وتقييم النظم الديناميكيه القائمه على قواعد التحكم في الأولوية لمركبات النقل العام في شبكات المرور في المناطق الحضرية

الملخص

إن مهمة إعداد معايير وحدة التحكم في حركة المرور للعمل على نحو فعال آنياً (في الوقت الفعلي) هي في الواقع مهمة صعبة، وتتطلب وضع معايير مختلفة لتقدم أفضل تطابق مع بعض ظروف حركة المرور المتوقعة. وتعرض هذه الدراسة الإطار (الشكل العام) والمنهجية المتبعة في تطبيق نموذج استجابة السطح (RSM)، وذلك لمعايرة أي نظام تحكم يتضمن الاستراتيجيات المتقدمة في إدارة حركة المرور (مثل نظام التحكم المتكامل في حركة المرور الذي طوره أحمد وحواس). إن النظام المتكامل هو نظام تحكم ارشادي يستجيب لظروف فعالة محددة، مثل الازدحام عند المصب، والكشف عن الحوادث، وإعطاء أولوية لمركبات النقل العام، وذلك بتغيير قيمة المنظومة المحسوبة مسبقا بمجموعة من المعايير المقابلة لهذه الشروط. إن النظام المتكامل يوفر تحكم آني للإشارات الفعالة في التقاطعات مع ترتيبات الطور المختلفة (المنفصلة والمحمية/الآمنة والمزدوجة).

إن مبدأ منهجية استجابة السطح (RSM) قائم على قدرة العمل لإنجاز وظيفة واحدة أو عدة وظائف محددة؛ وقد يكون بعضها متناقضاً مع بعضها البعض. فعلى سبيل المثال، قد يؤدي زيادة عدد رحلات النقل العام في النظام المتبع لأولوية النقل العام إلى التأثير على الوقت الإجمالي للرحلات لشبكة المواصلات ككل. وتتمثل المهمة الصعبة في تحقيق/توفير متطلبات مركبات النقل العام مقابل المركبات الأخرى في آن واحد.

كما يعمل نظام منهجية استجابة السطح (RSM) على معايرة معايير النظام المتكامل عن طريق اختيار القيم التي يمكن من خلالها تحقيق التدابير القصوى والأمثل للفعالية. وقد تمت معايرة نظام التحكم باستخدام تحليلات موسعة تستند إلى المحاكاة في ظل ظروف الحركة المرورية المرتفعة والمرتفعة جداً لمختلف أنواع التحكم في الإشارات المرورية: المنفصلة، والمحمية/الآمنة، والمزدوجة.

وقد تم استخدام نهج قائم على المحاكاة والذي بدوره يتضمن استخدام البرنامج المتعارف عليه (TSIS) مع نصوص برمجية تمثل منطق/أساس نظام التحكم المتكامل. حيث تم

استخدام/تطبيق بيئة المحاكاة لتوليد البيانات اللازمة لمتابعة واستكمال تحليل (RSM) ومعايرة النماذج.

كما وقد تم استخدام (RSM) لتحديد إعدادات المعايير الأمثل لكل نوع من أنواع التحكم ومستوى الحركة المرورية. وقد تم استخدامها أيضاً لتحديد المعايير الأكثر تأثيراً على الهدف (الأهداف) المحدد وتطوير نماذج للمعايير الفعالة الى جانب تفاعلها مع مقاييس أداء الشبكة بشكل عام.

كما يستخدم النظام المطور (RSM) ما يسمى بالقيمة المُرَكَّبة لتحقيق غاية معينة الى جانب تزامنها مع الغايات ذات الأهداف المتعددة وتقديرات المخرجات لتحديد أفضل المعايير (مثل السعي لغاية رفع كفاءة مركبات النقل العام بالتزامن مع خفض متوسط زمن الرحلة للمركبة). وقد أظهرت هذه الدراسة أيضاً كيفية تطوير نماذج "رياضية/حسابية" للتقدير التقريبي لمقاييس الأداء مقابل قيم المعايير المختلفة، بما في ذلك كيفية اثبات والتحقق من صحة الإعدادات الأمثل. وقد تم اثبات فعالية النماذج المعايرة.

وبالإضافة الى ذلك، فقد تم اختبار المعايير الأمثل لكل نوع من أنواع التحكم ومستوى الحركة المرورية للتأكد من فعالية استخدام النموذج، وما إذا كان بالإمكان استخدام مجموعة قيم موحَدة/شاملة من المعايير النسبية لكل نوع من أنواع أنماط التحكم. وبما يتعلق بمستوى الحركة المرورية، فإن المجموعة الأمثل من المعايير لمستوى مرتفع من الحركة المرورية هي أكثر قوة من تلك التي بمستوى حركة مرورية مرتفع جداً. إلى جانب ذلك، فإن الإعدادات الأمثل لنمط التحكم الفعال المزدوج ولمستوى حركة مرورية مرتفع جداً هو أكثر قوة (من إعدادات أنواع التحكم الأخرى) ويظهر أفضل أداء بينهم.

مفاهيم البحث الرئيسية: نموذج استجابة السطح (RSM)، نظام متكامل لمراقبة حركة المرور، TSIS، أولوية إشارة العبور، المعايرة، الأمثل، مرغوب فيه متعددة الأغراض، ميكروسيمولاتيون

Acknowledgements

It is my pleasure to express my sincere gratitude to some important people, and without the support of them, my research work would not have been possible.

I would like to express the deepest appreciation to my supervisor Professor Yaser E. Hawas, who continually and convincingly conveyed the spirit of research. It has been a great privilege and an honor to work with him. Without his guidance, and persistent assistance and support this work would not have been possible. I have the deepest regards for him.

I would express my deepest gratitude to my parents and wife for their endless support and blessings.

Last but not the least I am also very thankful to the Roadway Transportation and Traffic Safety Research Center (RTTSRC) for providing the financial support and work environment.

Dedication

To my beloved parents and family

Table of Contents

List of Tables

List of Figures

List of Notations

i	Intersection i of the urban road network.
t	Current time index t.
c	Private cars.
b	Normal-priority busses.
p	High priority busses.
V	Abbreviation of virtual queue of all types of vehicles on a specific approach.
$u^{/}$	Upstream approach.
$d^{/}$	Downstream approach.
ϕ_j	Abbreviation of individual phase j, j=1….8.

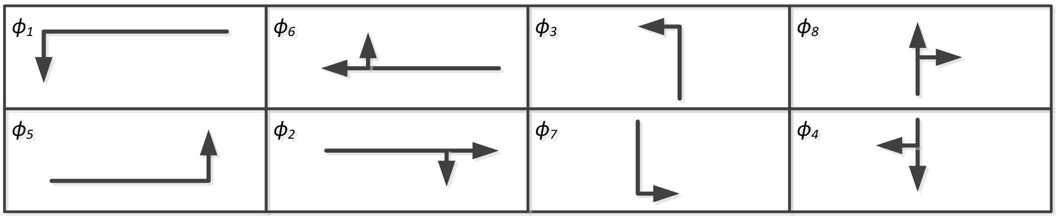

Φ_k	Abbreviation of a candidate phase set k, k=1,.....,8, where $\Phi_1 = \{\phi_1 \cup \phi_5\}$, $\Phi_2 = \{\phi_1 \cup \phi_6\}$, $\Phi_3 = \{\phi_2 \cup \phi_5\}$, $\Phi_4 = \{\phi_2 \cup \phi_6\}$, $\Phi_5 = \{\phi_3 \cup \phi_7\}$, $\Phi_6 = \{\phi_3 \cup \phi_8\}$, $\Phi_7 = \{\phi_4 \cup \phi_7\}$, $\Phi_8 = \{\phi_4 \cup \phi_8\}$
$\beta^{N}_{i,\phi_j,u^{/}}$	A coefficient for incidents on the upstream approach,$u^{/}$, of phase ϕ_j, at intersection i.
$\beta^{p}_{i,\phi_j,u^{/}}$	A coefficient for transit priority for high priority buses on the upstream approach,$u^{/}$, of phase ϕ_j, at intersection i.
$\beta^{b}_{i,\phi_j,u^{/}}$	A coefficient for transit priority for normal priority buses on the upstream approach,$u^{/}$, of phase ϕ_j, at intersection i.
$\beta^{B}_{i,\phi_j,d^{/}}$	A coefficient for blockage on the downstream exit link of phase $\phi_j$at intersection i;

$\beta^{V}_{i,\phi_j,u^{/}}$	A coefficient for virtual queue of vehicles on the upstream approach link of phase ϕ_j at intersection i;
$C^{b,t}_{i,\phi_j,u^{/}}$	The total counts of the normal priority buses, b, at time t on the upstream approach, $u^{/}$, of phase, ϕ_j , of intersection i.
$C^{c,t}_{i,\phi_j,u^{/}}$	The total counts of the cars, c, at time t on the upstream approach link, $u^{/}$, relevant to phase, ϕ_j , of intersection i.
$C^{p,t}_{i,\phi_j,u^{/}}$	The total counts of the high priority buses, p, at time t on the upstream approach, $u^{/}$, of phase, ϕ_j , of intersection i.
$O^{b}_{i,\phi_j,u^{/}}$	Average passenger occupancy for the normal priority buses on the upstream approach, $u^{/}$, of phase ϕ_j at intersection i.
$O^{c}_{i,\phi_j,u^{/}}$	Average passenger occupancy for the private cars on the upstream approach, $u^{/}$, of phase ϕ_j at intersection i.
$O^{p}_{i,\phi_j,u^{/}}$	Average passenger occupancy for the high priority buses on the upstream approach, $u^{/}$, of phase ϕ_j at intersection i.
$r^{V,t}_{i,\phi_j,u^{/}}$	The ratio of the vehicle queue length over the physical capacity of the corresponding link length, $l_{i,\phi_j,u^{/}}$.
$I^{B,t}_{i,\phi_j,d^{/}}$	The indicator of the presence of blockage at time index $(t-1)$ on the downstream link, relevant to phase, ϕ_j , of intersection i.
$I^{N,t}_{i,\phi_j,u^{/}}$	Indicator of the presence of incidents at time index $(t-1)$ on the upstream link, relevant to phase, ϕ_j , of intersection i.
$J^{/,t}_{i,\phi_j}$	The base congestion indicator of an individual phase, ϕ_j, in terms of the total virtual queue of passengers, without adjusting for the incident status on the approach link of the intersection i at time t for the individual phase, ϕ_j.
J^{t}_{i,ϕ_j}	The congestion indicator of an individual phase, ϕ_j in terms of the total virtual queue of passengers, adjusted for the incident status on the approach link of the intersection i at time t for the individual phase, ϕ_j.

A^{t}_{i,ϕ_j} — The actuation index of an individual phase ϕ_j of intersection i at time t.

Z^{t}_{i,Φ_k} — The actuation index of phase set,Φ_k, of intersection i at time t.

β^V — Abbreviation of the penalty coefficient of virtual queue of vehicles on the upstream approach link (same as $\beta^{V}_{i,\phi_j,u'}$).

β^b — Abbreviation of the penalty coefficient of normal priority bus (same as $\beta^{b}_{i,\phi_j,u'}$).

β^p — Abbreviation of the penalty coefficient of high priority bus (same as $\beta^{p}_{i,\phi_j,u'}$).

β^B — Abbreviation of the penalty coefficient of blockage on the downstream exit link (same as $\beta^{B}_{i,\phi_j,d'}$).

β^N — Abbreviation of the penalty coefficient of incidents (same as $\beta^{N}_{i,\phi_j,u'}$).

N_{bus} — A response variable (MOE) representing the total number of bus trips served during a specific analysis period (herein 1.5 hours).

T_t — A response variable (MOE) representing the total network travel time (in hours) during a specific analysis period (herein 1.5 hours).

t_m — A response variable (MOE) representing the mean vehicular travel time per trip (in seconds) during a specific analysis period (herein 1.5 hours).

$f_{N_{bus}}$ — Unknown non-linear function of the (N_{bus}) response variable.

f_{T_t} — Unknown non-linear function of the (T_t) response variable.

f_{t_m} — Unknown non-linear function of the (t_m) response variable.

$\varepsilon_{N_{bus}}$ — Statistical error of the function $f_{N_{bus}}$.

ε_{T_t} — Statistical error of the function f_{T_t}.

ε_{t_m} — Statistical error of the function f_{t_m}.

N — Number of experiments for Central Composite or Box-Behken designs.

k	Number of parameters to optimize (herein 3 representing $\beta^B, \beta^b = \beta^P, \beta^V$) .
C_0	Number of central points.
α	The axial point in Central Composite design.
$d_{\mathrm{N}_{bus}}$	The model estimated individual desirability index of the total bus trips (N_{bus}).
d_{T_t}	The model estimated individual desirability index of the network total travel time (T_t).
d_{t_m}	The model estimated individual desirability index of the trip mean travel time (t_m).
D	The model estimated composite desirability index; Destination.
$w_{\mathrm{N}_{bus}}$	The importance (weight) parameter of the total bus trips (N_{bus}).
w_{T_t}	The importance (weight) parameter of the network total travel time (T_t).
w_{t_m}	The importance (weight) parameter of the trip mean travel time (t_m).
$y_{\mathrm{N}_{bus}}$	The model response value representing the total bus trips (N_{bus}).
y_{T_t}	The model response value representing the network total travel time (T_t).
y_{t_m}	The model response value representing the trip mean travel time (t_m).
$T_{\mathrm{N}_{bus}}$	The model target value of total bus trips (N_{bus}).
T_{T_t}	The model target value of the network total travel time (T_t).
T_{t_m}	The model target value of the trip mean travel time (t_m).
$L_{\mathrm{N}_{bus}}$	The model lower bound value of the total bus trips (N_{bus}).
U_{T_t}	The model upper bound value of the network total travel time (T_t).
L_{t_m}	The model lower bound value of the trip mean travel time (t_m).
U_{t_m}	The model upper bound value of the trip mean travel time (t_m).

$r, (r_1, r_2)$	The weight value (s) of the individual desirability.
D_{Ej}	Destination j on the Eastern boundary of the test network.
D_{wj}	Destination j on the Western boundary of the test network.
D_{Nj}	Destination j on the Northern boundary of the test network.
D_{Sj}	Destination j on the Southern boundary of the test network.
O	Origin;
O_{Ej}	Origin j on the Eastern boundary of the test network.
O_{wj}	Origin j on the Western boundary of the test network.
O_{Nj}	Origin j on the Northern boundary of the test network.
O_{Sj}	Origin j on the Southern boundary of the test network.
BQL	Abbreviation used in model and graphics for the coefficient for virtual queue of vehicles on the upstream approach link, β^{V}.
BTP	Abbreviation used in model and graphics for the coefficient for transit priority (normal or high) bus.
BDC	Abbreviation used in model and graphics for the coefficient for downstream blockage penalty
MTT	Abbreviation used in model and graphics for the trip mean travel time (in seconds).
Trips	Abbreviation used in model and graphics for the total number of bus trips.
TTT	Abbreviation used in model and graphics for network total travel time (in hours).

List of Acronyms

ATCS	Adaptive Traffic Control Systems
ATMS	Advanced Traffic Management Systems
BBD	Box–Behnken Design
CCD	Central Composite Design
MOEs	Measures of Effectiveness
RSM	Response Surface Methodology
TSP	Transit Signal Priority

Chapter 1: Introduction

1.1 Research Problem and Motivation

Traffic demand in the urban area dynamically fluctuates with abrupt changes, and it is hard to predict future traffic accurately. Optimizing the controller settings in real time is a challenging task as it entails setting several parameters to best suit some predicted traffic conditions. There is nearly no logic that can accurately predict traffic conditions and additionally set the control parameters optimally to suit these conditions. There is the so-called dependency phenomenon, where the traffic conditions depend on the control decisions and vice versa. Not to mention the added complexity of additional functions such as incident detection, management, and transit priority systems (TSP) are active duties of the same controller. The optimization of such complex controllers requires analyses at different network loading levels and configurations. In a typical network, functions such as TSP may result in deterioration of performance to the regular vehicular traffic at the expense of favoring priority transit vehicles.

For any typical control system, such as signal control, parameters are commonly selected to fit specific traffic conditions. It is natural as such that such systems should be re-calibrated each time they are deployed to different conditions (that the system was not optimized for). What makes it more challenging is the dynamics of traffic and the evolution of the traffic demand over the day. A signal controller with some TSP functions may operate effectively during specific hours but then fails to run at other times because its parameters are adjusted for only some specific conditions (but not all). Such complex control systems commonly include multiple parameters that affect the performance, and as such the recalibration is certainly a challenging, difficult multi-dimensional task.

It is also practically impossible to readjust such control systems by carrying the optimization process online. Instead, a more appealing approach is to optimize such systems offline, but additionally one has to ensure the robustness of the optimized settings. The settings should provide optimal (or near) performance measures. In brief words, such control systems must be calibrated to provide good performance to the most prevailing traffic conditions in the network, keeping in mind that these circumstances would certainly change.

Regardless of the controller functions, strategy and methodology to implement, one has to ensure the robustness of adopted solutions. Robustness can only be assured with extensive analytical, simulation or field tests under variant traffic conditions and network configurations. In addition to robustness, there is also need to minimize the recalibration requirement; it is illogical and impractical to calibrate the system for every condition it may encounter. In a real-time operational environment, this is certainly an impossible task. In brief, there is a need to devise a methodology that can be used to assess the effectiveness of complex control systems, calibrate parameters to provide optimal (or at least close to optimal) control, and assess the robustness of its effective control under the varying conditions. The typical notion of a robust system is one that performs well across a range of (traffic, geometry, weather, etc.) conditions. Given that this study considers varying traffic conditions and control types, the robustness of the system should be assured at various levels (multi-dimensional). At the first level, the purpose is to ensure that for each control type (e.g. dual, protected or split) the sensitivity of relative ratios of the parameters. The idea here is to check whether there is a specific relative ratio among the parameters that makes the specific control type (dual, protected or split) robust under one specific traffic condition. The second level purpose is to identify for each control type the optimal robust relative ratio (identified at the first level) that makes each control type robust if applied to different traffic conditions. That is, when the traffic conditions vary, how to set the parameters of each specific controller to perform effectively under such varying traffic conditions. The third level purpose is to identify the “universal” relative parameters ratio that can be applied under varying traffic conditions for all control types together. The details regarding the study of robustness will be discussed later in the study in Chapters 5, 6 and 7.

The challenge of the devising such methodology is the complexity of the objective functions and the nonlinearity nature of it in response to the calibration parameters. Some of the signal controllers in the literature, for instance, are even integrated with other advanced ATMS components such as incident detection, management, and transit priority systems (Ahmed and Hawas, 2015), which makes the calibration of parameters even more challenging. Some of integrated control systems may have few parameters to calibrate, and some may have many. As such, no matter what methodology is used to calibrate these parameters, it should be functional with various control systems and parameters.

In general, Adaptive Traffic Control Systems (ATCSs) have been developed to adjust signal timing plans in dynamic real-time based on the current traffic situations, and transportation system capacity. According to a comprehensive study by Stevanovic (2010), each ATCS has unique features and identified several features to describe various adaptive traffic control logics. The distinctive working principles of various ATCS are detection, type of action, adjustment method, the time frame for adjustment, hierarchical levels, models for the status of traffic condition, signal timing parameters to be adjusted, flexibility to form regions, support for vehicle-actuated operations, and transit operations. None of the commonly used ATCS has the comprehensive function of TSP, incident detection, and management as well as congestion protocols altogether.

Nearly all the existing adaptive traffic control systems do not consider the combined effects of TSP and incidents, simultaneously (Ahmed and Hawas, 2015). Recently, Ahmed and Hawas (2015) developed a complex integrated traffic control system, which has the advanced traffic management strategies, such as transit signal priority, incident detection and management, and the recurrent congestion management. The developed integrated system prioritizes the competing phases of a traffic signal by the total expected throughputs (in terms of the number of passengers) among all competing phases.

This research study presents an attempt to enhance the previously developed integrated control system by the optimization of parameters. The control system by Ahmed and Hawas may be best classified as heuristically-based that reacts to specific triggering conditions (such as downstream signal congestion, incident detection, identification of priority transit vehicle(s) in the traffic stream) by penalizing some predefined objective function with a set of parameters corresponding to these conditions.

The system itself is not an optimization controller but a heuristic one. For instance, when a transit vehicle is detected, a transit vehicle parameter is activated to increase the value of the objective function for this traffic approach (and its corresponding signal phase) on which the transit vehicle is detected. Similarly, if the congestion downstream a specific phase is reaching the capacity of approach, the upstream phase objective function is penalized for reducing the green time allocation of this phase.

In their earlier work, Ahmed and Hawas carried out extensive analyses to identify the set of parameters that will suit specific traffic conditions. The analyses were conducted using trial and error; change the parameter values and assess the controller performance. Needless to say that the “optimal” settings of the earlier work corresponded to one of these trials. That is, there was no systematic procedure to identify the optimal set of parameters, nor to verify the optimality of the solutions and to ensure the robustness. Given the complexity of such integrated system by Ahmed and Hawas (2015) and the fact it includes multiple contradicting functions that affect the network performance, it will be used in this study to demonstrate how can the proposed methodology in this research be used to calibrate any complex control systems.

Advanced Traffic Management Systems (ATMS) are commonly studied, analyzed, and evaluated by using micro-simulation tools. These micro-simulation models mimic events, such as gap-acceptance to cross or merge the traffic, speed adjustment, lane changing, and car-following. There are also models like gap acceptance ones to predict driver’s behavior at signalized intersections (Teodorović and Janić, 2017). Various parameters are used in such models to describe the individual driver behavior and individual vehicle dynamics. These parameters also need calibration to replicate real life events accurately, and to minimize the discrepancy between the observed and simulated traffic conditions (Pande and Wolshon, 2016). This calibration is the crucial stage for any traffic simulation model (Hawas, 2002). Similarly, the integrated traffic control system has parameters to regulate traffic for improving the overall network productivity and efficiency, and these parameters must be calibrated to determine their values for optimal control.

This research has taken a step towards the calibration of the parameters for various real time traffic control systems (regardless of its complexity and number of parameters) under several traffic demand scenarios. The calibration guidelines with the application of the well-known simulation-based optimization method of Response Surface Methodology (RSM) is developed for ATMS systems calibration and robustness verification.

This research study aims to develop an RSM-based methodology that can be used to calibrate and improve the effectiveness and robustness of the solutions of advanced traffic control systems in general. The methodology would entail the selection of the optimal settings for the controller parameters. To demonstrate the details of the method and how it can be used for parameter setting and robustness verification, the Integrated Traffic Signal Control System developed by Ahmed and Hawas (2015), is used (as the controller to optimize). The proposed method can be effectively used to optimize parameters of multi-criteria contradicting objective functions within the same controller. Three criteria have been used in this study; maximize the transit vehicles throughput while minimizing the average vehicular travel time as well as the network overall vehicle travel time. These criteria may actually contradict each other; increasing transit throughput may increase delay and travel time for other vehicles.

1.2 Research Objectives

This study has set the following specific objectives:

- Carry out a detailed literature review to identify the characteristics of existing transit signal priority systems in specific as the most important function of any integrated traffic signal control system. The introduction of TSP function to a signal control has implications on its effectiveness as it commonly results in exceeding delays for nonpriority vehicles.
- Carry on the literature review on simulation based optimization methods along with the features of the Response Surface Methodology (RSM) and response optimization method.
- Develop the framework for complex controller optimization and robustness verification, and formulate a RSM-based methodology to optimize the multi-function integrated controller by Ahmed and Hawas (2015)
- Carry on the calibration exercise for the integrated controller under various traffic conditions, and signal type configurations
- Investigate the robustness features of the identified optimal settings of the different signal control types.
- Recommend some calibration guidelines and suggest further enhancement to the developed integrated traffic signal control system.

1.3 Research Question

The TSP is commonly integrated with a traffic signal controller (e.g. Ahmed and Hawas, 2015). The combination of TSP with the controller (integration) would have implications on the preset objective functions. For instance, maximizing transit throughput (by the TSP) is commonly accompanied by increase in vehicular traffic delays and travel times. Based on the nature of the controller (type and functions), and the TSP strategies, this study attempts to address the following research questions:

- What are the state-of-art and state-of-practice to implement TSP system in the urban network?
- How to calibrate TSP-based traffic control systems, especially if combined with other functions for signal control, incident and congestion management?
- What is the optimal set of parameters for each control type and traffic condition?
- How to study the robustness of the integrated controller?
- Are the identified optimal settings robust and to what extent?

1.4 Thesis Outline

This thesis is organized into seven chapters. Chapter 2 presents a detailed literature review of the existing transit signal priority (TSP) systems. The state-of-art and state-of-practice of the simulation based optimization methods are discussed in Chapter 3. It also incorporates all the relevant details of the Response Surface Methodology (RSM) and response optimization method. Chapter 4 presents the experimental model's setup with different traffic demand and supply conditions and data generation with RSM based model building and optimization process for this research study. Chapter 5 discusses the results, analyses, and robustness under high traffic demand scenario with different control settings. The results, analyses, and robustness under very high traffic demand scenario with different control settings are presented and discussed in Chapter 6. A synthesis of the main findings and the proposed direction for future research are presented in Chapter 7.

Chapter 2: Literature Review

2.1 Introduction

This research study addresses complex integrated advanced signal controllers coupled with transit systems priority (TSP). This chapter is intended to review the state-of-the-art design of traffic signals with TSP functions to identify the influence of calibration using simulation-based optimization. It reviews the existing methodologies of transit signal priority systems, both in practice and in theory. Section 2.2 discusses the general characteristics and features of transit signal priority (TSP) systems, such as TSP concepts like active, adaptive/real-time with or without optimization, TSP strategies, and the evaluation of TSP system. This section also provides a summary discussion of the TSP in general and concludes the main drives behind this research. The concept of the Integrated Traffic Signal Control System is presented in section 2.3. The simulation-based optimization methods are reviewed in section 2.4.

2.2 Transit Signal Priority (TSP)

Transit Signal Priority (TSP) can be defined as an operational strategy to facilitate the movement of transit vehicles by enhancing the performance, efficiency, and reliability of transit systems. This entails adjustments to the traffic signal control logic to integrate preferential treatment to the movement of transit vehicles as they approach intersections. In general, TSP strategies offer benefits in minimizing the delays of transit vehicles. The primary objective of TSP is to reduce the transit travel time or the transit vehicle throughput. It is believed that TSP can significantly increase the operational efficiency of the transit vehicles and maintain a better schedule adherence.

The priority treatment, given to emergency vehicles and the transit vehicles, is not same. Although both methods facilitate the movement of vehicles, preemption, which gives priority to emergency vehicles, interrupts the signal operation while priority changes or modifies the signal operation. The TSP is used for some priority service within the coordinated operation of traffic signals that can reduce delay for the transit vehicles with minimal impact on other traffic. In other words, preemption is a high degree of priority to facilitate a safe movement of specific vehicles through the signal with some consideration to the resulting delays.

The configuration and timing of traffic signal control, as well as physical design of streets, are often optimized to minimize average delay for all motor vehicles. However, since transit vehicles normally carry a higher number of passengers, this traffic signal control will not minimize the overall delay per person. Transit vehicles, therefore, need to be handled differently to minimize the overall delay per person. The transit lines sometimes use minor streets not the major arterial streets and have a different speed profile due to bus stops. Therefore, transit vehicles need to be prioritized to minimize the delay per person. There is also another important reason to “over compensate” transit vehicles; that is to promote travel by public transport to reduce pollution and congestion.

The benefits of TSP include also reducing costs of bus operation by reducing the delay of bus or passengers at signalized intersections and reducing passenger’s waiting time at the bus stops. Thus, the required number of transit vehicles to serve the predicted transit demand is minimized. Other significant benefits are improving the service of on-schedule public transit and increasing the ridership and discouraging the use of private vehicles. Besides these advantages, however, there are common two negative impacts or costs on non-priority approaches and neighboring intersections, such as increasing travel time in non-priority approaches and interruption on coordinated treatment at adjacent intersections.

Research studies along with methodologies on the TSP technologies, TSP concepts (active/passive/adaptive), priority strategies, evaluation methods, and design criteria are discussed in the following sections.

2.2.1 TSP Technologies

The transit vehicle detection system is a principal component of the advanced transit signal priority systems as it detects transit vehicles, and transmits this information to the signal controller. There are different types of media for detection such as sound, light, radio frequencies, wireless, and so on. Advanced technologies like global positioning systems (GPS) is commonly used for transit priority. TSP may be implemented locally in a single intersection or a centralized signal system controlling by the traffic management center. The effectiveness of TSP relies on transit vehicle detection and location methods. Usually, there are three types of vehicle detection methods: point detectors, zone detectors, and transit vehicle movement detectors (Automatic Vehicle Location – AVL and Automatic Passenger Count - APC). In the following section, the research studies on connected vehicle technologies to control the traffic signal are presented.

Ding et al. (2013) demonstrated a multimodal priority signal control system within an integrated traffic control framework using wireless communication, global positioning system, and connected vehicles. The framework has been developed and tested using a microscopic hardware-in-the-loop simulation (HILS) environment (based on VISSIM) and was demonstrated in a network of six intersections in Anthem, Arizona. The paper addresses the architecture of multiple priority requests signal control system (the Priority Request Generator and the Priority Request Server) and the HILS environment (The setup of HILS and various wireless communications among different components of HILS). Also, the functions like emergency vehicle (EV) preemption and transit priority are presented. The developed model was demonstrated in a real network with three case studies (An EV from conflicting phase to the bus, two EVs on concurrent phases but conflicting to the bus, and two EVs from conflicting phases). The three broad components of priority signal control system are the On-Board Equipment (OBE), Road Side Equipment (RSE), and the Actuated Signal Controller (ASC). The vehicle detection system and priority request generator (PRG) is realized by the OBE, while the communication medium is wireless, and the RSE realizes the priority request server (PRS). There is also communication between the RSE and ASC to implement the priority timing strategy from the PRS. The assumption for case studies included: 1) A case without EV, where the maximum green time extension is set to (1+a) multiples of the maximum green time extension for the transit vehicle, (typically, the value of a is $0<a<0.5$). This case had no allowed phase skipping, and actuated control on non-priority vehicle phases was available, 2) A case with EV, where the maximum green time extension is set equal to 240 seconds for EV requested phases, and additionally phases skipping be allowed.

2.2.2 Priority Concepts

At a traffic signal, the transit priority is granted in different methods. Among these methods are the active (conditional and unconditional) and passive priorities. Lin et al. (2015) presented a comprehensive review of existing TSP controls according to the application and theoretical aspects. Passive priority gives priority using historical data of transit vehicles arrivals, and Active priority uses a system for the transit vehicles arrivals and detections at the intersection. The active control can be further categorized into rule-based and model-based. There are different types of TSP concepts as described below.

Active Unconditional and Conditional Priority

Conditional priority gives transit vehicles priority under certain limits and conditions like transit vehicle's occupancy, time headway, and delay. The main objective of this concept is to operate the network efficiently without affecting non-transit vehicles. On the other hand, the unconditional priority provides priority to a transit vehicle whenever it is detected. The main aim of this concept is to reduce the transit vehicles' travel times for a better service and to encourage people to use it. Both conditional and unconditional control strategies attempt to improve system performance. Conditional control is more sophisticated and requires additional infrastructure/sensors.

Ekeila et al. (2009) presented the development and evaluation of a TSP control system in response to real-time traffic and transit conditions. Transit arrival time is defined with its upper and lower boundaries, and the implementation of the TSP decision is delayed to minimize the impact on cross street traffic. The Automatic Vehicle Location (AVL) system and the transit arrival prediction model are essential parts of the overall system. The TSP system by Ekeila et al. consists of three main components: a virtual detection system, a dynamic arrival prediction model, and a dynamic TSP algorithm. This system was evaluated through two case studies to compare its performance vis-a-vis some conventional TSP systems. The first case study entailed using a hypothetical four-legged intersection and the second one involved a Light Rail Transit (LRT) line with 17 signalized intersections on a corridor.

For both case studies, a virtual detection system was developed (in VISSIM), along with a linear travel-time arrival prediction model. Also, a dynamic TSP algorithm was developed to determine what TSP strategy to use and when to apply it. The results showed considerable time savings regarding transit delays. There are many limitations for this work, such as the Delayed TSP decision is not well explained; no evaluation in a typical network of intersections; single (not multiple) transit priority to consider during a cycle with offset recovery time.

Adaptive/Real-Time Priority

Automatic Vehicle Location (AVL) based TSP system has the potential to overcome the typical shortcomings of traditional active or passive TSP (e.g., traditional active or passive TSP does provide priority to the transit vehicle, but it fails to seize the opportunity to cross the intersection due to the lack of real-time location of transit vehicle). The real-time transit movement data from GPS can be used to estimate bus location as well as to predict bus arrival time to reach the bus stops and intersections. The accurate prediction of Transit's arrival time at an intersection can help to select the optimal time range to activate the traffic signal controller for priority service. A few of adaptive traffic signal control algorithms have been enhanced to embed TSP functions.

Ahmed and Hawas (2015) presented the functional modules of a distributed adaptive traffic control system to handle boundary conditions of recurrent and non-recurrent congestion with transit signal priority. The main objective of this model is to develop three functional modules (transit priority module, downstream blockage module, and Incident status module) to handle boundary conditions of recurrent and non-recurrent congestion with transit signal priority. The system employs multiple objective functions to improve the overall transit productivity (throughput) and efficiency (delay times) for all vehicles under heavily congested traffic demand scenarios. For this, the control system uses the link detectors' (upstream, mid-block, and downstream) data to determine the boundary conditions of all entry and exit links of the intersection.

The transit signal priority module estimates the number of priority and non-priority buses at every second using a GPS based bus detector device. The bus is considered as non-priority if it is bound to stop at some intermediate bus stop along the approach link. If the bus has already stopped or no bus stop along the approach link and the expected time of the bus to reach the stop line at the downstream end of the link is less than the green extension, then the bus is treated as a high priority bus only for actuated traffic control. The model by Ahmed and Hawas was thoroughly assessed with CORSIM micro-simulation for a grid network of 49 intersections with different types of signal phase settings. Various traffic demand flows starting from relatively low to high-traffic volume levels are adopted, and the directional movements on each link are estimated using User Equilibrium Assignment. The model has some limitations such as the number of required detectors on each link. Also, the initial results were only favorable for the pre-timed signal settings (with phase skipping strategy). There are also some inconsistencies among the set parameters within the control model and the CORSIM simulator.

Ma et al. (2013) presented some integrated operation for signal timings and bus speed. The idea is to provide priority to buses at isolated intersections using real-time adjustment of bus speed through Connected Vehicles technology. A set of integrated operational rules (such as impacts of preceding bus analysis rules, priority requests generation rules, priority passing rules, and speed adjustment without priority rules) are developed. The relevant rules are selected according to the passing and the arrival times windows for buses with and without schedule deviation with the objective of minimizing bus schedule deviation, bus fuel consumption, and emissions. This model was designed and evaluated with a VISSIM-based simulation platform. The model outperforms the no priority and common priority strategies. A sensitivity analysis was conducted under different levels of transit and vehicular demands, as well as accounting for critical factors that may affect model performance such as available priority time (maximum red truncation time and maximum green extension time) and bus speed limits. Some of the model limitations include; 1) No near-side bus stops; 2) Only green extension and red truncation can be used to provide transit signal priority; 3) There is an exclusive bus lane, and all buses will accept the recommend speed immediately and accurately. Furthermore, the model was tested at isolated intersections, and as such, it may underperform on corridor-wide or grid network.

Lin et al. (2013) presented a headway-based transit signal priority (TSP) model for multiple bus requests from different routes to benefit both bus riders and passenger-car users without increasing the total person delay on the arterial. The main objective of this model is to minimize the passenger waiting time at the next bus stop without significantly causing disruptions to the crossing street. This model utilizes the variable priority time technique to determine the duration of green extension for each intersection depending on the total person delay estimation and by considering the impacts of the downstream signal controller. To handle multiple priority requests based on headways, the model estimates the benefits of the bus passenger at the next bus stop, the in-bus passengers and the passenger-car users on the arterial before and after TSP control to determine the optimal priority time. The primary model assumptions are: 1) only grant the priority to traffic movements on the arterial; 2) no change to the common cycle time; the extra green time of prioritized movements is equal to truncated green time of through movements on the cross street; 3) the green time should be long enough to clear the initial queue for each movement, and 4) the passenger cars have no effect on buses in the entry/exit into/from the bus stop. This model was tested in a hypothetical arterial with six intersections, with only two intersections operated with the function of TSP. The results showed that the TSP control provides some benefits to transit vehicles with an increase of the cross-street passengers delay. Among the limitations of this model is that it applies only green extension strategy of TSP (of 15 seconds maximum).

Mirchandani and Lucas (2004) presented a strategy, referred to as Categorized Arrivals-based Phase Re-optimization at Intersections (CAPRI), which integrates transit signal priority and rail/emergency preemption within a dynamic programming-based real-time traffic adaptive signal control system like RHODES (Real-time Hierarchical Optimizing Distributed Effective System). The main objective of this paper is to enhance the RHODES by using varying weights for buses or transit vehicles based on the onboard number of passengers and its schedule. The weight is negative when the bus is earlier to its announced schedule and positive when it is late. This model was examined using a simulation environment. Results indicated a reduction in the variance of bus delays at the downstream bus stop when RHODES is implemented. The standard deviation for the delay decreased from 22.95 seconds (semi-actuated control- SAC) to 20.02 seconds (RHODES with no bus priority) and 18.65 seconds (RHODES-BP) at high cross street volumes. The reduction in bus delays on cross streets due to RHODES-BP is higher (4.46%) for relatively high cross street volumes (demand of 1100 vehicles/hour), with very little change in cross-street traffic delays

(16.24 versus 17.02 seconds). In evaluating the model, all intersections were considered isolated.

Adaptive/Real-Time Priority with Optimization

Adaptive/real-time priority with optimization control strategies predict the arrival of vehicles, and then, the optimization is done to minimize a cost function (like a weighted combination of stops and delays for all vehicles). Transit vehicles can be selectively detected and given a higher weight in the cost function. Therefore, the resulting signal timings will be more favorable towards the transit. Different routes, directions or late buses, can be given different weights to prioritize in different extents. In summary, this approach attempts to provide transit priority based on the optimization of performance criteria such as passenger delay, vehicle delay or some combinations of these measures.

Feng et al. (2015) presented a real-time adaptive signal phase allocation algorithm using connected vehicle data to optimize the phase sequence and duration by solving a two-level optimization problem (minimization of total vehicle delay and queue length). The main objective of this paper is to improve the controlled optimization of phases (COP), which is based on a sequence of stages (used in the Real-time Hierarchical Optimization Distributed Effective System, RHODES, adaptive traffic control system). This algorithm applies the two-level optimization scheme to a dual ring controller. Both phase sequence and duration are optimized simultaneously. Given the current low penetration rates, the location and speed of unequipped vehicles should be estimated accurately. An algorithm called EVLS (Estimation of Location and Speed) is used to construct a complete prediction arrival table by segmenting the road near an intersection into three regions: queuing region, slow-down region, and free-flow region. The two-level optimization algorithm assigns signal phase sequences and durations based on predicted vehicle arrivals. At the upper level, a dynamic program (DP) is applied to each barrier group.

The calculation of the performance function of the upper level is passed to the lower level, which is formulated as a utility minimization problem (total vehicle delay or queue length based on different operational policies). The sequence of barrier groups is assumed to be fixed, but the order of phases within each ring in each barrier group can vary. A real-world intersection is modeled in VISSIM to validate the algorithm. Different scenarios with two different demand levels and four penetration rates (100%, 75%, 50%, and 25%) are tested. The results with the various market penetration rates and demand levels are compared to well-tuned fully actuated control. In general, minimization of total vehicle delay generates lower total vehicle delay compared to minimization of queue length. When the demand is higher, the difference is more significant. The algorithm outperforms actuated control by reducing total delay by as much as 16.33% in a high penetration rate case.

Hu et al. (2015) presented a person-delay-based optimization method for a TSP logic that enables transit/signal cooperation and coordination among consecutive signals under the Connected Vehicle environment. A Coordinated TSP with Connected Vehicle (TSPCV-C) is proposed to secure the mobility benefit generated by the TSP logic along a corridor. The problem is formulated as a Binary Mixed Integer Linear Program (BMILP), solved by a standard branch-and-bound method, to minimize the person delay. The TSPCV-C is designed to be "conditional"; grants priority only when the bus is behind schedule and the grant of TSP causes no extra total person delay. The used assumptions include; 1) cycle length is fixed, 2) sequence of signal phases does not change, 3) general traffic rate is constant 4) a maximum of one TSP is granted within the signal cycle. The optimization algorithm is designed to find a set of decision variables that minimize the total delay (including bus and general traffic users). This algorithm was evaluated using both analytical and microscopic traffic simulation approaches. Four scenarios were compared: without TSP (NTSP), conventional TSP (CTSP), TSP with Connected Vehicle (TSPCV), and Coordinated TSP with Connected Vehicle (TSPCV-C). Transit delay and total travel time of all travelers were used as the measures of effectiveness. The performance of TSPCV-C is compared against conventional TSP (CTSP) under four congestion levels (v/c ratios are 0.5, 0.7, 0.9, and 1.0) and five intersection spacing (0.14 to 0.54 miles with 0.1 miles increment) cases. The results showed that the TSPCV-C greatly reduces bus delay for all congestion levels and intersection spacing cases. The TSPCV is not as efficient as TSPCV-C, but still, it can reduce delay up to 59% for not too closely spaced intersections. The TSPCV-C is recommended for intersections that are spaced less than 0.5 miles away, and it can reduce the bus delay between 55% and 75% compared to the conventional TSP. No significant negative effects were observed at congestion levels below capacity.

Dion and Hellinga (2002) presented a heuristic-based, distributed, real-time, traffic-responsive model named Signal Priority Procedure for Optimization in Real-Time (SPPORT) considering the impacts of transit vehicles. The model accounts for the interference caused to the general traffic by transit vehicles (stopping in the right of way to board and discharge passengers), and the potential effects of priority passage of transit vehicles on other traffic. This model was evaluated with 12 scenarios in an isolated intersection considering transit vehicles (yes, no), and various temporal (constant, peaking) travel demands (low, medium, high). The model was also compared with both fixed-time and traffic actuated control. Among the model limitations is the unrealistic setting of amber time (set to 2 seconds), which may create a dilemma for drivers (usually it should be 3-5 seconds). Also, the relative weights of priority were not considered in the sensitivity analysis. For the constant demand scenarios, the model performs worse than fixed timed signal control. The model is also reported to be time-consuming with short green extension settings.

Ghanim and Abu-Lebdeh (2015) presented a real-time traffic signal optimization approach for a coordinated network, integrating transit signal priority using genetic algorithms (GA). The model is aimed at overcoming the uncertainty in transit vehicle arrival times and difficulties associated with incorporating a TSP system within a coordinated traffic signal control network. Artificial neural networks (ANN) applications are used to predict the bus travel time (dwell time at individual stops along the route).

A Dynamic Signal Priority Optimization in Real-time Traffic (D-SPORT) control algorithm was developed with cost function formulation based on signal timing plans, ANN bus arrival prediction model and the GA optimization platform. The cost function combines weighted sub-functions of network general traffic performance, transit travel time, and transit schedule adherence. The ANN model predicts bus arrival times using the number of general traffic vehicles, observed average delay and travel time, average number of queued vehicles in through, right and left-turning traffic streams in the past 5 minutes, bus lateness, number of passengers in bus and at bus stop, and local signal time within signal cycle at which a bus is detected. The ANN model was trained, tested, and validated in a MATLAB environment using 8871 datasets generated by VISSIM. The decision variables of the GA algorithm are the cycle length, green times, and offsets. The model was tested in a simulation environment using VISSIM, using a network with two intersecting one-way streets (two through lanes and one exclusive left-turn lane with same cross-streets without turning bay) under coordinated signal operation. The tested signal control scenarios are pre-timed with and without TSP, fully actuated traffic control with and without TSP, real time without TSP, and D-SPORT. The results indicated that D-SPORT could reduce traffic delay and stops by 5% to 90% for the general traffic along the major corridors depending on the congestion level and control type in the most experimental scenarios. The model does not have an adverse impact on crossing streets traffic. Concerning the transit traffic, the model resulted in reducing transit delay and number of stops by 15% to 85%.

Zhou et al. (2007) presented an adaptive transit signal priority (TSP) model using a parallel genetic algorithm (PGA) to optimize the traffic signal control (phase plan, cycle length, and green splits) at isolated intersections considering the performance of both the transit and general vehicles. The model assigns weighting factors to individual transit vehicles that require TSP service. This weighting factor accounts for the passenger occupancy of the transit vehicle, the queuing conditions of all intersection movements, and the schedule lateness of the transit vehicle. The PGA searches for a near-optimal traffic signal timing solution to optimize the intersection average vehicle delay. This model was implemented and tested in a “star-like” network of one center and four adjacent intersections upstream the center intersection. The four adjacent intersections create traffic platoons and fluctuations. The simulation results showed that the PGA-based optimizer outperformed the fully actuated NEMA TSP control. Among the limitations are the use of single intersection for TSP evaluation, and also the huge computational resources needed for an arterial control.

2.2.3 Priority Strategies

TSP implementation is done through several strategies, such as extending greens, altering phase sequences, and including distinct phases without disrupting the coordination between adjacent intersections. The characteristics of these strategies are dependent on the selected priority concept. In the remaining part of this section, we highlight some of these strategies.

Passive Priority Strategies

Passive priority strategies are based on the schedules of the transit vehicles. They are developed based on the assumption that transit vehicles adhere to the planned schedule. When transit volume is higher (exceeds 60 buses per hour), the passive TSP with arterial coordination can provide much better performance than others (Lin et al., 2015). They are easy to implement and require low investment since no detection system is used. Passive priority strategies include green adjustment, phase splitting, cycle length reduction, transit coordination, metering vehicle, and queue jumps.

Green adjustment is two types; extending the green phase and truncating the red phase. The signal timing is changed depending on the arrival time of a transit vehicle. In phase splitting strategy, the signal phase is split into two equal phases without affecting the cycle length and the green time of cross streets traffic. The appropriateness of this strategy usually depends on transit and non-transit vehicles volumes. The cycle length reduction strategy is like the phase splitting strategy. However, the cycle length is reduced to decreases the stopping time of the transit vehicles. The strategy is likely to lessen the efficiency of control (by increasing the loss time), as the all red clearance times and the start-up delays at the beginning of each phase will be same for reduced cycle length. In transit coordination strategy, the offsets of the signals along the route of the transit vehicles are designed for signal coordination based on the schedule of the transit vehicles. Coordination is designed along the path of the transit vehicles if the transit vehicle path is not through an arterial. This strategy may not be effective due to the difficulty of predicting the dwell time at different stations along the route. A metering vehicle is an approach that limits the number of passenger cars to pass in the congested intersections or regions to increase the reliability and efficiency of transit vehicle operations. Finally, the queue jumps strategy is only suitable at intersections with designated transit vehicle lane(s). The transit vehicles are given early green times to jump the vehicle queues.

Active Priority Strategies

Active priority strategies are based on real-time conditions and are better than the passive strategies since they are responsive to traffic conditions. However, they require greater investment due to the essential implementation of a detection system. Active priority strategies include a green extension, red truncation or early green, phase insertion, phase rotation or substitution, and queue jumps. These strategies are like the ones used in the passive priority systems, but they are executed only when a transit vehicle is detected.

Zhou and Gan (2009) presented a signal control design for queue jumper lanes with actuated TSP strategies and compared its performance with that of the general actuated mixed-lane TSP. The associated signal control designs for the TSP and queue jumper lanes include phasing, phase splits, multiple bus services, and coordination recovery and green reimbursement. The model was evaluated in a micro-simulation environment by comparing its performance with that of the general mixed-lane TSP under various traffic volumes and bus stop locations. The results showed that the proposed TSP with queue jumper lanes could reduce more bus delays than can the commonly-used mixed-lane TSP, especially under high traffic volume conditions. Also, a nearside bus stop is superior to the far-side bus stop regarding bus delay (reduction of bus delay up to 25 percent) and overall intersection delay for the proposed design. Also, the impact of bus volumes on the general traffic on both major and minor streets is not significantly different from the mixed-lane TSP because of limiting the continuous calls for TSP to no more than two in one or two continuous signal cycles. The model is limited in the sense it accounts only for intersections with three phases (left turn are only permitted on the minor street). For four phase intersections, the results can be entirely different, and a new strategy has to be developed for coordination recovery and green reimbursement.

Green reallocation is another strategy that splits the original green times with respecting the phase transition sequence. Hu et al. (2015) demonstrated this strategy based on person-delay using optimization method for a TSP logic (Coordinated TSP with Connected Vehicle, TSPCV-C). This model is composed of three major components; a transit detection component, a TSP timing plan and transit speed calculation component, and finally a logic assessment and implementation component.

Signal Recovery/Compensation

Applying transit priority strategies may adversely affect other traffic and signal coordination. Signal compensation and offset recovery could be used to recover these effects. The additional green time given to the desired phase is taken from other phases in the following cycles to keep the same signal cycle time. This can cause delays and queues on the other phases especially if the frequency of transit signal priority is more.

The implementation of this strategy depends on the incidence frequency and characteristics of priority requests.

When a transit signal priority strategy is applied, the offsets of the signals may get altered, and that may disrupt the coordination of the signals on an arterial. The offset recovery is employed to recover the offset of the signal by adjusting the cycle lengths of the next two or three cycles. Signal recovery is usually applied on a network scale.

During the implementation of TSP, coordination can be interrupted due to the alteration of signal settings at intersections. Therefore, the strategy to incorporate TSP into a coordinated arterial should be thoroughly examined. He et al. (2014) presented the mathematical optimization model formulation of coordinated-actuated traffic signal priority control using Mixed-Integer Linear Program (MILP). The model was examined using a microsimulation tool. The model is designed to handle the multiple priority requests from different modes of vehicles and pedestrians with coordination and actuation simultaneously. Vehicle-To-Infrastructure (V2I) communication is used for getting the real-time information from the priority vehicle. Signal coordination is achieved by integrating virtual coordination requests, and when the signal coordination is not fulfilled, a penalty is added to the objective function. Two assumptions were used; the sequence of phases in a ring is fixed, and an existing off-line optimized signal coordination plan is available. The model was examined with three coordinated control methods, two bus frequencies and four different scenarios of nominal traffic volume (from low to high) for sensitivity analysis. The simulation experiment showed better results than the state-of-practice strategies. Results also indicated that greater coordination weight might cause some adverse impact to buses and pedestrians.

Conflicting/Multiple Priority Requests

Conflicting or multiple signal priority requests can occur. For instance, two transit lines crossing each other at an intersection can arrive at the same time requesting signal priority in different directions. Similarly, multiple priority requests of various modes of vehicles and pedestrians can occur. Also, buses on the same transit line initiate multiple priorities requests if they arrive successively with some time gaps, which results in calls at different stages of the traffic signal. Even two buses served by the same stage can cause various requests for signal priority if it is impossible for both buses to pass the intersection at the same green period. Typically, conventional controls, heuristic rules like first-come first served, are used to overcome this issue.

Zamanipour et al. (2014) presented a mathematical optimization model formulation to present a unified decision framework for multimodal traffic signal control. They used relative importance for different modes based on the information collected from connected vehicles and traditional detection system. The model is aimed to handle the multiple priority requests of various modes of vehicles and pedestrians. A policy-based integrated priority control framework is developed. National Electrical Manufacturers Association (NEMA) dual-ring eight-phase controller is used assuming the sequence of phases in each ring is fixed and phase skipping is not allowed. This model was evaluated with using two modes; Transit and Trucks. The model, although tested in the simulation model, does not account for delays due to coordination and green time extensions.

2.2.4 Evaluation

Lin et al. (2015) presented a comprehensive review of existing TSP controls according to the application and theoretical aspects by considering priority control methods, and system evaluations. This paper reviews three effective ways of system evaluations: analytical evaluation, simulation test, and field test. Moreover, this study analyzes field benefits of TSP in 24 cities around the world.

A critical step of the implementation of TSP is its assessment. Bus performance and reliability can measure the effectiveness of a transit signal priority. Bus performance is measured by bus travel time, delay, and speed, while bus reliability is measured by headway or schedule adherence. Moreover, the performance of the general vehicles and overall intersection/network is used to evaluate TSP system. The general vehicles performance is measured by vehicle delay and cross street vehicle delay, and the overall intersection/network performance is measured by total delay and total passenger delay. These performance measures are commonly determined by traffic simulation, analytical modeling, or actual TSP implementation.

Analytical Evaluation

The effects of active transit priority are difficult to model analytically due to the stochastic nature of the transit arrivals, which can be described as “events” rather than traffic flow. Analytical evaluation is done using queueing theory and regression models, to assess the efficiency and reliability of TSP control, and identify influenced factors.

Bagherian et al. (2015) presented an analytical method to enhance the evaluation of TSP at the network level using parameters such as traffic flow and signal characteristics. The model operational rules are: 1) pre-computed signal timing is utilized when no bus is approaching the intersection; 2) green extension (GE) would be granted if a bus is detected on an approach, the signal is green, the bus can pass the stop-line with this extension, and once the bus crosses the stop line, transition to the next phase is triggered; 3) red truncation (RT) is granted if a bus is detected on an approach and the signal is red; 4) the amounts of GE or RT time are compensated in the next cycle; 5) both prioritizing and compensation are ignored if a bus is detected in the next cycle; and 6) the effect of opposing flow rate is reflected in signal timing (i.e., allocated green time for each phase). The SIDRA model for traffic analysis is used to obtain sequence and phase times, and to compare the delay values vis-à-vis those obtained from the TSP delay function. The TSP model was examined by two case studies; first, an isolated T-intersection is used to address both TSP strategy and model efficiency, and second using a corridor in Australia. The results indicated that the delay estimated by the delay function closely matches micro simulation results.

Traffic Simulation Software

The microsimulation techniques have been widely used to evaluate and assess the efficiency and effectiveness of signal timing settings (Lin et al., 2015). For the preliminary study and planning of large transportation projects, traffic simulation software can provide more depth and analyses of project’s impacts. Simulation technologies have replaced traditional mathematical models for understanding and foreseeing the dynamics of traffic movements and control operations. Currently, there are several popular micro-simulation models, such as AIMSUM, CORSIM, VISSIM, TRANSMODELLER, and PARAMICS; however, engineering (statistical) judgment with calibration is required for adopting the most appropriate, efficient simulation tool for the particular type of project.

2.2.5 Discussion

This section summarizes the literature reviewed on various aspects of transit signal priority (TSP), such as the types of TSP concepts and strategies, the evaluations of these strategies, and the considerations for the planning and implementation of TSP.

TSP concepts are commonly categorized as Passive Priority, Active Priority or Adaptive/Real-Time Priority with or without optimization. Passive priority uses a pre-timed signal plan to favor bus operation without explicitly recognizing actual bus presence. Such passive priority strategies include green adjustment, phase splitting, cycle length reduction, transit coordination, metering vehicle, and queue jumps. Active priority alters the signal operation in response to the presence of a transit vehicle using detectors. Active priority strategies include a green extension, red truncation or early green, phase insertion, phase rotation or substitution, and the green reallocation (Hu et al., 2015). Depending on the location and capabilities of the bus detectors, active priority can also be classified as unconditional and conditional. Unconditional active priority grants priority to all transit priority requests; whereas, conditional active priority provides priority only to buses that meet certain predefined criteria, such as schedule or headway adherence, high passenger occupancy, or queue length of traffic. Based on real-time flow profiles of transit and general vehicles, adaptive priority develops signal timing plans to provide priority for transit vehicles while incurring the least delay to the transit passenger or total person (Lin et al., 2015). Adaptive priority entails using optimization models, Genetic algorithms and Artificial Neural Network (ANN) based control algorithm (Ghanim and Abu-Lebdeh, 2015).

The evaluation of TSP strategies is commonly based on the traffic performance, including the assessment of bus performance, bus reliability (headway or schedule adherence), general and cross street traffic performance and overall traffic performance. Also, evaluation methods can be categorized into three types: analytical evaluation, simulation test, and field test (Lin et al., 2015). In the majority of the literature, the TSP evaluation has been commonly reported with an improvement in transit performance (i.e., travel time, delay). However, the improvement gained regarding transit performance is typically accompanied by deterioration in the performance of the cross street traffic.

TSP may be applied at an isolated intersection, on an arterial, and over a network of intersections. Only very few papers have reported the performance of TSP in a complex urban traffic network with many overlapping or conflicting bus routes (Ahmed and Hawas, 2015). Transit signal priority at an isolated intersection needs a detection system for active priority. In the case of passive priority, an efficient arrival prediction model is required to get information regarding transit vehicles. When applied along an arterial with a group of signalized intersections, it is common to consider the coordinating between the adjacent intersections. For a network-based application, complex and advanced transit detection systems are essential (such as the Automatic Vehicle Location (AVL) and Automatic Passenger Count (APC), Connected Vehicle (CV)), and should be coupled with the non-transit vehicle queue detectors (Ding et al., 2013). The real-time detection system monitors the transit vehicles continuously, and the signal controller integrates the monitored vehicle's information with the non-transit flow data to provide priority to the transit vehicles. At this level, various priority strategies and different optimization models can be applied to optimize the network performance.

In general, TSP interrupts normal signal operations, and this creates delays to general traffic by serving priority requests. In some way, the performance of TSP control strategies relies on transit vehicle detection system, which in turn influences TSP operations. Short or long detection ranges may lead to less efficient TSP operations. Short detection range technology enables transit identification too near from the intersection, while the long detection range transit vehicles to be located at a far distance from the intersection. As such, short detection range implies late priority calls which would have limited lead time for treatment. On the other hand, long detection ranges can result in less predictability or inaccuracy of the transit vehicle's arrival at the intersection, due to the uncertainties of transit movements like dwelling at stops. Another important aspect is the location of bus stops (a near side stop is located before the intersection, and a far side stop is located after the intersection). In the case of far side bus stop, the TSP operation depends on the detection of the bus itself, but for nearside bus stop, the TSP operations should additionally account for the dwelling time at the bus stop.

Considering all these issues, Ahmed and Hawas (2015) developed an integrated traffic control system with TSP using a GPS based real-time bus detector system. The bus is considered as non-priority if it is bound to stop at some intermediate bus stop along the approach link. If the bus has already stopped or no bus stop along the approach link and its expected time to reach the stop line at the downstream end of the link is less than the green extension, then the bus is treated as a high priority bus. If the bus cannot reach the stop line within the green extension, the bus is regarded as a normal priority. This provides treatment to the issue of near or far side bus stop. Also, Ahmed and Hawas introduced mid-block detectors to overcome the problem of short or large detection range, but the impact of these detectors is not evaluated. Furthermore, despite the fact that the TSP system was tested with various signal controllers (split, protected, dual), there is no adequate discussion of the implications (pros and cons) of integrating the TSP with the different controllers.

The majority of the TSP systems in the literature lack some fundamental aspects that this research is attempting to address. First, the TSP s in literature have limited applicability to network operation (with overlapping and intersecting transit routes). Second, there is also another limitation because of the assumption that one point of transit vehicle's detection is sufficient for the system to operate. As indicated earlier there is advantages and disadvantages of both short and long term detection. Each detection range requires specific technology (with pros and cons), and as such, coupling both detection techniques (and ranges) might provide an edge. Third, nearly all the presented TSP's cannot be generalized to conditions beyond which the conditions they are calibrated for and tested. The robustness of a TSP system is verified if and only if it results in near optimal (or at least good) measures of performance in all conditions it may encounter in real life. A TSP working effectively for a specific traffic situation may not be as effective for another condition.

The TSP system parameters are commonly selected to fit specific traffic conditions. It is natural as such that such systems should be re-calibrated each time they are deployed to different conditions (that the system was not optimized for). What makes it more challenging is the dynamics of traffic and the evolution of the traffic demand over the day. A TSP may operate effectively during specific hours but then fails to run at other times because its parameters are adjusted for only some specific conditions (but not all). Furthermore, TSP systems commonly include multiple parameters that affect the performance, and as such the recalibration is certainly a challenging, difficult multi-dimensional task. It is not clear from the literature how were most of the TSP systems calibrated and how parameters were estimated.

Apparently, it seems like a trial and error calibration approach. It is certainly unclear also how general ATMS systems (and specifically complex TSPs) are calibrated for real time operation to function effectively at various demand levels and network configurations. A rule of thumb is no TSP system fits all traffic conditions.

Regardless of the TSP strategy and methodology to implement, one has to ensure the robustness of adopted solutions. Robustness can only be assured with extensive analytical, simulation or field tests under variant traffic conditions and network configurations. In addition to robustness, there is also need to minimize the recalibration requirement; it is illogical and impractical to calibrate the system for every condition it may encounter. In a real-time operational environment, this is certainly an impossible task. In brief, there is a need to devise a methodology that can be used to assess the effectiveness of complex TSP based systems, calibrate its parameters to provide optimal (or at least close to optimal) control, and assess the robustness of its effective control under the varying conditions. The challenge of the devising such methodology is the complexity of the objective functions and the nonlinearity nature of it. Some of the TSP s found in the literature are even integrated with other advanced ATMS components such as incident detection and management (Ahmed and Hawas, 2015), which makes the calibration of parameters even more challenging. Some of the TSP s may have few parameters to calibrate, and some may have many. As such, no matter what methodology is used to calibrate these parameters, it should be functional with various TSP systems and parameters. In the remaining part of this thesis, we highlight the main features of the proposed solution methodology and demonstrate how it can be used for optimizing the parameters through various case studies and ensure consistency and robustness of solution effectiveness at different operating conditions. To demonstrate the methodology, the integrated system developed by Ahmed and Hawas (2015) shall be used. Any other TSP algorithm can also be used instead; the Ahmed and Hawas (2015) was merely used because it is one of the most complicated TSP-based systems published recently, and it applies to all traffic control types (split, protected and dual).

2.3 Integrated Traffic Signal Control System

Traffic signals operate in pre-timed and actuated (semi-actuated and full-actuated) control modes. In pre-timed control, the control parameters (e.g. cycle length, phase splits, and phase sequence) are preset based on average traffic demand from historical data at different time periods of the day. In actuated control (based on the vehicle actuation), the control parameters (e.g. cycle length, phase splits, and sequence) vary in response to the current traffic situation. However, still, these control parameters depend on preset fixed parameters, such as unit extension, minimum, and maximum green. Therefore, these signal control systems can handle the recurrent congestion efficiently, but they do not have the ability to cope with non-recurrent congestion. *Adaptive Traffic Control Systems* (ATCSs) have been developed to adjust signal timing plans in dynamic real-time based on the current traffic situations, and transportation system capacity. According to a comprehensive study by Stevanovic (2010), each ATCS has unique features. This study identified several features to describe various adaptive traffic control logics. Among the potential features, the following functions can help in the identification of the distinctive working principles of each respective ATCS, as shown in Figure 2.1. This list does not include other features that are nearly as important (e.g. handling non-recurrent traffic conditions in urban streets). It is evident that none has the function of incident detection and

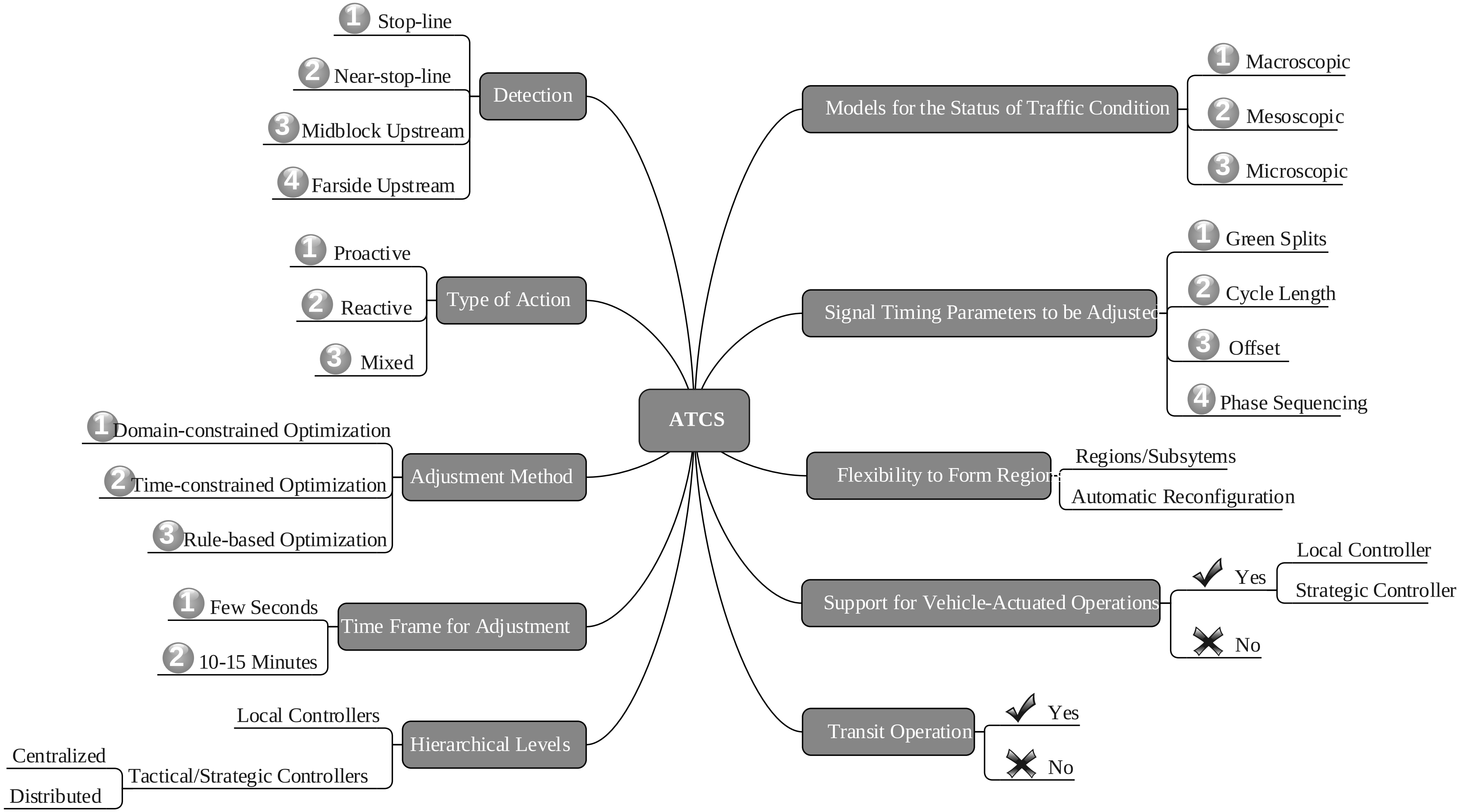

Figure 2.1: Features of various adaptive traffic control logics

management protocols. Therefore, an alternative control logic was developed by Ahmed and Hawas (2015) to combine incident detection and management protocols, transit signal priority, along with the recurrent congestion management into one integrated control system.

The control system by Ahmed and Hawas (2015) may be best classified as heuristically-based system that reacts to specific triggering conditions (such as downstream signal congestion, incident detection, identification of priority transit vehicle(s) in the traffic stream) by penalizing some predefined objective function with a set of parameters corresponding to these conditions.

The objective function of the controller is to maximize the throughput of passengers. This is not a typical optimization (maximization) process over a specific extended time-period, but rather an optimization at specific time instants (triggers). At any time (triggered by activating specific conditions), following the minimum green of the current phase, the system allocates the green to the phase (either current or the competing one) that has the estimated maximum queue of passengers.

In estimating the queue of passengers for any phase, the model accounts of passengers on priority buses (increases the passenger queue with more priority buses). For instance, when a transit vehicle is detected, a transit vehicle parameter is activated to increase the value of the objective function for this traffic approach (and its corresponding signal phase) on which the transit vehicle is detected. The model also accounts for downstream congestion status (decreases the passengers queue with downstream blockage conditions). If the congestion downstream a specific phase is reaching the capacity of approach, the upstream phase queue of passengers is readjusted to reduce the green time allocation of the phase(s) that are likely affected by the downstream congestion. The model also reacts to incident alarms on a specific approach by increasing the passenger queue of the phase serving this approach to allow incident recovery.

Ahmed and Hawas (2015) suggested that the system should undertake some actuation decisions of a currently running green phase based on the “establishment” of some boundary conditions, as shown in Figure 2.2. There are four modules, which are deployed to check the so-called boundary conditions. According to Ahmed and Hawas (2015), the traffic regime state module estimates the congestion status of the upstream link to a signalized intersection, the incident status module determines the likelihood of an incident on the link, the transit priority module estimates if the link is flagged for transit priority based on the transit vehicle location and type, and the downstream blockage module scans all downstream links of the intersection and determines their recurrent blockage (spillback) conditions.

The *transit signal priority* module estimates the number of priority buses and their type (normal or high). A bus will be flagged as no priority and as such will not be accounted for in the logic, if it is bound to stop at some intermediate bus stop along the approach link at time *t*. i.e., the bus is yet to stop. If the bus has already stopped (or no bus stop along the approach link), we check the expected time of the bus to reach the stop line at the downstream end of the link. If the bus is expected to reach the stop line within some interval, $\triangle g_{i,\Phi_k}$, the bus is treated as a *high* priority bus. If the bus is to reach the stop line beyond $\triangle g_{i,\Phi_k}$, the bus is treated as a *normal* priority one. $\triangle g_{i,\Phi_k}$ is the pre-specified time extension period for the actuated signal. The logic identifies the numbers of no priority, normal and high priority buses, and is capable of treating them differently by separate penalty values. Nonetheless, in this research, the penalty of both normal and high priority buses are set equal.

The *downstream blockage* module declares if any downstream blockage condition exists (physical constraint on the downstream exit link(s) for an individual phase, ϕ_j) at each detector data aggregation interval. This module checks the *balance* between the *number of vehicles to be served* for the time $\Delta g_{i,\Phi_k}$ from the upstream approach link, and the *available physical spaces* on the downstream exit link. The presence of downstream blockage condition is indicated if the estimated number of vehicles to be served (from the upstream demand side) exceeds the number of vehicles that could be accommodated physically (with the downstream supply side), at the time *t*. It is to be noted that the available number of vehicles that could be accommodated on a downstream exit link is estimated considering the jam condition as the worst case scenario.

The actuation module then estimates the so-called actuation index for each individual phase and then optimize to identify the next candidate phase set based on the signal control type (e.g. dual, protected, split). The controller then deploys the best-identified candidate phase set.

According to Ahmed and Hawas (2015), the proposed system operates in a manner similar to fully actuated signal (with split phase or protected phase or dual ring phase settings). The system has a continuously running *actuation module* which decides the "most deserving" phase set to go green from the inputs of the four modules at each control decision check point. While deploying the *actuation module*, the system also scans all feasible phase sets (including the current one). The system then estimates the value of the so-called *actuation index* for all the feasible phase sets, and determines the optimum (most deserving) *candidate* phase set; the one that possesses the maximum actuation index value, to serve green.

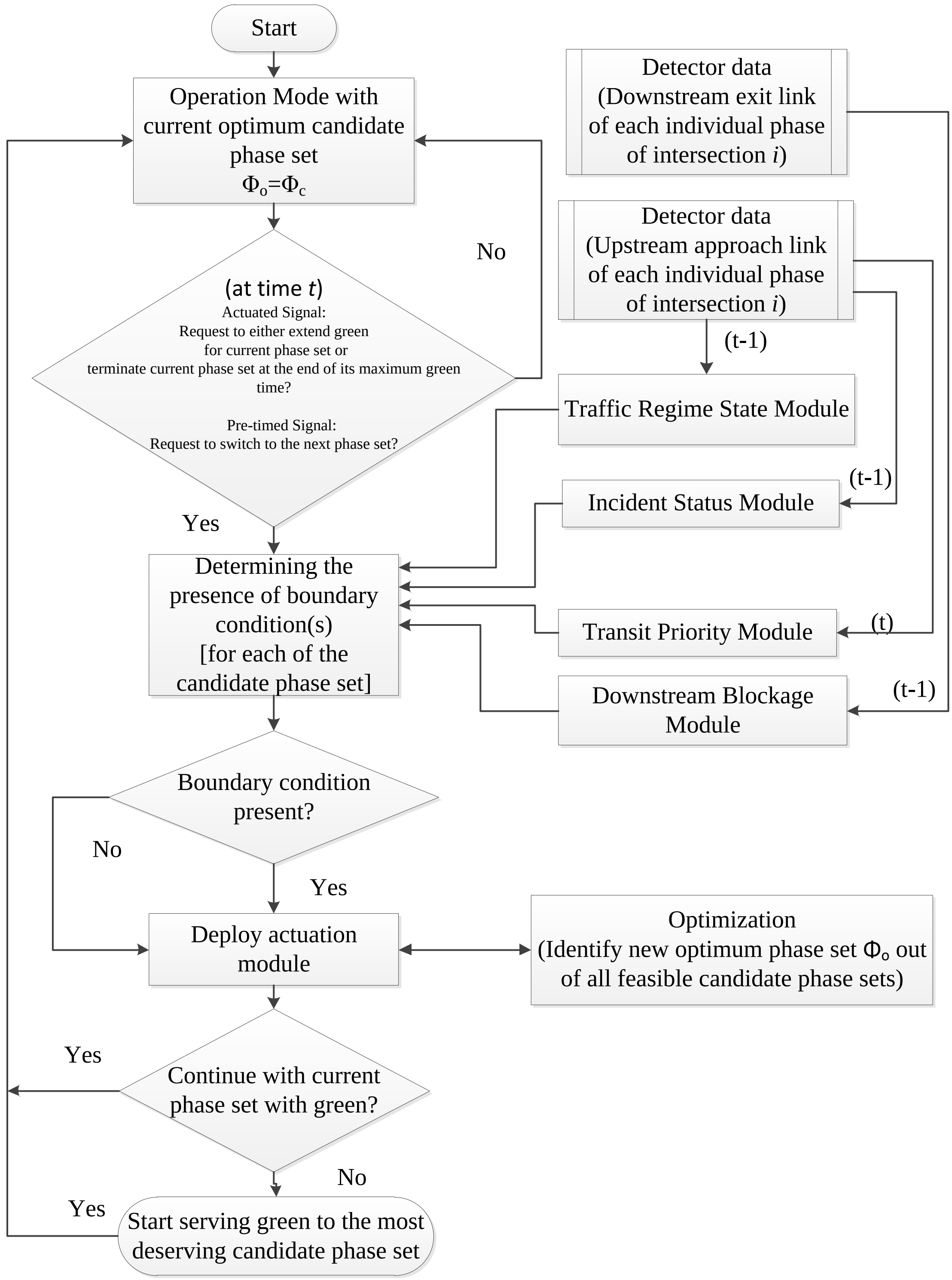

Figure 2.2: The architecture of the integrated traffic signal control system (source: Ahmed and Hawas, 2015)

For the *actuated* controllers, the first check point is the pre-selected minimum green-time $\mathrm{g}_{\mathrm{i},\Phi_{\mathrm{c}}}^{\mathrm{min}}$ (of the current phase set Φ_c at intersection *i*). If the *actuation module* identifies the currently running green phase set as the optimum (most deserving) candidate phase set at this first check point, then the green time is extended for a period of $\Delta\mathrm{g}_{\mathrm{i},\Phi_{\mathrm{c}}}$,where $\Delta\mathrm{g}_{\mathrm{i},\Phi_{\mathrm{c}}}$ is the adopted (pre-selected) green time extension seconds for the phase set Φ_c at intersection *i*. The whole control system logic is repeated then (a loop) at each $\Delta\mathrm{g}_{\mathrm{i},\Phi_{\mathrm{c}}}$ interval, which forms the consecutive check points and this process is constrained with some limiting conditions.

If the optimum (most deserving) candidate phase set is currently red flagged, then the current green phase set is truncated to switch to this optimum candidate phase with the maximum actuation index value. The control system logic is repeated when the current phase set reaches the first check point i.e. the minimum green time of a phase set.

In order to determine the optimum phase set Φ_o at any time *t*, the actuation module acts as an optimization model with a maximization problem. At any time *t* at the intersection *i*, while the current green phase set is Φ_c, the aim of this maximization problem is to search the best deserving candidate phase set Φ_k out of Ψ_c, which is a set of all feasible candidate phase sets while the current phase set is Φ_c. The best candidate phase set is termed as the phase set(s) which would produce the maximum actuation index, Z_{i,Φ_k}^{t}value(s). The optimum phase set, Φ_o is selected from either $\Phi_{k^{*1}}$ or $\Phi_{k^{*2}}$ (based on the type of control and the time with respect to maximum green), where, $\Phi_{k^{*1}}$ and $\Phi_{k^{*2}}$ refer the index of the best candidate phase set of the highest and second highest Z_{i,Φ_k}^{t} values, respectively, given that the current *green* phase set is Φ_c and the set of feasible candidate phase sets, Ψ_c.

As any phase set consists of two individual phases (as per the dual ring operation phase settings format), the final *adjusted virtual queue of passengers* of the feasible phase set is estimated by summing the *adjusted virtual queue of passengers* of the two corresponding individual phases. The phase set incurring the highest *adjusted virtual queue of passengers* is denoted as the optimum or most deserving candidate phase.

The *base congestion indicator* on the upstream of an individual phase ϕ_j denoted by $J_{i,\phi_j}^{/,t}$ refers to the *virtual queue of passengers* on the upstream approach of that individual phase ϕ_j at time *t*, and could be estimated from Eq. (2.1). This base *congestion indicator* ($J_{i,\phi_j}^{/,t}$) is estimated without any adjustment for the incident status on the upstream approach of that individual phase ϕ_j at time *t*. That is, Eq. (2.1) applies only to normal recurrent conditions; that is if no incident is detected on the upstream approach of phase ϕ_j .

$$J_{i,\phi_j}^{/,t} = \begin{bmatrix} \left(C_{i,\phi_j,u^/}^{c,t} \times O_{i,\phi_j,u^/}^{c} \times 1\right) + \\ \left(C_{i,\phi_j,u^/}^{b,t} \times O_{i,\phi_j,u^/}^{b} \times \beta_{i,\phi_j,u^/}^{b}\right) + \\ \left(C_{i,\phi_j,u^/}^{p,t} \times O_{i,\phi_j,u^/}^{p} \times \beta_{i,\phi_j,u^/}^{p}\right) + \\ \left\{\left(C_{i,\phi_j,u^/}^{c,t} \times O_{i,\phi_j,u^/}^{c} + C_{i,\phi_j,u^/}^{b,t} \times O_{i,\phi_j,u^/}^{b} + C_{i,\phi_j,u^/}^{p,t} \times O_{i,\phi_j,u^/}^{p}\right) \times r_{i,\phi_j,u^/}^{V,t} \times \beta_{i,\phi_j,u^/}^{V}\right\} \end{bmatrix} \tag{2.1}$$

Where $C_{i,\phi_j,u^/}^{c,t}$, $C_{i,\phi_j,u^/}^{b,t}$,and $C_{i,\phi_j,u^/}^{p,t}$ are the total vehicular counts of the cars, *c*, normal priority buses, *b*, and high priority buses, *p*, respectively, at time *t* on the *upstream* approach link, $u^/$, relevant to phase, ϕ_j , of intersection *i*. $O_{i,\phi_j,u^/}^{c}$, $O_{i,\phi_j,u^/}^{b}$and $O_{i,\phi_j,u^/}^{p}$ are the average passenger occupancies of cars, *c*, normal priority buses, *b*, and high priority buses, *p*, respectively. The parameters $\beta^{b}_{i,\phi_j,u^/}$ and $\beta^{p}_{i,\phi_j,u^/}$ are coefficients for *transit priority* for normal and high priority buses, respectively. $r^{V,t}_{i,\phi_j,u^/}$ is the *ratio of the vehicular queue length* to the physical capacity of the corresponding link length $l_{i,\phi_j,u^/}$. $\beta^{V}_{i,\phi_j,u^/}$ is a coefficient for *virtual queue of vehicles*.

If an incident is detected $\left(i.e.\ I^{N,t}_{i,\phi_j,u^/} = 1\right)$, the value of the *base congestion indicator*, $J^{/,t}_{i,\phi_j}$ is adjusted (increased) by the incident penalty coefficient $\beta^{N}_{i,\phi_j,u^/}$ to account for the potential incident on the upstream approach, $u^/$, as shown in Eq. (2.2):

$$J^{t}_{i,\phi_j} = \left(1 + \beta^{N}_{i,\phi_j,u^/} \times I^{N,t}_{i,\phi_j,u^/}\right) \times J^{/,t}_{i,\phi_j} \tag{2.2}$$

The J^{t}_{i,ϕ_j} value (in Eq. 2.2) is further adjusted (decreased) as shown in Eq. (2.3) by applying a *downstream blockage penalty* coefficient $\beta^{B}_{i,\phi_j,d^/}$ to account for blockage on the downstream exit link of phase ϕ_j. This applies only if the indicator of the downstream congestion $I^{B,t}_{i,\phi_j,d^/} = 1.$ If the downstream congestion indicator; $I^{B,t}_{i,\phi_j,d^/} = 0$, the denominator value $\left[\left(1 + I^{B,t}_{i,\phi_j,d^/}\right)^{\beta^{B}_{i,\phi_j,d^/}}\right]$ →1, and $A^{t}_{i,\phi_j} = J^{t}_{i,\phi_j}$. The value of A^{t}_{i,ϕ_j} is referred to as the *actuation index of the individual phase* ϕ_j .

$$A^{t}_{i,\phi_j} = \frac{J^{t}_{i,\phi_j}}{\left[\left(1+I^{B,t}_{i,\phi_j,d^/}\right)^{\beta^{B}_{i,\phi_j,d^/}}\right]} \tag{2.3}$$

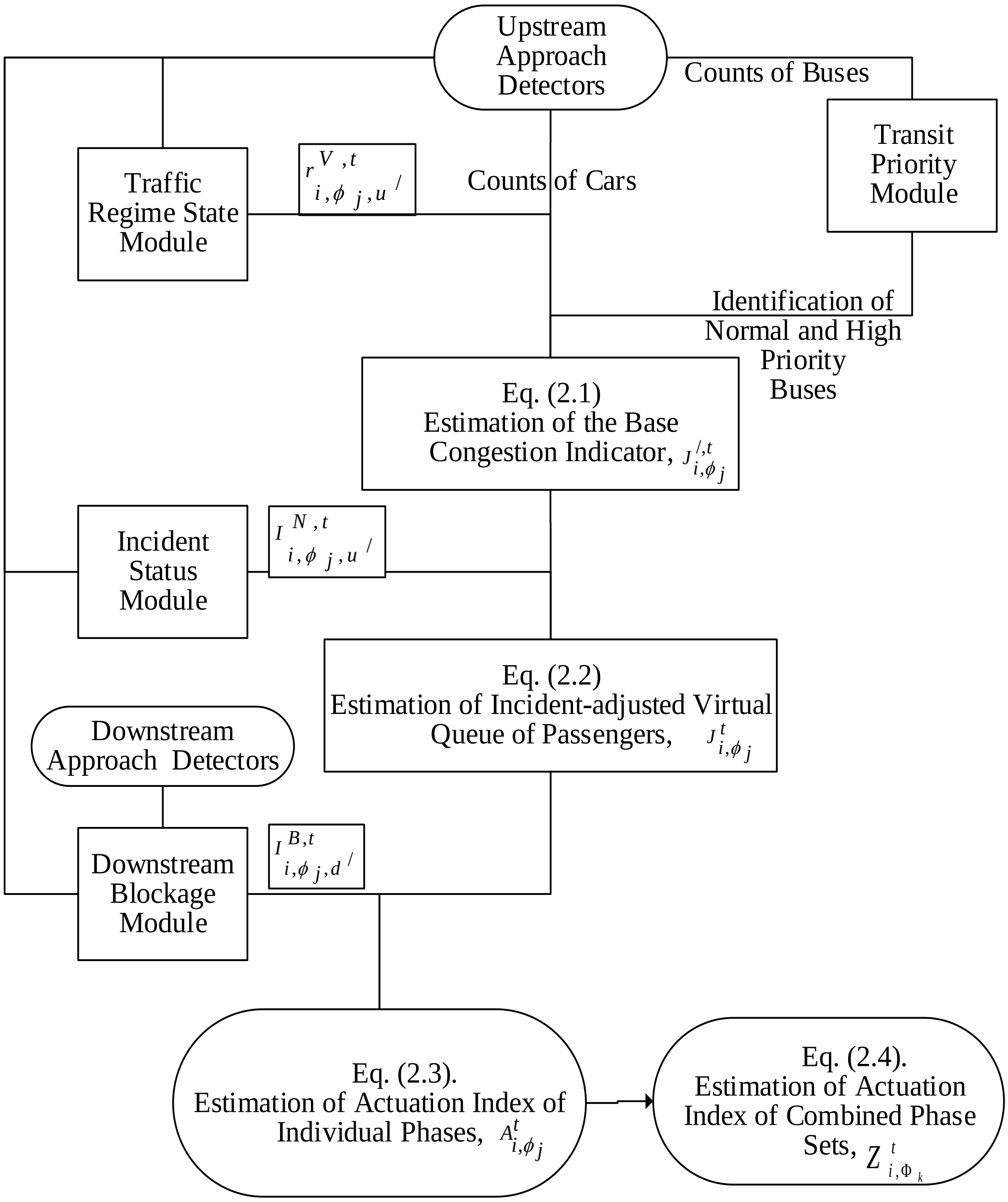

Figure 2.3: Mathematical model of the Integrated Traffic Control System

It is important to note though that all links of the network have detectors. That is, the downstream (exit) link of a phase is simultaneously an upstream link of another phase at the downstream intersection, and as such, it is naturally equipped with detectors. The congestion on the downstream link is estimated using the information extracted from the downstream (exit) link detectors as indicated in Eq. (2.3). The actuation index of a candidate phase set Z^{t}_{i,Φ_k} is the sum of the actuation indexes of the two concurrent individual phases of the candidate phase set, Φ_k, $\Phi_k = \{\phi^{k,1} \cup \phi^{k,2}\}$.

$$Z_{i,\Phi_k}^t = A_{i,\phi^{k,1}}^t + A_{i,\phi^{k,2}}^t \qquad (2.4)$$

The Z_{i,Φ_k}^t index represents the final *adjusted virtual queue of passengers* considering the estimated impact of all the relevant boundary conditions which are represented by respective modules. The most deserving candidate phase set is the one of the maximum Z_{i,Φ_k}^tvalue.

Eq. (2.3) is introduced to penalize the links that have full or partial blockage; if one link is fully blocked, the upstream phases of this particular link will be "penalized" and as such lesser green times to these phases that feed vehicles to such blocked link. This will prevent any further blockage on the incident links, reduce the likelihood of full blockage and prevent spill backs from and along fully blocked incident links.

Eqns. (2.1), (2.2) and (2.3) are all used to estimate the congestion indicator (base or adjusted), but their values will depend on the met identified boundary conditions. For instance, the transit priority parameters and terms in Eq. (2.1) accounts for priority buses. If a priority bus is detected, these terms will be processed and as such the base congestion indicator will give different results as compared to the case where no priority buses are detected. The downstream congestion (in Eq. 2.3) as well is a boundary condition that is flagged by a blockage on downstream links (if and only if downstream exit links are flagged with blockage).

2.4 Simulation-based optimization

Contemporary simulation-based optimization methods can be categorized as discussed by Carson and Maria (1997) and shown in Figure 2.4 into Gradient-Based

Search, Stochastic Optimization, Response Surface Methodology, Heuristic Methods, A-Teams, and Statistical. Gradient-Based Search Methods estimate the response function gradient to assess the shape of the objective function and employ deterministic mathematical programming techniques. Also, commonly used gradient estimation methods are Finite Difference Estimation, Likelihood Ratio Estimators (Treiber and Kesting, 2013), Perturbation Analysis, and Frequency Domain Experiments.

Stochastic optimization is the way of finding a local optimum for an objective function using an iterative method based on gradient estimation. It has two features relevant to the calibration of micro-simulation traffic models: (1) considering the presence of measurement errors in the objective function explicitly and (2) the results are usually faster to identify solutions than many other algorithms (Daamen et al., 2015). Stochastic optimization has been used for the traffic simulation models by Balakrishna et al. (2007), Ma et al. (2007), Lee and Ozbay (2009), Vaze et al. (2009), Ciuffo and Punzo (2010), (Hale et al., 2015b), Mudigonda and Ozbay (2015), and Paz et al. (2015b).

Response surface methodology is a process for fitting a regression model to the output variable(s) of a simulation model. More details about this method are presented in the following sections. The response surface methodology has been used for the optimization of transportation systems by Joshi et al. (1995), and Jafarzadeh-Ghoushchi (2015).

Heuristic (direct search) methods require function values to balance exploration with efficient global search strategies (Genetic Algorithms, Evolutionary Strategies, Simulated Annealing, Tabu Search, and Simplex Search). Genetic algorithms are the most widely used for calibrating microscopic traffic simulation models (Daamen et al., 2015, Manjunatha et al., 2013, Vasconcelos et al., 2014a, 2014b, Ma and Abdulhai, 2002, Schultz and Rilett, 2004, Kim et al., 2005, Ma et al., 2007, Ciuffo and Punzo, 2010). Simulated annealing is a method for solving unconstrained and bound-constrained global optimization problems, and it has been used in numerous transportation applications by Chang et al. (2002), Chen et al. (2005), and Ciuffo and Punzo (2010).

Asynchronous team (A-team) is a method that involves combining various problem solving strategies so that they can interact synergistically (Carson and Maria, 1997, Abdalhaq and Baker, 2014, Paz and Molano, 2014, Hale et al., 2015a, Osorio and Chong, 2015, Osorio et al., 2015, Li et al., 2016, Paz et al., 2015a).

OptQuest/Multistart algorithm is a type of the A-team methods, which is at the same time a scatter search heuristic and a gradient-based algorithm. A shortcoming of this approach is a large number of objective function evaluations (i.e., traffic simulations) it requires (Daamen et al., 2015). This has been applied in the microscopic traffic simulation models by Ciuffo et al. (2008), Ciuffo and Punzo (2010).

The statistical methods include the Importance Sampling, Ranking and Selection, and Multiple Comparison. Additionally, Zhong (2016) used a cross-entropy method with probabilistic sensitivity analysis framework for calibrating microscopic traffic models.

In simulation-based optimization, the best parameter values are chosen from a set of candidate parameter settings. In this research, Response Surface Methodology (RSM) will be used to get the best parameter configurations, as RSM requires a smaller number of simulation experiments than that of the Gradient-based method (Carson and Maria, 1997). The idea of RSM is to construct a mathematical surrogate model(s) to approximate the underlying function (Deng, 2007).

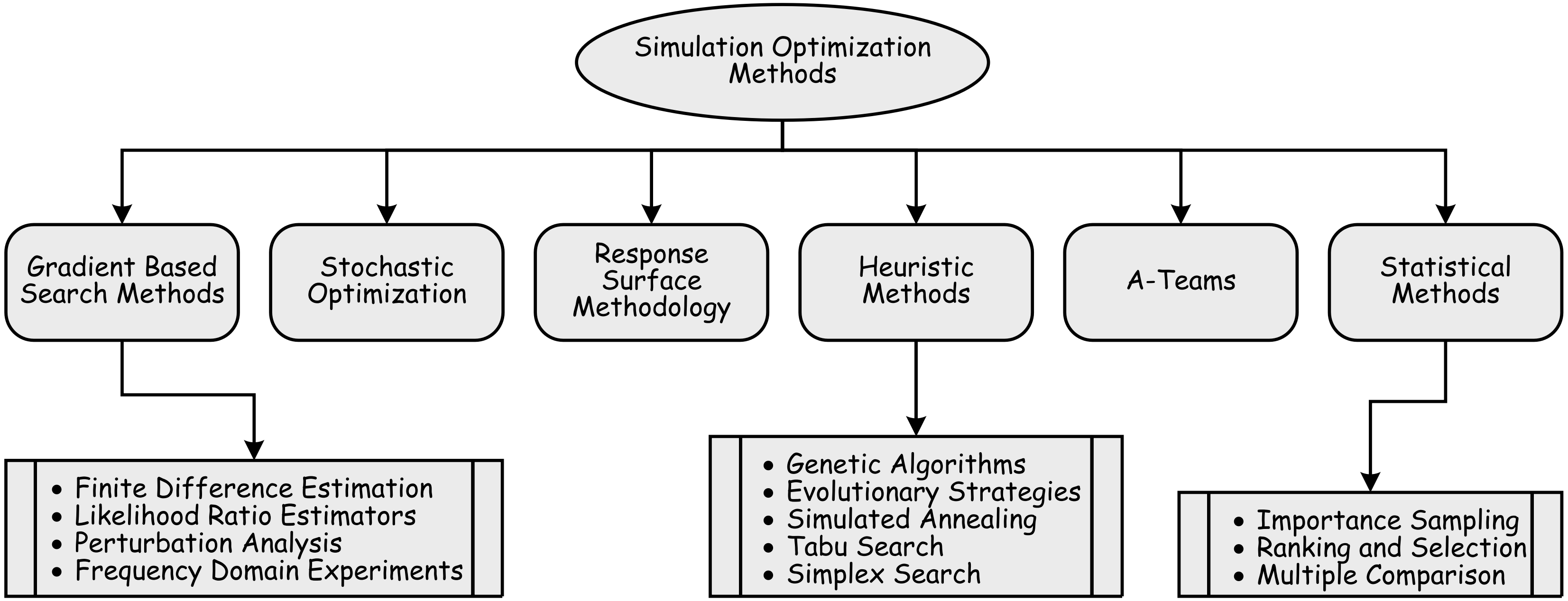

Figure 2.4: Simulation Optimization Methods (source: Carson and Maria, 1997)

RSM can be divided into two general methods; Central Composite Design (CCD) and Box–Behnken Design (BBD) (Fu, 2015). In this research study, Box–Behnken method is used to get the optimum solutions (of the parameters vis-à-vis the specified MOE’s) as the BBD is slightly more efficient than the CCD (Ferreira et al., 2007). The following sections provide more details about the RSM with different design methods and the procedure to optimize the responses.

Chapter 3: Methodology

3.1 Introduction

This chapter presents the methodology to calibrate the parameters of Integrated Traffic Signal Control System (Ahmed and Hawas, 2015) using the Response Surface Methodology (RSM). The parameters of Integrated Traffic Signal Control System are discussed in Section 3.2 briefly. Then, the features of RSM including the experimental design (Central Composite Design or Box–Behnken Design) methods and response optimization strategy are presented. Finally, the RSM procedures (design, data importing, model building for each response, and optimization) in Minitab are introduced.

3.2 Parameters of Integrated Traffic Signal Control System

To apply the Integrated Traffic Signal Control System developed by Ahmed and Hawas (2015) for real-time traffic signal control, there are parameters that must be calibrated and their values to be determined for optimal control, as they affect the estimates of the actuation index, A^{t}_{i,ϕ_j} as explained earlier. These parameters are:

1. The coefficient for virtual queue of vehicles on the upstream approach link (β^{V}); an abbreviation of the coefficient of *virtual queue of vehicles* ($\beta^{V}_{i,\phi_j,u^{/}}$) on the *upstream approach link* of phase ϕ_j at intersection *i*.
2. The coefficients for transit priority (β^{b} or β^{p}); abbreviations of coefficients for *transit priority* for high priority buses ($\beta^{p}_{i,\phi_j,u^{/}}$) and normal priority buses ($\beta^{b}_{i,\phi_j,u^{/}}$) on the upstream approach, $u^{/}$, of phase

ϕ_j, at intersection *i*. In this study, it is assumed that both coefficients have equal values for simplicity.

3. The downstream blockage penalty coefficient (β^B); an abbreviation of the coefficient for *blockage* on the *downstream exit link* ($\beta^B_{i,\phi_j,d^/}$) of phase $\phi_j$at intersection i.
4. The incident penalty coefficient (β^N); an abbreviation of the coefficient of incidents ($\beta^N_{i,\phi_j,u^/}$) on the upstream approach,$u^/$, of phase ϕ_j, at intersection i.

In this study, we focus only on estimating the optimal control strategies for recurrent conditions. That is, no incident scenarios are considered. For more on incident situation control, the reader is referred to Ahmed and Hawas (2015). In typical recurrent congestion situations, the values of the parameters β^V, β^bor β^p, and β^B (while β^N is not considered) are likely to affect the network performance as a result of different penalty values via the signal control. The performance of the traffic network is represented herein by three output variables or MOEs; these are: total number of bus trips served during a specific analysis period, N_{bus}, total network travel time (in hrs), T_t , and the trip mean travel time in seconds, t_m. Figure 3.1 shows the schematic presentation of the control system. It is to be noted that the mid-block of the figure (simulation) is acting herein as the medium for evaluating the MOE's in response to the changes of the various control coefficients. The study adopts a simulation-based optimization approach to model the relationships between the control parameters and the resulting MOE's.

In brief, this study aims at studying the impact of these control parameters on the network MOE's, to develop models for explaining the relationships between these parameters and the resulting MOE's for various signal control types and congestion conditions. One can regard the problem in hand as an optimization problem of input parameters β^V, β^b or β^p, and β^B, to maximize the total number bus trips, and to minimize the total and mean travel times. For simplicity, in this study both high and normal bus priority parameters β^b and β^p are assumed equal.

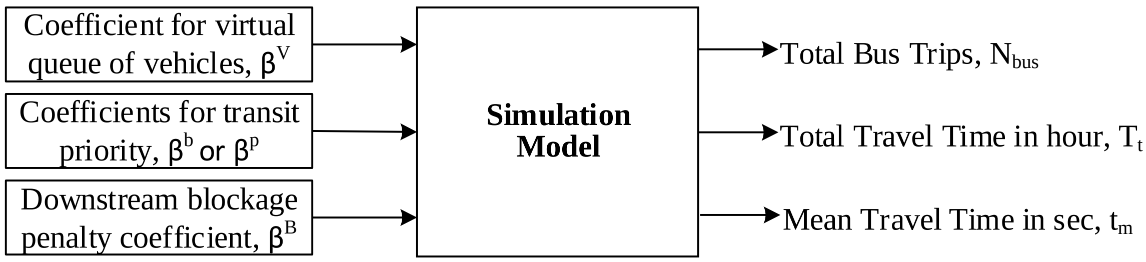

Figure 3.1: Schematic presentation of input parameters and resulting MOE's

Figures 3.2 and 3.3 show the 3D scatter plots for the responses of N_{bus} and t_m for various parameters of β^V, β^b or β^p, and β^B. The data for these plots are taken from the simulation of a specific network (that will be discussed later) operated by the integrated control system using different 135 input variable settings. Each setting is simulated ten times. That is, 1350 simulation runs were done to produce these data. The responses as drawn on the figures (total bus trips in Figure 3.2, and the mean travel time in Figure 3.3) are the average values of the ten simulation runs of each of the 135 settings. As apparent in figures 3.2 and 3.3, the responses are quite dispersed. It is not possible to identify the set (among these 135 settings) that correspond to the maximum total bus trips and simultaneously the least mean travel time. In Figure 3.2, the black dots refer to the bus trips of more than 160 (the maximum number of bus trips obtained from simulating the 1350 cases is 161.3).

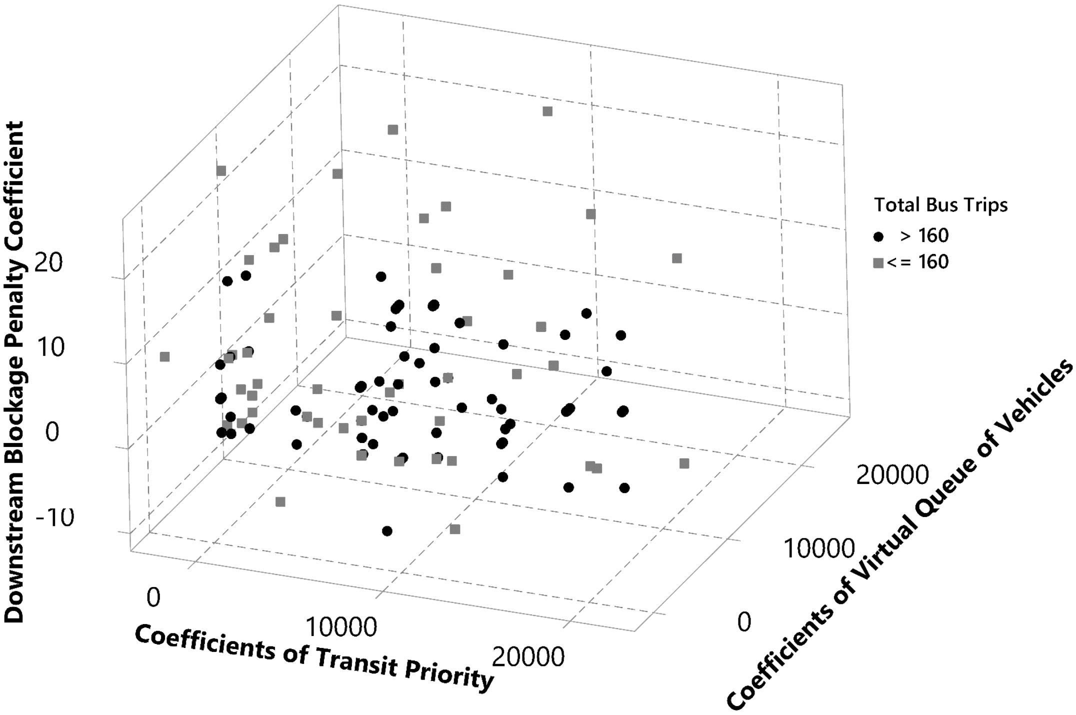

Figure 3.2: Scatter 3D plot of N_{bus} for various parameters of β^V, β^bor β^p, and β^B for split actuated control under high traffic demand

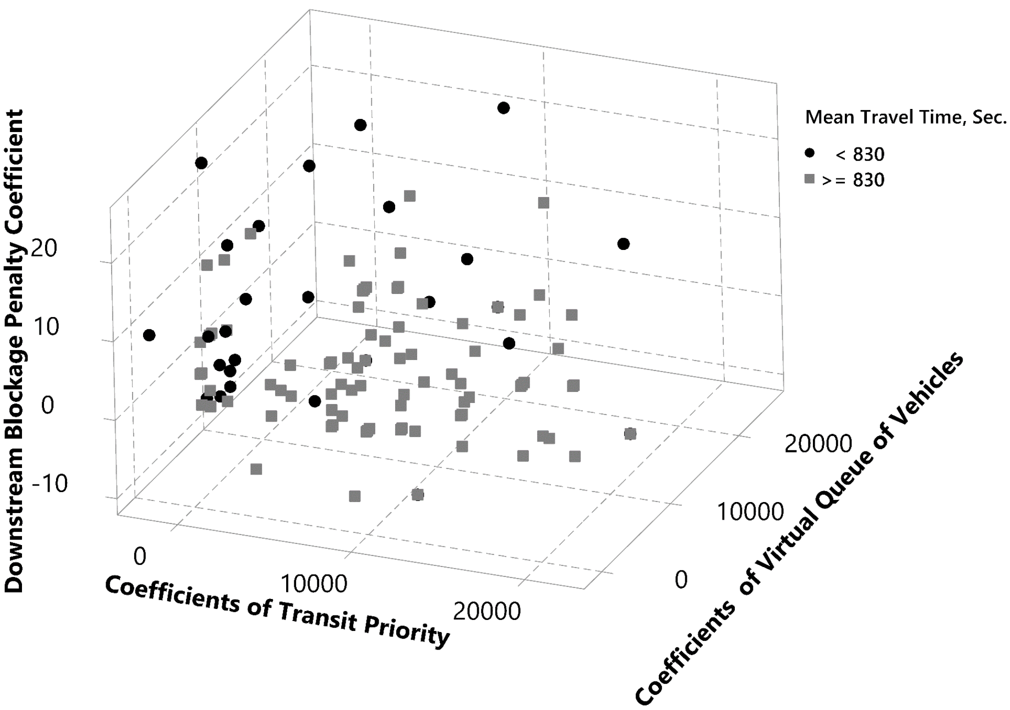

Figure 3.3: Scatter 3D plot of t_m for various parameters of β^V, β^bor β^p, and β^B for split actuated control under high traffic demand

In Figure 3.3, the black dots refer to the mean travel time of fewer than 830 seconds (the least mean travel time was 809.4 seconds). The question then becomes whether is there a specific parameter set that can be used to obtain more than (or as close as possible) 161.3 bus trips and simultaneously have mean travel time fewer than 830 seconds. Therefore, to identify the optimal setting, it is necessary to use some optimization method to satisfy all conditions. The Response Surface Methodology is chosen to perform this task.

3.3 Response Surface Methodology (RSM)

Response Surface Methodology (RSM) was originated and described by Box and Wilson (1951). RSM consists of techniques (mathematical and statistical), to define the relationships between the response and independent variables (inputs). It determines the effect (alone or in combination) of the independent variables on the processes. To analyze the consequences of the independent variables, RSM generates a metamodel. The graphical perspective of this metamodel has led to the term Response Surface Methodology.

In this research study, the relationships between the responses or MOE's (N_{bus}, T_t and t_m) and the inputs parameters (β^V, β^b or β^p, and β^B) are mathematically expressed by Eqs. (3.1 to 3.3):

$$N_{bus} = f_{N_{bus}}(\beta^V, \beta^b \text{ or } \beta^p, \text{ and } \beta^B) + \varepsilon_{N_{bus}} \tag{3.1}$$

$$T_t = f_{T_t}(\beta^V, \beta^b \text{ or } \beta^p, \text{ and } \beta^B) + \varepsilon_{T_t} \tag{3.2}$$

$$t_m = f_{t_m}(\beta^V, \beta^b \text{ or } \beta^p, \text{ and } \beta^B) + \varepsilon_{t_m} \tag{3.3}$$

N_{bus}, T_t, and t_m are the responses (MOE's) of total bus trips, total network travel time, and trip mean travel time, respectively. $f_{N_{bus}}$, f_{T_t}, and f_{t_m} represent the unknown functions (metamodels) of responses (N_{bus}, T_t, and t_m, respectively). β^V, β^bor β^p, and β^B denote the input variables (coefficient for virtual queue of vehicles, coefficient for transit priority, and downstream blockage penalty coefficient, respectively. $\varepsilon_{N_{bus}}$, ε_{T_t}, and ε_{t_m} are some statistical errors that represent other sources of variability not accounted for by the functions. The error terms are assumed to follow a normal distribution with the mean of zero and some variance.

3.3.1 Steps for RSM

The application of RSM as an optimization technique are as follows (Bezerra et al., 2008):

1. The selection of independent variables through screening and the delimitation of the experimental region, according to the objective and the experience of the researcher. In this research study, the three independent variables are previously selected (β^V, β^bor β^p, and β^B) as they relate to the parameters affecting the objective function (as explained earlier in Section 2.3).
2. The choice of the experimental design and accomplishing the experiments according to the selected experimental matrix. In this research study, Box-Behnken Design (BBD) is used.
3. The mathematic-statistical treatment of the obtained experimental data through the fit of a polynomial function, using the p-value of 0.1;
4. The evaluation of the model's fitness;
5. The verification of the necessity and possibility of performing a displacement in direction to the optimal region; and
6. Obtaining the optimum values for each studied variable.

3.4 Experimental Designs with Computer Simulation Models

RSM can be applied to computer simulation models of physical systems (Myers et al., 2009). In such applications, RSM is used to build a metamodel of the system (being modeled by the computer simulation), and optimization is carried out on the metamodel. The assumption is that if the computer simulation model is a reliable representation of the real system, then the RSM optimization will result in an adequate determination of the optimum settings for the actual system. It is worthy to note traffic simulation models could be stochastic or deterministic. In the stochastic simulation models, the output responses are somehow random variables whereas deterministic models are typically mathematical functions that yield deterministic outputs (not random). In this research study, an experimental network is simulated by a stochastic model.

The RSM approach is based on a philosophy of sequential experimentation, with the objective of approximating the response surface with a low-order polynomial function in a relatively small region of interest that contains the optimum solution. RSM can be carried out using either Central Composite Design (CCD) or Box–Behnken Design methods (Fu, 2015), as discussed in the following sections.

3.4.1 Box–Behnken Design

Box-Behnken Design (BBD) suggests how to select points from the three-level factorial arrangement, which allows the efficient approximation of the first- and second-order coefficients of the mathematical model. BBD is more efficient and economical than the similar three-level full factorial designs (Bezerra et al., 2008). The BBD principal characteristics are:

1. The number of experiments (N) required in BBD is defined as $N = 2k(k-1) + C_0$, (where k and C_0 are the number of factors and central points, respectively). In this study, k and C_0 are both equal to three (3). Thus, the number of experiments will be 15 ($N = 2*3*(3-1)+3$). For comparison; the number of experiments for a Central Composite Design (CCD) is $N = 2^k + 2k + C_0$, which would be 20 ($N = 2^3 + 2*3 + 6$) with three factors and six central points.
2. All factor levels have to be set only at three levels (−1, 0, +1) with equally spaced intervals between these levels.

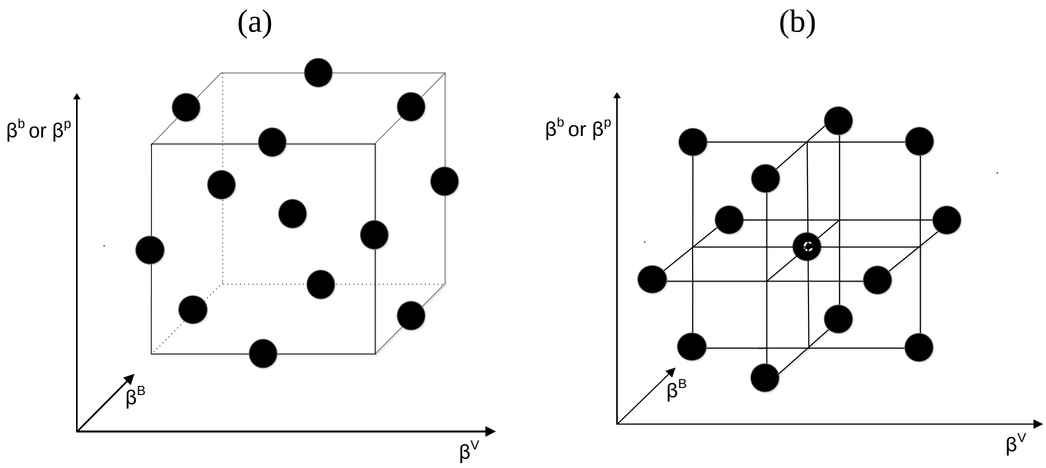

Figure 3.4: (a) The cube for BBD, and (b) three interlocking two-level full factorial design (modified version of the source figure from Ferreira et al., 2007).

For three factors, the BBD graphical representation can be seen in two forms (Ferreira et al., 2007):

1. A cube that consists of the central point and the middle points of the edges, as can be seen in Figure 3.4a.

2. An illustration of three interlocking two-level full factorial designs and a central point, as shown in Figure 3.4b.

Table 3.1: Coded factor levels for a BBD of three-variable matrices with 3 center points in a single block

Experiment	Point Type	β^V	β^b or β^p	β^B
1	Edge	−1	−1	0
2	Edge	1	−1	0
3	Edge	−1	1	0
4	Edge	1	1	0
5	Edge	−1	0	−1
6	Edge	1	0	−1
7	Edge	−1	0	1
8	Edge	1	0	1
9	Edge	0	−1	−1
10	Edge	0	1	−1
11	Edge	0	−1	1
12	Edge	0	1	1
13	Center	0	0	0
14	Center	0	0	0
15	Center	0	0	0

Table 3.1 presents the coded values of the experimental matrices of BBD. For a BBD, the Minitab represents the settings with -1 for the low factor setting, 0 for the middle setting, and +1 for the high setting.

The BBD is a good design for the RSM (Ferreira et al., 2007). It permits (i) estimation of the parameters of the full/ partial quadratic model with the building of sequential designs; (ii) detection of lack of fit of the model; and (iii) use of blocks. A comparison between the BBD and other RSM designs (central composite, and three-level full factorial design) has demonstrated that the BBD is slightly more efficient than the CCD, and much more efficient than the three-level full factorial designs (Ferreira et al., 2007).

3.4.2 Central Composite Design

The Central Composite Design (CCD) was presented by Box and Wilson (1951) and consists of the following parts: (1) a full factorial or fractional factorial design with an additional design, often a star design in which experimental points are at a distance α from its center; and (2) a central point (Bezerra et al., 2008). Figure 3.5 illustrates the full CCD of three variables for optimization.

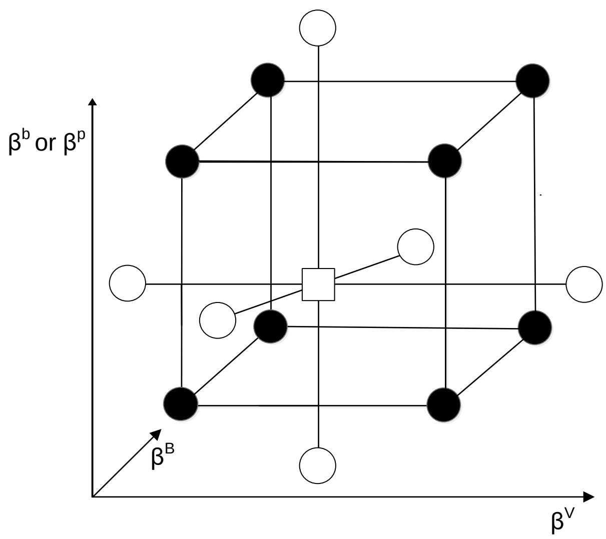

Figure 3.5: The CCD of three variables system

The full CCD presents the following characteristics:

1. The required number of experiments is $N = 2^k + 2k + C_0$, where k is the factor number and C_0 is the replicate number of the central point. In this

research study, $(N = 2^3 + 2 * 3 + 6)$ which 20 with three factors and six central points;

2. α-values depend on the number of input variables and is calculated by for Spherical design ($\alpha = \sqrt{k}$), and for Rotatable design ($\alpha = 2^{k/4}$) , where k is the number of factors;
3. All factors are considered in five levels (−α, −1, 0, +1, +α).

Table 3.2: The coded values of the CCD experimental matrices

Experiment	**Point Type**	β^V	β^b or β^p	β^B
1	Corner	-1	-1	1
2	Corner	1	-1	-1
3	Corner	-1	1	1
4	Corner	1	1	-1
5	Corner	1	-1	1
6	Corner	-1	1	-1
7	Corner	-1	-1	-1
8	Corner	1	1	1
9	Axial	0	1.681793	0
10	Axial	1.681793	0	0
11	Axial	0	0	1.681793
12	Axial	0	-1.68179	0
13	Axial	0	0	-1.68179
14	Axial	-1.68179	0	0
15	Center	0	0	0
16	Center	0	0	0
17	Center	0	0	0
18	Center	0	0	0
19	Center	0	0	0
20	Center	0	0	0

Table 3.2 presents the coded values of the experimental matrices of CCD. For a CCD, Minitab represents the settings as follows:

- -1 indicates the low factor level
- 1 indicates the high level
- 0 indicates the middle point between the low and high level
- -1.68179 and 1.68179 indicate the low and high axial levels, respectively

3.5 Response optimization

The variable settings (β^V, β^bor β^p, and β^B) are obtained using Minitab®'s Response Optimizer in accordance to some objective functions on the set of responses (N_{bus}, T_t and t_m). Herein, the objectives are to maximize N_{bus} and to simultaneously minimize both T_t and t_m.

The so-called desirability function approach (as outlined by Derringer and Suich, 1980) is used the multi-objective simultaneous consideration of the responses. Initially, each response is converted into an individual desirability, which varies over the range from zero to one dimensionless scale. The individual desirabilities are, then, used to estimate the composite desirability (D) using the following geometric mean formula:

$$D = (d_{\mathrm{N}_{bus}} * d_{T_t} * d_{t_m})^{\frac{1}{3}} \qquad (3.4)$$

Where, $d_{\mathrm{N}_{bus}}$is the individual desirability of total number of bus trips (N_{bus}), d_{T_t} is the individual desirability of the network’s total travel time (T_t), and $d_{t_m}$is the individual desirability of trip’s mean travel time (t_m).

The estimated composite desirability value depends on the specific set goal (lower, target, upper) of each individual desirability element (response), the weight

(r) which defines the form shape of desirability function for each response, and the importance parameters (w) of the various desirability items that are combined into a single composite desirability.

Given the aimed objectives (e.g. maximize N_{bus} and to simultaneously minimize both T_t and t_m), the individual desirabilities are stated, and overall the problem in hand is transformed into maximizing the composite desirability. The composite desirability unifies the individual desirabilities of all the response variables into a single measure and emphasis is placed on the response variables with the importance parameter (w). The importance parameters reflect the relative importance of the individual desirabilities in estimating the composite one as shown in Equation 3.8 (weighted geometric mean):

$$D = \left[\left(d_{\mathrm{N}_{bus}}\right)^{w_{N_{bus}}} \times \left(d_{T_t}\right)^{w_{T_t}} \times \left(d_{t_m}\right)^{w_{t_m}}\right]^{1/3} \tag{3.5}$$

Where, $w_{\mathrm{N}_{bus}}$is the importance parameter of N_{bus}, $w_{\mathrm{T}_t}$is the importance parameter of T_t, and $w_{\mathrm{t}_m}$is the importance parameter of t_m. The importance parameter determines the influence of each response on the composite desirability. For instance, if the importance of $d_{\mathrm{N}_{bus}}$ is 1, whereas the importance of d_{T_t} is 2, then, d_{T_t} will have a greater (not double) influence on the composite desirability. By default, Minitab® places equal importance on the responses and assigns each an importance value of one. In this research study, all importance parameters of individual desirability are set equal to one (1). That is, $w_{\mathrm{N}_{bus}} = w_{T_t} = w_{t_m} = 1$.

The goal is interpreted with regard to the target parameter for the response. If the goal is minimizing a response, the desirability is one for all response values less than or equal to a specific lower bound target. Alternatively, if the goal is maximizing a response, then the desirability is one for all values equal to or above a specific upper bound target. Finally, if the goal is to get the response at target (located between the lower and upper bound), then the desirability is one at the target.

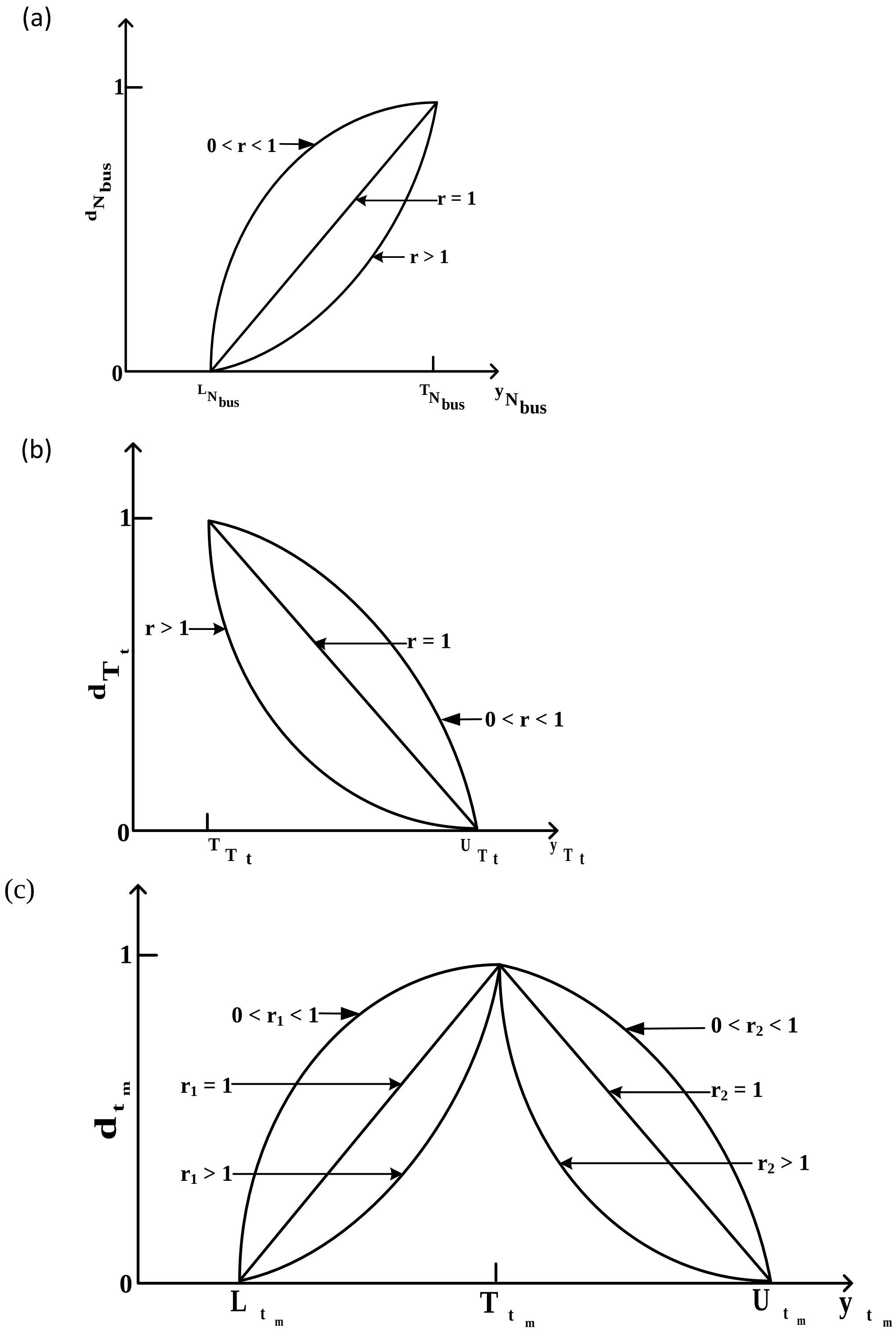

Figure 3.6: The forms of individual desirability functions for different goals: maximization; (b) minimization; (c) a particular target value.

For example, if the goal for the response of the total bus trips ($y_{N_{bus}}$) is a maximum value, the individual desirability function $d_{N_{bus}}$is defined as follows:

$$d_{N_{bus}} = \begin{cases} 0 & y_{N_{bus}} < L_{N_{bus}} \\ \left(\frac{y_{N_{bus}} - L_{N_{bus}}}{T_{N_{bus}} - L_{N_{bus}}}\right)^r & L_{N_{bus}} \leq y_{N_{bus}} \leq T_{N_{bus}} \\ 1 & y_{N_{bus}} > T_{N_{bus}} \end{cases} \quad (3.6)$$

Where, the value of $\left(\frac{y_{N_{bus}} - L_{N_{bus}}}{T_{N_{bus}} - L_{N_{bus}}}\right)^r$ ranges from zero to one. r is the weight that defines the functional form of the desirability function; if $r = 1$, the desirability function is linear, as shown in Figure 3.6a. $L_{N_{bus}}$ and $T_{N_{bus}}$ are the lower bound and target values of the response (N_{bus}), respectively.

If the goal for the response is a minimum value (e.g. minimal network total travel time y_{T_t}), the individual desirability for the response $d_{T_t}$is defined as follows:

$$d_{T_t} = \begin{cases} 1 & y_{T_t} < T_{T_t} \\ \left(\frac{U_{T_t} - y_{T_t}}{U_{T_t} - T_{T_t}}\right)^r & T_{T_t} \leq y_{T_t} \leq U_{T_t} \\ 0 & y_{T_t} > U_{T_t} \end{cases} \quad (3.7)$$

Where, the value of $\left(\frac{U_{T_t} - y_{T_t}}{U_{T_t} - T_{T_t}}\right)^r$ ranges from zero to one. r is the weight that defines the functional form of the desirability function; if $r = 1$, the desirability function is linear, as shown in Figure 3.6b. U_{T_t} and T_{T_t} are the upper bound and target of the response (T_t), respectively.

Likewise, if the goal for the response is to achieve a specific target (e.g. trip mean trip time for the network y_{t_m} is set to a target value T_{t_m}), the two-sided individual desirability is defined as follows:

$$d_{t_m} = \begin{cases} 0 & y_{t_m} < L_{t_m} \\ \left(\frac{y_{t_m} - L_{t_m}}{T_{t_m} - L_{t_m}}\right)^{r_1} & L_{t_m} \le y_{t_m} \le T_{t_m} \\ \left(\frac{U_{t_m} - y_{t_m}}{U_{t_m} - T_{t_m}}\right)^{r_2} & T_{t_m} \le y_{t_m} \le U_{t_m} \\ 0 & y_{t_m} > U_{t_m} \end{cases} \tag{3.8}$$

Where, the values of $\left(\frac{y_{t_m} - L_{t_m}}{T_{t_m} - L_{t_m}}\right)^{r_1}$ and $\left(\frac{U_{t_m} - y_{t_m}}{U_{t_m} - T_{t_m}}\right)^{r_2}$ range from zero to one. r_1 and r_2 are the desirability function weights (if r_1 = r_2 = 1, the desirability function is linear, as shown in Figure 3.6c, L_{t_m}, U_{t_m} , and T_{t_m} are the lower bound, upper bound and target values of the response (t_m), respectively.

It is important to note that in this research, the goal for a specific target value of any response is not used. The goals of maximizing the response (N_{bus}) and minimizing the responses (T_t, and t_m) are used.

The weights of the desirability function (r_1, r_2, and r) define the shape of the individual desirability function as shown in Figure 3.6. Choosing $r > 1$ places more emphasis on being close to the target value of the response and choosing $0 < r < 1$ makes this less important (Myers et al., 2009).

In summary, in maximizing a response, the desirability value increases as response values increase from the lower limit to the target, and it becomes one for all values at or above the set target. In minimizing a response, the desirability is one for all response values less than or equal to the target. If the goal is a specific target, then the desirability is one and only one at the target value, and it decreases as the response deviates more from the target in either direction. In conclusion, desirability is an objective function, which ranges from zero outside of the limits to one at the goal. The features of the goal can be modified by adjusting the weight and/or importance parameters.

For multiple responses and factors, all goals get united into composite a desirability function. It is worth noting that always trying to get a very high desirability value is not useful, as the value is completely dependent on how closely the lower and upper limits are set relative to the actual best set of conditions (Design-Expert, 2015). Rather, the goal of optimization is to find the best set of conditions for satisfying all the goals. That is, in this study, the aim is to find the best set parameters β^{V}, β^{b}or β^{p}, and β^{B} that maximize N_{bus} and to simultaneously minimize both T_t and t_m, regardless of the achieved composite desirability index. Achieving a maximum composite desirability index by itself is not the study objective.

3.6 Response Surface Modeling in Minitab

The steps of Response Surface Modelling design, data importing, model building for each response, and the optimization in Minitab are explained in Appendix A. First, it depicts the Response Surface Modelling design (Appendix A.1.1). Second, it shows the steps for building the RSM model for the responses, the analyses of the model terms (interactions between the factors and their squares) to identify the significant terms, as described in details in Appendix A.1.2. Finally, it depicts the steps of optimization of the responses considering the objective function(s) described in details in Appendix A.1.3.

Chapter 4: Experimental Models Setup, Data Generation, and Model Building Process

This chapter summarizes simulation experimental setup for the integrated control system described in the previous chapter with the various signal control types (Split Actuated, Dual Actuated, and Protected Actuated). The network topologies together with the different traffic demand levels used for testing are described. The well-known TSIS-CORSIM (TSIS-CORSIM, 2010) is used for the simulation. The results of the simulation are then used, by Minitab® (Minitab, 2016), for the Response Surface modeling and optimization of the previously described coefficients. The data generation and the RSM building processes are also described briefly.

4.1 Experimental Traffic Network

A grid-type network of 49 intersections is used in this study. Due to the extensive set of simulation-based runs and the corresponding RSM optimization in this study, it is decided to focus the scope of this research on networks exhibiting high to very high traffic volume levels.

The network consists of one short link (i.e. 300 m) and one long link (i.e. 600 m) side by side, on alternatively in both vertical and horizontal dimensions, as shown in Figure 4.1. This is a typical grid network with a mix of non-uniform link lengths (next to each other). This network has seven (7) horizontal and seven (7) vertical arterials and the origin (O) and destination (D) are chosen from the Eastern, Western, Northern and Southern boundary link entrances and exits, respectively. In this network, there are 49 intersections and each intersection has four approach links (from the East, West, North, and South) and four exit links with three continuous lanes (all over the link length) and two additional left-turn lanes with 80 m storage length each.

The network has seven origins and destinations at each of the four boundary sides as shown in Figure 4.1.

The adopted “car” trip distribution for any demand case is as follows: From any origin j on the Eastern boundary (O_{Ej}), 60% of the total originated trips are split equally among the destinations on the Western boundary (i.e. D_{W1} to D_{W7}). Furthermore, 20% of the total originated trips are split equally among the destinations on the Northern boundary (i.e. D_{N1} to D_{N7}). Finally, the remaining 20% of the total originated trips are split equally among the destinations on the Southern boundary (i.e. D_{S1} to D_{S7}). Similar directional distributions are followed for any origin j on the Western (O_{wj}), Northern (O_{Nj}) and Southern (O_{Sj}) boundaries.

Two different levels of traffic demand are configured based on the origin nodes traffic volumes and the characteristics of the bus routes. The adopted traffic demand conditions or cases are shown in Table 4.1. The demand cases of “E” and “F” correspond to the high and very high car traffic volume of 1000 and 1500 per hour, respectively. For the demand cases of “E”, from any origin j along the Eastern (O_{Ej}) or Western (O_{wj}) or Northern (O_{Nj}) or Southern (O_{Sj}) boundaries, the hourly traffic volume is set as 1000 cars/hour. Therefore, the network demand for cars is 28,000 per hour (or 42,000 per the analysis period of 1.5 hours). For the demand cases of “F”, from any origin j along the Eastern (O_{Ej}) or Western (O_{wj}) or Northern (O_{Nj}) or Southern (O_{Sj}) boundaries, the hourly traffic volume is set as 1,500 cars/hour. Therefore, the network demand for cars is 42,000 per hour (or 63,000 per the analysis period of 1.5 hours). The demand cases “E” and demand cases “F” are tested with the mean headway along the bus routes is 10 minutes and 5 minutes, respectively. Both demand cases are tested with the maximum green time (of any individual phase or phase set) of 45 seconds.

Table 4.1:Different Traffic Demand Case Scenarios

Demand Case	***Car Demands (Cars/hour)***				***Network Demand (Cars/1.5 hours) as offered load***	***Mean Bus Headway (in Minutes) for all Routes***	***Maximum Green time for Phase/Phase Set (Seconds)***
	Eastern (O_{Ej})	**Western (O_{wj})**	**Northern (O_{Nj})**	**Southern (O_{Sj})**			
E	1000	1000	1000	1000	42000	10	45
F	1500	1500	1500	1500	63000	5	45

As indicated in Figure 4.2, a fixed bus route network comprising 18 directional routes are introduced for the two demand case scenarios (Ahmed and Hawas, 2015). The devised integrated logic allows bus priority in grid networks in cross directions not only along specific arterials and bus routes operate with uniform headways. According to the demand of the car trips, proportionate levels of bus trip headway and bus occupancy are considered. The origins and destinations on the Eastern and Western boundaries are considered, as the bus flow directions shown in Figure 4.2. Some of the bus routes overlap on some of the links and some intersections have both left- and right-turning bus trips on their associated approach links.

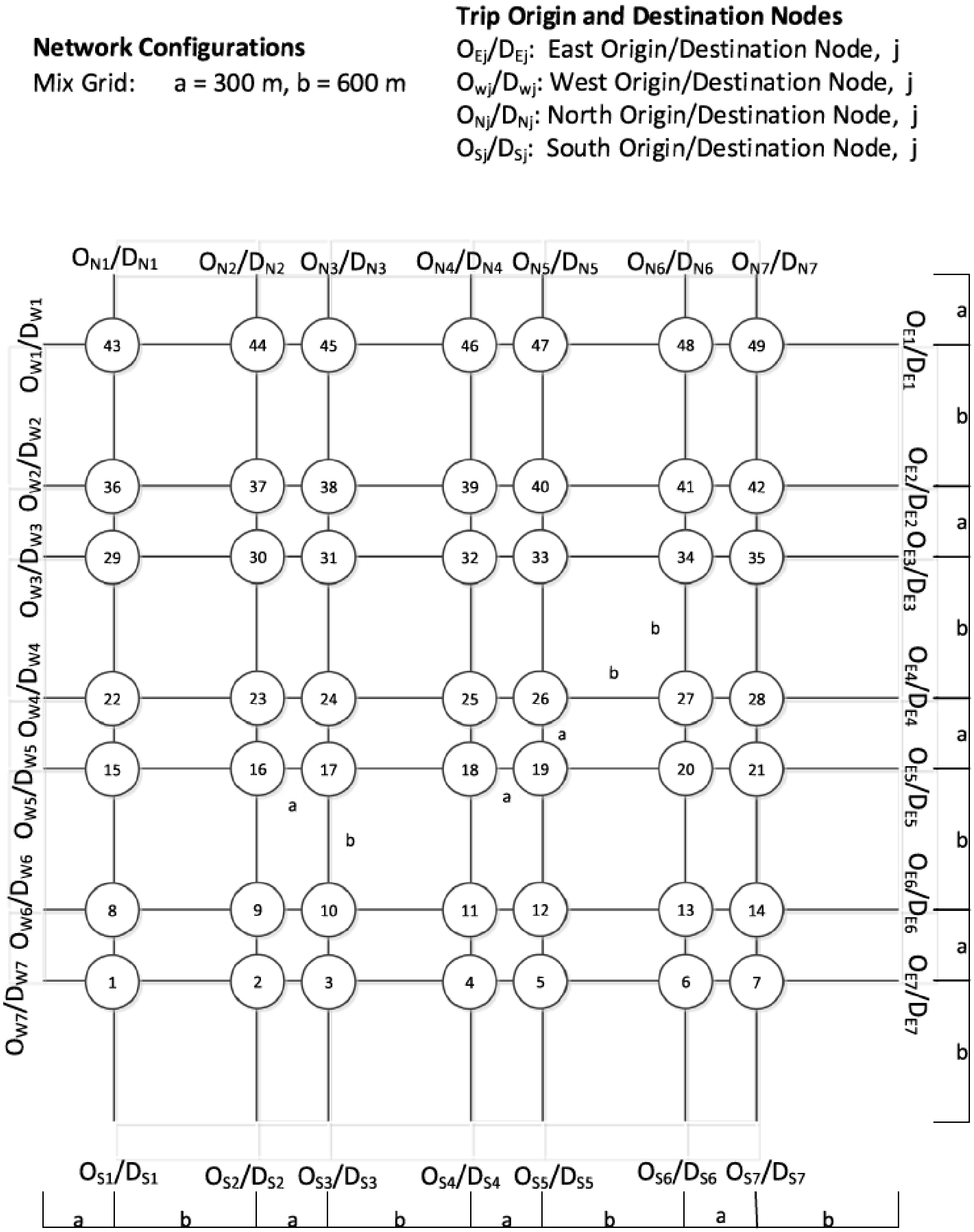

Figure 4.1: Layout of hypothetical test bed network (Ahmed and Hawas, 2015)

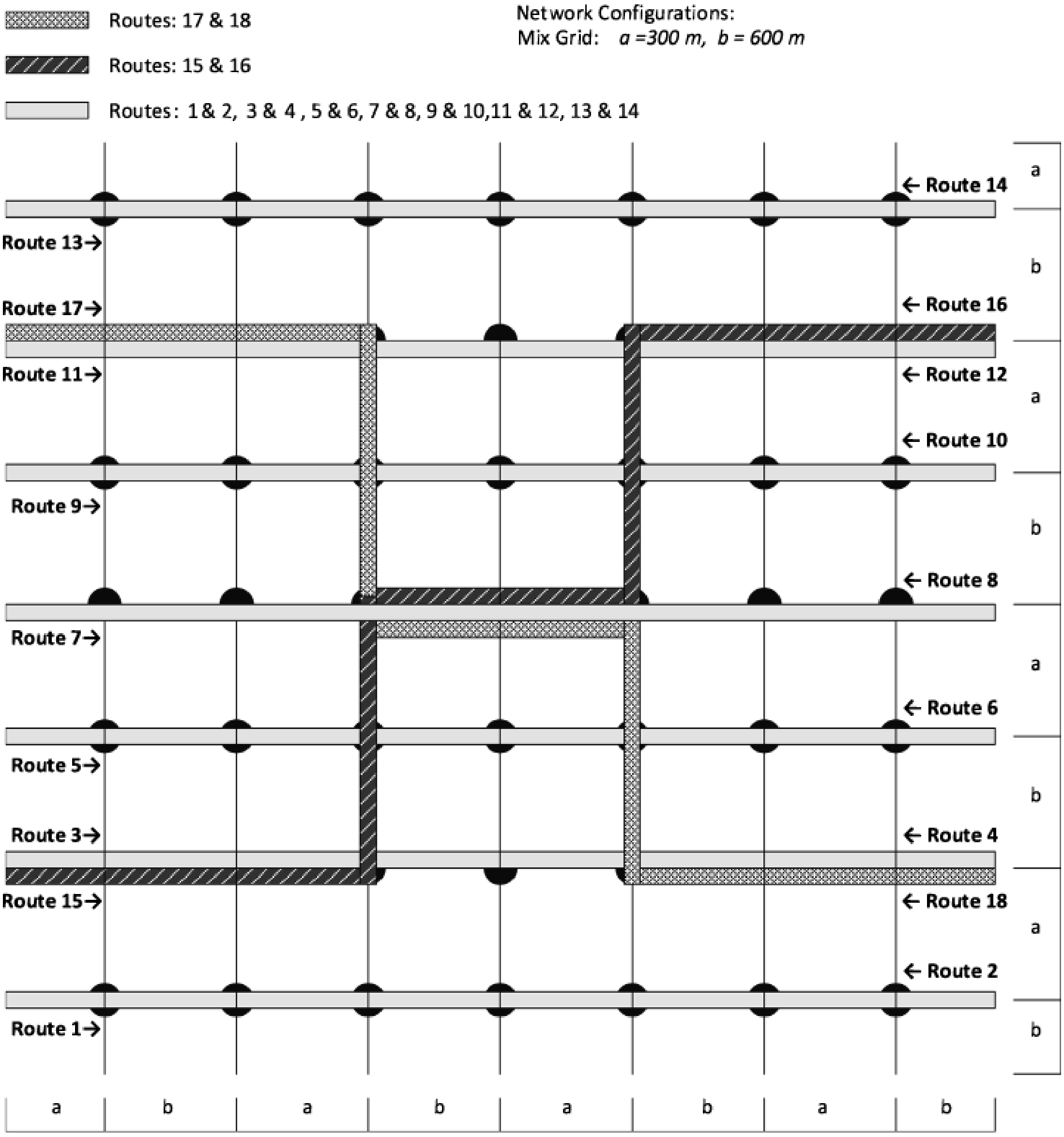

Figure 4.2: Layout of bus route network (Ahmed and Hawas, 2015)

4.2 Data Generation Process

This section describes the steps of simulation-based data generation using the TSIS-CORSIM model:

1. Selection of the input variables levels range. A range is set for each value of β^V, β^b or β^p, and β^B.

2. Designing the Response Surface Model (RSM) in Minitab for the selected variables; details are provided in the Appendix A.

3. For each combination of β^V, β^b or β^p, and β^B the simulation model is run for ten times (10) using different seeds. A folder is then created for each case according to the RSM design.

4. Executing the Simulation model using TSIS-CORSIM. The various coefficients of β^V, β^b or β^p, and β^B are modified in Visual Studio according to the case's coefficients.

5. Extracting the MOE's (response variables) from the simulation; the total number of bus trips, the network total travel time (in hours), and the trip's mean travel time (in seconds).

6. Importing the response variables to Excel to estimate the MOE average response from the ten runs of each case.

7. Importing the Excel data to Minitab to model each response for the input variables; details are provided in Appendix A.

8. Optimizing the Response Surface Model for each response; details are provided in Appendix A.

9. Interpreting the results and model analysis (based on the model significance and boundary values of the coefficients).

4.3 Model Building Process

An important step in RSM is to perform a displacement to the variables β^V, β^b or β^p, and β^B (change in the region) in the direction to the optimal region (Bezerra et al., 2008). The steepest ascent method is commonly used to decide on the direction of displacement (Myers et al., 2009). In this research study, this was not followed in this calibration process of the RSM. The reason is that downstream blockage penalty coefficient (β^B) was found to be insignificant in most of the studied cases. Furthermore, the steepest ascent method requires the fitting of a first-order (linear) model with the factors (Myers et al., 2009).

In this research study, the regions of the factors for the first model are initially chosen arbitrarily, yet guided by the preliminary findings of Ahmed and Hawas (2015), whom used a simplified Brute-Force search to identify the optimal coefficient values. The earlier study (Ahmed and Hawas, 2015) however was limited in the sense that it used a Brute-Force sequential process to identify the best value of one parameter at a time, while all others are kept fixed. This earlier approach could also lead to local (not global) optimal solutions, keeping in mind that the optimal values are strongly affected by the initial values of the parameters. Furthermore, deploying a Brute-Force search method was very time consuming and did not allow for verification of global optimal solution nor for model calibration of responses vis-à-vis the control parameters β^V, β^b or β^p, and β^B.

To overcome these limitations, the RSM is used to allow full consideration of interactions among the control parameters and to insure obtaining global optimal solutions. The findings of Ahmed and Hawas (2015) were used to specify the initial control parameter regions. The establishment of the RSM followed an iterative smart guided search. The initial control parameters were used to develop RSM. The "learning" from the established relationships of the first model were then used to specify (modify) the region of the control parameters, and as such developing a second RSM. The analysis of the 2nd model was then used to modify as needed the parameters' ranges as needed. The later models are processed similarly considering the output of contour plot from the data of previous models. When the established model satisfies the objective functions properly (maximizing the network bus trips and simultaneously minimizing the network travel time and the trip mean travel time), the model is thoroughly analyzed, and then verification stage is carried out to validate the results from the model. Chapter 5 and Appendix A illustrate the process of model building through a step-by-step example.

Chapter 5: RSM Results and Analyses under the High Traffic (E) Demand Scenario

This chapter summarizes the results and the analyses of the optimization of the calibrated RSM on the coefficients for the integrated control system described in Chapter 3 for the various control types (Split Actuated, Protected Actuated, and Dual Actuated) under the demand scenario designated as (E) and the associated network topology. The (E) letter herein refers to the traffic demand scenarios of “high” traffic volume as explained earlier in more details in Chapter 4.

This chapter is divided into three subsections to demonstrate the results and analyses for the Split Actuated control, followed by the ones for the Protected Actuated control, and finally for the Dual Actuated control.

5.1 Split Actuated Control

The outputs for the Split Actuated control system are presented in Table 5.1 for nine (9) RSM models, as discussed in Chapter 3 and Appendix A in details. Table 5.1 summarizes the input variable ranges, the optimal settings, and the resulting composite desirability. The optimization results of the nine models are plotted in Figure 5.1 to Figure 5.9 for the three input parameters of coefficient for virtual queue of vehicles, β^V (BQL), coefficient for transit priority, $\beta^b or\ \beta^p$ (BTP), and downstream blockage penalty coefficient, β^B (BDC), as well as the three responses of the total bus trips, N_{bus} $(Trips)$, total network travel time, T_t (TTT), and the trip average travel time, t_m (MTT).

Table 5.1: Optimal values of split actuated control under “E” demand scenario

Model NO.	Factor ranges			Optimal factor settings (β^V, β^bor β^p, β^B)	Composite Desirability, D
	β^V (BQL)	β^bor β^p (BTP)	β^B (BDC)		
1	-1000 – 15000	-2000 – 10000	-5 – 25	3040, -2000, 10	0.629
2	2500 – 25000	1500 – 15000	-10 – 20	25000, 10363, -10	0.526
3	1000 – 25000	5000 – 20000	-7 – 20	1000, 5000, -2.9	0.610
4	500 – 5500	1000 – 19000	1 – 19	2924, 1000, 1	0.619
5*	100 – 3500	9000 – 15000	5 – 15	100, 15000, 15	0.933
6	2 – 200	2000 – 22000	2 – 20	2, 22000, 20	0.745
7	2 – 200	1000 – 19000	1 – 19	2, 19000, 19	0.901
8	2 – 200	500 – 15500	1 – 9	2, 14742, 1	0.863
9	100 – 3000	1000 – 8000	1 – 5	100, 1000, 1	0.626

* Little variation in responses and the models are not significant.

Figures 5.1 and 5.2 illustrate the optimization plots for models 1 and 2 considering the three input parameters and the three responses. The composite desirability of models 1 and 2 are 0.629 and 0.526, respectively. Only the 1st model considered possible negative values for BQL and BTP coefficients. It is worth noting that when such negative values are used simultaneously (for the coefficients of BQL and BTP in model 1), the resulting $Trips$ are very low (almost zero), and as such, no further negative values were used anymore in other models.

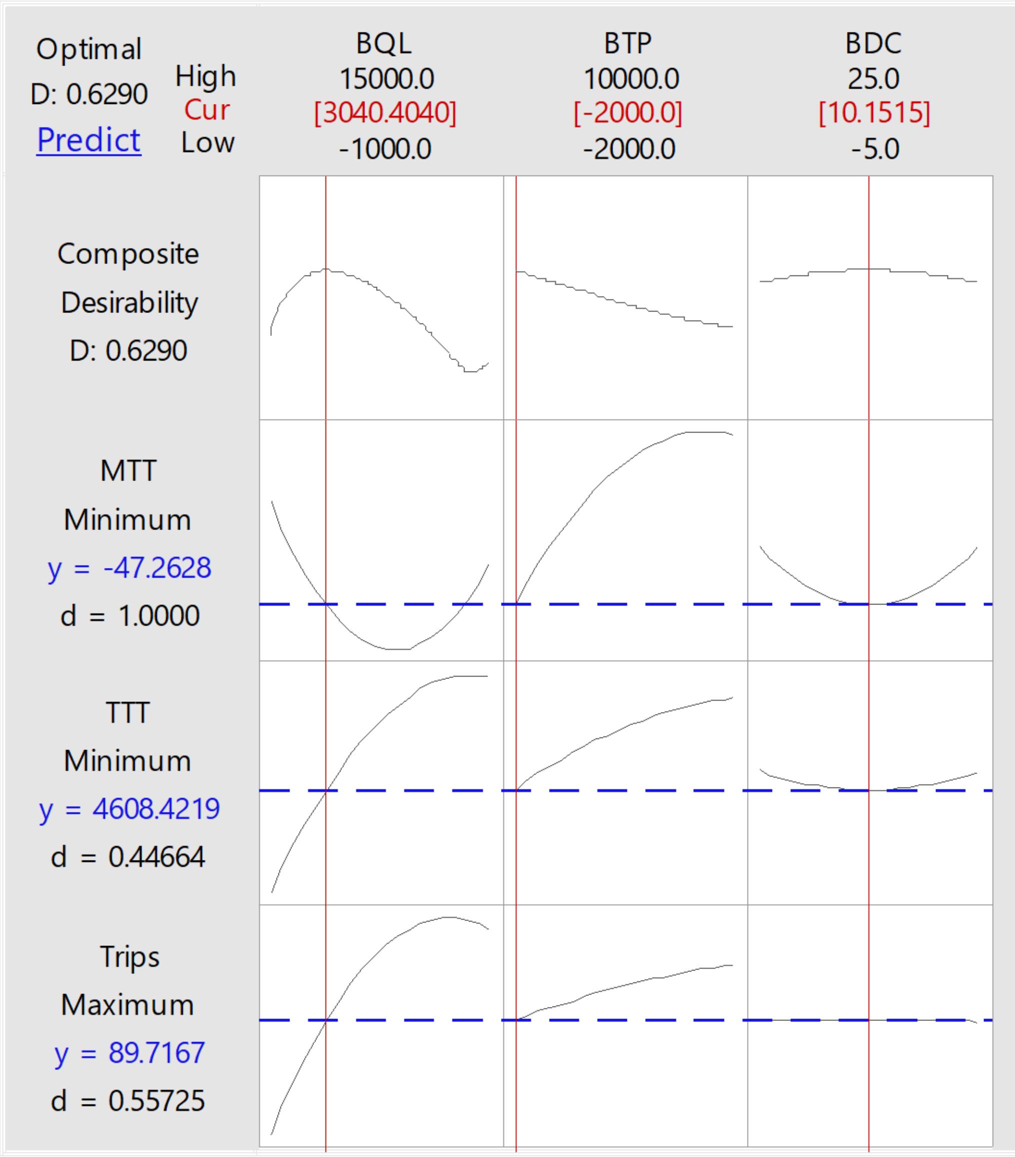

Figure 5.1: Model 1 individual and composite desirability D for the responses of N_{bus} $(Trips)$, T_t (TTT) and t_m (MTT) for various parameters of β^V (BQL), β^bor β^p (BTP), and β^B (BDC), for split actuated control under "E" demand scenario

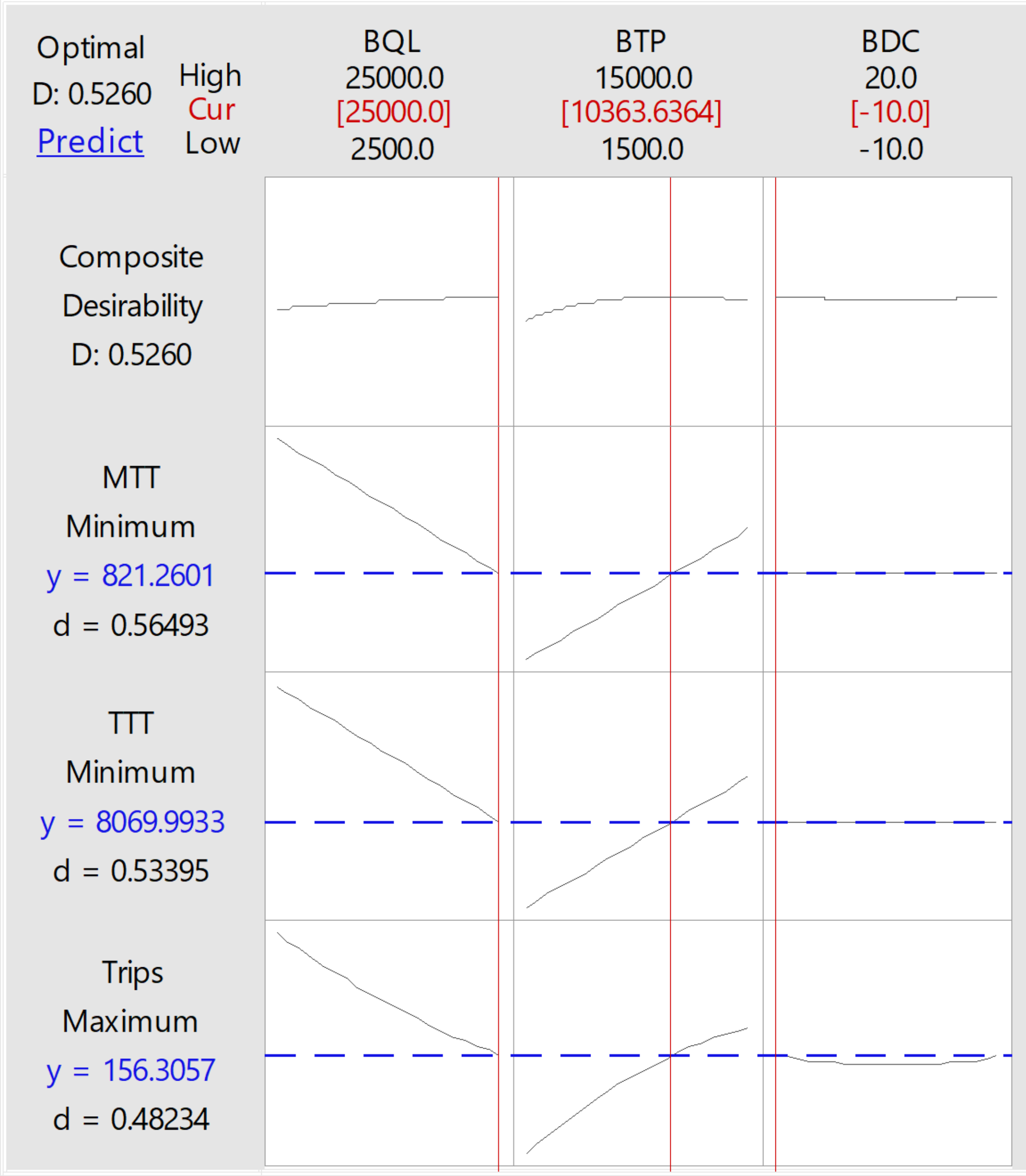

Figure 5.2: Model 2 individual and composite desirability D for the responses of N_{bus} $(Trips)$, T_t (TTT) and t_m (MTT) for various parameters of β^V (BQL), β^bor β^p (BTP), and β^B (BDC), for split actuated control under "E" demand scenario

Figures 5.3, 5.4, 5.5 and 5.6 illustrate the optimization plots for models 3, 4, 5 and 6. The composite desirability values of these models are 0.61, 0.62, 0.93, and 0.75, respectively.

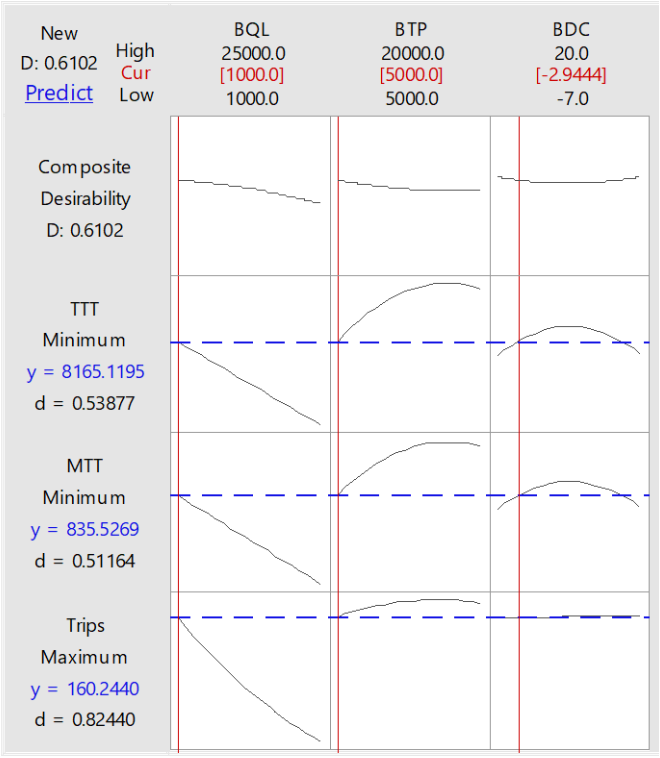

Figure 5.3: Model 3 individual and composite desirability D for the responses of N_{bus} $(Trips)$, T_t (TTT) and t_m (MTT) for various parameters of β^V (BQL), β^bor β^p (BTP), and β^B (BDC), for split actuated control under "E" demand scenario

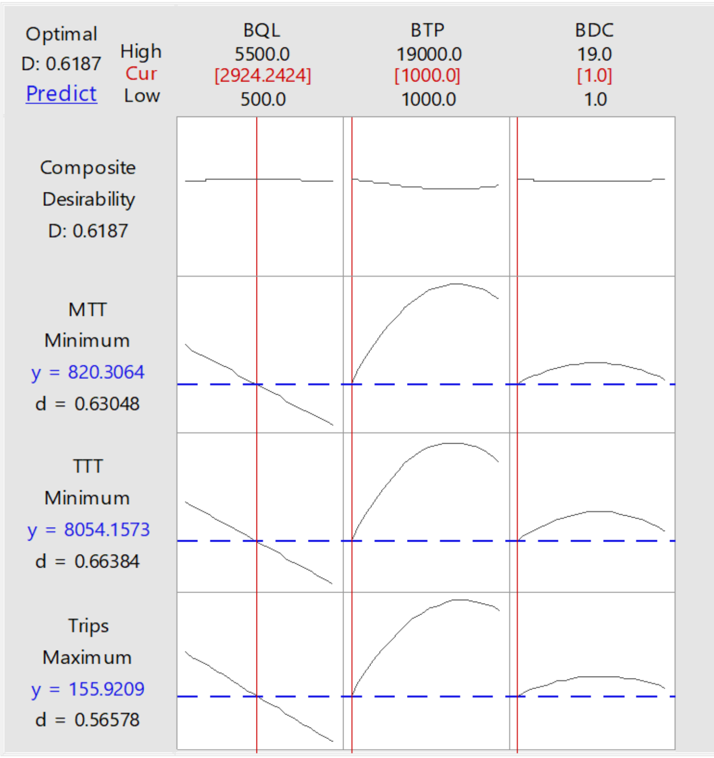

Figure 5.4: Model 4 individual and composite desirability D for the responses of N_{bus} $(Trips)$, T_t (TTT) and t_m (MTT) for various parameters of β^V (BQL), β^bor β^p (BTP), and β^B (BDC), for split actuated control under "E" demand scenario

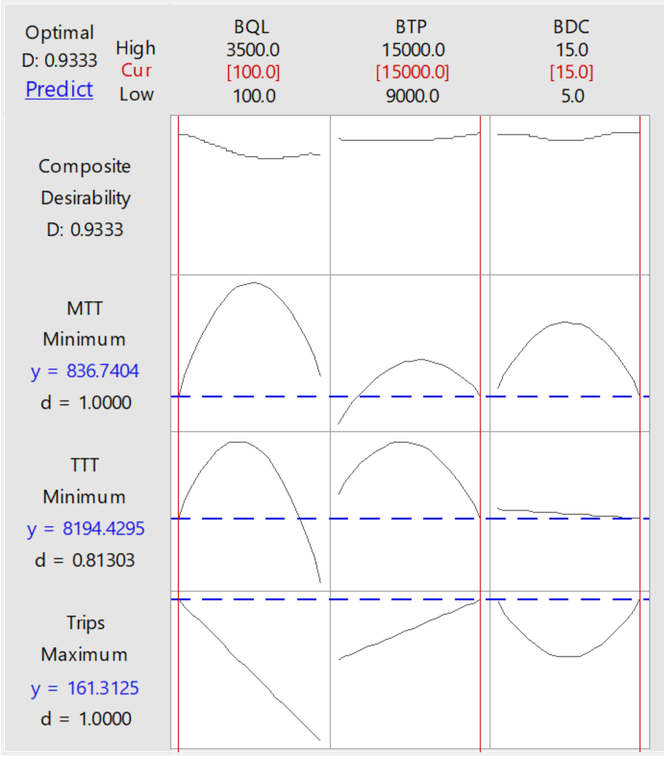

Figure 5.5: Model 5 individual and composite desirability D for the responses of N_{bus} $(Trips)$, T_t (TTT) and t_m (MTT) for various parameters of β^V (BQL), β^bor β^p (BTP), and β^B (BDC), for split actuated control under "E" demand scenario

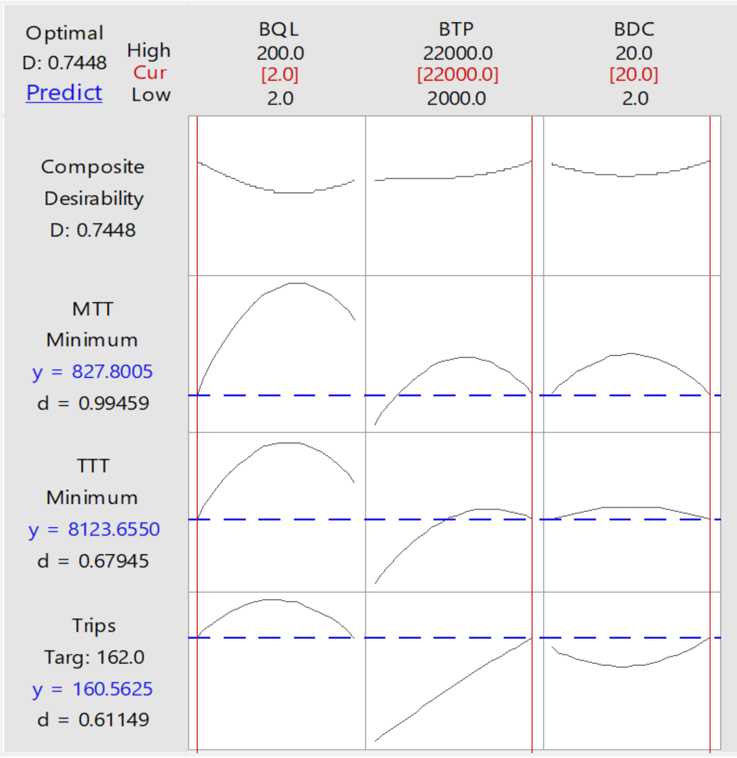

Figure 5.6: Model 6 individual and composite desirability D for the responses of N_{bus} $(Trips)$, T_t (TTT) and t_m (MTT) for various parameters of β^V (BQL), β^bor β^p (BTP), and β^B (BDC), for split actuated control under "E" demand scenario

Figures 5.7, 5.8, and 5.9 illustrate the optimization plots for models 7, 8 and 9. The composite desirability values of these models are 0.90, 0.86, and 0.63, respectively.

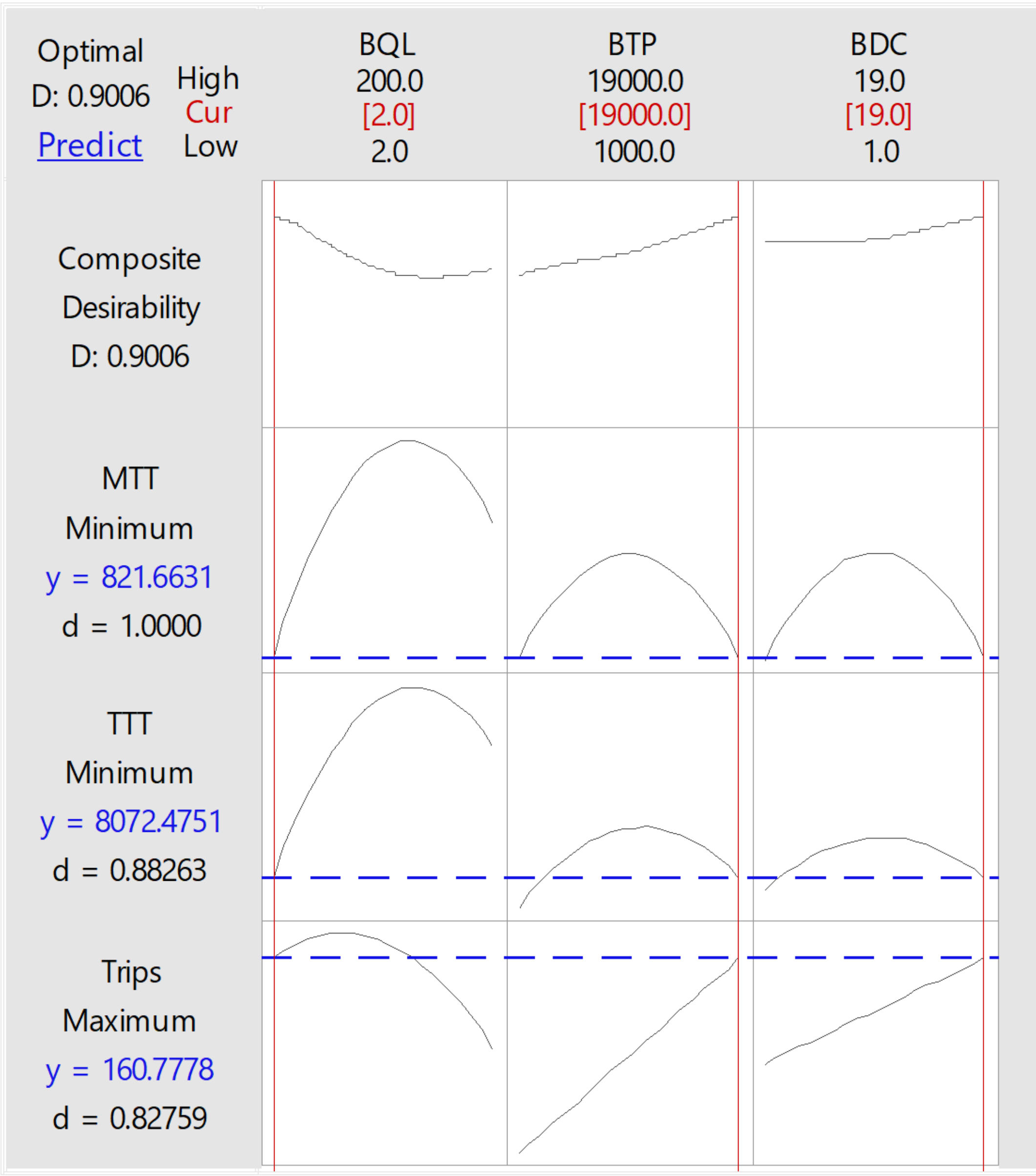

Figure 5.7: Model 7 individual and composite desirability D for the responses of N_{bus} $(Trips)$, T_t (TTT) and t_m (MTT) for various parameters of β^V (BQL), β^bor β^p (BTP), and β^B (BDC), for split actuated control under "E" demand scenario

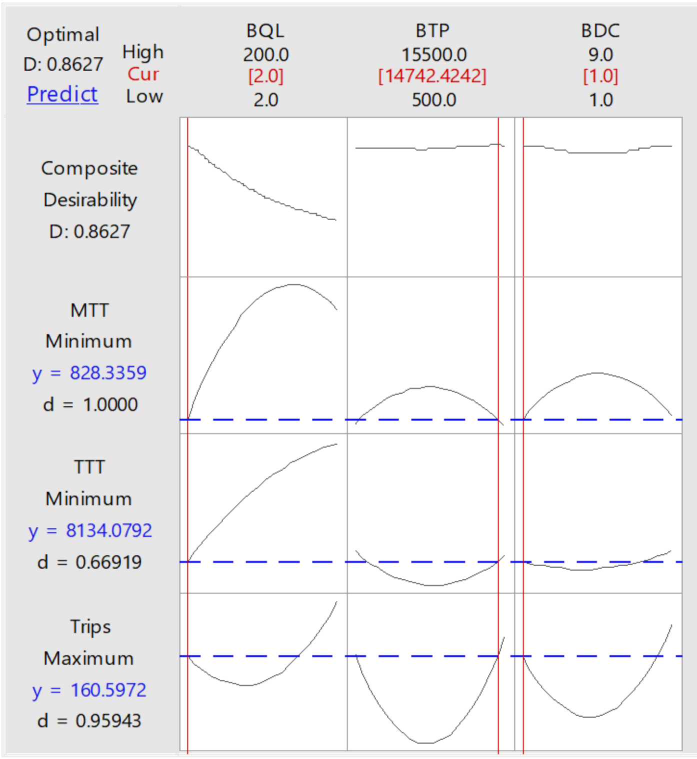

Figure 5.8: Model 8 individual and composite desirability D for the responses of N_{bus} $(Trips)$, T_t (TTT) and t_m (MTT) for various parameters of β^V (BQL), β^bor β^p (BTP), and β^B (BDC), for split actuated control under "E" demand scenario

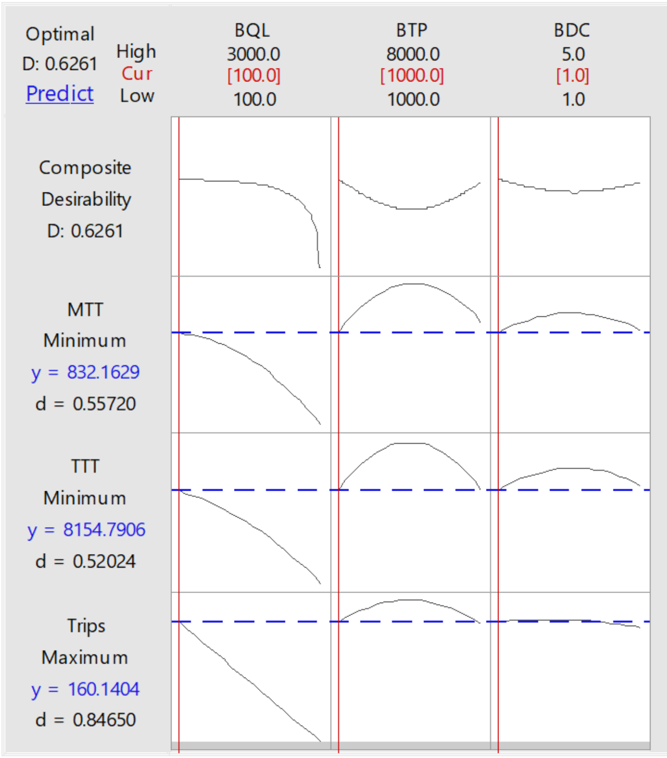

Figure 5.9: Model 9 individual and composite desirability D for the responses of N_{bus} $(Trips)$, T_t (TTT) and t_m (MTT) for various parameters of β^V (BQL), β^bor β^p (BTP), and β^B (BDC), for split actuated control under "E" demand scenario

A contour plot was developed for the three responses of N_{bus} *(*Trips*)*, T_t *(*TTT*) and* t_m *(*MTT*)* for various parameters of β^V *(*BQL*)*, β^b or β^p *(*BTP*), and* β^B *(*BDC*) as* shown in Figure 5.10. The data for the contour plot was taken from a total of 135 input variable settings (data of models 1 to 9). These variant input settings correspond to a total of 1350 simulation runs, as each parameter setting is executed for 10 multiple runs.

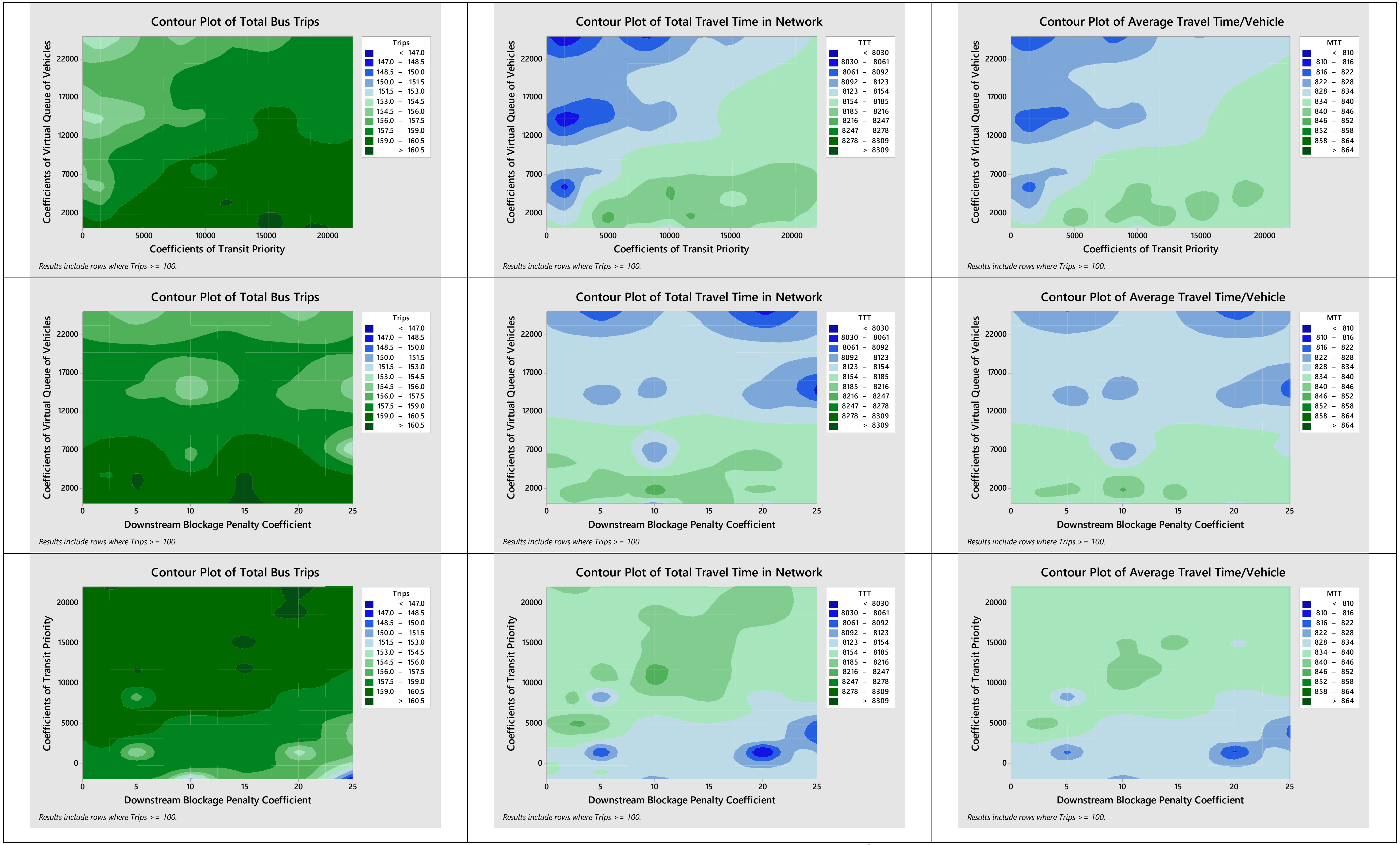

Figure 5.10: Contour plot of the three responses of N_{bus} $(Trips)$, T_t (TTT) and t_m (MTT) for various parameters of β^V (BQL), β^bor β^p (BTP), and β^B (BDC) for split actuated control and demand case "E"

5.1.1 Analysis

None of the above models resulted in acceptable desirability levels (within the model input range) using the set three objective functions (maximizing of N_{bus} ($Trips$), while simultaneously minimizing both T_t (TTT) and t_m (MTT)). The optimum values of the coefficients are mostly border values (upper bound or lower bound of the specified regions). Furthermore, the variability of the responses is very little, for instance N_{bus} ($Trips$) are 150 – 160, T_t (TTT) is 8000 – 8300 hours and t_m (MTT) is 810 – 860 seconds.

Further analysis is done for the all the models using only either double or single objective function(s). The conducted analyses still led to optimal solutions at the borders of the parameter regions. Only model 9 has shown good performance, and it is discussed hereafter.

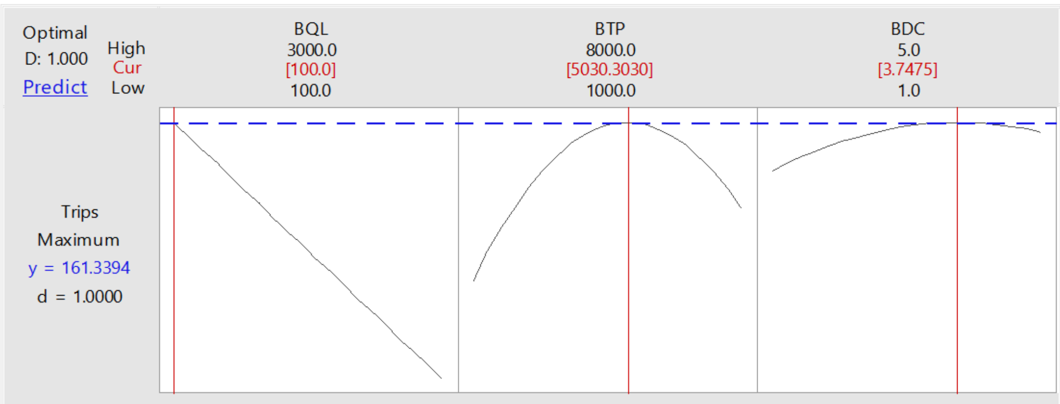

Figure 5.11: Optimization of N_{bus} ($Trips$) for various parameters of β^V (BQL), β^bor β^p (BTP), and β^B (BDC), for split actuated control under "E" demand scenario

First, the optimization is done only using one objective function (maximizing of N_{bus} ($Trips$)) as shown in Figure 5.11. The resulting optimal variable setting is presented in Table 5.2. This setting is 100, 5030, and 3.75 for the β^V (BQL), β^bor β^p

(BTP), and β^B (BDC), respectively, with the response N_{bus} $(Trips)$ of 161.34, and 0.291 (95% CI = 160.7, 162.1) standard error (SE).

Table 5.2: Optimal variable setting of coefficients for the response of N_{bus} $(Trips)$ for split actuated control with demand case "E"

Coefficients			**Responses**	
β^V (BQL)	β^b or β^p (BTP)	β^B (BDC)	N_{bus} $(Trips)$	SE (95% CI)
100	5030	3.75	161.339	0.291 (160.7, 162.1)

The optimization is done afterward considering two objective functions (maximizing of N_{bus} $(Trips)$, while simultaneously minimizing t_m (MTT)), as shown in Figure 5.12. The resulting optimal parameter setting is presented in Table 5.3. This setting is 305, 1000, and 2.91 for β^V (BQL), β^b or β^p (BTP), and β^B (BDC), respectively. The optimal responses are 159.9 for N_{bus} $(Trips)$ with a standard error (SE) of 0.4 (95% CI = 159, 160.8) and 834.7 seconds for t_m (MTT) with a standard error (SE) of 3.4 (95% CI = 827.0, 842.4).

Table 5.3: Optimal variable setting of coefficients for the responses of N_{bus} $(Trips)$ and t_m (MTT) for split actuated control with demand case "E"

Coefficients			**Responses**			
β^V (BQL)	β^b or β^p (BTP)	β^B (BDC)	N_{bus} $(Trips)$	SE (95% CI)	t_m (MTT) (seconds)	SE (95% CI)
305	1000	2.1	159.9	0.4 (159, 160.8)	834.71	3.4 (827.0, 842.4)

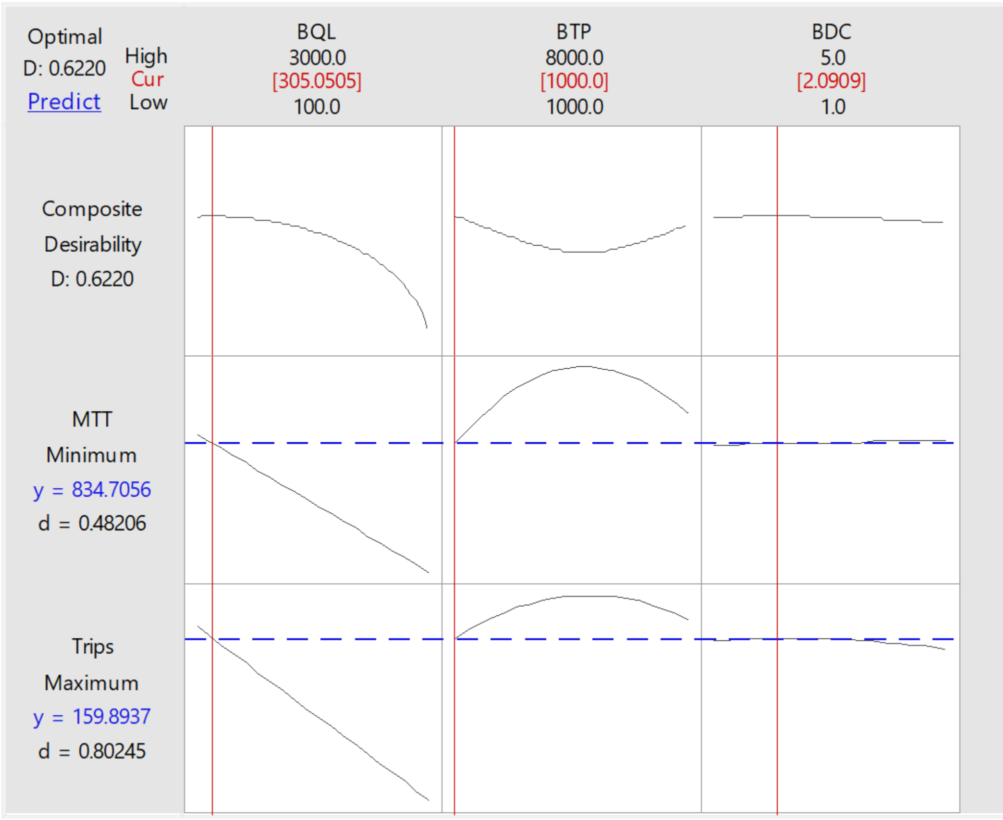

Figure 5.12: Optimization of N_{bus} $(Trips)$, and t_m (MTT) for various parameters of β^V (BQL), β^bor β^p (BTP), and β^B (BDC), for split actuated control under "E" demand scenario

RSM Statistics (ANOVA table)

Regardless of the number and nature of used objective function(s) to identify the optimal setting (single, dual or triple), the model itself is the same. Only the optimal settings vary according to the preset objective function(s). For the 9th model (with design explained in Table 5.1), the response surface model of N_{bus} $(Trips)$ is significant (R-square = 94.56%), as p-value for each parameter is less than 0.01, as shown in Table 5.4. Only β^B (BDC) is not significant with a p-value greater than 0.1. There is a supporting evidence that there is little variation with different values of β^B (BDC) as shown in the contour plots of Figure 5.10. This may be attributed to the prevailing traffic conditions under the E demand level, as the downstream approaches may not likely to be flagged as congested (the necessary condition to apply the downstream congestion adjustment as explained in Chapter 2- Equation 2.3).

Table 5.4: Summary of ANOVA for N_{bus} $(Trips)$ versus various β^V (BQL), β^bor β^p (BTP), and β^B (BDC) for split actuated control of "E" demand scenario

Source		Sum of Squares	df	Mean Square	F
Linear		27.2125	3	9.0708	39**
	β^V	10.58	1	10.58	45.49**
	β^p	16.5312	1	16.5312	71.07**
	β^B	0.1013	1	0.1013	0.44*
Square	$\beta^p * \beta^p$	2.8934	1	2.8934	12.44**
2-Way Interaction	$\beta^V * \beta^p$	6.25	1	6.25	26.87**
Lack-of-Fit		2.0467	7	0.2924	12.53*
Total		38.4493	14		

*p > 0.1
**p < 0.1

The second order regression equation of N_{bus} $(Trips)$ versus β^V (BQL), β^bor β^p (BTP), and β^B (BDC) is:

N_{bus} $(Trips)$ (Split Actuated Control under "E" Demand Scenario)

$$= 159.518 - 0.001901\,\beta^V + 0.000676\,\beta^p + 0.0563\,\beta^B$$

$$- 0.0000001\beta^p * \beta^p + 0.0000001\beta^V * \beta^p$$

Additionally, the response model of t_m (MTT) is significant (R-square = 80.94%), as p-value for each parameter is less than 0.1, as shown in Table 5.5. Only β^B (BDC) is not significant with a p-value greater than 0.1.

Table 5.5: Summary of ANOVA for t_m (MTT) versus various β^V (BQL), β^bor β^p (BTP), and β^B (BDC) for split actuated control of "E" demand scenario

Source		Sum of Squares	df	Mean Square	F
Linear		442.406	3	147.469	7.08**
	β^V	66.387	1	66.387	3.19**
	β^p	375.58	1	375.58	18.04**
	β^B	0.44	1	0.44	0.02*
Square	β^p*β^p	218.051	1	218.051	10.47**
2-Way Interaction	β^V*β^p	135.185	1	135.185	6.49**
Lack-of-Fit		145.159	7	20.737	0.98*
Total		983.01	14		

*p > 0.1
**p < 0.1

The second order regression equation of t_m (MTT) versus β^V (BQL), β^bor β^p (BTP), and β^B (BDC) is:

t_m (MTT) (Split Actuated Control under "E" Demand Scenario) (seconds)

$$= 831.12 - 0.00714\,\beta^V + 0.00580\,\beta^p + 0.117\,\beta^B$$

$$- 0.000001\,\beta^p * \beta^p + 0.000001\,\beta^V * \beta^p$$

Finally, the response model of T_t (TTT) is significant (R-square = 87.19%), as the p-value for each parameter is less than 0.1 shown in Table 5.6. Only β^B (BDC) is not significant with a p-value greater than 0.1.

Table 5.6: Summary of ANOVA for T_t (TTT) versus various β^V (BQL), β^bor β^p (BTP), and β^B (BDC) for split actuated control of "E" demand scenario

Source		**Sum of Squares**	**df**	**Mean Square**	**F**
Linear		18218.8	3	6072.9	7.87**
	β^V	3532.5	1	3532.5	4.58**
	β^p	14597.6	1	14597.6	18.93**
	β^B	88.6	1	88.6	0.11*
Square		16767.4	2	8383.7	10.87**
	$\beta^p * \beta^p$	15026.3	1	15026.3	19.48**
	$\beta^B * \beta^B$	2537.6	1	2537.6	3.29**
2-Way Interaction	$\beta^V * \beta^p$	6993.5	1	6993.5	9.07**
Lack-of-Fit		4224.9	6	704.1	0.72*
Total		48149.6	14		

*p > 0.1
**p < 0.1

The second order regression equation of T_t (TTT) versus β^V (BQL), β^bor β^p (BTP), and β^B (BDC) is:

T_t (TTT) (Split Actuated Control under "E" Demand Scenario) (hours) =

$$8093.3 - 0.0516\,\beta^V + 0.0462\ \beta^p + 40.9\,\beta^B$$

$$-\,0.000005\ \beta^p * \beta^p - 6.53\,\beta^B * \beta^B + 0.000008\,\beta^V * \beta^p$$

5.1.2 Optimum selection (model validation)

For different objective functions, different optimal settings are obtained. In specific, herein we refer to the optimum settings of the coefficients of β^V (BQL), β^bor β^p (BTP), and β^B (BDC) related to the solutions:

I. where only N_{bus} $(Trips)$ is maximized (as indicated in Table 5.2)

II. where N_{bus} $(Trips)$ is maximized and t_m (MTT) is minimized (as indicated in Table 5.3)

In order to select only one set of values to generalize its use with the split actuated controller under the E demand scenario, a verification/validation process is deployed. The validation process entails running the simulation with the identified values (in Tables 5.2 and 5.3). Each dataset was used in ten (10) multiple runs and the resulting responses were then averaged and reported as shown in Table 5.7. The resulting average N_{bus} $(Trips)$, t_m (MTT) and T_t (TTT) of the 10 simulation runs (as shown in Table 5.7) lie within the 95% confidence interval (corresponding values) extracted from the response surface model (as shown in Table 5.2 for variable setting I, and Table 5.3 for variable setting II).

The 2nd set of variables (II) (β^V $(BQL) = 305$, β^bor β^p $(BTP) = 1000$, and β^B (BDC)= 2.1) is selected as the default general setting of the split actuated controller under the demand case "E". The set results in higher values of N_{bus} $(Trips)$ and lesser values of t_m (MTT) and T_t (TTT) as shown in Table 5.7.

It is worth noting that the total network travel time T_t (TTT) was not explicitly used an optimization criterion in any of the above two solutions (I and II). Nonetheless, it is legitimate to say that T_t (TTT) was implicitly accounted in obtaining the optimal settings II; as it directly relates to the trip's average travel time, t_m (MTT) through the formula $\mathrm{t_m} = \frac{\mathrm{T_t}}{\mathrm{N_{trips}}} * 3600$, where $\mathrm{N_{trips}}$ is the total number of vehicles in the network. That is, explicit minimization of t_m (MTT) implies implicit minimization (not explicit) of T_t (TTT).

Table 5.7: Optimal variable settings of β^V (BQL), β^bor β^p (BTP), and β^B (BDC) and corresponding simulation-based MOE's (N_{bus} $(Trips)$, t_m (MTT) (seconds), T_t (TTT) (hours)) for split actuated control of "E" demand scenario

Variable Settings	Coefficients			Responses		
	β^V (BQL)	β^bor β^p (BTP)	β^B (BDC)	N_{bus} $(Trips)$	t_m (MTT) (seconds)	T_t (TTT) (hours)
I. (only N_{bus} $(Trips)$ is maximized)	100	5030	3.75	160.9	839.26	8205.25
II. (N_{bus} $(Trips)$ is maximized and t_m (MTT) is minimized)	305	1000	2.1	**161.0**	**838.26**	**8190.57**

5.2 Protected Actuated Control

The outputs for the Protected Actuated control system is presented in Table 5.8 for three (3) RSM models, as discussed in Chapter 3 and Appendix A in details. Table 5.8 summarizes the input variable ranges, the optimal variable setting, and the resulting composite desirability. The optimization results of the three models are plotted in Figure 5.13 to 5.15 for three input parameters of coefficient for virtual queue of vehicles, β^V (BQL), coefficient for transit priority, $\beta^b or\ \beta^p$ (BTP), and downstream blockage penalty coefficient, β^B (BDC), as well as the three responses of the total bus trips, N_{bus} $(Trips)$, total network travel time, T_t (TTT), and the trip average travel time, t_m (MTT).

Table 5.8: Optimal values of protected actuated control under "E" demand scenario

Model NO.	**Factor ranges**			**Optimal factor settings (β^V, β^bor β^p, β^B)**	**Composite Desirability, *D***
	β^V (BQL)	**β^bor β^p (BTP)**	**β^B (BDC)**		
1	2 – 3000	1000 – 15000	1 – 10	3000, 14434, 1	0.941
2	1000 – 6000	2000 – 20000	2 – 8	1000, 16545, 2	0.963
3	100 – 4000	3000 – 18000	3 – 6	4000, 18000, 3	0.916

Figure 5.13, 5.14, and 5.15 depict the optimization plots for models 1, 2, and 3 considering the three input parameters and the three responses. The composite desirability values of these models are 0.941, 0.963, and 0.916, respectively.

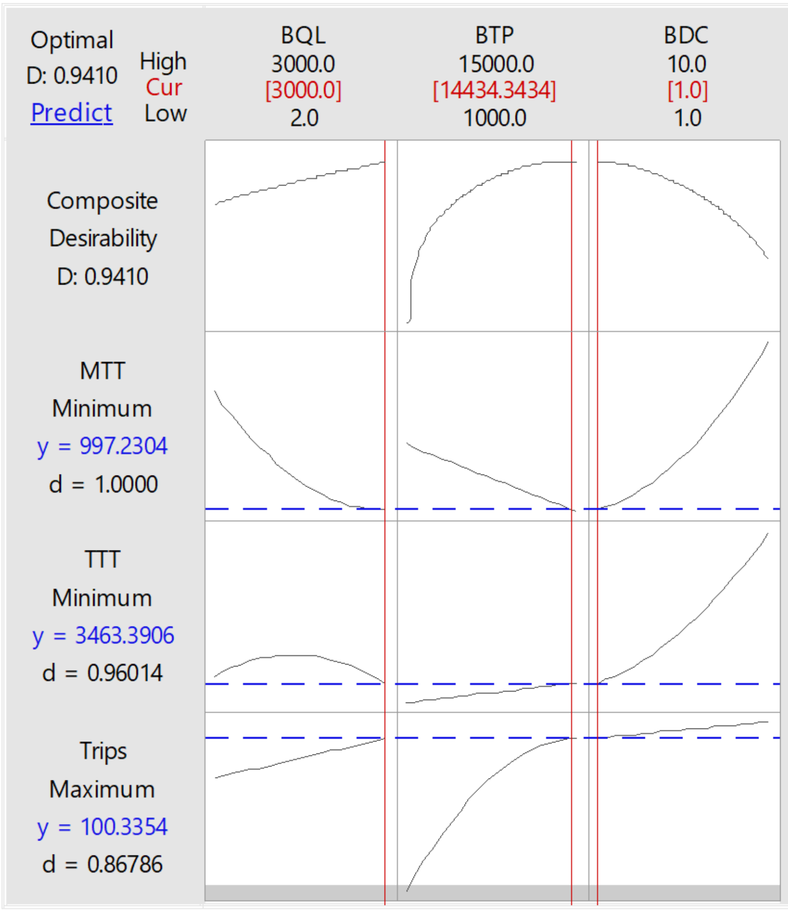

Figure 5.13: Model 1 individual and composite desirability D for the responses of N_{bus} $(Trips)$, T_t (TTT) and t_m (MTT) for various parameters of β^V (BQL), β^bor β^p (BTP), and β^B (BDC), for protected actuated control under "E" demand scenario

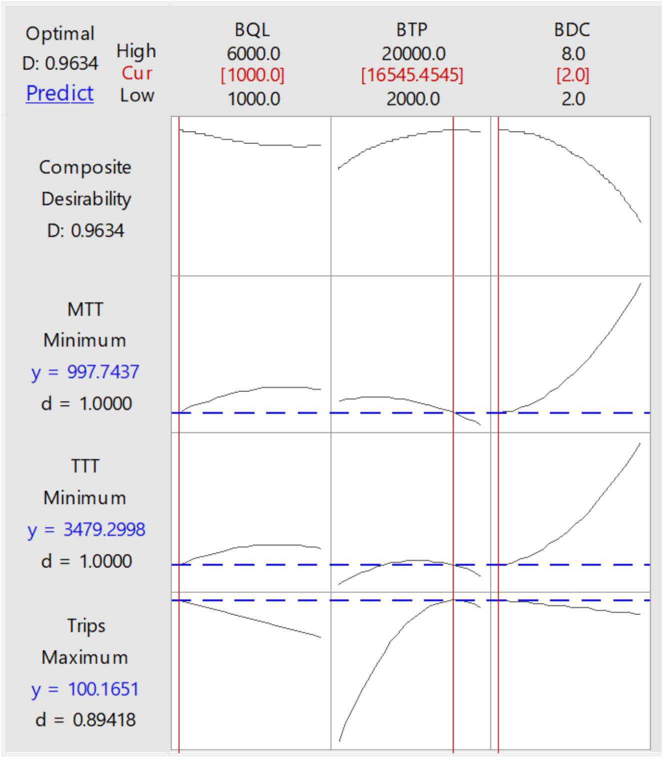

Figure 5.14: Model 2 individual and composite desirability D for the responses of N_{bus} $(Trips)$, T_t (TTT) and t_m (MTT) for various parameters of β^V (BQL), β^bor β^p (BTP), and β^B (BDC), for protected actuated control under “E” demand scenario

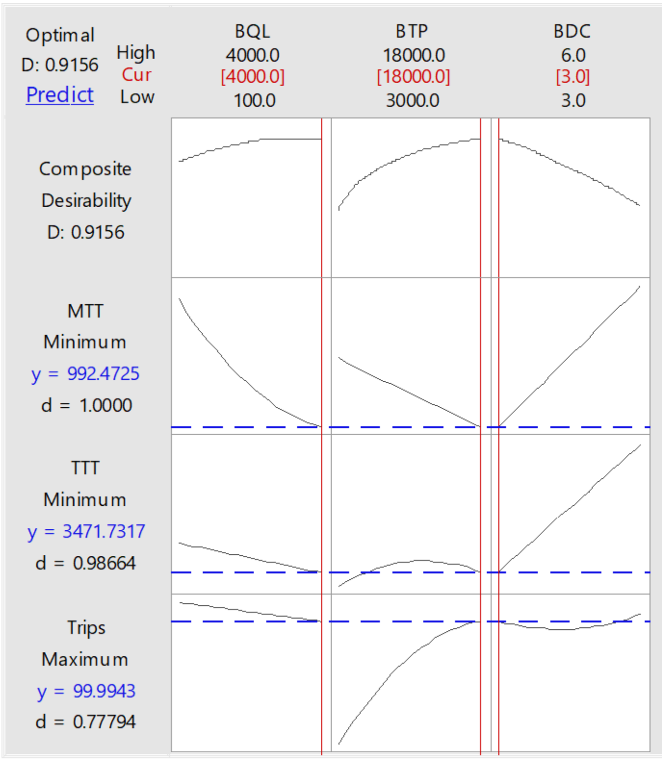

Figure 5.15: Model 3 individual and composite desirability D for the responses of N_{bus} $(Trips)$, T_t (TTT) and t_m (MTT) for various parameters of β^V (BQL), β^bor β^p (BTP), and β^B (BDC), for protected actuated control under “E” demand scenario

A contour plot was developed for the three responses of N_{bus} *(*Trips*)*, T_t *(*TTT*) and* t_m *(*MTT*)* for various parameters of β^V *(*BQL*)*, β^bor β^p *(*BTP*), and* β^B *(*BDC*) as* shown in Figure 5.16. The data of the control plots were taken from a total of 45 input variable settings (data of models 1 to 3). These variant input settings correspond to a total of 450 simulation runs, as each parameter setting is executed for 10 multiple runs.

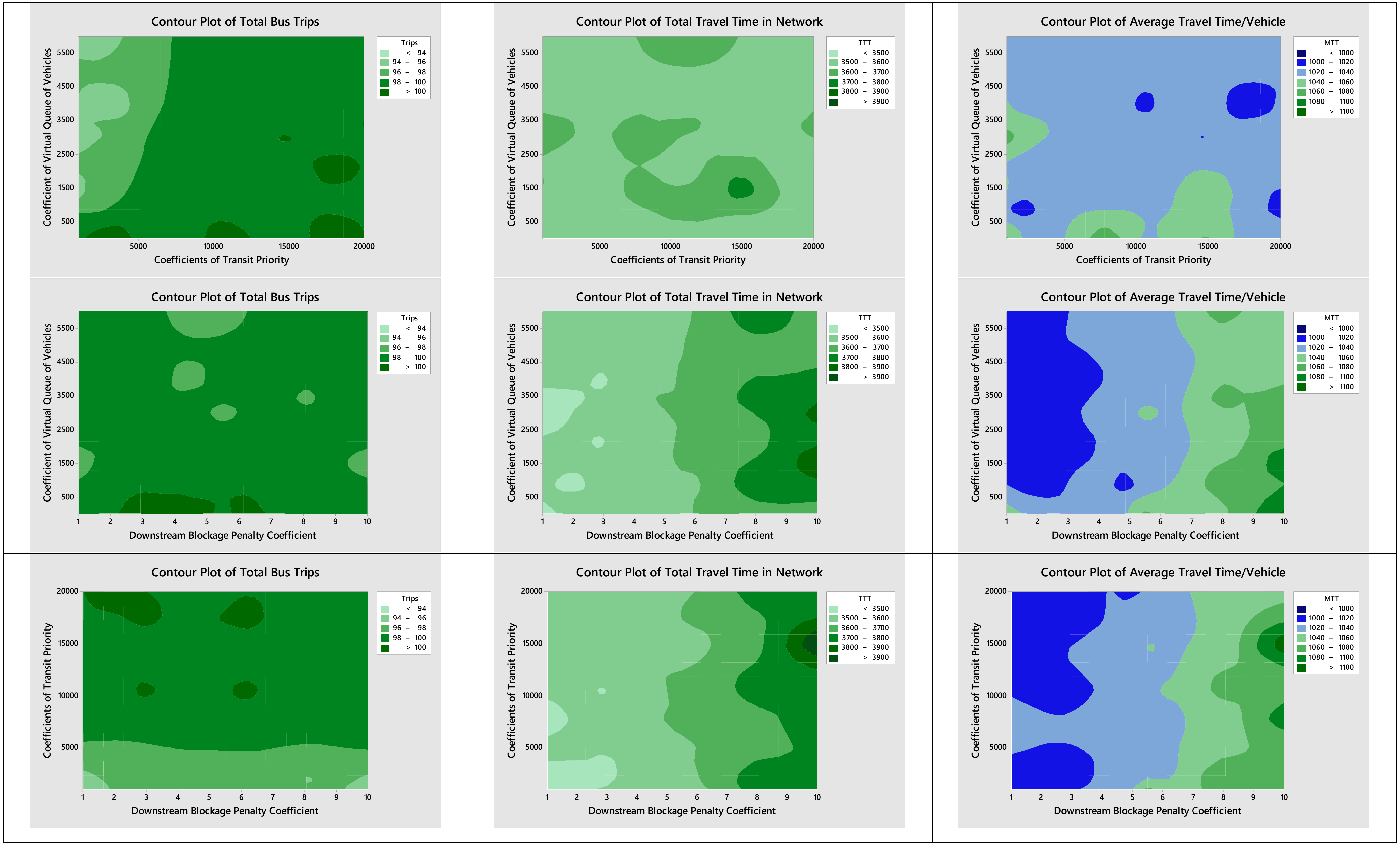

Figure 5.16: Contour plot of the three responses of N_{bus} $(Trips)$, T_t (TTT) and t_m (MTT) for various parameters of β^V (BQL), β^bor β^p (BTP), and β^B (BDC) for protected actuated control and demand case "E"

5.2.1 Analysis

The multi-objective optimization methodology (maximizing of N_{bus} $(Trips)$, while simultaneously minimizing both T_t (TTT) and t_m (MTT)) is used to solve these three models by the composite desirability function, as described in Chapter 3. None of the above models resulted in acceptable desirability levels (within the model input range) using the set three objective functions (maximizing of N_{bus} $(Trips)$, while simultaneously minimizing both T_t (TTT) and t_m (MTT)). The optimum values of the coefficients are mostly border values (upper bound or lower bound of the specified regions).

Further analysis is done for the all the models using only either double or single objective function(s). The conducted analyses still led to optimal solutions at the borders of the parameter regions. Only model 3 has shown good performance only for the double objective functions (maximizing of N_{bus} $(Trips)$, while simultaneously minimizing t_m (MTT)) and it is discussed hereafter.

The optimization is done only using two objective functions (maximizing of N_{bus} $(Trips)$, while simultaneously minimizing t_m (MTT)) as shown in Figure 5.17. The resulting optimal variable setting is presented in Table 5.9. This setting is 2503, 17242, and 3 for β^V (BQL), β^bor β^p (BTP), and β^B (BDC), respectively. The optimal responses are 100.3 for N_{bus} $(Trips)$ with a standard error (SE) of 0.6 (95% CI = 99.0, 101.6) and 999.3 seconds for t_m (MTT) with a standard error (SE) of 3.9 (95% CI = 990.5, 1008.1).

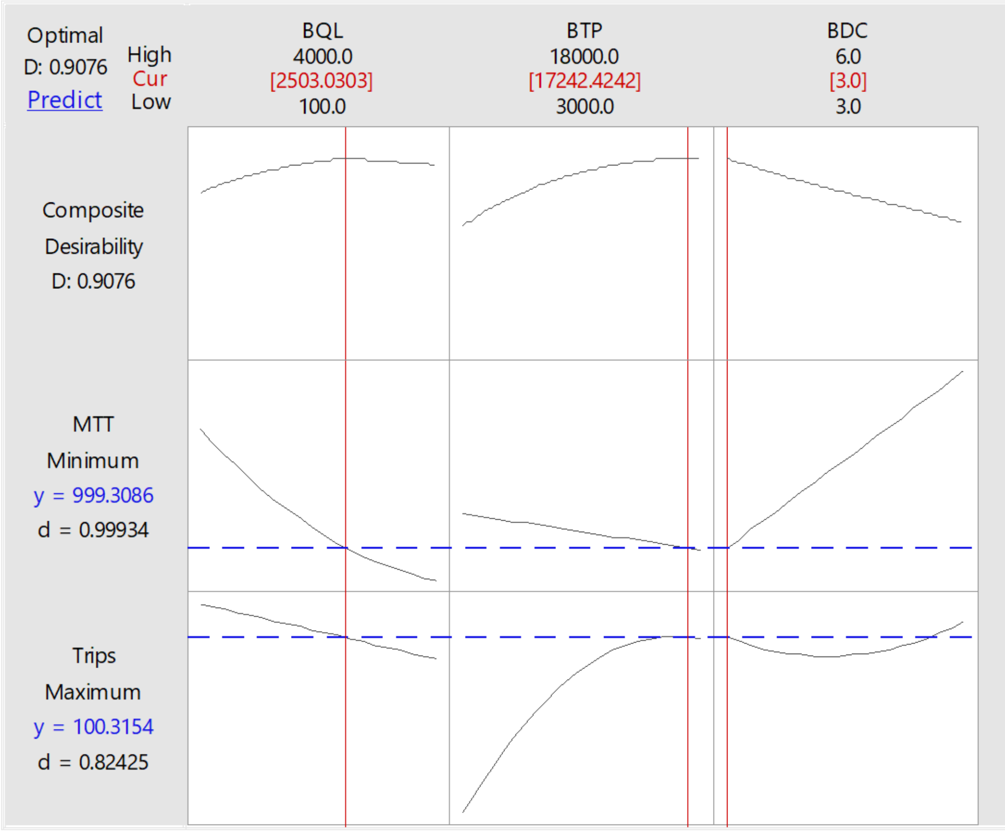

Figure 5.17: Optimization of N_{bus} $(Trips)$, and t_m (MTT) for various parameters of β^V (BQL), β^bor β^p (BTP), and β^B (BDC), for protected actuated control under "E" demand scenario

Table 5.9: Optimal variable setting of coefficients for the response of N_{bus} $(Trips)$ and t_m (MTT) for protected actuated control with demand case "E"

Coefficients			**Responses**			
β^V (BQL)	β^bor β^p (BTP)	β^B (BDC)	N_{bus} $(Trips)$	SE (95% CI)	t_m (MTT) (seconds)	SE (95% CI)
2503	17242	3	100.3	0.6 (99.0, 101.6)	999.3	3.9 (990.5, 1008.1)

RSM Statistics (ANOVA table)

Regardless of the number and nature of used objective function(s) to identify the optimal setting (single, dual or triple), the model itself is the same. Only the optimal settings vary according to the preset objective function(s). In 3rd model (with design explained in Table 5.8), the response surface model of total bus trips is significant (R-square = 86.42%), as shown in Table 5.10. β^B (BDC) and its square effect are not significant with a p-value greater than 0.1.

Table 5.10: Summary of ANOVA for N_{bus} $(Trips)$ versus various β^V (BQL), β^bor β^p (BTP), and β^B (BDC) for protected actuated control of "E" demand scenario

Source		**Sum of Squares**	**df**	**Mean Square**	**F**
Linear		31.163	3	10.3877	12.8**
	β^V	19.0159	1	19.0159	23.43**
	β^p	12.005	1	12.005	14.79**
	β^B	0.142	1	0.142	0.18*
Square		4.6465	2	2.3232	2.86**
	$\beta^p*\beta^p$	3.677	1	3.677	4.53**
	$\beta^B*\beta^B$	0.7143	1	0.7143	0.88*
2-Way Interaction	$\beta^V*\beta^p$	5.5225	1	5.5225	6.8**
Lack-of-Fit		5.1059	6	0.851	1.23*
Total		47.8246	14		

*p > 0.1
**p < 0.1

The second order regression equation of N_{bus} $(Trips)$ versus β^V (BQL), β^bor β^p (BTP), and β^B (BDC) is:

N_{bus} $(Trips)$ (Protected Actuated Control under "E" Demand Scenario)

$$= 103.06 - 0.001634\,\beta^V + 0.000370\ \beta^p - 1.67\,\beta^B$$

$$-0.0000001\ \beta^p * \beta^p + 0.195\,\beta^B * \beta^B + 0.0000001\,\beta^V * \beta^p$$

Additionally, the response model of t_m (MTT) is significant (R-square = 89.26%), as shown in Table 5.11. Only β^p (BTP) is not significant with a p-value greater than 0.1.

Table 5.11: Summary of ANOVA for t_m (MTT) versus various β^V (BQL), β^b or β^p (BTP), and β^B (BDC) for protected actuated control of "E" demand scenario

Source		Sum of Squares	df	Mean Square	F
Linear		2802.64	3	934.21	22.98**
	β^V	614.87	1	614.87	15.13**
	β^p	30.67	1	30.67	0.75*
	β^B	2157.1	1	2157.1	53.06**
Square	$\beta^V*\beta^V$	96.75	1	96.75	2.38**
2-Way Interaction	$\beta^V*\beta^p$	142.62	1	142.62	3.51**
Lack-of-Fit		170.18	7	24.31	0.25*
Total		3407.87	14		

*p > 0.1
**p < 0.1

The second order regression equation of t_m (MTT) versus β^V (BQL), β^b or β^p (BTP), and β^B (BDC) is:

t_m (MTT) (Protected Actuated Control under "E" Demand Scenario)

$$\text{(seconds)} = 980.03 - 0.00570\,\beta^V + 0.000576\,\beta^p + 10.95\,\beta^B + 0.000001\,\beta^V * \beta^V - 0.0000001\,\beta^V * \beta^p$$

Finally, the response model of T_t (TTT) is significant (R-square = 93.35%), as shown in Table 5.12. Only β^p (BTP) is not significant with a p-value greater than 0.1.

Table 5.12: Summary of ANOVA for T_t (TTT) versus various β^V (BQL), β^b or β^p (BTP), and β^B (BDC) for protected actuated control of "E" demand scenario

Source		Sum of Squares	df	Mean Square	F
Linear		41253.4	3	13751.1	45.3**
	β^V	2041	1	2041	6.72**
	β^p	428.1	1	428.1	1.41*
	β^B	38784.3	1	38784.3	127.77**
Square	$\beta^p * \beta^p$	1348.7	1	1348.7	4.44**
Lack-of-Fit		1986.5	8	248.3	0.47*
Total		45637.6	14		

*p > 0.1
**p < 0.1

The second order regression equation of T_t (TTT) versus β^V (BQL), β^bor β^p (BTP), and β^B (BDC) is:

$$T_t\ (TTT)\ \text{(Protected Actuated Control under "E" Demand Scenario) (hours)} = 3329.4 - 0.00819\,\beta^V + 0.00807\ \beta^p + 46.42\,\beta^B - 0.0000001\ \beta^p * \beta^p$$

5.2.2 Optimum selection (model validation)

In order to select the set of values to generalize its use with the protected actuated controller under the E demand scenario, a verification/validation process is deployed. The validation process entails running the simulation with the identified values (in Table 5.9). The dataset was used in ten (10) multiple runs and the resulting responses were then averaged and reported as shown in Table 5.13. The resulting average N_{bus} $(Trips)$, t_m (MTT) and T_t (TTT) of the 10 simulation runs (as shown in Table 5.13) lie within the 95% confidence interval (corresponding values) extracted from the response surface model (as shown in Table 5.9). Therefore, the set of variables (β^V $(BQL) = 2503$, β^bor β^p $(BTP) = 17242$, and β^B (BDC)= 3) is selected as the default general setting of the protected actuated controller under the demand case "E".

Table 5.13: Optimal variable settings of β^V (BQL), β^bor β^p (BTP), and β^B (BDC) and corresponding simulation-based MOE's (N_{bus} $(Trips)$, t_m (MTT) (seconds), T_t (TTT) (hours)) for protected actuated control of "E" demand scenario

Coefficients			Responses		
β^V (BQL)	β^bor β^p (BTP)	β^B (BDC)	N_{bus} $(Trips)$	t_m (MTT) (seconds)	T_t (TTT) (hours)
2503	17242	3	100.1	1012.7	3536.98

It is worth noting that the total network travel time T_t (TTT) was not explicitly used an optimization criterion in the above solution. Nonetheless, it is legitimate to say that T_t (TTT) was implicitly accounted in obtaining the optimal settings; as it directly relates to the trip's average travel time, t_m (MTT) through the formula $\mathrm{t_m} = \frac{\mathrm{T_t}}{\mathrm{N_{trips}}} * 3600$, where $\mathrm{N_{trips}}$ is the total number of vehicles in the network. That is, explicit minimization of t_m (MTT) implies implicit minimization (not explicit) of T_t (TTT).

5.3 Dual Actuated Control

The outputs of the Dual Actuated control system are presented in the Table 5.14 for five (5) RSM models, as discussed in Chapter 3 and Appendix A in details. Table 5.14 summarizes the input variable ranges, the optimal variable setting, and the resulting composite desirability. The optimization results of the five models are plotted in Figure 5.18 to 5.22 for three input parameters of coefficient for virtual queue of vehicles, β^V (BQL), coefficient for transit priority, $\beta^b or\, \beta^p$ (BTP), and downstream blockage penalty coefficient, β^B (BDC), as well as the three responses of the total bus trips, N_{bus} $(Trips)$, total network travel time, T_t (TTT), and the trip average travel time, t_m (MTT).

Table 5.14: Optimal values of dual actuated control under "E" demand scenario

Model NO.	**Factor ranges**			**Optimal factor settings (β^V, β^bor β^p, β^B)**	**Composite Desirability, *D***
	β^V (BQL)	**β^bor β^p (BTP)**	**β^B (BDC)**		
1	100 – 5000	1000 – 20000	1 – 10	100, 1000, 10	0.973
2	1 – 3000	500 – 15000	2 – 20	2547.96, 15000, 20	0.994
3	1000 – 4000	2000 – 10000	3 – 30	1000, 10000, 3	0.916
4	500 – 6000	3000 – 30000	4 – 40	6000, 30000, 40	0.983
5	2 – 3500	2500 – 13000	5 – 34	1839.3, 13000, 5	0.933

Figure 5.18 to 5.22 depict the optimization plots for the models 1 to 5, respectively, considering the three input parameters and the three responses. The composite desirability values of the models 1 to 5 are 0.973, 0.994, 0.916, 0.983, and 0.933, respectively.

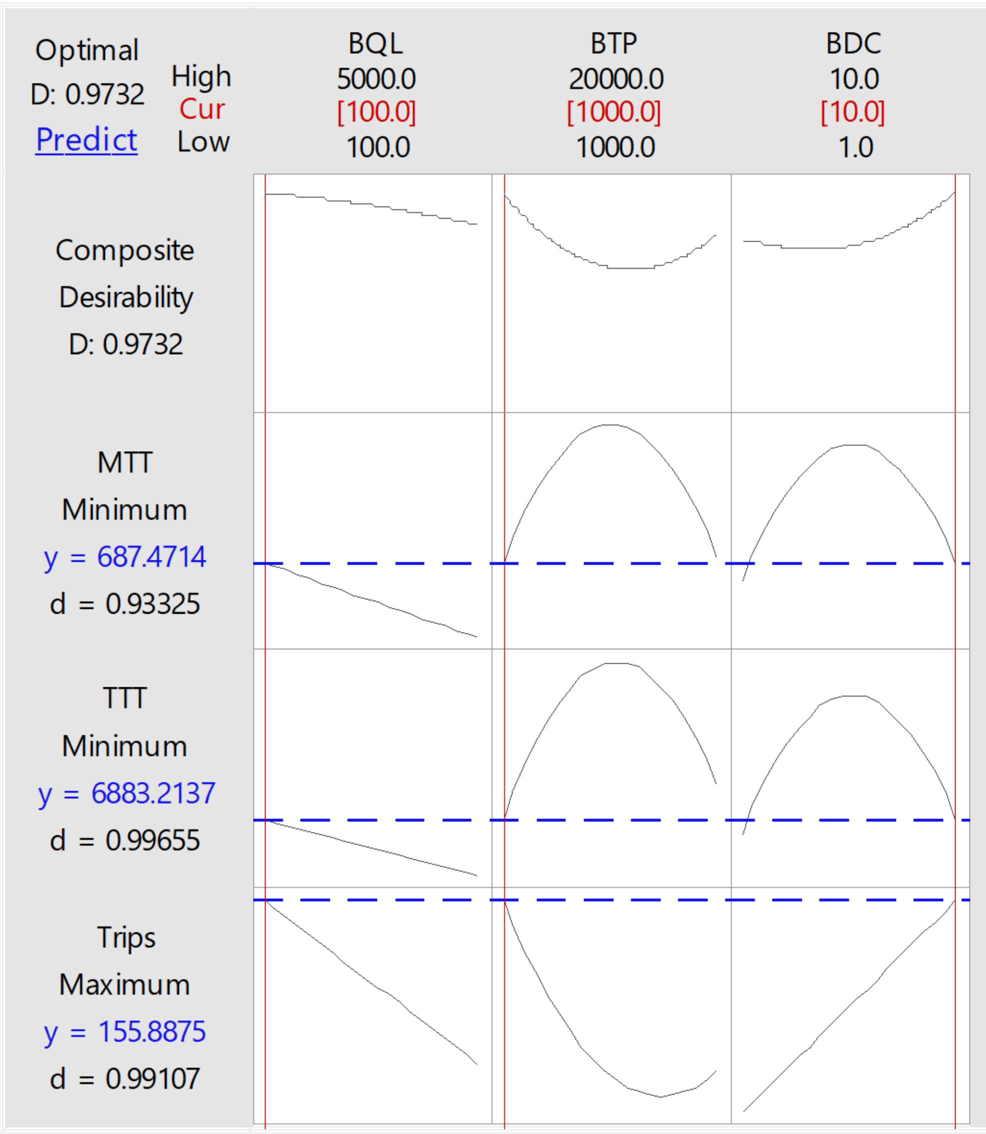

Figure 5.18: Model 1 individual and composite desirability D for the responses of N_{bus} $(Trips)$, T_t (TTT) and t_m (MTT) for various parameters of β^V (BQL), β^b or β^p (BTP), and β^B (BDC), for dual actuated control under "E" demand case

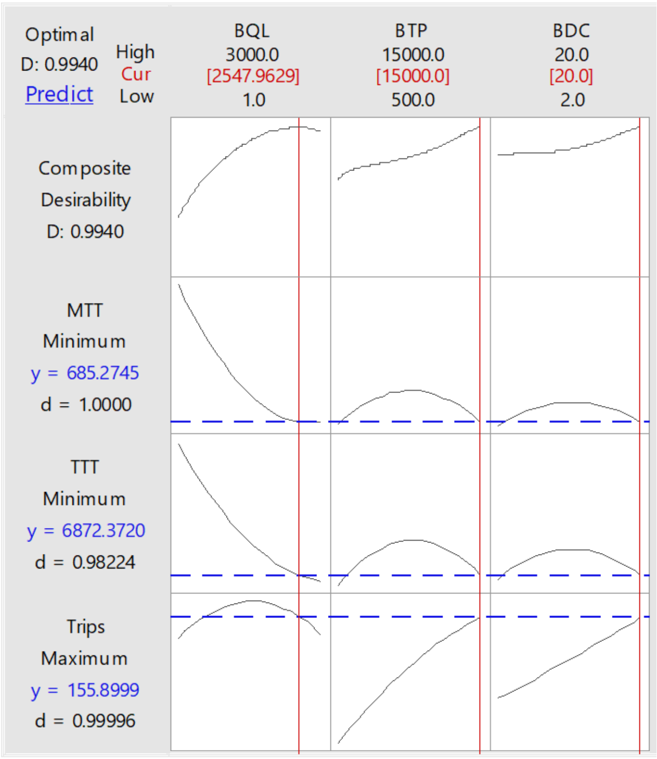

Figure 5.19: Model 2 individual and composite desirability D for the responses of N_{bus} ($Trips$), T_t (TTT) and t_m (MTT) for various parameters of β^V (BQL), β^bor β^p (BTP), and β^B (BDC), for dual actuated control under "E" demand case"

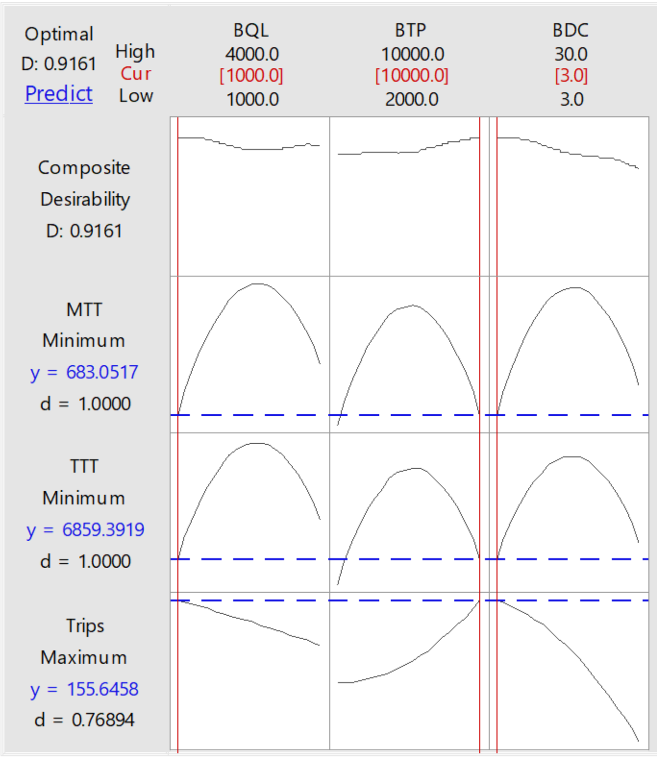

Figure 5.20: Model 3 individual and composite desirability D for the responses of N_{bus} ($Trips$), T_t (TTT) and t_m (MTT) for various parameters of β^V (BQL), β^bor β^p (BTP), and β^B (BDC), for dual actuated control under "E" demand case

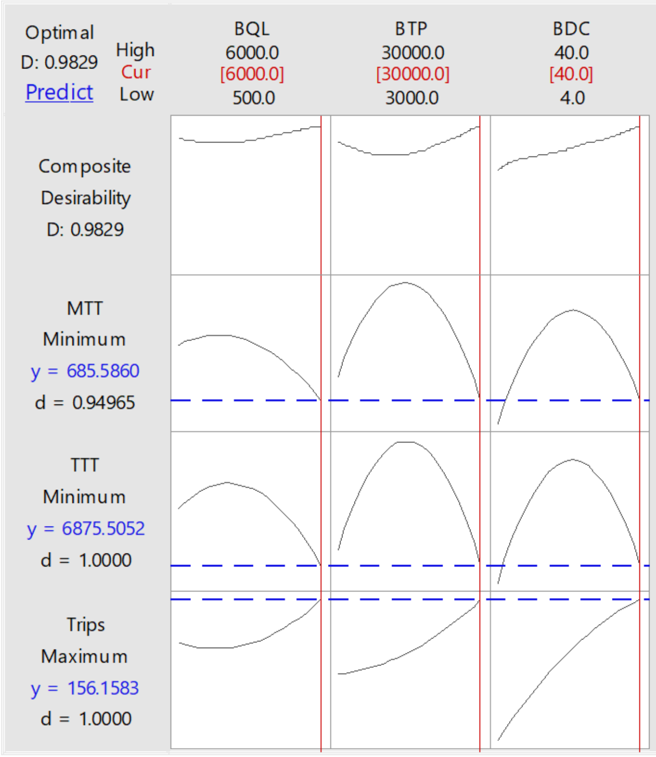

Figure 5.21: Model 4 individual and composite desirability D for the responses of N_{bus} $(Trips)$, T_t (TTT) and t_m (MTT) for various parameters of β^V (BQL), β^bor β^p (BTP), and β^B (BDC), for dual actuated control under "E" demand case

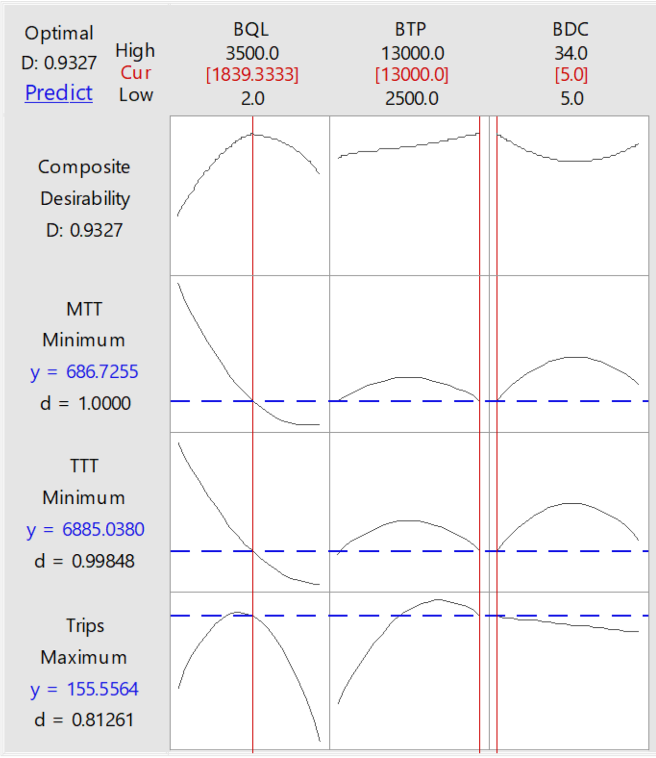

Figure 5.22: Model 5 individual and composite desirability D for the responses of N_{bus} $(Trips)$, T_t (TTT) and t_m (MTT) for various parameters of β^V (BQL), β^bor β^p (BTP), and β^B (BDC), for dual actuated control under "E" demand case

A contour plot was developed for the three responses of N_{bus} *(*Trips*)*, T_t *(*TTT*) and* t_m *(*MTT*)* for various parameters of β^V *(*BQL*)*, β^bor β^p *(*BTP*), and* β^B *(*BDC*) as* shown in Figure 5.23. The data for the control plot is taken from a total of 75 input variable settings (data of models 1 to 5). These variant input settings correspond to a total of 750 simulation runs, as each parameter setting is executed for 10 multiple runs.

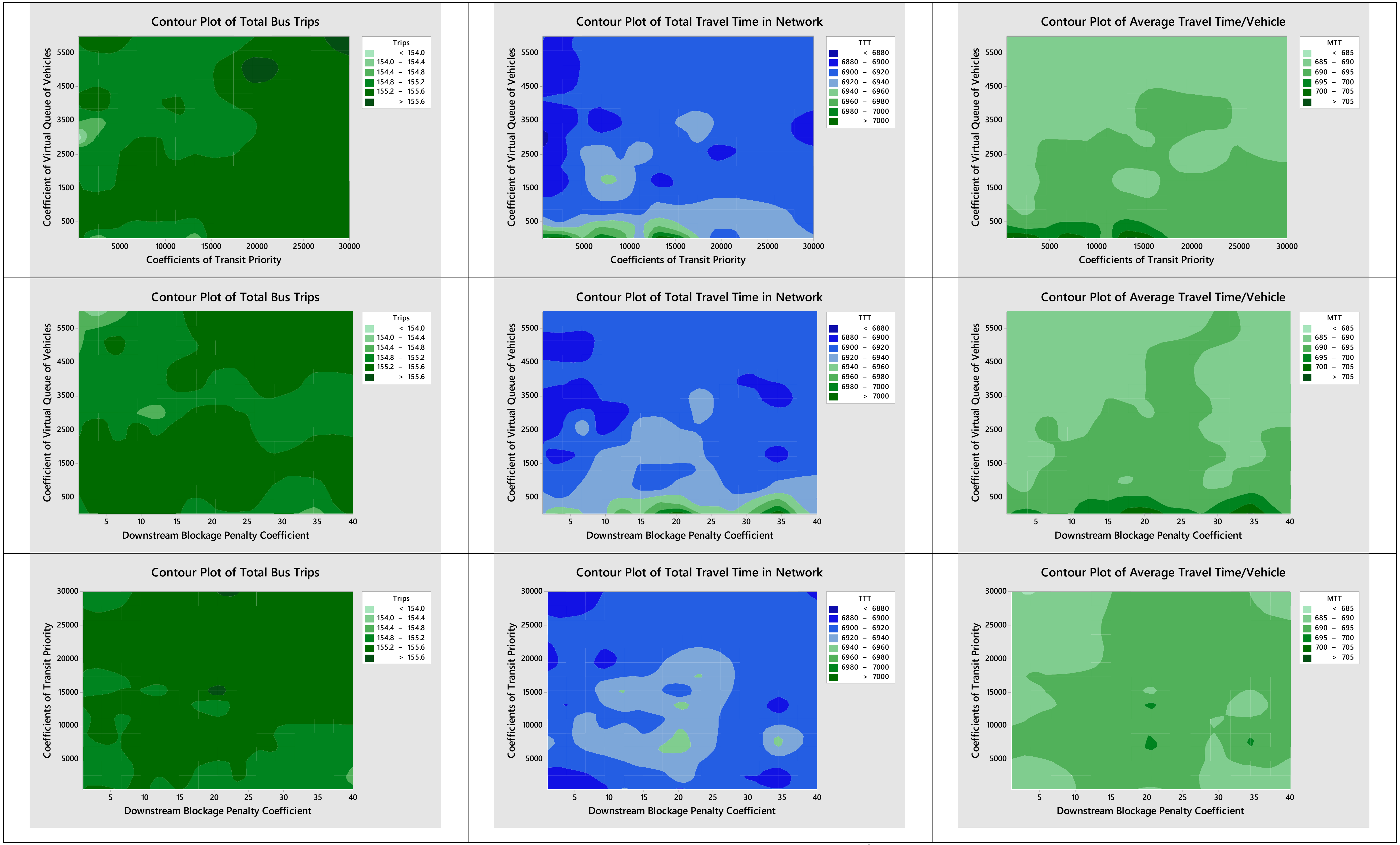

Figure 5.23: Contour plot of the three responses of N_{bus} $(Trips)$, T_t (TTT) and t_m (MTT) for various parameters of β^V (BQL), β^bor β^p (BTP), and β^B (BDC) for dual actuated control and demand case "E"

5.3.1 Analysis

The multi-objective optimization methodology (maximizing of N_{bus} $(Trips)$, while simultaneously minimizing both T_t (TTT) and t_m (MTT)) is used to solve these five models by the composite desirability function, as described in Chapter 3. None of the above models resulted in acceptable desirability levels (within the model input range) using the set three objective functions (maximizing of N_{bus} $(Trips)$, while simultaneously minimizing both T_t (TTT) and t_m (MTT)). The optimum values of the coefficients are mostly border values (upper bound or lower bound of the specified regions).

Further analysis is done for the all the models using only either double or single objective function(s). The conducted analyses still led to optimal solutions at the borders of the parameter regions. Only model 3 has shown good performance, and it is discussed hereafter.

First, the optimization is done only using one objective function (maximizing of N_{bus} $(Trips)$) as shown in Figure 5.24. The resulting optimal variable setting is presented in Table 5.15. This setting is 1274, 9941, and 5 for the β^V (BQL), β^bor β^p (BTP), and β^B (BDC), respectively, with the response N_{bus} $(Trips)$ of 155.7, and 0.146 (95% CI = 155.4, 156.0) standard error (SE).

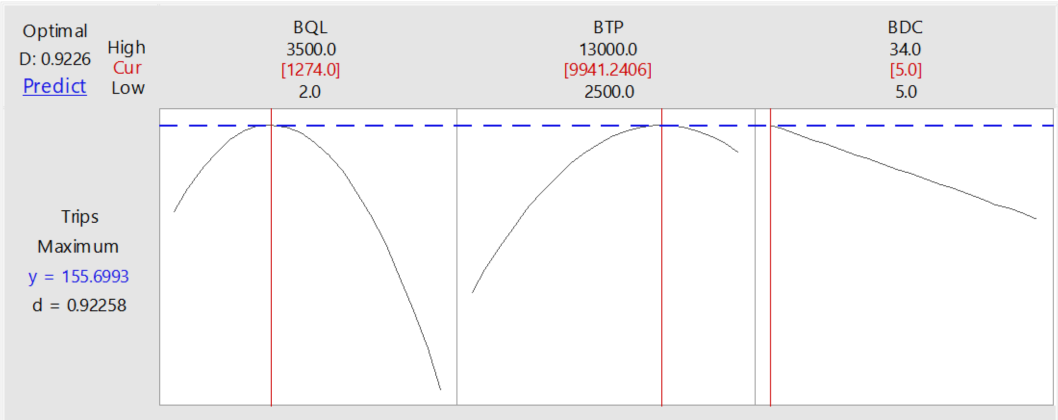

Figure 5.24: Optimization of N_{bus} $(Trips)$ for various parameters of β^V (BQL), β^bor β^p (BTP), and β^B (BDC), for dual actuated control under "E" demand scenario

Table 5.15: Optimal variable setting of coefficients for the response of N_{bus} $(Trips)$ for dual actuated control with demand case "E"

Coefficients			**Responses**	
β^V (BQL)	β^bor β^p (BTP)	β^B (BDC)	N_{bus} $(Trips)$	SE (95% CI)
1274	9941	5	155.7	0.146 (155.4, 156.0)

The optimization is done afterward considering two objective functions (maximizing of N_{bus} $(Trips)$, while simultaneously minimizing t_m (MTT)), as shown in Figure 5.25. The resulting optimal variable setting is presented in Table 5.16. This setting is 2652, 11727, and 34 for β^V (BQL), β^bor β^p (BTP), and β^B (BDC), respectively. The optimal responses are 155.6 for N_{bus} $(Trips)$ with a standard error (SE) of 0.16 (95% CI = 155.25, 155.99) and 687.19 seconds for t_m (MTT) with a standard error (SE) of 2.42 (95% CI = 681.6, 692.8).

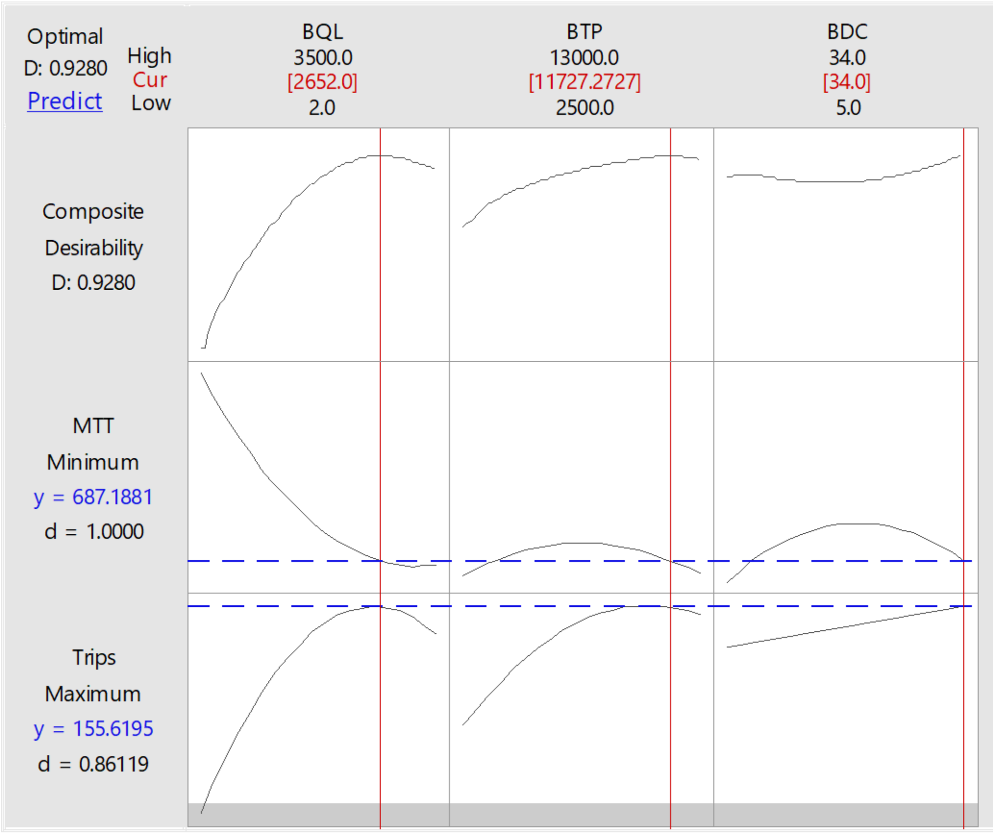

Figure 5.25: Optimization of N_{bus} $(Trips)$, and t_m (MTT) for various parameters of β^V (BQL), β^bor β^p (BTP), and β^B (BDC), for dual actuated control under "E" demand scenario

Table 5.16: Optimal variable setting of coefficients for the response for dual actuated control of "E" demand scenario

Coefficients			**Responses**			
β^V (BQL)	β^bor β^p (BTP)	β^B (BDC)	N_{bus} $(Trips)$	SE (95% CI)	t_m (MTT) (seconds)	SE (95% CI)
2652	11727	34	155.6	0.16 (155.25, 155.99)	687.19	2.42 (681.6, 692.8)

RSM Statistics (ANOVA table)

Regardless of the number and nature of used objective function(s) to identify the optimal setting (single, dual or triple), the model itself is the same. Only the optimal settings vary according to the preset objective function(s). In 5th model, the response surface model of N_{bus} $(Trips)$ is significant (R-square = 82.40%), as shown in Table 5.17.

Table 5.17: Summary of ANOVA for N_{bus} $(Trips)$ versus various β^V (BQL), β^bor β^p (BTP), and β^B (BDC) for dual actuated control of "E" demand scenario

Source		Sum of Squares	df	Mean Square	F
Linear		0.5025	3	0.1675	2.66**
	β^V	0.02	1	0.02	0.32*
	β^p	0.45125	1	0.45125	7.17**
	β^B	0.03125	1	0.03125	0.5*
Square		1.36423	2	0.68212	10.84**
	β^V*β^V	1.14727	1	1.14727	18.24**
	β^p*β^p	0.2928	1	0.2928	4.65**
2-Way Interaction	β^V*β^B	0.49	1	0.49	7.79**
Lack-of-Fit		0.3966	6	0.0661	1.24*
Total		2.86	14		

*p > 0.1
**p < 0.1

The second order regression equation of N_{bus} $(Trips)$ versus β^V (BQL), β^bor β^p (BTP), and β^B (BDC) is:

N_{bus} $(Trips)$ (Dual Actuated Control under "E" Demand Scenario)

$$= 154.53 + 0.000396\,\beta^V + 0.000203\ \beta^p - 0.0285\,\beta^B$$

$$- 0.0000001\,\beta^V * \beta^V - 0.0000001\ \beta^p * \beta^p + 0.000014\,\beta^V * \beta^B$$

Additionally, the response model of t_m (MTT) is significant (R-square = 82.67%), as shown in Table 5.18.

Table 5.18: Summary of ANOVA for t_m (MTT) versus various β^V (BQL), β^bor β^p (BTP), and β^B (BDC) for dual actuated control of "E" demand scenario

Source		**Sum of Squares**	**df**	**Mean Square**	**F**
Linear		558.055	3	186.018	10.87**
	β^V	551.51	1	551.51	32.22**
	β^p	0.012	1	0.012	0*
	β^B	6.533	1	6.533	0.38*
Square		176.896	2	88.448	5.17**
	$\beta^V*\beta^V$	106.517	1	106.517	6.22**
	$\beta^B*\beta^B$	58.226	1	58.226	3.4**
Lack-of-Fit		37.842	7	5.406	0.09*
Total		889.007	14		

*p > 0.1
**p < 0.1

The second order regression equation of t_m (MTT) versus β^V (BQL), β^bor β^p (BTP), and β^B (BDC) is:

t_m (MTT) (Dual Actuated Control under "E" Demand Scenario) (seconds) =

$$698.47 - 0.01088\,\beta^V + 0.000007\ \beta^p + 0.797\,\beta^B$$

$$+ 0.000002\,\beta^V * \beta^V - 0.0188\,\beta^B * \beta^B$$

Finally, the response model of T_t (TTT) is significant (R-square = 84.89%), as shown in Table 5.19. Only β^B (BDC) is not significant.

Table 5.19: Summary of ANOVA for T_t (TTT) versus various β^V (BQL), β^bor β^p (BTP), and β^B (BDC) for dual actuated control of "E" demand scenario

Source		**Sum of Squares**	**df**	**Mean Square**	**F**
Linear		27341.2	3	9113.7	10.81**
	β^V	27181.5	1	27181.5	32.24**
	β^p	9.5	1	9.5	0.01*
	β^B	150.2	1	150.2	0.18*
Square		10568	3	3522.7	4.18**
	$\beta^V * \beta^V$	3034.1	1	3034.1	3.6**
	$\beta^p * \beta^p$	2545.2	1	2545.2	3.02**
	$\beta^B * \beta^B$	4431.5	1	4431.5	5.26**
Lack-of-Fit		179.2	6	29.9	0.01*
Total		44654.4	14		

*p > 0.1
**p < 0.1

The second order regression equation of T_t (TTT) versus β^V (BQL), β^bor β^p (BTP), and β^B (BDC) is:

$$T_t\ (TTT)\ (Dual\ Actuated\ Control\ under\ "E"\ Demand\ Scenario)\ \text{(hours)}$$
$$= 6911.8 - 0.0661\,\beta^V + 0.01497\ \beta^p + 6.73\,\beta^B$$
$$+ 0.000009\,\beta^V * \beta^V - 0.000001\ \beta^p * \beta^p - 0.1648\,\beta^B * \beta^B.$$

5.3.2 Optimum selection (model validation)

For different objective functions, different optimal settings are obtained. In specific, herein we refer to the optimum settings of the coefficients of β^V (BQL), β^bor β^p (BTP), and β^B (BDC) related to the solutions:

I. where only N_{bus} $(Trips)$ is maximized (as indicated in Table 5.15)

II. where N_{bus} $(Trips)$ is maximized and t_m (MTT) is minimized (as indicated in Table 5.16)

In order to select only one set of values to generalize its use with the dual actuated controller under the E demand scenario, a verification/validation process is deployed. The validation process entails running the simulation with the identified values (in Tables 5.15 and 5.16). Each dataset was used in ten (10) multiple runs and the resulting responses were then averaged and reported as shown in Table 5.20. The resulting average N_{bus} $(Trips)$, t_m (MTT) and T_t (TTT) of the 10 simulation runs (as shown in Table 5.20) lie within the 95% confidence interval (corresponding values) extracted from the response surface model (as shown in Table 5.15 for variable setting I, and Table 5.16 for variable setting II).

The 2nd set of variables (II) (β^V $(BQL) = 2652$, β^bor β^p $(BTP) = 11727$, and β^B (BDC)= 34) is selected as the default general setting of the dual actuated controller under the demand case "E". The set results nearly same values of N_{bus} $(Trips)$, but lesser values of t_m (MTT) and T_t (TTT) as shown in Table 5.20.

Table 5.20: Optimal variable settings of β^V (BQL), β^bor β^p (BTP), and β^B (BDC) and corresponding simulation-based MOE's (N_{bus} $(Trips)$, t_m (MTT) (seconds), T_t (TTT) (hours)) for dual actuated control of "E" demand scenario

Variable Settings	**Coefficients**			**Responses**		
	β^V (BQL)	β^bor β^p (BTP)	β^B (BDC)	N_{bus} $(Trips)$	t_m (MTT) (seconds)	T_t (TTT) (hours)
I. (only N_{bus} $(Trips)$ is maximized)	1274	9941	5	155.5	701.56	6993.85
II. (N_{bus} $(Trips)$ is maximized and t_m (MTT) is minimized)	2652	11727	34	155.2	688.71	6901.98

It is worth noting that the total network travel time T_t (TTT) was not explicitly used an optimization criterion in any of the above two solutions (I and II). Nonetheless, it is legitimate to say that T_t (TTT) was implicitly accounted in obtaining the optimal settings II; as it directly relates to the trip's average travel time, t_m (MTT) through the formula $\mathrm{t_m} = \frac{\mathrm{T_t}}{\mathrm{N_{trips}}} * 3600$, where $\mathrm{N_{trips}}$ is the total number of vehicles in the network. That is, explicit minimization of t_m (MTT) implies implicit minimization (not explicit) of T_t (TTT).

5.4 Discussion

The optimal variable settings for various controls and their responses with characteristics are discussed in this section. The selected optimal variable settings for the Split Actuated control, Protected Actuated control, and Dual Actuated control under the demand scenario "E" ('E' refers to the traffic demand scenario of "high" traffic volume) are presented in Table 5.21. Also, the corresponding simulation-based MOE's (N_{bus} ($Trips$), t_m (MTT) (seconds), T_t (TTT) (hours)) for each setting are shown. From these settings, the split actuated and dual actuated control performed better than the protected actuated, as they delivered more total bus trips (N_{bus} ($Trips$)) with less average travel time per trip (t_m (MTT)). In addition, the dual actuated control has shown best performance considering the average travel time per trip (688.71 seconds vs. 838.26 seconds); although, it has less total bus trips (155.2 vs. 161) than the split actuated control.

Table 5.21: Optimal variable settings of β^V (BQL), β^bor β^p (BTP), and β^B (BDC) and corresponding simulation-based MOE's (N_{bus} $(Trips)$, t_m (MTT) (seconds), T_t (TTT) (hours)) for various controls of "E" demand scenario

Control	Coefficients			Responses		
	β^V (BQL)	β^bor β^p (BTP)	β^B (BDC)	N_{bus} $(Trips)$	t_m (MTT) (seconds)	T_t (TTT) (hours)
Split Actuated	305	1000	2.1	161.0	838.26	8190.57
Protected Actuated	2503	17242	3	100.1	1012.7	3536.98
Dual Actuated	2652	11727	34	155.2	688.71	6901.98

In general, optimization deals with finding the best outputs (MOEs) by selecting the input variable settings and often in simulation-based optimization, the input variable settings follow a ratio among them to yield the similar output(s), as they have a similar effect on output(s). Therefore, the effect of various input variable settings using the selected optimal input variable settings is discussed in this section.

As indicated in Chapter 1, the typical notion of a robust system is one that performs well across a range of (traffic, geometry, weather, etc.) conditions. The robustness of the system must be ensured at various levels of congestion and across different control types (namely three levels). At the first level, the purpose is to ensure that for each control type (e.g. dual, protected or split) the sensitivity of relative ratios of the parameters. The idea is to check whether there is a specific relative ratio among the parameters that makes the specific control type (dual, protected or split) robust under one specific traffic condition.

Here, the "robustness" is examined in the context of the degree of sensitivity of the control system performance as a function of the scale of the input variable, while holding the relative ratio between these variables constant. The conclusion from this analysis is that the system is robust because (for most cases) performance of the system remains relatively constant regardless of the absolute magnitude of the parameter values as long as the relative ratios of the parameter values remain constant. The other two levels of robustness checking are summarized in Chapter 7.

More specifically, this section focuses on testing the "robustness" of the various controllers under fixed relative proportions among the various inputs. That is, will the performance of a specific controller change if the absolute values of the penalty coefficients (inputs) change, but the relative proportions among these penalties remain the same? It is believed that no matter what are the absolute values of these penalty coefficients, what determines the optimal setting is a specific "relative" proportion among them for each specific controller. If the controller performance does not change with the change of the absolute penalty values (while keeping the relative proportions fixed), this is a reflection of system robustness.

In the remaining part of this section, the robustness testing of the split actuated control is presented first, followed by the ones for the protected actuated control, and finally for the dual actuated control.

5.4.1 Split Actuated Control

The selected optimal variable settings (β^V $(BQL) = 305$, β^bor β^p $(BTP) = 1000$, and β^B (BDC)= 2.1) for split actuated controls under "E" demand scenario is presented in Table 5.22. These absolute values if rounded would result in the relative ratios of 150:495:1 (β^V (BQL) : β^bor β^p (BTP): β^B (BDC)). Using this fixed relative ratio, several input variable settings were developed and simulated. Each setting as indicated in Table 5.23 was simulated 100 times, and the average MOE's of these runs were reported. The results of the various settings (with the same relative ratio) are shown in Table 5.23. The results (in Table 5.23) show that the responses using this fixed ratio are more or less similar, and closely identical to the responses obtained with the selected optimal input variable settings (Table 5.22).

Table 5.22: Selected optimal variable settings of β^V (BQL), β^bor β^p (BTP), and β^B (BDC) and corresponding simulation-based MOE's (N_{bus} ($Trips$), t_m (MTT) (seconds), T_t (TTT) (hours)) for split actuated controls of "E" demand scenario

Coefficients			Responses		
β^V (BQL)	β^bor β^p (BTP)	β^B (BDC)	N_{bus} ($Trips$)	t_m (MTT) (seconds)	T_t (TTT) (hours)
305	1000	2.1	161.0	838.26	8190.57

Table 5.23: Several variable settings with the ratio of optimal variable settings of β^V (BQL), β^bor β^p (BTP), and β^B (BDC) and corresponding simulation-based (from 100 runs) MOE's (N_{bus} ($Trips$), t_m (MTT) (seconds), T_t (TTT) (hours)) for split actuated controls of "E" demand scenario

Coefficients			Responses		
β^V (BQL)	β^bor β^p (BTP)	β^B (BDC)	N_{bus} ($Trips$)	t_m (MTT) (seconds)	T_t (TTT) (hours)
150	495	1	160.1	842.5	8223.0
450	1485	3	160.6	842.8	8223.5
750	2475	5	160.5	844.0	8241.3
1500	4950	10	160.4	842.2	8229.0
3000	9900	20	160.5	842.8	8232.8

Figure 5.26 shows the rolling average of 10 runs of total bus trips (Trips) from 100 simulation runs for several variable settings using the ratio of optimal variable settings of β^V (BQL), β^bor β^p (BTP), and β^B (BDC) for split actuated controls under "E" demand scenario. There is a similarity among the several variable settings, with the total bus trips (Trips) ranges from 159.6 to 161.5, which are close to the response (total bus trips=161.0) of selected optimal variable settings of β^V (BQL), β^bor β^p (BTP), and β^B (BDC). The variations of the three responses under the various tested scenarios (Table 5.23) is almost negligible, and it clearly indicates the robustness of

the split actuated controllers using the fixed relative ratio of 150:495:1 for the β^V (BQL): β^bor β^p (BTP): β^B (BDC).

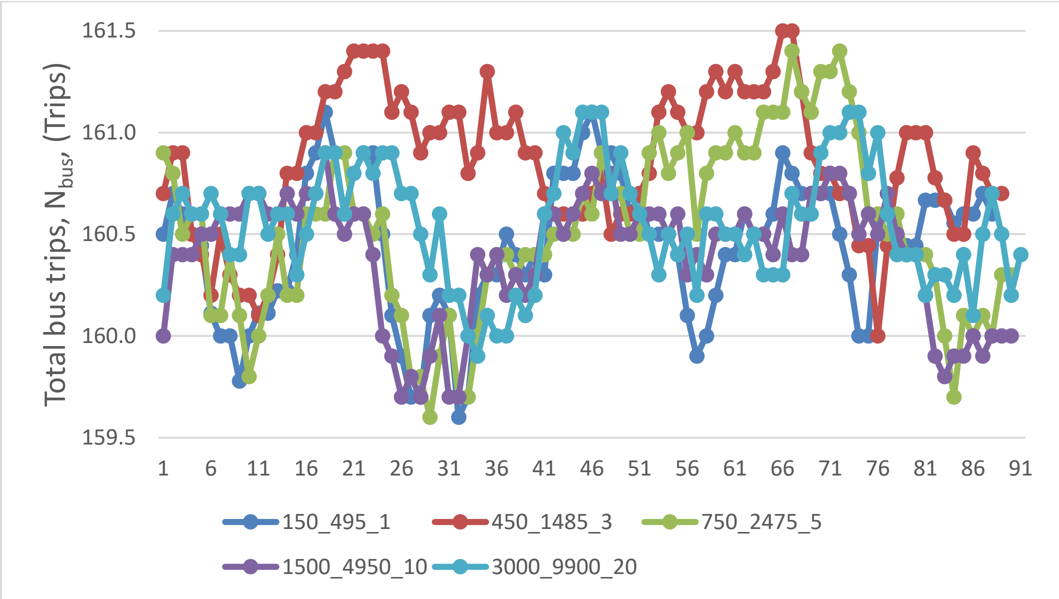

Figure 5.26: Ten runs rolling average of total bus trips (Trips) for several variable settings with the fixed ratio of optimal variable settings of β^V (BQL), β^bor β^p (BTP), and β^B (BDC) for the split actuated controller of "E" demand scenario

5.4.2 Protected Actuated Control

The selected optimal variable settings (β^V $(BQL) = 2503$, β^bor β^p $(BTP) = 17242$, and β^B (BDC)= 3) for protected actuated controls under "E" demand scenario is presented in Table 5.24. These absolute values if rounded would result in the relative ratios of 830:5810:1 (β^V (BQL) : β^bor β^p (BTP): β^B (BDC)).

Using this fixed relative ratio, several input variable settings were developed and simulated. Each setting as indicated in Table 5.25 was simulated 100 times, and the average MOE's of these runs were reported. The results of the various settings (with the same relative ratio) are shown in Table 5.25. The results (in Table 5.25) indicate that the responses using this fixed ratio are more or less similar, and closely identical to the responses obtained with the selected optimal input variable settings (Table 5.24).

Table 5.24: Selected optimal variable settings of β^V (BQL), β^bor β^p (BTP), and β^B (BDC) and corresponding simulation-based MOE's (N_{bus} $(Trips)$, t_m (MTT) (seconds), T_t (TTT) (hours)) for protected actuated controls of "E" demand scenario

Coefficients			**Responses**		
β^V (BQL)	β^bor β^p (BTP)	β^B (BDC)	N_{bus} $(Trips)$	t_m (MTT) (seconds)	T_t (TTT) (hours)
2503	17242	3	100.1	1012.7	3536.98

Table 5.25: Several variable settings with the ratio of optimal variable settings of β^V (BQL), β^bor β^p (BTP), and β^B (BDC) and corresponding simulation-based (from 100 runs) MOE's (N_{bus} $(Trips)$, t_m (MTT) (seconds), T_t (TTT) (hours)) for protected actuated controls of "E" demand scenario

Coefficients			**Responses**		
β^V (BQL)	β^bor β^p (BTP)	β^B (BDC)	N_{bus} $(Trips)$	t_m (MTT) (seconds)	T_t (TTT) (hours)
830	5810	1	99.1	1015.99	3493.65
2490	17430	3	99.9	1013.1	3489.1
4150	29050	5	99.8	1029.26	3572.93
8300	58100	10	100.3	1101.5	3896.7
16600	116200	20	100.2	1116.1	3947.7

Figure 5.27 shows the rolling average of 10 runs of total bus trips (Trips) from 100 simulation runs for several variable settings using the ratio of optimal variable settings of β^V (BQL), β^bor β^p (BTP), and β^B (BDC) for protected actuated controls under "E" demand scenario. There is a similarity among the several variable settings, with the total bus trips (Trips) ranges from 95.4 to 104.3, which are close to the response (total bus trips=100.1) of selected optimal variable settings of β^V (BQL), β^bor β^p (BTP), and β^B (BDC). The variations of the three responses under the various tested scenarios (Table 5.25) is moderate, and it clearly indicates a moderate level of

robustness of the protected actuated controllers using the fixed relative ratio of 830:5810:1 for the β^V (BQL): β^bor β^p (BTP): β^B (BDC).

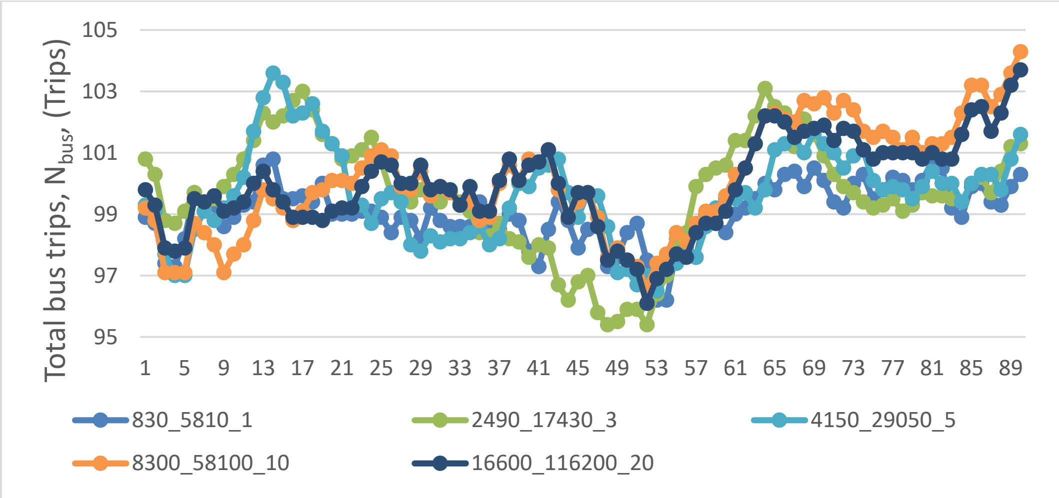

Figure 5.27: Ten runs rolling average of total bus trips (Trips) for several variable settings with the fixed ratio of optimal variable settings of β^V (BQL), β^bor β^p (BTP), and β^B (BDC) for the protected actuated controller of "E" demand scenario

5.4.3 Dual Actuated Control

The selected optimal variable settings (β^V $(BQL) = 2652$, β^bor β^p $(BTP) = 11727$, and β^B $(BDC)= 34$) for dual actuated controls under "E" demand scenario is presented in Table 5.26. These absolute values if rounded would result in the relative ratios of 80:350:1 (β^V (BQL) : β^bor β^p (BTP): β^B (BDC)).

Table 5.26: Selected optimal variable settings of β^V (BQL), β^bor β^p (BTP), and β^B (BDC) and corresponding simulation-based MOE's (N_{bus} $(Trips)$, t_m (MTT) (seconds), T_t (TTT) (hours)) for dual actuated controls of "E" demand scenario

Coefficients			Responses		
β^V (BQL)	β^bor β^p (BTP)	β^B (BDC)	N_{bus} $(Trips)$	t_m (MTT) (seconds)	T_t (TTT) (hours)
2652	11727	34	155.2	688.71	6901.98

Using this fixed relative ratio, several input variable settings were developed and simulated. Each setting as indicated in Table 5.27 was simulated 100 times, and the average MOE's of these runs were reported. The results of the various settings (with the same relative ratio) are shown in Table 5.27. The results (in Table 5.27) indicate that the responses using this fixed ratio are more or less similar, and closely identical to the responses obtained with the selected optimal input variable settings (Table 5.26).

Table 5.27: Several variable settings with the ratio of optimal variable settings of β^V (BQL), β^bor β^p (BTP), and β^B (BDC) and corresponding simulation-based (from 100 runs) MOE's (N_{bus} ($Trips$), t_m (MTT) (seconds), T_t (TTT) (hours)) for dual actuated controls of "E" demand scenario

Coefficients			Responses		
β^V (BQL)	β^bor β^p (BTP)	β^B (BDC)	N_{bus} ($Trips$)	t_m (MTT) (seconds)	T_t (TTT) (hours)
80	350	1	155.4	693.70	6947.05
240	1050	3	155.3	692.98	6938.53
400	1750	5	155.5	692.33	6935.31
800	3500	10	155.1	693.34	6938.64
1600	7000	20	155.6	692.97	6936.31

Figure 5.28 shows the rolling average of 10 runs of total bus trips (Trips) from 100 simulation runs for several variable settings using the ratio of optimal variable settings of β^V (BQL), β^bor β^p (BTP), and β^B (BDC) for dual actuated controls under "E" demand scenario. There is a similarity among the several variable settings, with the total bus trips (Trips) ranges from 154.3 to 156.4, which are close to the response (total bus trips=155.2) of selected optimal variable settings of β^V (BQL), β^bor β^p (BTP), and β^B (BDC). The variations of the three responses under the various tested scenarios (Table 5.27) is almost negligible, and it clearly indicates the robustness of

the dual actuated controllers using the fixed relative ratio of 80:350:1 for the β^V (BQL): β^bor β^p (BTP): β^B (BDC).

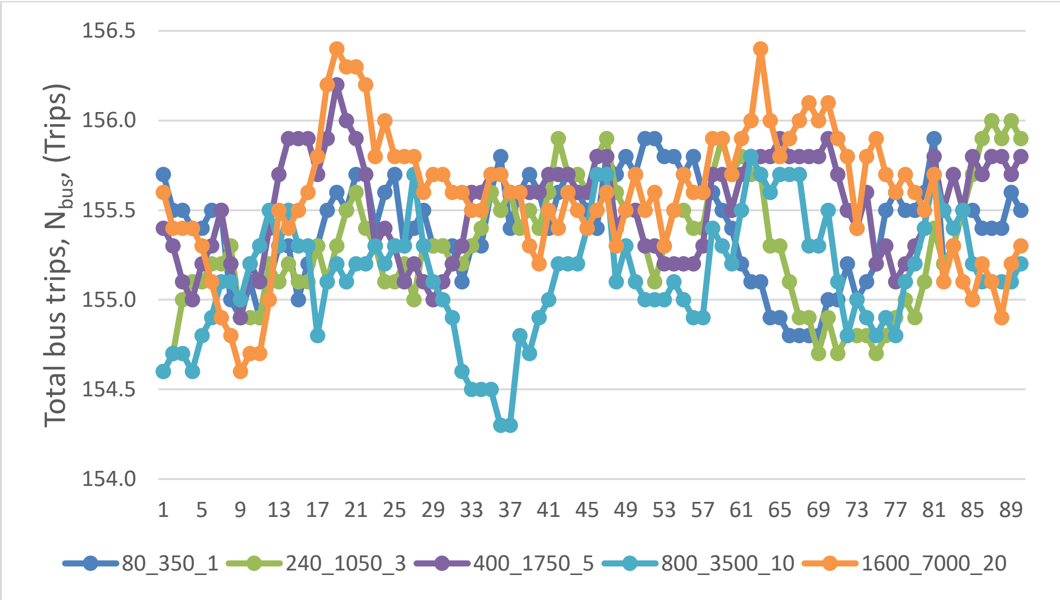

Figure 5.28: Ten runs rolling average of total bus trips (Trips) for several variable settings with the fixed ratio of optimal variable settings of β^V (BQL), β^bor β^p (BTP), and β^B (BDC) for the dual actuated controller of "E" demand scenario

Chapter 6: RSM Results and Analyses under the Very High Traffic (F) Demand Scenario

This chapter summarizes the results and the analyses of the optimization of the calibrated RSM on the coefficients for the integrated control system described in Chapter 3 for the various control types (Split Actuated, Protected Actuated, and Dual Actuated) under the demand scenario designated as (F) and the associated network topology. The (F) letter herein refers to the traffic demand scenarios of "very high" traffic volume as explained earlier in more details in Chapter 4.

This chapter is divided into three subsections to demonstrate the results and analyses for the Split Actuated control, followed by the ones for the Protected Actuated control, and finally for the Dual Actuated control.

6.1 Split Actuated Control

The output of the Split Actuated control system is presented in Table 6.1 for two (2) RSM models, as discussed in Chapter 3 and Appendix A in details. Table 6.1 summarizes the input variable ranges, the optimal settings, and the resulting composite desirability. The optimization results of the two models are plotted in Figures 6.1 and 6.2 for the three input parameters of coefficient for virtual queue of vehicles, β^V (BQL), coefficient for transit priority, $\beta^b or\, \beta^p$ (BTP), and downstream blockage penalty coefficient, β^B (BDC), as well as the three responses of the total bus trips, N_{bus} ($Trips$), total network travel time, T_t (TTT), and the trip average travel time, t_m (MTT).

Table 6.1: Optimal values of split actuated control under “F” demand scenario

Model NO.	Factor ranges			Optimal factor settings (β^V, β^bor β^p, β^B)	Composite Desirability, D
	β^V (BQL)	β^bor β^p (BTP)	β^B (BDC)		
1	100 – 3000	1000 – 8000	1 – 5	100, 8000, 1.32	0.792
2	1 – 3000	1000 – 8000	1 – 5	1, 4818.18, 1.20	0.887

Figures 6.1 and 6.2 depict the optimization plot for the models 1 and 2 considering the three input parameters and the three responses. The composite desirability values of models 1 and 2 are 0.792 and 0.887, respectively.

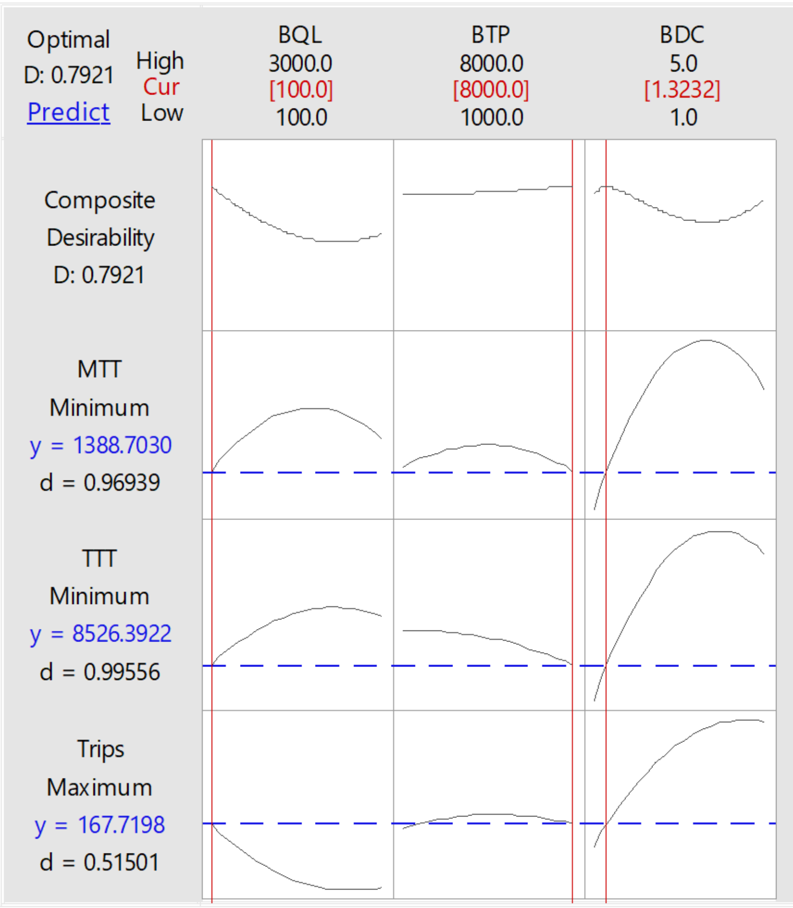

Figure 6.1: Model 1 individual and composite desirability D for the responses of N_{bus} $(Trips)$, T_t (TTT) and t_m (MTT) for various parameters of β^V (BQL), β^bor β^p (BTP), and β^B (BDC), for split actuated control under “F” demand scenario

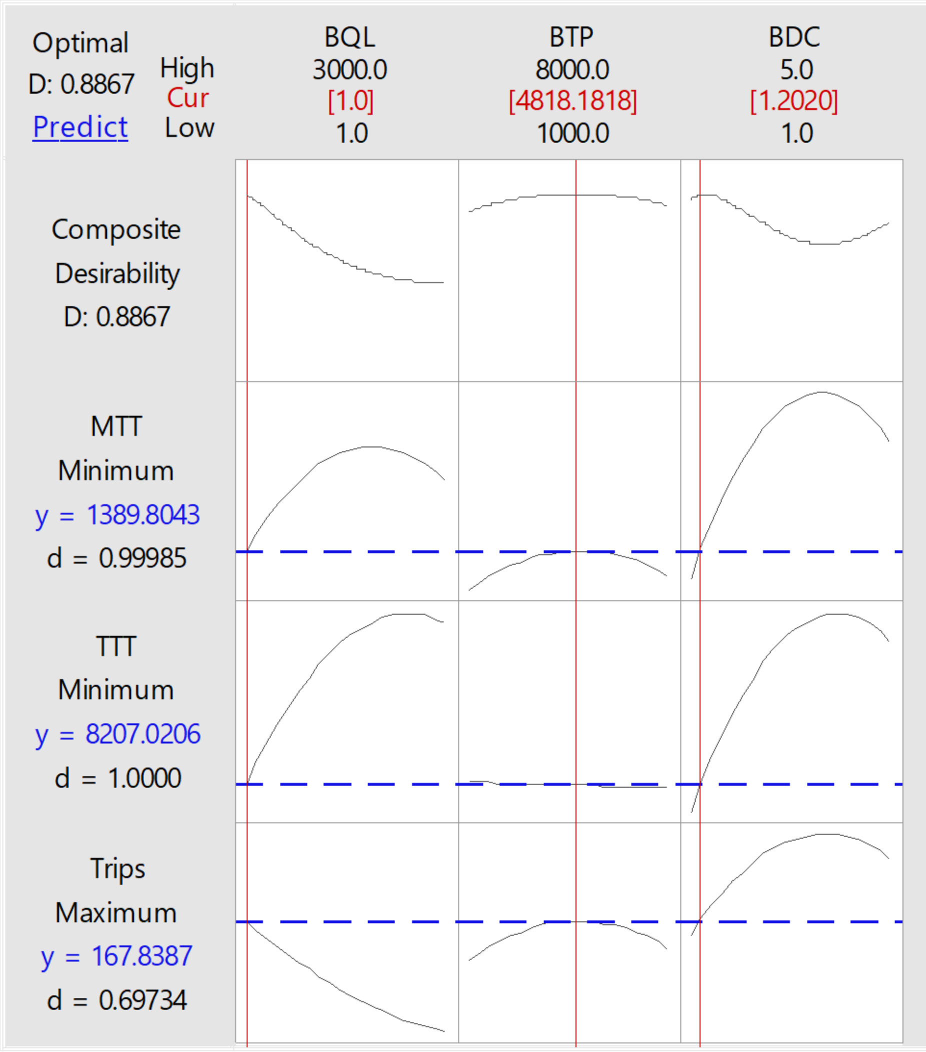

Figure 6.2: Model 2 individual and composite desirability D for the responses of N_{bus} $(Trips)$, T_t (TTT) and t_m (MTT) for various parameters of β^V (BQL), β^bor β^p (BTP), and β^B (BDC), for split actuated control under "F" demand scenario

A contour plot was developed for the three responses of N_{bus} (Trips), T_t (TTT) *and* t_m (MTT) for various parameters of β^V (BQL), β^bor β^p (BTP), *and* β^B (BDC) *as* shown in Figure 6.3. The data for the contour plot were taken from a total of 15 coded input variable settings for each model as indicated in Chapter 3 according to the Box-Behnkan design (Table 3.1) (a total of 30 input settings for models 1 and 2). These variant input settings correspond to a total of 300 simulation runs, as each parameter setting is executed for 10 multiple runs.

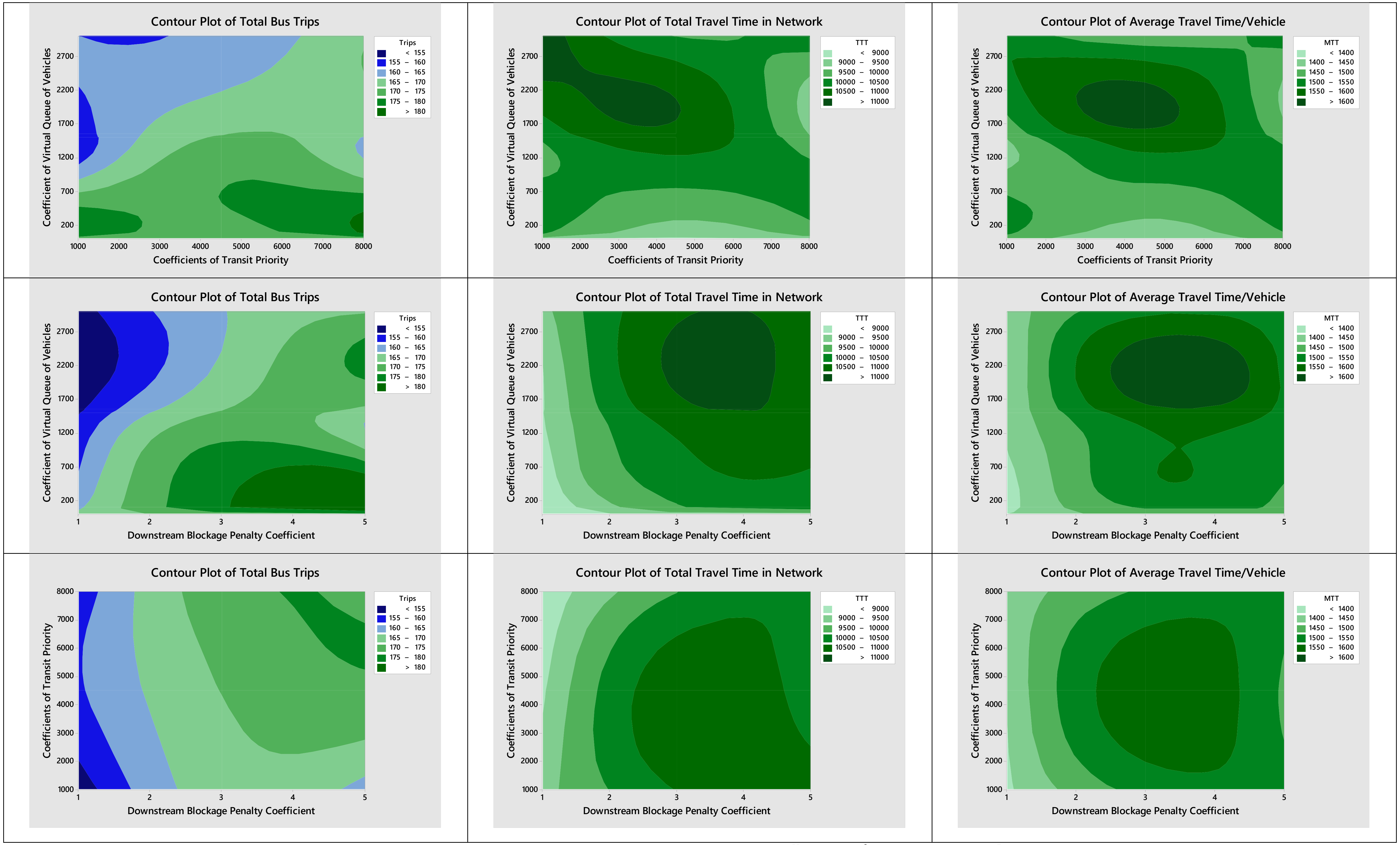

Figure 6.3: Contour plot of the three responses of N_{bus} $(Trips)$, T_t (TTT) and t_m (MTT) for various parameters of β^V (BQL), β^bor β^p (BTP), and β^B (BDC) for split actuated control and demand case “F”

6.1.1 Analysis

The multi-objective optimization methodology (maximizing of N_{bus} ($Trips$), while simultaneously minimizing both T_t (TTT) and t_m (MTT)) is used to solve these two models by the composite desirability function, as described in Chapter 3. The second model satisfied the proper desirability within the input variable levels, as the optimum values of the coefficients are within the border (upper bound or lower bound) as shown in Figure 6.2, except for the coefficient for virtual queue of vehicles and it is lowest positive value. Further analysis is done for the second model using only either double or single objective function(s) and it is discussed hereafter.

First, the optimization is done considering two objective functions (maximizing of N_{bus} ($Trips$), while simultaneously minimizing t_m (MTT)), as shown in Figure 6.4 and the optimal variable setting is presented in Table 6.2. The results are similar to the earlier ones shown in Figure 6.2. This setting is 1, 4818.18, and 1.20 for β^V (BQL), β^bor β^p (BTP), and β^B (BDC), respectively. The optimal responses are 167.84 for N_{bus} ($Trips$) with a standard error (SE) of 1.35 (95% CI = 164.53, 171.15) and 1389.8 seconds for t_m (MTT) with a standard error (SE) of 14.4 (95% CI = 1356.6, 1423.0).

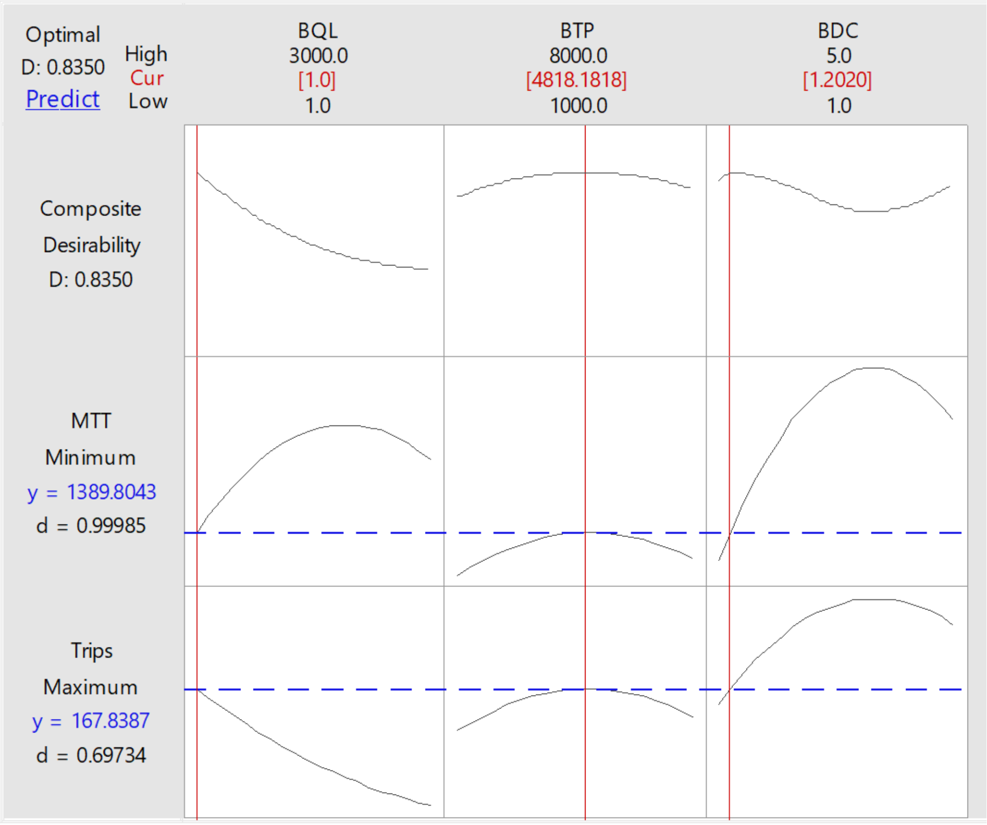

Figure 6.4: Optimization of N_{bus} $(Trips)$, and t_m (MTT) for various parameters of β^V (BQL), β^bor β^p (BTP), and β^B (BDC), for split actuated control under "F" demand scenario

Table 6.2: Optimal variable setting of coefficients for the response for split actuated control of "F" demand scenario

Coefficients			**Responses**			
β^V (BQL)	β^bor β^p (BTP)	β^B (BDC)	N_{bus} $(Trips)$	SE (95% CI)	t_m (MTT) (seconds)	SE (95% CI)
1	4818.18	1.20	167.84	1.35 (164.53, 171.15)	1389.8	14.4 (1356.6, 1423.0)

The optimization is done afterward considering only one objective function (maximizing of N_{bus} $(Trips)$) as shown in Figure 6.5. The resulting optimal variable setting is presented in Table 6.3. This setting is 1, 4818.18, and 3.67 for the β^V (BQL), β^bor β^p (BTP), and β^B (BDC), respectively, with the response N_{bus} $(Trips)$ of 177.05 and 1.08 (95% CI = 174.41, 179.70) standard error (SE).

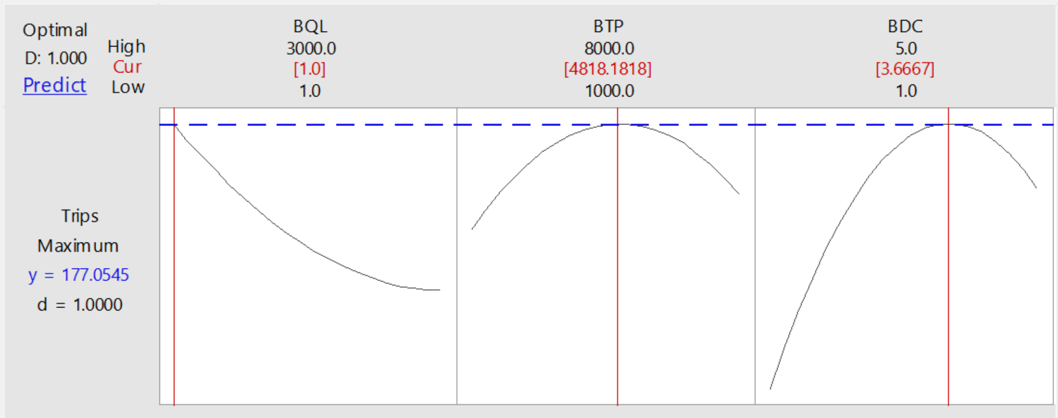

Figure 6.5: Optimization of N_{bus} $(Trips)$ for various parameters of β^V (BQL), β^bor β^p (BTP), and β^B (BDC), for split actuated control under "F" demand scenario

Table 6.3: Optimal variable setting of coefficients for the response of N_{bus} $(Trips)$ for split actuated control with demand case "F"

Coefficients			**Responses**	
β^V (BQL)	β^bor β^p (BTP)	β^B (BDC)	N_{bus} $(Trips)$	SE (95% CI)
1	4818.18	3.67	177.05	1.08 (174.41, 179.70)

RSM Statistics (ANOVA table)

Regardless of the number and nature of used objective function(s) to identify the optimal setting (single, dual or triple), the model itself is the same. Only the optimal settings vary according to the preset objective function(s). In 2nd model (with design explained in Table 6.1), the response surface model of N_{bus} $(Trips)$ is statistically significant (R-square = 94.56%), as p-value for each parameter is less than 0.1, as shown in Table 6.4, except the square of coefficient for virtual queue of vehicles ($\beta^V * \beta^V$, p-value = 0.117).

Table 6.4: Summary of ANOVA for N_{bus} $(Trips)$ versus various β^V (BQL), β^bor β^p (BTP), and β^B (BDC) for split actuated control of "F" demand scenario

Source		**Sum of Squares**	**df**	**Mean Square**	**F**
Linear		527.142	3	175.714	61.52**
	β^V	147.061	1	147.061	45.49**
	β^p	77.501	1	77.501	71.07**
	β^B	302.580	1	302.580	0.44**
Square		188.468	3	62.823	22.00**
	$\beta^V * \beta^V$	9.551	1	9.551	3.34*
	$\beta^p * \beta^p$	46.314	1	46.314	16.22**
	$\beta^B * \beta^B$	133.663	1	133.663	46.8**
2-Way Interaction		40.263	2	20.131	7.05**
	$\beta^V * \beta^p$	23.04	1	23.04	8.07**
	$\beta^V * \beta^B$	17.223	1	17.223	6.03**
Lack-of-Fit		11.850	4	2.963	1.12*
Total		773.009	14		

*p > 0.1
**p < 0.1

The second order regression equation of N_{bus} $(Trips)$ versus β^V (BQL), β^bor β^p (BTP), and β^B (BDC) is:

N_{bus} $(Trips)$ (Split Actuated Control under "F" Demand Scenario) =

$$149.92 - 0.00914\,\beta^V + 0.002805\,\beta^p + 11.06\,\beta^B + 0.000001\beta^V * \beta^V - 0.0000001\beta^p * \beta^p - 1.504\beta^B * \beta^B + 0.0000001\beta^V\beta^p + 0.000692\beta^V\beta^B$$

Additionally, the response model of t_m (MTT) is significant (R-square = 93.91%), as p-value for each parameter is less than 0.1 as shown in Table 6.5, except the β^p(BTP), as p-value greater than 0.1.

Table 6.5: Summary of ANOVA for t_m (MTT) versus various β^V (BQL), β^bor β^p (BTP), and β^B (BDC) for split actuated control of "F" demand scenario

Source		Sum of Squares	df	Mean Square	F
Linear		26876	3	8958.7	18.86**
	β^V	5609.4	1	5609.4	11.81**
	β^p	289	1	289	0.61*
	β^B	20977.5	1	20977.5	44.15**
Square		31749.3	3	10583.1	22.28**
	$\beta^V * \beta^V$	8654.7	1	8654.7	18.22**
	$\beta^p * \beta^p$	2196.1	1	2196.1	4.62**
	$\beta^B * \beta^B$	24286.9	1	24286.9	51.12**
Lack-of-Fit		3157.8	6	526.3	1.64*
Total		62426.1	14		

*p > 0.1
**p < 0.1

The second order regression equation of t_m (MTT) versus β^V (BQL), β^bor β^p (BTP), and β^B (BDC) is:

t_m (MTT) (Split Actuated Control under "F" Demand Scenario) (seconds)

$$= 1193.6 + 0.0823\,\beta^V + 0.01964\,\beta^p + 147.3\,\beta^B$$
$$- 0.000022\,\beta^V * \beta^V - 0.000002\,\beta^p * \beta^p - 20.28\,\beta^B * \beta^B$$

Finally, the response model of T_t (TTT) is significant (R-square = 94.57%), as p-value for each parameter is less than 0.1, as shown in Table 6.6, except the interaction between the coefficient for virtual queue of vehicles and coefficient for transit priority ($\beta^V * \beta^p$, p-value = 0.16).

Table 6.6: Summary of ANOVA for T_t (TTT) versus various β^V (BQL), β^bor β^p (BTP), and β^B (BDC) for split actuated control of "F" demand scenario

Source		Sum of Squares	df	Mean Square	F
Linear		8161969	3	2720656	33.04**
	β^V	3752929	1	3752929	45.58**
	β^p	466049	1	466049	5.66**
	β^B	3942991	1	3942991	47.89**
Square		3120424	2	1560212	18.95**
	$\beta^V * \beta^V$	1098124	1	1098124	13.34**
	$\beta^B * \beta^B$	2229928	1	2229928	27.08**
2-Way Interaction	$\beta^V * \beta^p$	192960	1	192960	2.34*
Lack-of-Fit		588067	6	98011	2.78*
Total		12134027	14		

*p > 0.1
**p < 0.1

The second order regression equation of T_t (TTT) versus β^V (BQL), β^bor β^p (BTP), and β^B (BDC) is:

$$T_t\ (TTT)\ \text{(Split Actuated Control under "F" Demand Scenario) (hours)} =$$

$$6696 + 1.371\,\beta^V - 0.0062\ \beta^p + 1513\,\beta^B$$

$$-\,0.000242\ \beta^V * \beta^V - 193.7\,\beta^B * \beta^B - 0.000042\,\beta^V * \beta^p$$

6.1.2 Optimum selection (model validation)

For different objective functions, different optimal settings are obtained. In specific, herein we refer to the optimum settings of the coefficients of β^V (BQL), β^bor β^p (BTP), and β^B (BDC) related to the solutions:

III. where N_{bus} ($Trips$) is maximized and t_m (MTT) is minimized (as indicated in Table 6.2)

IV. where only N_{bus} ($Trips$) is maximized (as indicated in Table 6.3)

To select only one set of values, to generalize its use with the split actuated controller under the "F" demand scenario), a verification/validation process is deployed. The validation process entails running the simulation with the identified values (in Tables 6.2 and 6.3). Each dataset was used in ten (10) multiple runs and the resulting responses were then averaged and reported as shown in Table 6.7. The resulting average N_{bus} $(Trips)$, t_m (MTT) and T_t (TTT) of the 10 simulation runs (as shown in Table 6.7) lie within the 95% confidence interval (corresponding values) extracted from the response surface model (as shown in Table 6.2 for variable setting I, and Table 6.3 for variable setting II).

Table 6.7: Optimal variable settings of β^V (BQL), β^bor β^p (BTP), and β^B (BDC) and corresponding simulation-based MOE's (N_{bus} $(Trips)$, t_m (MTT) (seconds), T_t (TTT) (hours)) for split actuated control of "F" demand scenario

Variable Setting	**Coefficients**			**Responses**		
	β^V (BQL)	β^bor β^p (BTP)	β^B (BDC)	N_{bus} $(Trips)$	t_m (MTT) (seconds)	T_t (TTT) (hours)
I. (N_{bus} $(Trips)$ is maximized and t_m (MTT) is minimized)	1	4818.18	1.2	163.2	1393.9	8408.5
II. (only N_{bus} $(Trips)$ is maximized)	1	4818.18	3.2	**175.1**	**1462.2**	**9335.6**

The 2nd set of variables (II) (β^V $(BQL) = 1$, β^bor β^p $(BTP) = 4818.18$, and β^B (BDC)= 3.2) is selected as the default general setting of the split actuated controller under the demand case "F". The set has nearly 12 more total bus trips. It is usual that with more trips, the average travel time and total travel time in the network will increase.

6.2 Protected Actuated Control

The outputs for the Protected Actuated control system are presented in Table 6.8 for two (2) RSM models, as discussed in Chapter 3 and Appendix A in details. Table 6.8 summarizes the input variable ranges, the optimal variable setting, and the resulting composite desirability. The optimization results of the two models are plotted in Figures 6.6, and 6.7 for three input parameters of coefficient for virtual queue of vehicles, β^V (BQL), coefficient for transit priority, $\beta^b or\ \beta^p$ (BTP), and downstream blockage penalty coefficient, β^B (BDC), as well as the three responses of the total bus trips, N_{bus} $(Trips)$, total network travel time, T_t (TTT), and the trip average travel time, t_m (MTT).

Table 6.8: Optimal values of protected actuated control under "F" demand scenario

Model NO.	**Factor ranges**			**Optimal factor settings (β^V, β^bor β^p, β^B)**	**Composite Desirability, D**
	β^V (BQL)	**β^bor β^p (BTP)**	**β^B (BDC)**		
1	100 – 4000	3000 – 18000	3 – 6	100, 9212.12, 3	0.891
2	1 – 5000	3000 – 18000	1 – 5	1, 10575, 1.52	0.836

Figures 6.6, and 6.7 depict the optimization plots for models 1, and 2 considering the three input parameters and the three responses. The composite desirability values of these models are 0. 891, and 0.836, respectively.

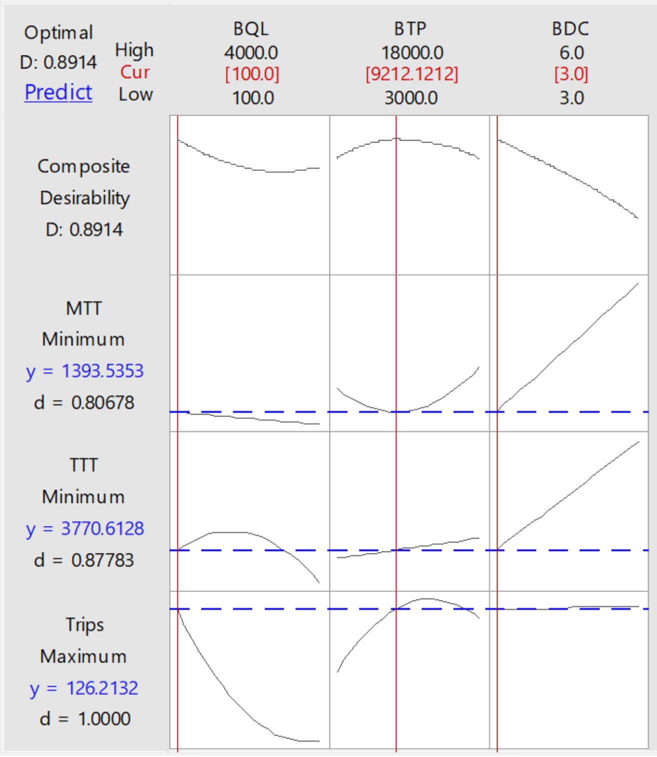

Figure 6.6: Model 1 individual and composite desirability D for the responses of N_{bus} $(Trips)$, T_t (TTT) and t_m (MTT) for various parameters of β^V (BQL), β^bor β^p (BTP), and β^B (BDC), for protected actuated control under "F" demand scenario

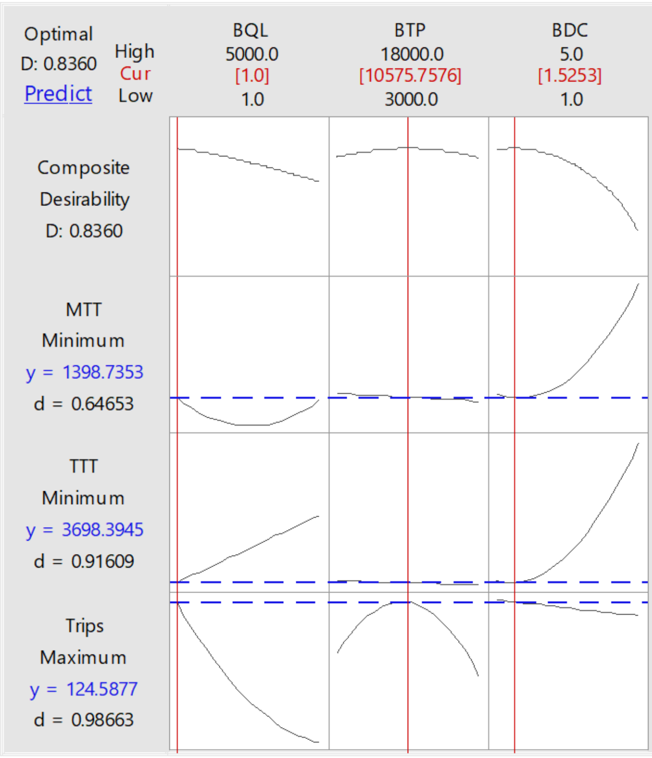

Figure 6.7: Model 2 individual and composite desirability D for the responses of N_{bus} $(Trips)$, T_t (TTT) and t_m (MTT) for various parameters of β^V (BQL), β^bor β^p (BTP), and β^B (BDC), for protected actuated control under "F" demand scenario

A contour plot was developed for the three responses of N_{bus} *(*Trips*)*, T_t *(*TTT*)* *and* t_m *(*MTT*)* for various parameters of β^V *(*BQL*)*, β^bor β^p *(*BTP*), and* β^B *(*BDC*) as* shown in Figure 6.15. The data for the contour plot were taken from a total of 15 coded input variable settings for each model as indicated in Chapter 3 according to the Box-Behnkan design (Table 3.1) (a total of 30 input settings for models 1 and 2). These variant input settings correspond to a total of 300 simulation runs, as each parameter setting is executed for 10 multiple runs.

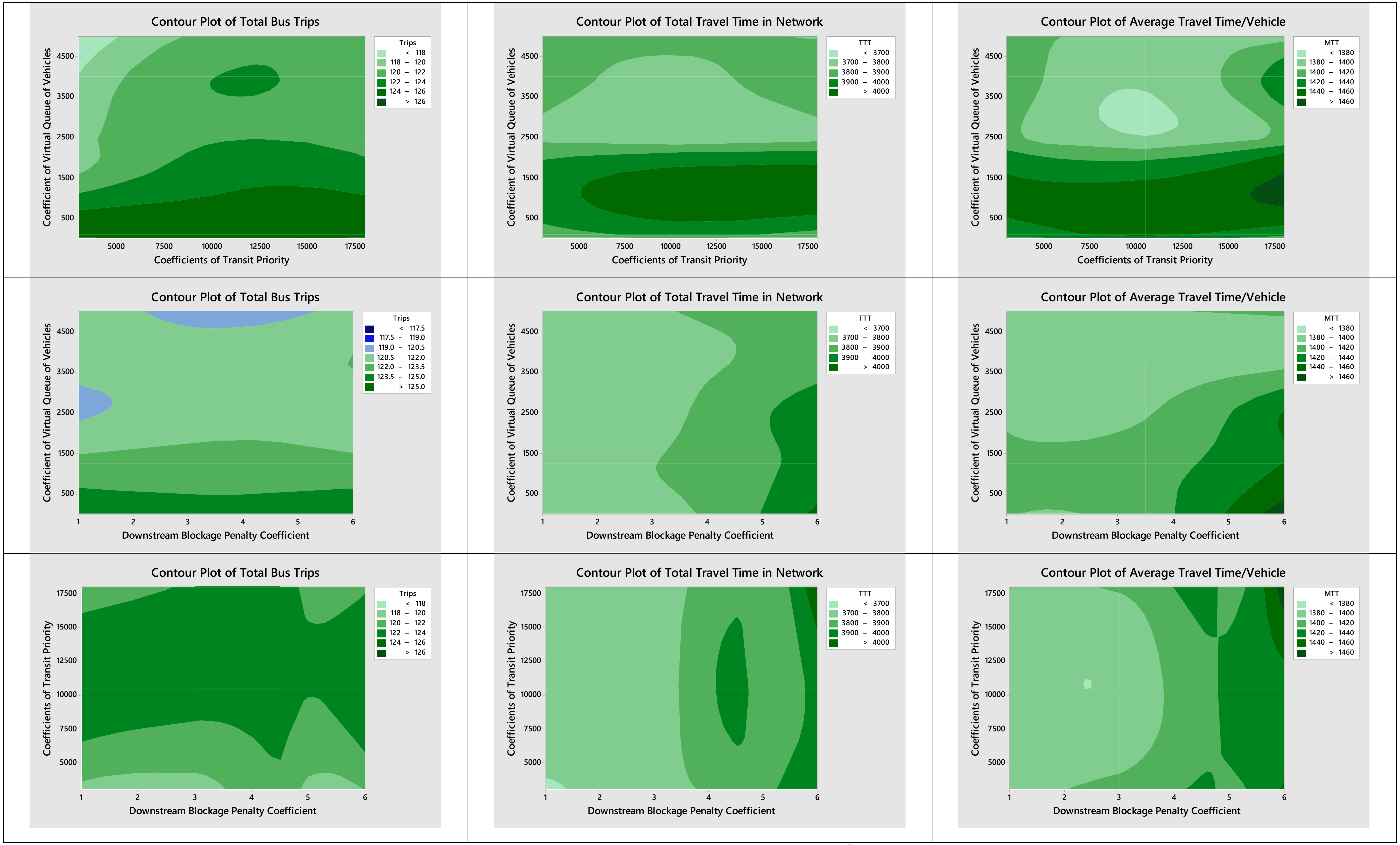

Figure 6.8: Contour plot of the three responses of N_{bus} $(Trips)$, T_t (TTT) and t_m (MTT) for various parameters of β^V (BQL), β^bor β^p (BTP), and β^B (BDC) for protected actuated control and demand case “F”

6.2.1 Analysis

The multi-objective optimization methodology (maximizing of N_{bus} ($Trips$), while simultaneously minimizing both T_t (TTT) and t_m (MTT)) is used to solve these two models by the composite desirability function, as described in Chapter 3. None of the above models resulted in acceptable desirability levels (within the model input range) using the set three objective functions (maximizing of N_{bus} ($Trips$), while simultaneously minimizing both T_t (TTT) and t_m (MTT)). The optimum values of the coefficients are mostly border values (upper bound or lower bound of the specified regions).

Further analysis is done for the all the models using only either double or single objective function(s). The conducted analyses still indicated the optimal solutions at the borders of the parameter regions. Only model 2 has shown good performance, and it is discussed hereafter.

First, the optimization is done considering two objective functions (maximizing of N_{bus} ($Trips$), while simultaneously minimizing t_m (MTT)), as shown in Figure 6.9. The resulting optimal variable setting is presented in Table 6.9. This setting is 303.97, 10727.27, and 1.69 for β^V (BQL), β^bor β^p (BTP), and β^B (BDC), respectively. The optimal responses are 124.18 for N_{bus} ($Trips$) with a standard error (SE) of 0.32 (95% CI = 123.5, 124.9) and 1395.8 seconds for t_m (MTT) with a standard error (SE) of 6.71 (95% CI = 1380.3, 1411.2).

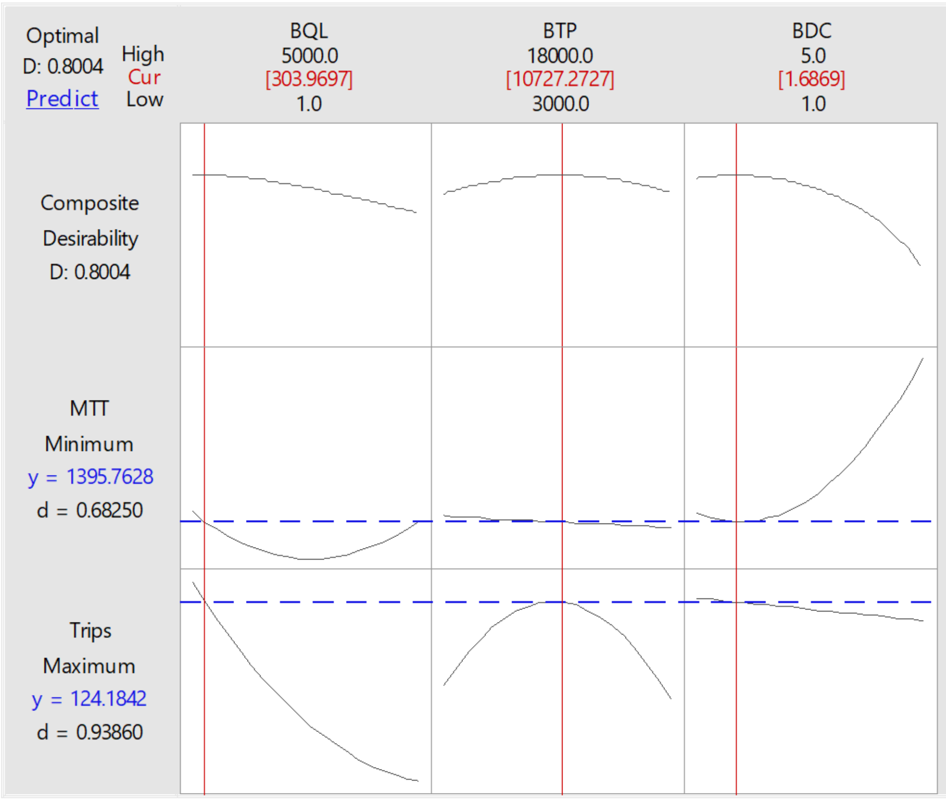

Figure 6.9: Optimization of N_{bus} $(Trips)$, and t_m (MTT) for various parameters of β^V (BQL), β^bor β^p (BTP), and β^B (BDC), for protected actuated control under "F" demand scenario

Table 6.9: Optimal variable setting of coefficients for the response of N_{bus} $(Trips)$ and t_m (MTT) for protected actuated control with demand case "F"

Coefficients			**Responses**			
β^V (BQL)	β^bor β^p (BTP)	β^B (BDC)	N_{bus} $(Trips)$	SE (95% CI)	t_m (MTT) (seconds)	SE (95% CI)
303.97	10727.27	1.69	124.18	0.32 (123.5, 124.9)	1395.8	6.71 (1380.3, 1411.2)

The optimization is done afterward considering only one objective function (maximizing of N_{bus} $(Trips)$) as shown in Figure 6.10. The resulting optimal variable setting is presented in Table 6.10. This setting is 1, 9818.18, and 1 for the β^V (BQL), β^bor β^p (BTP), and β^B (BDC), respectively, with the response N_{bus} $(Trips)$ of 124.66 and 0.38 (95% CI = 123.8, 125.5) standard error (SE).

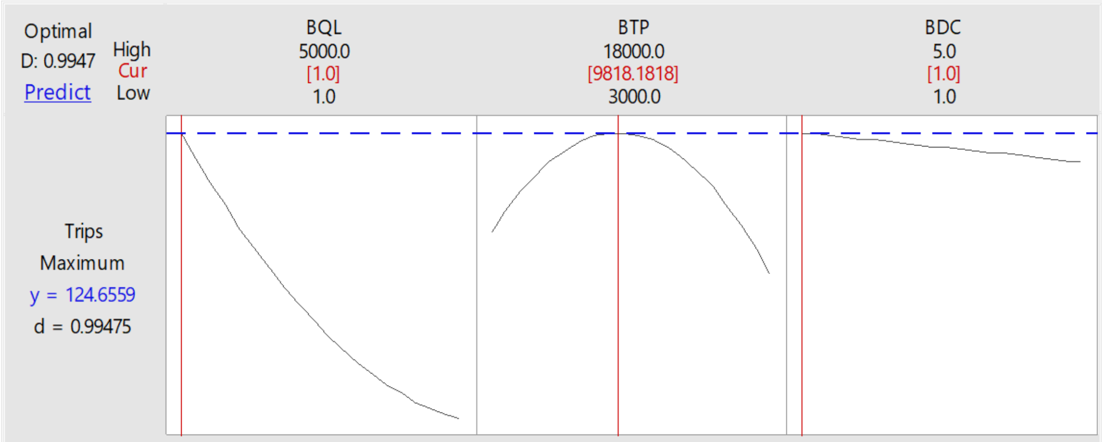

Figure 6.10: Optimization of N_{bus} $(Trips)$ for various parameters of β^V (BQL), β^bor β^p (BTP), and β^B (BDC), for split actuated control under "F" demand scenario

Table 6.10: Optimal variable setting of coefficients for the response of N_{bus} $(Trips)$ for split actuated control with demand case "F"

Coefficients			**Responses**	
β^V (BQL)	β^bor β^p (BTP)	β^B (BDC)	N_{bus} $(Trips)$	SE (95% CI)
1	9818.18	1	124.66	0.38 (123.8, 125.5)

RSM Statistics (ANOVA table)

Regardless of the number and nature of used objective function(s) to identify the optimal setting (single, dual or triple), the model itself is the same. Only the optimal settings vary according to the preset objective function(s). In 2nd model (with design explained in Table 6.8), the response surface model of total bus trips is significant (R-square = 95.59%), as shown in Table 6.11. Only β^B (BDC) is not significant with a p-value greater than 0.1.

Table 6.11: Summary of ANOVA for N_{bus} $(Trips)$ versus various β^V (BQL), β^bor β^p (BTP), and β^B (BDC) for protected actuated control of "F" demand scenario

Source		Sum of Squares	df	Mean Square	F
Linear		33.0422	3	11.0141	33.59**
	β^V	27.4259	1	27.4259	83.64**
	β^p	5.2963	1	5.2963	16.15**
	β^B	0.32	1	0.32	0.98*
Square		12.5219	2	6.261	19.1**
	β^V*β^V	1.8907	1	1.8907	5.77**
	β^p*β^p	9.9478	1	9.9478	30.34**
2-Way Interaction	β^V*β^p	7.5625	1	7.5625	23.06**
Lack-of-Fit		2.1364	6	0.3561	1.46*
Total		59.5	14		

*p > 0.1
**p < 0.1

The second order regression equation of N_{bus} $(Trips)$ versus β^V (BQL), β^bor β^p (BTP), and β^B (BDC) is:

N_{bus} $(Trips)$ (Protected Actuated Control under "F" Demand Scenario)

$$= 121.94 - 0.002076\,\beta^V + 0.000573\ \beta^p - 0.1\beta^B$$

$$+ 0.0000001\,\beta^V * \beta^V - 0.0000001\ \beta^p * \beta^p + 0.0000001\,\beta^V * \beta^p$$

Additionally, the response model of t_m (MTT) is significant (R-square = 77.02%), as shown in Table 6.12. Only β^p (BTP) is not significant with a p-value greater than 0.1.

Table 6.12: Summary of ANOVA for t_m (MTT) versus various β^V (BQL), β^bor β^p (BTP), and β^B (BDC) for protected actuated control of "F" demand scenario

Source		Sum of Squares	df	Mean Square	F
Linear		3500.9	3	1166.97	8.24**
	β^V	1691.63	1	1691.63	11.94**
	β^p	19.77	1	19.77	0.14*
	β^B	2113.49	1	2113.49	14.92**
Square		1558.09	2	779.05	5.5**
	β^V*β^V	503.42	1	503.42	3.55**
	β^B*β^B	1155.69	1	1155.69	8.16**
2-Way Interaction	β^V*β^B	586.62	1	586.62	4.14**
Lack-of-Fit		719.97	6	120	0.58*
Total		4931.66	14		

*p > 0.1
**p < 0.1

The second order regression equation of t_m (MTT) versus β^V (BQL), β^bor β^p (BTP), and β^B (BDC) is:

$$t_m\ (MTT)\ \text{(Protected Actuated Control under “F” Demand Scenario)}$$

$$\text{(seconds)} = 1413.5 - 0.00576\,\beta^V - 0.00021\ \beta^p - 14.96\,\beta^B + 0.000002\,\beta^V * \beta^V + 4.41\beta^B * \beta^B - 0.00242\,\beta^V * \beta^B$$

Finally, the response model of T_t (TTT) is significant (R-square = 66.91%), as shown in Table 6.13. Only β^p (BTP) is not significant with a p-value greater than 0.1.

Table 6.13: Summary of ANOVA for T_t (TTT) versus various β^V (BQL), β^bor β^p (BTP), and β^B (BDC) for protected actuated control of "F" demand scenario

Source		Sum of Squares	df	Mean Square	F
Linear		26734.3	3	8911.4	4.17**
	β^V	7232.9	1	7232.9	3.39**
	β^p	19	1	19	0.01*
	β^B	19482.5	1	19482.5	9.13**
Square	$\beta^B * \beta^B$	5462.3	1	5462.3	2.56**
Lack-of-Fit		4933.5	8	616.7	0.08*
Total		64506.9	14		

*p > 0.1
**p < 0.1

The second order regression equation of T_t (TTT) versus β^V (BQL), β^bor β^p (BTP), and β^B (BDC) is:

T_t (TTT) (Protected Actuated Control under "F" Demand Scenario) (hours) =

$$3718.8 - 0.01203\,\beta^V - 0.00021\ \beta^p - 26.5\,\beta^B + 9.56\ \beta^B * \beta^B$$

6.2.2 Optimum selection (model validation)

For different objective functions, different optimal settings are obtained. In specific, herein we refer to the optimum settings of the coefficients of β^V (BQL), β^bor β^p (BTP), and β^B (BDC) related to the solutions:

I. where N_{bus} $(Trips)$ is maximized and t_m (MTT) is minimized (as indicated in Table 6.9)

II. where only N_{bus} $(Trips)$ is maximized (as indicated in Table 6.10)

To select the set of values, to generalize its use with the protected actuated controller under the "F" demand scenario, a verification/validation process is deployed. The validation process entails running the simulation with the identified values (in Tables 6.9 and 6.10). The dataset was used in ten (10) multiple runs and the resulting responses were then averaged and reported as shown in Table 6.14. The resulting average N_{bus} $(Trips)$, t_m (MTT) and T_t (TTT) of the 10 simulation runs (as shown in Table 6.14) lie within the 95% confidence interval (corresponding values) extracted from the response surface model (as shown in Table 6.9 for variable setting I, and Table 6.10 for variable setting II).

Table 6.14: Optimal variable settings of β^V (BQL), β^bor β^p (BTP), and β^B (BDC) and corresponding simulation-based MOE's (N_{bus} $(Trips)$, t_m (MTT) (seconds), T_t (TTT) (hours)) for protected actuated control of "F" demand scenario

Variable Setting	**Coefficients**			**Responses**		
	β^V (BQL)	β^bor β^p (BTP)	β^B (BDC)	N_{bus} $(Trips)$	t_m (MTT) (seconds)	T_t (TTT) (hours)
I. (N_{bus} $(Trips)$ is maximized and t_m (MTT) is minimized)	303.97	10727.27	1.69	**124.8**	**1391.8**	**3750.8**
II. (only N_{bus} $(Trips)$ is maximized)	1	9818.18	1	124.7	1401.5	3720.4

The 1st set of variables (I) (β^V $(BQL) = 303.97$, β^bor β^p $(BTP) = 10727.27$, and β^B (BDC)= 1.69) is selected as the default general setting of the dual actuated controller under the demand case "F". The set has similar total bus trips (N_{bus}) but less average travel time (t_m).

It is worth noting that the total network travel time T_t (TTT) was not explicitly used an optimization criterion in the above solution. Nonetheless, it is legitimate to say that T_t (TTT) was implicitly accounted in obtaining the optimal settings; as it directly relates to the trip's average travel time, t_m (MTT) through the formula $\mathrm{t_m}=\frac{\mathrm{T_t}}{\mathrm{N_{trips}}} *$

3600, where N_{trips} is the total number of vehicles in the network. That is, explicit minimization of t_m (MTT) implies implicit minimization (not explicit) of T_t (TTT).

6.3 Dual Actuated Control

The outputs of the Dual Actuated control system are presented in the Table 6.15 for three (3) RSM models, as discussed in Chapter 3 and Appendix A in details. Table 6.15 summarizes the input variable ranges, the optimal variable setting, and the resulting composite desirability. The optimization results of the three models are plotted in Figure 6.11 to 6.13 for three input parameters of coefficient for virtual queue of vehicles, β^V (BQL), coefficient for transit priority, $\beta^b or\ \beta^p$ (BTP), and downstream blockage penalty coefficient, β^B (BDC), as well as the three responses of the total bus trips, N_{bus} ($Trips$), total network travel time, T_t (TTT), and the trip average travel time, t_m (MTT).

Table 6.15: Optimal values of dual actuated control under "F" demand scenario

Model NO.	**Factor ranges**			**Optimal factor settings (β^V, β^bor β^p, β^B)**	**Composite Desirability, *D***
	β^V (BQL)	**β^bor β^p (BTP)**	**β^B (BDC)**		
1	2 – 3500	2500 – 13000	5 – 34	3500, 3380.29, 5	0.751
2	1 – 5000	2500 – 13000	1 – 25	5000, 2500, 9.48	0.586
3	1 – 2500	2000 – 10000	1 – 11	1767.97, 2000, 5.55	0.629

Figures 6.11 to 6.13 depict the optimization plots for the models 1 to 3, respectively, considering the three input parameters and the three responses. The composite desirability values of the models 1 to 3 are 0.751, 0.586, and 0.629, respectively.

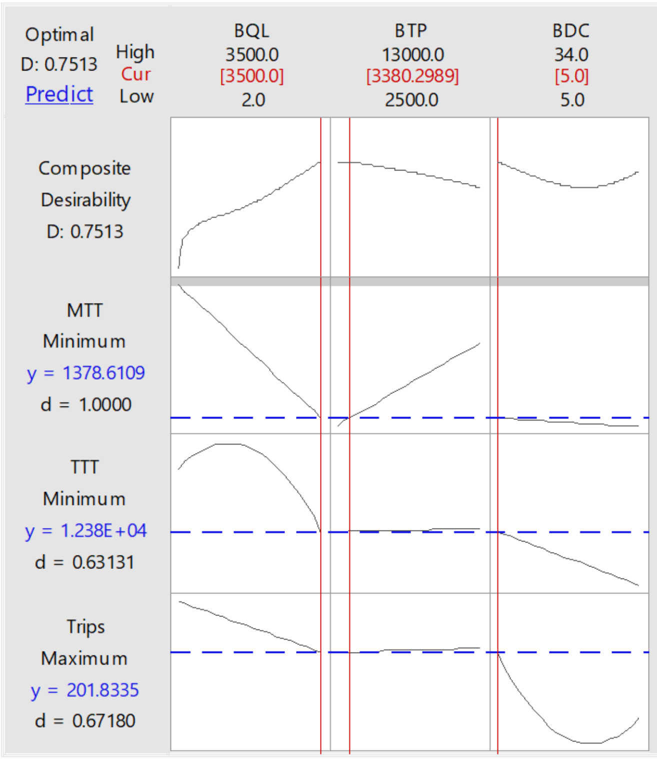

Figure 6.11: Model 1 individual and composite desirability D for the responses of N_{bus} $(Trips)$, T_t (TTT) and t_m (MTT) for various parameters of β^V (BQL), β^bor β^p (BTP), and β^B (BDC), for dual actuated control under "F" demand case

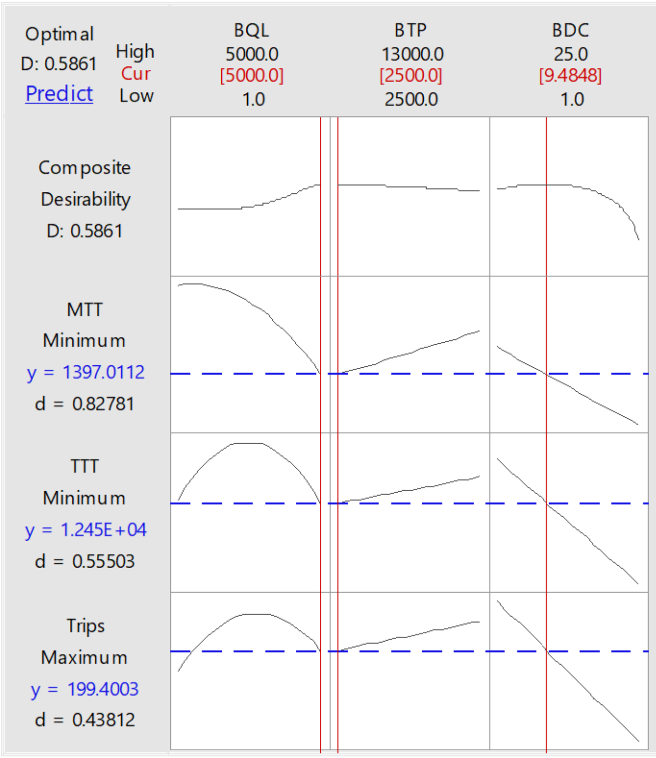

Figure 6.12: Model 2 individual and composite desirability D for the responses of N_{bus} $(Trips)$, T_t (TTT) and t_m (MTT) for various parameters of β^V (BQL), β^bor β^p (BTP), and β^B (BDC), for dual actuated control under "F" demand case"

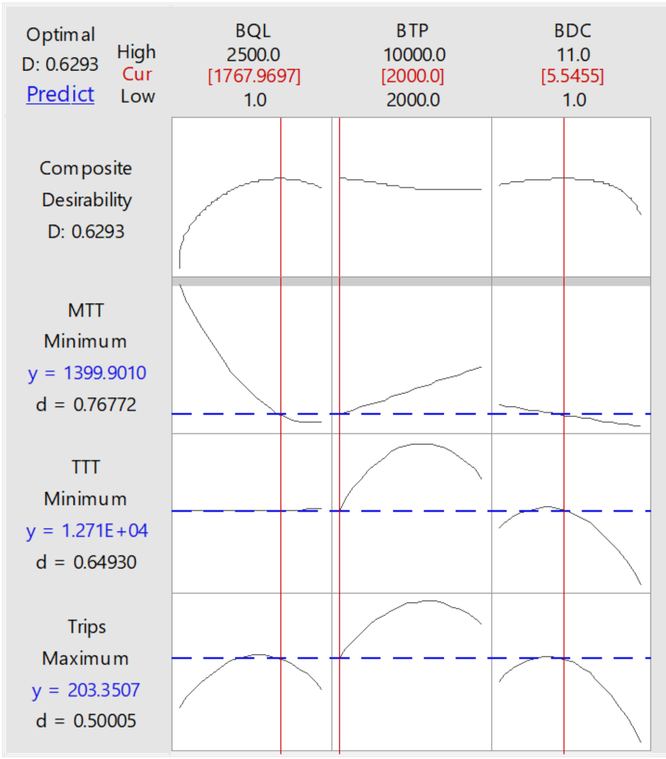

Figure 6.13: Model 3 individual and composite desirability D for the responses of N_{bus} $(Trips)$, T_t (TTT) and t_m (MTT) for various parameters of β^V (BQL), β^bor β^p (BTP), and β^B (BDC), for dual actuated control under "F" demand case

A contour plot was developed for the three responses of N_{bus} (Trips), T_t (TTT) *and* t_m (MTT) for various parameters of β^V (BQL), β^bor β^p (BTP), *and* β^B (BDC) *as* shown in Figure 6.14. The data for the contour plot were taken from a total of 15 coded input variable settings for each model as indicated in Chapter 3 according to the Box-Behnkan design (Table 3.1) (a total of 45 input settings for models 1 to 3). These variant input settings correspond to a total of 450 simulation runs, as each parameter setting is executed for 10 multiple runs.

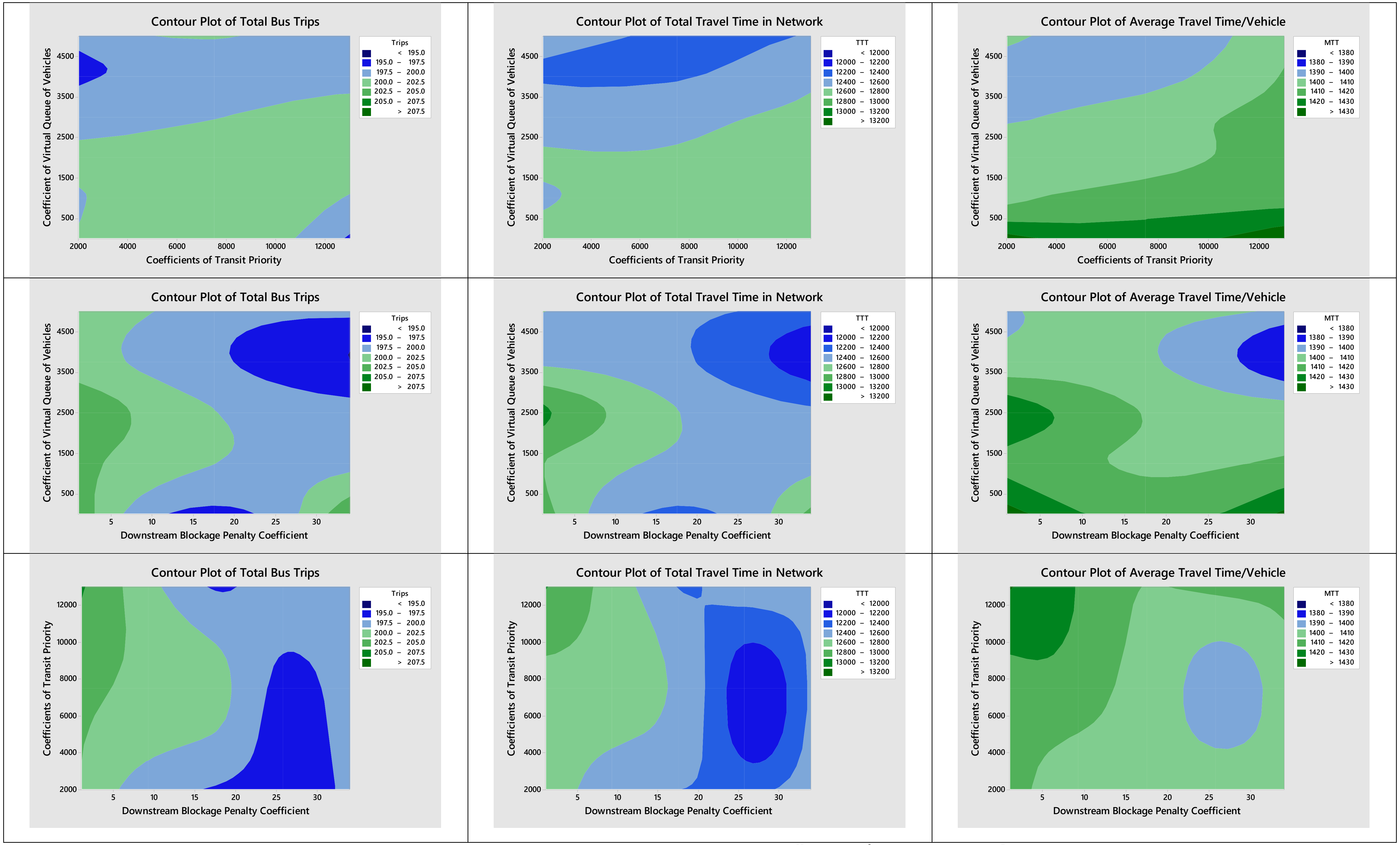

Figure 6.14: Contour plot of the three responses of N_{bus} $(Trips)$, T_t (TTT) and t_m (MTT) for various parameters of β^V (BQL), β^bor β^p (BTP), and β^B (BDC) for dual actuated control and demand case “F”

6.3.1 Analysis

The multi-objective optimization methodology (maximizing of N_{bus} ($Trips$), while simultaneously minimizing both T_t (TTT) and t_m (MTT)) is used to solve these three models by the composite desirability function, as described in Chapter 3. None of the above models resulted in acceptable desirability levels (within the model input range) using the set three objective functions (maximizing of N_{bus} ($Trips$), while simultaneously minimizing both T_t (TTT) and t_m (MTT)). The optimum values of the coefficients are mostly border values (upper bound or lower bound of the specified regions).

Further analysis is done for the all the models using either double or single objective function(s). The conducted analyses still indicated optimal solutions at the borders of the parameter regions. Only model 3 has shown good performance, and it is discussed hereafter.

First, the optimization is done only considering one objective function (maximizing of N_{bus} ($Trips$)) as shown in Figure 6.15. The resulting optimal variable setting is presented in Table 6.16. This setting is 1389.3, 6848.48, and 4.54 for the β^V (BQL), β^bor β^p (BTP), and β^B (BDC), respectively, with the response N_{bus} ($Trips$) of 207.6, and 1.22 (95% CI = 204.82, 210.43) standard error (SE).

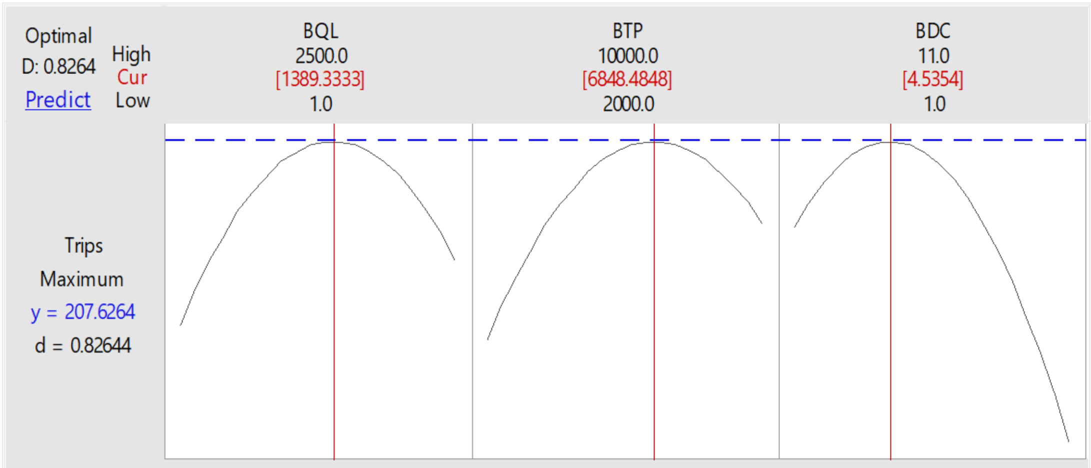

Figure 6.15: Optimization of N_{bus} $(Trips)$ for various parameters of β^V (BQL), β^bor β^p (BTP), and β^B (BDC), for dual actuated control under "F" demand scenario

Table 6.16: Optimal variable setting of coefficients for the response of N_{bus} $(Trips)$ for dual actuated control with demand case "F"

Coefficients			**Responses**	
β^V (BQL)	β^bor β^p (BTP)	β^B (BDC)	N_{bus} $(Trips)$	SE (95% CI)
1389.3	6848.48	4.54	207.6	1.22 (204.8, 210.4)

The optimization is done afterward considering two objective functions (maximizing of N_{bus} $(Trips)$, while simultaneously minimizing t_m (MTT)), as shown in Figure 6.16. The resulting optimal variable setting is presented in Table 6.17. This setting is 1767.97, 5151.5, and 5.24 for β^V (BQL), β^bor β^p (BTP), and β^B (BDC), respectively. The optimal responses are 206.8 for N_{bus} $(Trips)$ with a standard error (SE) of 1.19 (95% CI = 204.1, 209.5) and 1405.4 seconds for t_m (MTT) with a standard error (SE) of 4.40 (95% CI = 1395.4, 1415.4).

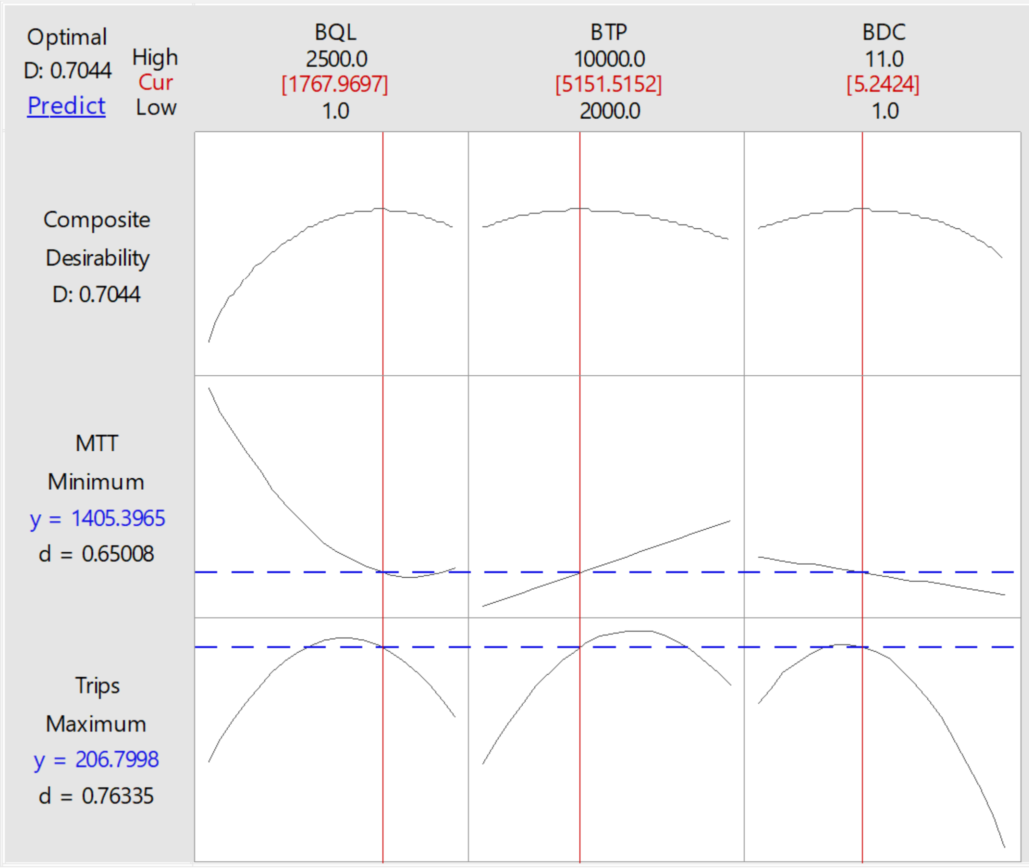

Figure 6.16: Optimization of N_{bus} $(Trips)$, and t_m (MTT) for various parameters of β^V (BQL), β^bor β^p (BTP), and β^B (BDC), for dual actuated control under "F" demand scenario

Table 6.17: Optimal variable setting of coefficients for the response for dual actuated control of "F" demand scenario

Coefficients			**Responses**			
β^V (BQL)	β^bor β^p (BTP)	β^B (BDC)	N_{bus} $(Trips)$	SE (95% CI)	t_m (MTT) (seconds)	SE (95% CI)
1767.97	5151.5	5.24	206.8	1.19 (204.1, 209.5)	1405.4	4.40 (1395.4, 1415.4)

RSM Statistics (ANOVA table)

Regardless of the number and nature of used objective function(s) to identify the optimal setting (single, dual or triple), the model itself is the same. Only the optimal settings vary according to the preset objective function(s). In 3rd model, the response surface model of N_{bus} $(Trips)$ is significant (R-square = 77.71%), as shown in Table 6.18.

Table 6.18: Summary of ANOVA for N_{bus} $(Trips)$ versus various β^V (BQL), β^bor β^p (BTP), and β^B (BDC) for dual actuated control of "F" demand scenario

Source		**Sum of Squares**	**df**	**Mean Square**	**F**
Linear		47.695	3	15.898	3.29**
	β^V	3.125	1	3.125	0.65*
	β^p	10.125	1	10.125	2.09*
	β^B	34.445	1	34.445	7.12**
Square		87.216	3	29.072	6.01**
	$\beta^V*\beta^V$	31.159	1	31.159	6.44**
	$\beta^p*\beta^p$	25.056	1	25.056	5.18**
	$\beta^B*\beta^B$	44.075	1	44.075	9.11**
Lack-of-Fit		16.755	6	2.792	0.25*
Total		173.6	14		

*p > 0.1
**p < 0.1

The second order regression equation of N_{bus} $(Trips)$ versus β^V (BQL), β^bor β^p (BTP), and β^B (BDC) is:

N_{bus} $(Trips)$ (Dual Actuated Control under "F" Demand Scenario)

$$= 193.59 + 0.00515\,\beta^V + 0.002235\ \beta^p + 1.243\,\beta^B$$

$$- 0.000002\,\beta^V * \beta^V - 0.0000001\ \beta^p * \beta^p - 0.1382\,\beta^B * \beta^B$$

Additionally, the response model of t_m (MTT) is significant (R-square = 62.75%), as shown in Table 6.19.

Table 6.19: Summary of ANOVA for t_m (MTT) versus various β^V (BQL), β^bor β^p (BTP), and β^B (BDC) for dual actuated control of "F" demand scenario

Source		**Sum of Squares**	**df**	**Mean Square**	**F**
Linear		1604.96	3	534.99	3.68**
	β^V	1384.32	1	1384.32	9.53**
	β^p	146.85	1	146.85	1.01*
	β^B	73.79	1	73.79	0.51*
	β^V*β^V	455.81	1	455.81	3.14**
	β^V*β^p	140.8	1	140.8	0.97*
Lack-of-Fit		716.73	7	102.39	0.35*
Total		3508.24	14		

*p > 0.1
**p < 0.1

The second order regression equation of t_m (MTT) versus β^V (BQL), β^bor β^p (BTP), and β^B (BDC) is:

t_m (MTT) (Dual Actuated Control under "F" Demand Scenario) (seconds) =

$$14440.3 - 0.0354\,\beta^V - 0.00041\ \beta^p - 0.607\,\beta^B$$

$$+\,0.000007\,\beta^V * \beta^V + 0.000001\,\beta^V * \beta^p$$

Finally, the response model of T_t (TTT) is significant (R-square =54.49%), as shown in Table 6.20.

Table 6.20: Summary of ANOVA for T_t (TTT) versus various β^V (BQL), β^bor β^p (BTP), and β^B (BDC) for dual actuated control of "F" demand scenario

Source		**Sum of Squares**	**df**	**Mean Square**	**F**
Linear		175291	3	58430	1.29*
	β^V	110	1	110	0*
	β^p	40086	1	40086	0.89*
	β^B	135095	1	135095	2.99**
Square		312028	2	156014	3.45**
	$\beta^p * \beta^p$	188109	1	188109	4.16**
	$\beta^B * \beta^B$	146002	1	146002	3.23**
Lack-of-Fit		143542	7	20506	0.16*
Total		894250	14		

*p > 0.1
**p < 0.1

The second order regression equation of T_t (TTT) versus β^V (BQL), β^bor β^p (BTP), and β^B (BDC) is:

$$T_t\ (TTT)\ (Dual\ Actuated\ Control\ under\ "F"\ Demand\ Scenario)\ \text{(hours)}$$
$$= 12250 + 0.003\,\beta^V + 0.1865\ \beta^p + 69.2\,\beta^B$$
$$- 0.000014\ \beta^p * \beta^p - 7.93\,\beta^B * \beta^B.$$

6.3.2 Optimum selection (model validation)

For different objective functions, different optimal settings are obtained. In specific, herein we refer to the optimum settings of the coefficients of β^V (BQL), β^bor β^p (BTP), and β^B (BDC) related to the solutions:

III. where only N_{bus} $(Trips)$ is maximized (as indicated in Table 6.16)

IV. where N_{bus} $(Trips)$ is maximized and t_m (MTT) is minimized (as indicated in Table 6.17)

To select only one set of values, to generalize its use with the dual actuated controller under the "F" demand scenario, a verification/validation process is deployed. The validation process entails running the simulation with the identified values (in Tables 6.16 and 6.17). Each dataset was used in ten (10) multiple runs and the resulting responses were then averaged and reported as shown in Table 6.21. The resulting average N_{bus} $(Trips)$, t_m (MTT) and T_t (TTT) of the 10 simulation runs (as shown in Table 6.21) lie within the 95% confidence interval (corresponding values) extracted from the response surface model (as shown in Table 6.16 for variable setting I, and Table 6.17 for variable setting II).

The 1st set of variables (I) (β^V $(BQL) = 1389.3$, β^bor β^p $(BTP) = 6848.48$, and β^B (BDC)= 4.54) is selected as the default general setting of the dual actuated controller under the demand case "F". The set results more values of N_{bus} $(Trips)$, as well as less values of t_m (MTT) and T_t (TTT) than another set as shown in Table 6.21.

Table 6.21: Optimal variable settings of β^V (BQL), β^bor β^p (BTP), and β^B (BDC) and corresponding simulation-based MOE's (N_{bus} $(Trips)$, t_m (MTT) (seconds), T_t (TTT) (hours)) for dual actuated control of "F" demand scenario

Variable Settings	**Coefficients**			**Responses**		
	β^V (BQL)	β^bor β^p (BTP)	β^B (BDC)	N_{bus} $(Trips)$	t_m (MTT) (seconds)	T_t (TTT) (hours)
I. (only N_{bus} $(Trips)$ is maximized)	1389.3	6848.48	4.54	**206.1**	**1418.4**	**13075.3**
II. (N_{bus} $(Trips)$ is maximized and t_m (MTT) is minimized)	1767.97	5151.5	5.24	204.5	1423.1	13085.9

It is worth noting that the total network travel time T_t (TTT) was not explicitly used an optimization criterion in any of the above two solutions (I and II). Nonetheless, it is legitimate to say that T_t (TTT) was implicitly accounted in obtaining the optimal settings II; as it directly relates to the trip's average travel time, t_m (MTT) through the formula $\mathrm{t_m} = \frac{\mathrm{T_t}}{\mathrm{N_{trips}}} * 3600$, where $\mathrm{N_{trips}}$ is the total number of vehicles in the network. That is, explicit minimization of t_m (MTT) implies implicit minimization (not explicit) of T_t (TTT).

6.4 Discussion

The optimal variable settings for various controls and their responses with characteristics are discussed in this section. The selected optimal variable settings for the Split Actuated control, Protected Actuated control, and Dual Actuated control under the demand scenario "F" ("F" refers to the traffic demand scenario of "very high" traffic volume) are presented in Table 6.22. Also, the corresponding simulation-based MOE's (N_{bus} $(Trips)$, t_m (MTT) (seconds), T_t (TTT) (hours)) for each setting are shown. From these settings, the dual actuated control has shown best performance, as it delivered more total bus trips (N_{bus}) with similar or less average travel time per trip (t_m). In addition, the split actuated control has shown better performance than protected actuated control considering the total bus trips (N_{bus}) (175.1 vs. 124.8), although it required more average travel time per trip (t_m) (1462.2 vs. 1391.8).

Table 6.22: Optimal variable settings of β^V (BQL), β^bor β^p (BTP), and β^B (BDC) and corresponding simulation-based MOE's (N_{bus} $(Trips)$, t_m (MTT) (seconds), T_t (TTT) (hours)) for various controls of "F" demand scenario

Control	**Coefficients**			**Responses**		
	β^V (BQL)	β^bor β^p (BTP)	β^B (BDC)	N_{bus} $(Trips)$	t_m (MTT) (seconds)	T_t (TTT) (hours)
Split Actuated	1	4818.18	3.2	175.1	1462.2	9335.6
Protected Actuated	303.97	10727.27	1.69	124.8	1391.8	3750.8
Dual Actuated	1389.3	6848.48	4.54	206.1	1418.4	13075.3

In general, optimization deals with finding the best outputs (MOEs) by selecting the input variable settings and often in simulation-based optimization, the input variable settings follow a ratio among them to yield the similar output(s), as they have a similar effect on output(s). Therefore, the effect of various input variable settings using the selected optimal input variable settings is discussed in this section.

As indicated in Chapter 1 and Chapter 5, the typical notion of a robust system is one that performs well across a range of (traffic, geometry, weather, etc.) conditions. The robustness of the system must be ensured at various levels of congestion and across different control types (namely three levels). At the first level, the purpose is to ensure that for each control type (e.g. dual, protected or split) the sensitivity of relative ratios of the parameters.

Here, the "robustness" is examined in the context of the degree of sensitivity of the control system performance as a function of the scale of the input variable, while holding the relative ratio between these variables constant. The conclusion from this analysis is that the system is robust because (for most cases) performance of the system remains relatively constant regardless of the absolute magnitude of the parameter values as long as the relative ratios of the parameter values remain constant. The other two levels of robustness checking are summarized in Chapter 7.

More specifically, this section focuses on testing the "robustness" of the various controllers under fixed relative proportions among the various inputs. That is, will the performance of a specific controller change if the absolute values of the penalty coefficients (inputs) change, but the relative proportions among these penalties remain the same? It is believed that no matter what are the absolute values of these penalty coefficients, what determines the optimal setting is a specific "relative" proportion among them for each specific controller. If the controller performance does not change with the change of the absolute penalty values (while keeping the relative proportions fixed), this reflects system robustness.

In the remaining part of this section, the robustness testing of the split actuated control is presented first, followed by the ones for the protected actuated control, and finally for the dual actuated control.

6.4.1 Split Actuated Control

The selected optimal variable settings (β^V $(BQL) = 1$, β^bor β^p $(BTP) = 4818.18$, and β^B $(BDC)= 3.2$) for split actuated controls under "F" demand scenario is presented in Table 6.23. These absolute values if rounded would result in the relative ratios of 0.3:1505.7:1 (β^V (BQL) : β^bor β^p (BTP): β^B (BDC)). Using this fixed relative ratio, several input variable settings were developed and simulated. Each setting as indicated in Table 6.24 was simulated 100 times, and the average MOE's of these runs were reported. The results of the various settings (with the same relative ratio) are shown in Table 6.24. The results (in Table 6.24) show that the responses using this fixed ratio are not similar (increasing towards the higher absolute values, especially at 6.3, 30113.6, 20 (β^V (BQL) : β^bor β^p (BTP): β^B (BDC)), and decreasing towards the lower absolute values at 0.3, 1505.7, 1 (β^V (BQL) : β^bor β^p (BTP): β^B (BDC)).

Table 6.23: Selected optimal variable settings of β^V (BQL), β^bor β^p (BTP), and β^B (BDC) and corresponding simulation-based MOE's (N_{bus} $(Trips)$, t_m (MTT) (seconds), T_t (TTT) (hours)) for split actuated controls of "F" demand scenario

Coefficients			**Responses**		
β^V (BQL)	β^bor β^p (BTP)	β^B (BDC)	N_{bus} $(Trips)$	t_m (MTT) (seconds)	T_t (TTT) (hours)
1	4818.18	3.2	175.1	1462.2	9335.6

Table 6.24: Several variable settings with the ratio of optimal variable settings of β^V (BQL), β^bor β^p (BTP), and β^B (BDC) and corresponding simulation-based (from 100 runs) MOE's (N_{bus} $(Trips)$, t_m (MTT) (seconds), T_t (TTT) (hours)) for split actuated controls of "F" demand scenario

Coefficients			**Responses**		
β^V (BQL)	β^bor β^p (BTP)	β^B (BDC)	N_{bus} $(Trips)$	t_m (MTT) (seconds)	T_t (TTT) (hours)
0.3	1505.7	1	162.8	1365.2	8136.2
0.9	4517.1	3	173.2	1466.1	9357.5
1.6	7528.4	5	173.6	1442.0	9302.0
3.1	15056.8	10	173.6	1453.3	9360.6
6.3	30113.6	20	184.7	1549.9	10665.8

Figure 6.17 shows the rolling average of 10 runs of total bus trips (Trips) from 100 simulation runs for several variable settings using the ratio of optimal variable settings of β^V (BQL), β^bor β^p (BTP), and β^B (BDC) for split actuated controls under "F" demand scenario. If the least and highest values are excluded, there is a similarity among the several variable settings. The total bus trips (Trips) ranges from 156.6 to 191.1.

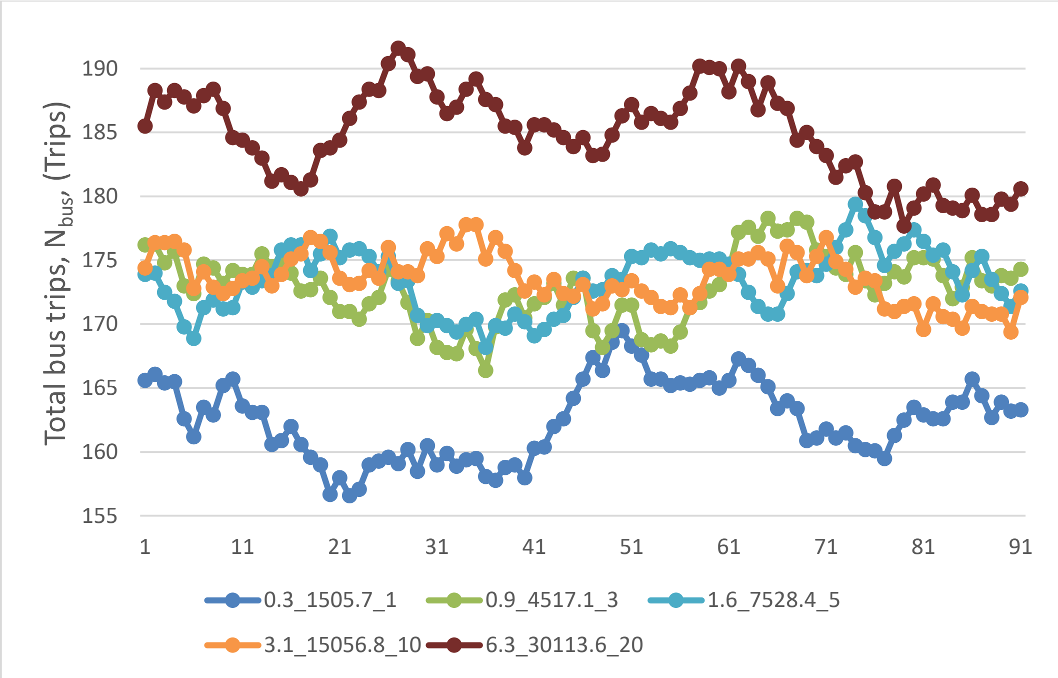

Figure 6.17: Ten runs rolling average of total bus trips (Trips) for several variable settings with the fixed ratio of optimal variable settings of β^V (BQL), β^bor β^p (BTP), and β^B (BDC) for the split actuated controller of "F" demand scenario

6.4.2 Protected Actuated Control

The selected optimal variable settings (β^V $(BQL) = 303.97$, β^bor β^p $(BTP) =$ 10727.27, and β^B (BDC)= 1.69) for protected actuated controls under "F" demand scenario is presented in Table 6.25. These absolute values if rounded would result in the relative ratios of 179.9:6347.5:1 (β^V (BQL) : β^bor β^p (BTP): β^B (BDC)).

Using this fixed relative ratio, several input variable settings were developed and simulated. Each setting as indicated in Table 6.26 was simulated 100 times, and the average MOE's of these runs were reported. The results of the various settings (with the same relative ratio) are shown in Table 6.26. The results (in Table 6.26) indicate that the responses using this fixed ratio are more or less similar, and closely identical to the responses obtained with the selected optimal input variable settings (Table 6.25).

Table 6.25: Selected optimal variable settings of β^V (BQL), β^bor β^p (BTP), and β^B (BDC) and corresponding simulation-based MOE's (N_{bus} $(Trips)$, t_m (MTT) (seconds), T_t (TTT) (hours)) for protected actuated controls of "F" demand scenario

Coefficients			**Responses**		
β^V (BQL)	β^bor β^p (BTP)	β^B (BDC)	N_{bus} $(Trips)$	t_m (MTT) (seconds)	T_t (TTT) (hours)
303.97	10727.27	1.69	124.8	1391.8	3750.8

Table 6.26: Several variable settings with the ratio of optimal variable settings of β^V (BQL), β^bor β^p (BTP), and β^B (BDC) and corresponding simulation-based (from 100 runs) MOE's (N_{bus} $(Trips)$, t_m (MTT) (seconds), T_t (TTT) (hours)) for protected actuated controls of "F" demand scenario

Coefficients			**Responses**		
β^V (BQL)	β^bor β^p (BTP)	β^B (BDC)	N_{bus} $(Trips)$	t_m (MTT) (seconds)	T_t (TTT) (hours)
179.9	6347.5	1	123.9	1398.1	3734.9
539.6	19042.5	3	124.2	1397.8	3767.5
899.3	31737.5	5	124.2	1429.3	3937.8
1798.6	63475.0	10	126.2	1530.6	4407.5
3597.3	126949.9	20	126.1	1557.4	4528.0

Figure 6.18 shows the rolling average of 10 runs of total bus trips (Trips) from 100 simulation runs for several variable settings using the ratio of optimal variable settings of β^V (BQL), β^bor β^p (BTP), and β^B (BDC) for protected actuated controls under "F" demand scenario. There is a similarity among the several variable settings, with the total bus trips (Trips) ranges from 119.7 to 128.9, which are close to the response (total bus trips=124.8) of selected optimal variable settings of β^V (BQL), β^bor β^p (BTP), and β^B (BDC). However, the values of the three responses under the various tested scenarios (Table 6.26) indicate some moderate variations, and some moderate level of robustness of the protected actuated controllers using the fixed relative ratio of 179.9:6347.5:1 for the β^V (BQL): β^bor β^p (BTP): β^B (BDC).

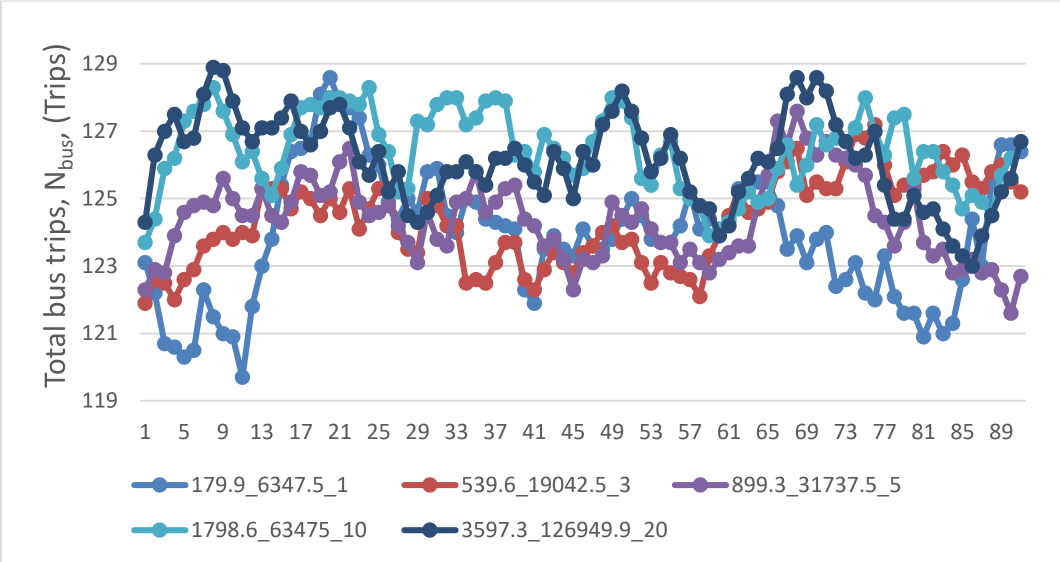

Figure 6.18: Ten runs rolling average of total bus trips (Trips) for several variable settings with the fixed ratio of optimal variable settings of β^V (BQL), β^bor β^p (BTP), and β^B (BDC) for the protected actuated controller of "F" demand scenario

6.4.3 Dual Actuated Control

The selected optimal variable settings (β^V $(BQL) = 1389.3$, β^bor β^p $(BTP) = 6448.48$, and β^B (BDC)= 4.54) for dual actuated controls under "F" demand scenario is presented in Table 6.27. These absolute values if rounded would result in the relative ratios of 306:1508.5:1 (β^V (BQL) : β^bor β^p (BTP): β^B (BDC)).

Using this fixed relative ratio, several input variable settings were developed and simulated. Each setting as indicated in Table 6.28 was simulated 100 times, and the average MOE's of these runs were reported. The results of the various settings (with the same relative ratio) are shown in Table 6.28. The results (in Table 6.28) show that the responses using this fixed ratio are nearly close to a great extent to the responses obtained with the selected optimal input variable settings (Table 6.27).

Table 6.27: Selected optimal variable settings of β^V (BQL), β^bor β^p (BTP), and β^B (BDC) and corresponding simulation-based MOE's (N_{bus} $(Trips)$, t_m (MTT) (seconds), T_t (TTT) (hours)) for dual actuated controls of "F" demand scenario

Coefficients			Responses		
β^V (BQL)	β^bor β^p (BTP)	β^B (BDC)	N_{bus} $(Trips)$	t_m (MTT) (seconds)	T_t (TTT) (hours)
1389.3	6848.48	4.54	206.1	1418.4	13075.3

Table 6.28: Several variable settings with the ratio of optimal variable settings of β^V (BQL), β^bor β^p (BTP), and β^B (BDC) and corresponding simulation-based (from 100 runs) MOE's (N_{bus} $(Trips)$, t_m (MTT) (seconds), T_t (TTT) (hours)) for dual actuated controls of "F" demand scenario

Coefficients			Responses		
β^V (BQL)	β^bor β^p (BTP)	β^B (BDC)	N_{bus} $(Trips)$	t_m (MTT) (seconds)	T_t (TTT) (hours)
306.0	1508.5	1	208.4	1424.2	13223.2
918.0	4525.4	3	208.5	1427.1	13259.5
1530.1	7542.4	5	207.5	1419.6	13159.6
3060.1	15084.8	10	204.6	1409.2	12873.7
6120.3	30169.5	20	203.0	1404.6	12686.2

Figure 6.19 shows the rolling average of 10 runs of total bus trips (Trips) from 100 simulation runs for several variable settings using the ratio of optimal variable settings of β^V (BQL), β^bor β^p (BTP), and β^B (BDC) for dual actuated controls under "F" demand scenario. There is a similarity among the several variable settings, with the total bus trips (Trips) ranges from 197.9 to 213.8, which are close to the response (total bus trips=206.1) of selected optimal variable settings of β^V (BQL), β^bor β^p (BTP), and β^B (BDC). The variations of the three responses under the various tested scenarios (Table 6.28) is almost negligible, and it clearly indicates the robustness of the dual actuated controllers using the fixed relative ratio of 306:1508.5:1 for the β^V (BQL): β^bor β^p (BTP): β^B (BDC).

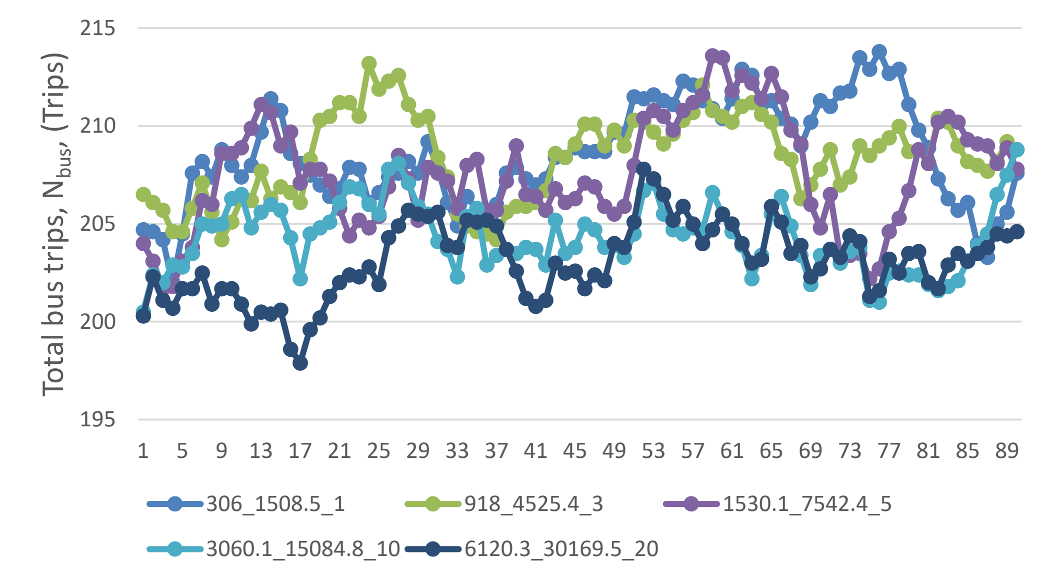

Figure 6.19: Ten runs rolling average of total bus trips (Trips) for several variable settings with the fixed ratio of optimal variable settings of β^V (BQL), β^bor β^p (BTP), and β^B (BDC) for the dual actuated controller of "F" demand scenario

Chapter 7: Conclusions

This chapter concludes with summarizing the major findings of this research in Section 7.1. Section 7.2 highlights the main research contribution. Section 7.3 highlights some of the limitations of this study followed by practical application in section 7.4. Finally, Section 7.5 suggests several future research directions.

7.1 Overview and Summary of Findings

This study provides a thorough review of various aspects of traffic control systems with transit signal priority (TSP), such as the types of TSP concepts and strategies, and the evaluations of these strategies. The study also describes how to implement the Response Surface Methodology (RSM) with single/multiple objective functions to calibrate the parameters of the integrated control system (Ahmed and Hawas, 2015). RSM applies the desirability function approach using the multi-objective simultaneous consideration of the responses. The composite desirability is estimated using the own desirability of each response, which varies from zero to one in dimensionless scale. Then, calibration is done to find the best outputs (optimal measures of effectiveness) by selecting the input variable settings (coefficient for virtual queue of vehicles on the upstream approach link (β^V), coefficients for transit priority (β^b or β^p), and downstream blockage penalty coefficient (β^B)). This is performed under high (“E”) and very high (“F”) traffic demand scenarios for various traffic controllers, such as split actuated, protected actuated, and dual actuated.

Table 7.1 summarizes the major findings of various controllers under high (E) and very high (F) traffic demand scenarios. It shows that all the controllers are robust under different traffic demand scenarios (“E” and “F”) except the split actuated controller under very high traffic demand scenario. The control types are also ranked considering the measures of effectiveness under each traffic demand scenario. The measures of effectiveness are the total number of bus trips served during a specific analysis period, N_{bus}, the trip mean travel time in seconds, t_m, and total network travel time (in hours), T_t. It is evident that the dual actuated control type is performing best under both traffic demand scenarios considering the MOEs of N_{bus} and t_m. It is worthy of note that the rank based on T_t can give the wrong perception. As an example, the protected actuated control type under both traffic demand scenarios is the best, but this is due to the fewer trips (transit and non-transit) which result in lesser total travel time.

Table 7.1: Summary of findings of various controllers under "E" and "F" traffic demand

Control type	**Split Actuated**		**Protected Actuated**		**Dual Actuated**	
Traffic demand	**High (E)**	**Very high (F)**	**High (E)**	**Very high (F)**	**High (E)**	**Very high (F)**
Robustness	Yes	No	Yes	~Yes	Yes	~Yes
Rank based on N_{bus}	1	2	3	3	2	1
Rank based on t_m	2	3	3	1	1	2
Rank based on T_t	3	2	1	1	2	3

* "~" denotes the moderate level of robustness

The performance of the optimal variable settings of various controllers under high ("E") traffic demand, is shown in Table 7.2 compared with the sample mean that is calculated considering all the model's data as explained in Chapters 5 and 6. The sample mean is dependent on the attempted number of cases. The sample mean reflects the average performance of the integrated control system in case it is not appropriately calibrated. The optimal variable settings of the various controllers give the best performance (the highest total bus trips and lowest mean travel time), including the number of non-transit vehicles. Table 7.2 indicates that the split actuated control under "E" traffic demand scenario gives the best performance, as it increases the total bus trips (by nearly 4%) and decreases the mean travel time (by 11%). Other control types (protected actuated, dual actuated) also shows better performance than the corresponding sample mean, as the total bus trips, $\mathrm{N_{bus}}$, is more and mean travel time, $\mathrm{t_m}$, is less.

Table 7.2: Performance of the selected optimal variable settings of β^V , β^bor β^p, and β^B of various controllers under "E" traffic demand

Control type	**Split actuated**		**Protected actuated**		**Dual actuated**	
MOEs	**$\mathbf{N_{bus}}$ (Trips)**	**$\mathbf{t_m}$ (seconds)**	**$\mathbf{N_{bus}}$ (Trips)**	**$\mathbf{t_m}$ (seconds)**	**$\mathbf{N_{bus}}$ (Trips)**	**$\mathbf{t_m}$ (seconds)**
Sample Mean	155.5	942.1	98.8	1034.9	155.2	691.6
Using optimal setting	161.0	838.3	100.1	1012.7	155.2	688.7
Performance	+3.6%	-11.0%	+1.3%	-2.1%	0.0%	-0.4%

Similarly, the performance of the optimal variable of various controllers under very high ("F") traffic demand, is shown in Table 7.3 compared with the sample mean of all the attempted model's data. The split actuated control under "F" traffic demand scenario also shows the best performance, as it gives nearly 5% more total bus trips and 2.4 % lesser mean travel time. Other control types (protected actuated, dual actuated) also shows better performance than the sample mean, as the total bus trips,

N_{bus}, is more and mean travel time, t_m , is less. Only the dual actuated control resulted in very marginal average travel time increase (+0.4%).

Table 7.3: Performance of the selected optimal variable settings of β^V , β^bor β^p, and β^B of various controllers under "F" traffic demand

Control type	**Split actuated**		**Protected actuated**		**Dual actuated**	
MOEs	$\mathbf{N_{bus}}$ **(Trips)**	$\mathbf{t_m}$ **(seconds)**	$\mathbf{N_{bus}}$ **(Trips)**	$\mathbf{t_m}$ **(seconds)**	$\mathbf{N_{bus}}$ **(Trips)**	$\mathbf{t_m}$ **(seconds)**
Sample Mean	166.9	1498.1	121.9	1411.7	200.7	1412.2
Using optimal setting	175.1	1462.2	124.8	1391.8	206.1	1418.4
Performance	+4.9%	-2.4%	+ 2.4%	-1.4%	+2.7%	+0.4%

As indicated in Chapter 1, the robustness of the system must be ensured at various levels of congestion and across different control types (namely three levels). In Chapters 5 and 6, we presented the first level of robustness checking to ensure that for each control type (e.g. dual, protected or split) the sensitivity of relative ratios of the parameters.

The second level of robustness checking is necessary to identify for each control type the optimal robust relative ratio (identified at the first level) that makes each control type effective under different traffic conditions. That is, when the traffic conditions vary, how to set the parameters of each specific controller to perform effectively under such varying traffic conditions. The third level purpose is to identify the "universal" relative parameters ratio that can be applied under varying traffic conditions for all control types together. In the remaining part of this section, we discuss briefly the second and third levels of robustness checking.

For the second level of robustness checking, the purpose is to select the parameter set that can perform efficiently under various traffic demand levels. Given the diversity of traffic conditions a controller may be applied for, and only for the purpose of demonstration, we assume that some intersection is dominantly operated under two traffic demand conditions ("E" and "F"), and each condition corresponds to a different optimal parameter setting. Here, the use of only two traffic conditions is merely to simplify the robustness checking procedure for the reader (not a limitation). In fact, the same methodology can be applied to whatever the number and durations of the prevailing traffic conditions the system may typically operate under.

To ensure the robustness of the controller, some information would be needed about the traffic conditions it is applied to, and the durations. A controller operating under say the F conditions most of the time is different from the one operating under E most of the time. The proportions (and durations) of such traffic conditions may certainly affect the selection of the most robust set of parameters.

Here, an attempt is made to formulate the process of robustness checking. Let's say, "E" is dominant for t_E (hrs.) and "F" is dominate for t_F (hrs.). The total network travel times $T^E_{t_{\beta^E}}$, $T^F_{t_{\beta^E}}$, $T^E_{t_{\beta^F}}$ and $T^F_{t_{\beta^F}}$ are estimated using the two parameter sets β^E, and β^F for "E" and "F" traffic demand conditions, respectively. $T^E_{t_{\beta^E}}$and $T^F_{t_{\beta^E}}$ are the resulting total network travel times (per hour) if the parameter set β^E (identified optimal set for the "E" traffic demand) is used under the "E" and "F" conditions, respectively. Similarly, $T^E_{t_{\beta^F}}$ and $T^F_{t_{\beta^F}}$ are the resulting total network travel times (per hour) if the parameter set β^F (identified optimal set for the "F" traffic demand) is used under the "E" and "F" conditions, respectively. The values of β^E, and β^F are already identified in Chapters 5 and 6.

The total network travel times (T_{β^E}, and T_{β^F}) during the t_E (hrs.) and t_F (hrs.) are calculated as follows:

$$T_{\beta^E} = t_E \times T^E_{t_{\beta^E}} + \; t_F \times T^F_{t_{\beta^E}} \tag{7.1}$$

$$T_{\beta^F} = t_E \times T^E_{t_{\beta^F}} + \; t_F \times T^F_{t_{\beta^F}} \tag{7.2}$$

Comparing between T_{β^E} and T_{β^F} can be simply used to identify the most robust set for a specific controller type. The set that results in lesser total travel time can be identified as the most robust set should be chosen as a default parameter set. For instance, if T_{β^E} is greater than T_{β^F}, then the parameter set of "F" (β^F) will be chosen as a default value and vice versa. In this way, the calibrated parameters under various traffic demands can operate the traffic control system robustly.

The robustness can also be checked using other measures of effectiveness (MOEs) like N_{bus} ($Trips$). The total bus trips (N_{β^E} and N_{β^F}) during the t_E (hrs.) and t_F (hrs.) are calculated using the following equations:

$$N_{\beta^E} = t_E \times N^E_{bus_{\beta^E}} + \; t_F \times N^F_{bus_{\beta^E}} \tag{7.3}$$

$$N_{\beta^F} = t_E \times N^E_{bus_{\beta^F}} + \; t_F \times N^F_{bus_{\beta^F}} \tag{7.4}$$

$N^E_{bus_{\beta^E}}$and $N^F_{bus_{\beta^E}}$ are the total bus trips using the optimal parameter set of "E" traffic demand (β^E) under the traffic demand scenarios of "E" and "F". $N^E_{bus_{\beta^F}}$ and $N^F_{bus_{\beta^F}}$ are also the total bus trips using the optimal parameter set of "F" traffic demand (β^F) under the traffic demand scenarios of "E" and "F". Comparing between N_{β^E} and N_{β^F}, if N_{β^E} is greater than N_{β^F}, then the parameter set of "E" (β^E) is more robust and will be chosen as a default value and vice versa.

To demonstrate the process, we assume a hypothetical condition where each controller operates under the E and F traffic conditions equally for say 1.5 hrs each.

That is, assuming equal t_E and t_F of 1.5 hrs. The total travel times ($T^E_{t_{\beta^E}}$, $T^F_{t_{\beta^E}}$, $T^E_{t_{\beta^F}}$ and $T^F_{t_{\beta^F}}$) are estimated using the two parameter sets for the dual actuated control as shown in Table 7.4. The total travel times (T_{β^E}, and T_{β^F}) are calculated using the Eqs. (7.1) and (7.2) (T_{β^E} is 19583.7 hours and T_{β^F} is 19953.8 hours). Since T_{β^E} is lesser than T_{β^F}, then the parameter set of "E" (β^E) is more robust and is chosen as a default value. Moreover, N_{β^E}, and N_{β^F} are also calculated using the Eqs. (7.3) and (7.4) (N_{β^E} is 358 trips and N_{β^F} is 361.6 trips). Since N_{β^E} is lesser than N_{β^F}, then the parameter set of "F" (β^F) can be chosen as a default value. Due to the different conclusions in studying various MOE (travel times or number of bus trips), a subjective judgment should be made weighing the overall pros and cons. Here, the parameter set of "F" (β^F) is considered more robust given higher weight to the set that maximizes the bus trips throughput. In conclusion, β^F is selected as the most robust parameter set for the dual TSP integrated controller.

Table 7.4: Simulation-based MOE's (N_{bus} (Trips), t_m (seconds), T_t (hours)) using different optimal variable settings for dual actuated controls under "E" and "F" demand scenarios

Traffic demand	**Optimal parameter set**	**Responses**			**Total**	
		$\boldsymbol{N_{bus}}$ $\boldsymbol{(trips)}$	$\boldsymbol{t_m}$ **(seconds)**	$\boldsymbol{T_t}$ **(hours)**	$\boldsymbol{N_{bus}}$ $\boldsymbol{(trips)}$	$\boldsymbol{T_t}$ **(hours)**
"E"	β^E	155.2	688.7	6901.9	358.1	19583.7
"F"	β^E	202.9	1409.7	12681.8		
"E"	β^F	155.5	686.0	6878.5	361.6	19953.8
"F"	β^F	206.1	1418.4	13075.3		
Conclusion: $\boldsymbol{\beta^F}$ is more robust considering the priority of bus trips					β^F	β^E

Tables 7.5 and 7.6 show the results of robustness for the split and protected actuated controllers under "E" and "F" traffic demand scenarios. The parameter set of "F" (β^F) is clearly more robust as shown in tables 7.5 and 7.6, as T_{β^E} is greater than T_{β^F} and N_{β^E} is lesser than N_{β^F} for both traffic control types. Therefore, the parameter set of "F" (β^F) is more robust for the split and protected controllers.

Table 7.5: Simulation-based MOE's (N_{bus} (Trips), t_m (seconds), T_t (hours)) using different optimal variable settings for split actuated controls under "E" and "F" demand scenarios

Traffic demand	Optimal parameters set	Responses			Total	
		N_{bus} ($trips$)	t_m (seconds)	T_t (hours)	N_{bus} ($trips$)	T_t (hours)
"E"	β^E	161.0	838.3	8190.6	328.8	18239.7
"F"	β^E	167.8	1502.1	10049.1		
"E"	β^F	160.8	831.7	8152.4	335.9	17488
"F"	β^F	175.1	1462.2	9335.6		
		Conclusion: $\boldsymbol{\beta^F}$ is more robust.			β^F	β^F

Table 7.6: Simulation-based MOE's (N_{bus} (Trips), t_m (seconds), T_t (hours)) using different optimal variable settings for protected actuated controls under "E" and "F" demand scenarios

Traffic demand	Optimal parameters set	Responses			Total	
		N_{bus} ($trips$)	t_m (seconds)	T_t (hours)	N_{bus} ($trips$)	T_t (hours)
"E"	β^E	100.1	1012.7	3536.9	221.3	7372.6
"F"	β^E	121.2	1425.7	3835.7		
"E"	β^F	101.1	998.8	3444.1	225.9	7194.9
"F"	β^F	124.8	1391.8	3750.8		
		Conclusion: $\boldsymbol{\beta^F}$ is more robust.			β^F	β^F

If the traffic demand in an intersection is not similar to the calibrated demand scenarios ("E" and "F"), then it is suggested to recalibrate the system under that traffic demand condition for better performance. The performance of the system is dependent on the parameters (as discussed in Eq. 2.1 to Eq. 2.3) that are likely to change due to the alteration of traffic demand as well as traffic control phasing (split, protected, and dual). As such, it is advisable to calibrate the system under all prevailing traffic conditions individually, then to identify the most robust set of parameters using equations 7.1 through 7.4 as explained earlier.

Tables 7.4 and 7.5 show that the parameter set of “F” (β^F) gives better performance than the parameter set of “E” (β^E). To identify the “universal” set of parameters that can be applied among the various control types and under all traffic conditions, one should examine the effectiveness of the identified robust parameters for all control types.

The parameter set of “F” (β^F) of dual actuated controller produces the best performance when applied for all traffic control types (split, protected, and dual) under both “E” and “F” traffic demand conditions, as shown in Table 7.7. The results from Table 7.7 show that the β^F for dual actuated control produces quite similar MOEs (N_{bus} (trips), t_m (seconds), T_t (hours)) compared to the optimal parameter set using RSM for the control type under the particular traffic demand (“E” or “F”) in almost all scenarios (except for the split actuated control under “F” traffic demand but similar bus trips are produced). Therefore, the β^F for dual actuated control is identified as the most robust parameter set for various control types (split, protected, and dual) under both traffic demand of “E” and “F” considering the bus trips.

Table 7.7: Simulation-based MOE's (N_{bus} (trips), t_m (seconds), T_t (hours)) using different optimal variable settings for various control types under traffic demand of "E" and "F"

Traffic demand	Control type	Optimal parameter set	Responses		
			N_{bus} ($trips$)	t_m (seconds)	T_t (hours)
"E"	Split	β^E of split control (using RSM)	161.0	838.3	8190.6
		$\boldsymbol{\beta^F}$ **of dual control**	161.5	844.5	8249.0
"E"	Protected	β^E of protected control (using RSM)	100.1	1012.7	3536.9
		$\boldsymbol{\beta^F}$ **of dual control**	100.7	1017.4	3535. 7
"E"	Dual	β^E of dual control (using RSM)	155.2	688.7	6901.9
		$\boldsymbol{\beta^F}$ **of dual control**	155.5	686.0	6878.5
"F"	Split	β^F of split control (using RSM)	175.1	1462.2	9335.6
		$\boldsymbol{\beta^F}$ **of dual control**	174.0	1556.9	10675.7
"F"	Protected	β^F of protected control (using RSM)	124.8	1391.8	3750.8
		$\boldsymbol{\beta^F}$ **of dual control**	124.2	1379.5	3855.8

Figure 7.1 compares the N_{bus} obtained from different optimal variable settings (optimal parameter set from RSM that was obtained for each control type under the traffic demand of "E" and "F") versus the optimal parameter set, β^F, of the dual actuated control under "F" traffic demand) for various control types under traffic

demand of "E" and "F". In all scenarios, the obtained bus trips by β^F of the dual actuated control under "F" traffic demand are almost similar to others.

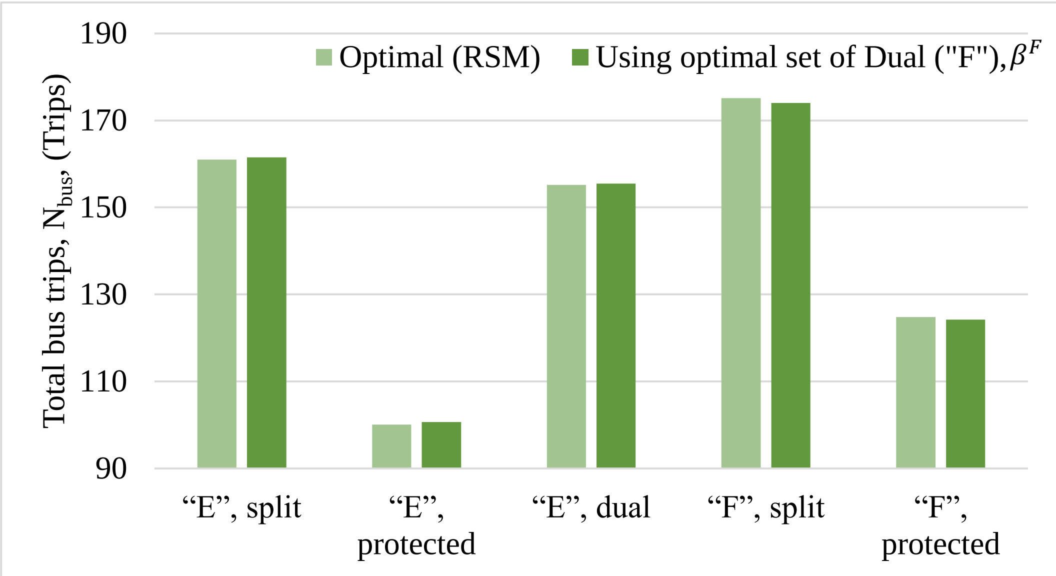

Figure 7.1: Comparison of optimal variable settings (optimal from RSM vs. β^F of dual control) using N_{bus} (trips) for various control types under "E" and "F"

The obtained mean travel times by β^F of the dual actuated control under "F" traffic demand are also similar to the mean travel times using the optimal set of the parameters of the controller itself as shown in Figure 7.2 (except for the split actuated control under "F" traffic demand, where β^F of the dual control under "F" traffic demand produces more mean travel time (1556.9 sec) than the optimal parameter set using RSM (1462.2 seconds)). Similarly, comparison of the total travel times T_t is presented in Figure 7.3. The β^F of the dual control under "F" traffic demand produces similar total travel times compared to the values of the optimal parameter sets (except for the split controller case under "F", where than the optimal parameter set using RSM yields total travel time of 9335.6 hours versus 10675.7 hours when the β^F of the dual control are used). Therefore, the parameter set (β^F) of the dual control under "F" traffic demand is quite robust, even if applied among all other controllers, it still produces MOEs quite close to the values obtained if the optimal parameter sets of the controller type itself are used. This identifies the (β^F) of the dual control to be the most robust parameter set and as such it should be used as the default for the various control types under both traffic demand of “E” and “F”.

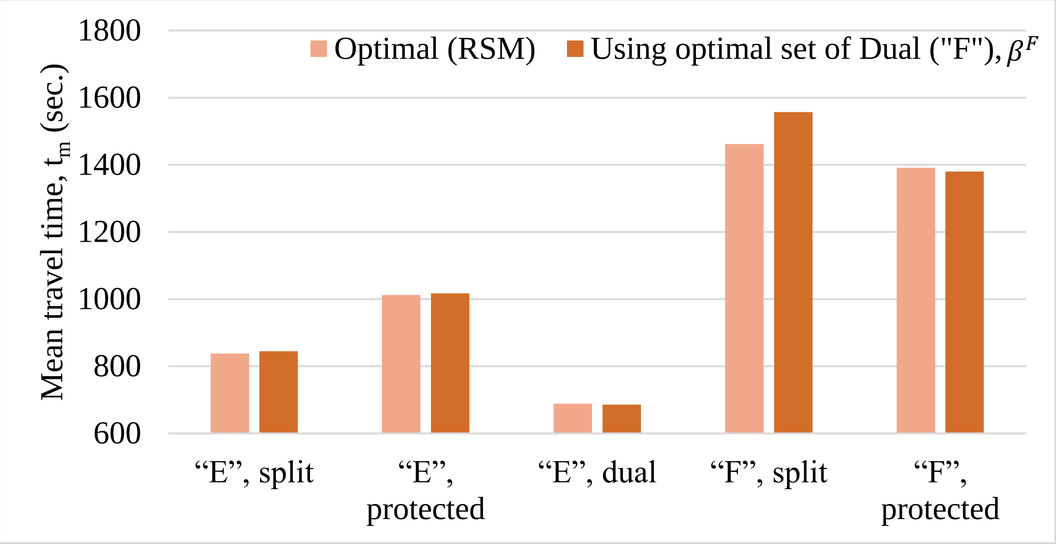

Figure 7.2: Comparison of optimal variable settings (optimal from RSM vs. β^F of dual control) using t_m (seconds) for various control types under “E” and “F”

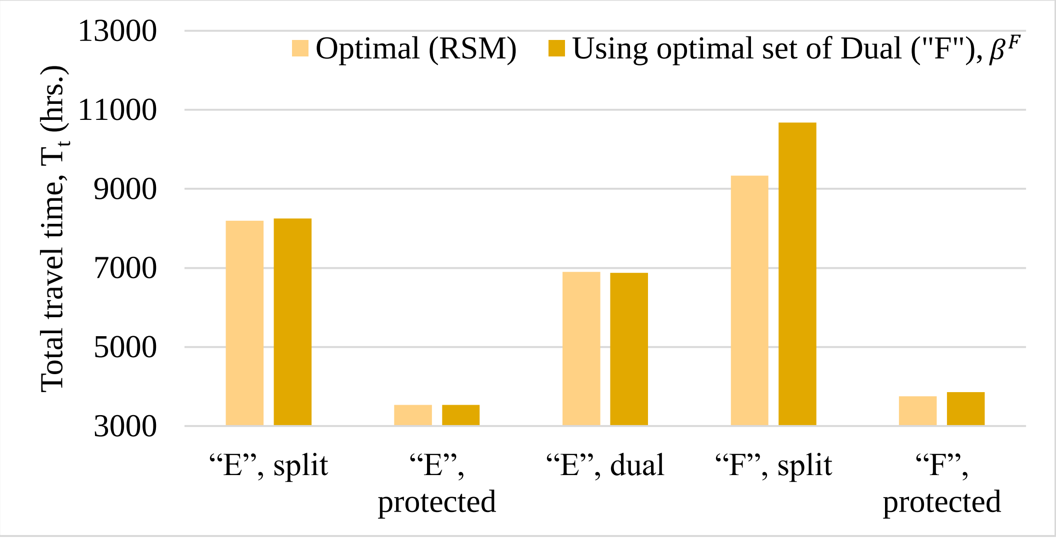

Figure 7.3: Comparison of optimal variable settings (optimal from RSM vs. β^F of dual control) using T_t (hours) for various control types under “E” and “F”

Calibrating the traffic control system for each traffic demand is impractical. Therefore, the robust control type should be chosen for the different demand levels. As an example, under very high ("F") traffic demand scenario, split actuated controller is not robust, but the dual actuated controller is. Furthermore, dual actuated controller shows the best performance considering measures of effectiveness (total bus trips, N_{bus}, and mean travel time, $\mathrm{t_m}$). Also, β^F of dual control has proven to be the most robust set even when applied to other controller types under either the E or F conditions, As such, it is preferable to use dual actuated controller settings at the very high demand levels; as this will certainly provide best performance and robust solutions.

7.2 Research Contributions

The primary contribution of this thesis is setting the framework and method that entails the application of the Response Surface Methodology (RSM) to calibrate the complex integrated traffic control system. The suggested method was assessed via extensive case study analysis of the integrated control system developed by Ahmed and Hawas (2015). The system has the advanced traffic management strategies, such as transit signal priority, incident detection, and management. The suggested RSM calibrates the parameters of the integrated system by selecting the values that can produce the best measures of effectiveness. The challenging task is to satisfy the requirements of transit and non-transit vehicles, which are very often diverse and conflicting. As an example, if transit signal priority is active in one approach, then the opposite side street would certainly encounter adverse impacts in the form of more delay travel time. RSM uses the desirability function approach as well as the simultaneous multi-objective desirability of the responses.

Another interesting feature of the suggested RSM method is its amenability to handle various control systems with different applications and multiple parameters. There is no limitation on the number of parameters to set optimally, and in fact, the data needed for the search for the optimal settings will not be significantly increased with the higher number of parameters. In brief, no matter what is the control system, its complexity, functions, and number of parameters, the suggested RSM approach can be used.

This research study also presented how to use either single or multiple objective functions to identify the optimal settings. Some of these objective functions may also be contradicting in nature, such as increasing throughput of transit trips and minimizing overall travel time. At first, three objective functions were used to calibrate the traffic control system. If the identified optimal solutions are always at boundary values not a mid-points of the specified model's regions, then single or double objective functions were alternatively considered. After identifying the optimal set, it (the set) was verified by simulation with 95% confidence interval.

This study also demonstrated how to develop "mathematical" models for estimation of the performance measures vis-à-vis the various parameter values. The calibrated models were proven to be significant. The study also indicated how to validate these optimal settings and ensure their robustness.

7.3 Limitations of the Research

This research study indicated how to apply the suggested RSM to any advanced control systems. To demonstrate the RSM procedure, it was applied to the integrated traffic signal control system developed by Ahmed and Hawas (2015). The integrated control system itself (by Ahmed and Hawas) has some limitations regarding specific assumptions to some variables and parameters. Some of these limitations include:

- Assumed specific geometric parameters such as the number of lanes, phase arrangements, link length, link speed, lane width, saturation flow rate, passenger car length, and heavy vehicle length.
- Specific traffic parameters were assumed such as the right turn percentage, through movement percentage, left turn percentage, peak hour factor, and the percentage of heavy vehicles.

The parameter calibration and the testing of robustness were carried out under certain boundary region. The selected optimal setting of the parameters can be dependent on this boundary region. The process of calibration itself cannot also be applied online; in fact, it is designed to provide off-line optimization of parameters.

7.4 Practical Application (Implementation)

The success of the research is to implement the proposed method for parameter settings in field, and therefore, the guidelines to implement the findings of this study are provided as follows:

- It is found that the parameter values for dual actuated control under “F” traffic demand scenario is robust for all control types (split actuated, protected actuated, and dual actuated) under “E” and “F” traffic demands. Therefore, to implement the Integrated Traffic Signal Control System (Ahmed and Hawas, 2015) in the field in case E” or “F” are the prevailing traffic conditions, it is recommended to use these parameters (β^F of the dual control under “F” traffic demand), if deemed necessary to use various control types.

- The field traffic demand may not be equal to the studied traffic demands (E" and "F"), and as such, the prevailing field traffic demand should be measured, and the corresponding robust parameters should be obtained, verified, and endorsed as shown in this research using the Response Surface Methodology (RSM).

7.5 Future Research Directions

Some of the suggested future research directions include:

- Calibrating the parameters of the traffic signal control itself:

    In the application of the RSM to the integrated control system, it was assumed that the parameters of the signal controller itself would remain fixed; just to narrow down the number of parameters to calibrate and ease tracking the process for the reader. The specific traffic signal parameters such as the minimum green, the maximum green, the vehicular extension period can also be optimized. Future research direction would increase the optimization number of parameters by considering the specific signal control parameters.

- The inclusion of environmental aspects

    Given that the developed framework and the RSM can be applied to multiple objective functions, it should also be valuable to add some measures of performance that reflect the network environmental quality and vehicular emissions explicitly. An additional objective function to minimize the negative environmental impacts can be beneficial.

- Calibration with arterial coordination:

The integrated control system could also be calibrated for coordination of traffic signals along a major arterial corridor for various traffic demands as well as various control types.

References

Abdalhaq, B.K., Baker, M.I.A., 2014. Using Meta Heuristic Algorithms to Improve Traffic Simulation. Journal of Algorithms and Optimization. Oct. 2014, Vol. 2 Iss. 4, PP. 110-128.

Ahmed, F., Hawas, Y.E., 2015. An integrated real-time traffic signal system for transit signal priority, incident detection and congestion management. Transportation Research Part C: Emerging Technologies 60, 52-76.

Bagherian, M., Mesbah, M., Ferreira, L., 2015. Using delay functions to evaluate transit priority at signals. Public Transport 7(1), 61–75.

Balakrishna, R., Antoniou, C., Ben-Akiva, M.E., Koutsopoulos, H.N., Wen, Y., 2007. Calibration of Microscopic Traffic Simulation Models: Methods and Application. Transportation Research Record: Journal of the Transportation Research Board (Vol. 1999), pp 198-207.

Bezerra, M.A., Santelli, R.E., Oliveira, E.P., Villar, L.S., Escaleira, L.A., 2008. Response surface methodology (RSM) as a tool for optimization in analytical chemistry. Talanta 76(5), 965-977.

Box, G.E.P., Wilson, K.B., 1951. On the Experimental Attainment of Optimum Conditions. Journal of the Royal Statistical Society. Series B (Methodological) 13(1), 1-45.

Carson, Y., Maria, A., 1997. Simulation Optimization: Methods And Applications, Simulation Conference, 7-10 Dec. 1997., pp. 118-126.

Chang, T.H., Li, Z.Y., 2002. Optimization of Mainline Traffic Via an Adaptive Coordinated Ramp Metering Control Model with Dynamic OD Estimation. Transportation Research Part C: Emerging Technologies 10(2), p. 99-120.

Chen, C.-H., Schonfeld, P., Paracha, J., 2005. Work Zone Optimization for Two-Lane Highway Resurfacing Projects with an Alternate Route. Transportation Research Record: Journal of the Transportation Research Board (Vol.1911), 51-66.

Ciuffo, B.F., Punzo, V., 2010. Verification of Traffic Micro-simulation Model Calibration Procedures: Analysis of Goodness-of-Fit Measures, Proceedings of 89th Annual Meeting. Washington, DC: Transportation Research Board., p. 20p.

Ciuffo, B.F., Punzo, V., Torrieri, V., 2008. Comparison of Simulation-Based and Model-Based Calibrations of Traffic-Flow Microsimulation Models.

Transportation Research Record: Journal of the Transportation Research Board (Vol. 2088), pp 36-44.

Daamen, W., Buisson, C., Hoogendoorn, S.P., 2015. Traffic simulation and data : validation methods and applications.

Deng, G., 2007. Simulation-based Optimization, Mathematics and Computation in Engineering. University of Wisconsin, Madison, p. 248.

Derringer, G., Suich, R., 1980. Simultaneous Optimization of Several Response Variables. Journal of Quality Technology , vol 12, 1980, pp. 214-219.

Design-Expert, 2015. Design Expert software, Version 10. Stat-Ease, Inc. 2021 E. Hennepin Ave. Suite 480, Minneapolis, MN 55413-2726, USA.

Ding, J., He, Q., Head, K.L., Saleem, F., Wu, W., 2013. Development and Testing of Priority Control System in Connected Vehicle Environment. TRB 92th Annual Meeting.

Dion, F., Hellinga, B., 2002. A rule-based real-time traffic responsive signal control system with transit priority: Application to an isolated intersection. Transportation Research Part B: Methodological 36(4), 325–343.

Ekeila, W., Sayed, T., El Esawey, M., 2009. Development of Dynamic Transit Signal Priority Strategy. Transportation Research Record: Journal of the Transportation Research Board Vol. 2111, 1–9.

Feng, Y., Head, K.L., Khoshmagham, S., Zamanipour, M., 2015. A real-time adaptive signal control in a connected vehicle environment. Transportation Research Part C: Emerging Technologies 55, 460–473.

Ferreira, S.L., Bruns, R.E., Ferreira, H.S., Matos, G.D., David, J.M., Brandao, G.C., da Silva, E.G., Portugal, L.A., Dos Reis, P.S., Souza, A.S., Dos Santos, W.N., 2007. Box-Behnken design: an alternative for the optimization of analytical methods. Anal Chim Acta 597(2), 179-186.

Fu, M.C., 2015. Handbook of Simulation Optimization. Springer New York, New York, NY.

Ghanim, M.S., Abu-Lebdeh, G., 2015. Real-Time Dynamic Transit Signal Priority Optimization for Coordinated Traffic Networks Using Genetic Algorithms and Artificial Neural Networks. Journal of Intelligent Transportation Systems, 1–12.

Hale, D.K., Antoniou, C., Brackstone, M., Michalaka, D., Moreno, A.T., Parikh, K., 2015a. Comparison of Optimization Methods for Assisted Calibration of

Traffic Micro-Simulation, Transportation Research Board 94th Annual Meeting. Transportation Research Board, Washington, DC, United States.

Hale, D.K., Antoniou, C., Brackstone, M., Michalaka, D., Moreno, A.T., Parikh, K., 2015b. Optimization-based assisted calibration of traffic simulation models. Transportation Research Part C: Emerging Technologies 55, 100-115.

Hawas, Y.E., 2002. Calibrating Simulation Models for Advanced Traveler Information Systems/Advanced Traffic Management Systems Applications. Journal of Transportation Engineering 128(1), 80-88.

Hawas, Y.E., Ahmed, F., 2016. A binary logit-based incident detection model for urban traffic networks. Transportation Letters, 1-14.

He, Q., Head, K.L., Ding, J., 2014. Multi-modal traffic signal control with priority, signal actuation and coordination. Transportation Research Part C: Emerging Technologies 46, 65–82.

Hu, J., Park, B.B., Lee, Y.-J., 2015. Coordinated transit signal priority supporting transit progression under Connected Vehicle Technology. Transportation Research Part C: Emerging Technologies 55, 393–408.

Jafarzadeh-Ghoushchi, S., 2015. Optimization of Transportation System Based on Combined Model Using Artificial Neural Networks and Response Surface Methodology. International Journal of Technical Research and Applications e-ISSN: 2320-8163, www.ijtra.com Special Issue 23 (June-July 2015), PP. 69-76.

Joshi, S.S., Rathi, A.K., Tew, J.D., 1995. An improved response surface methodology algorithm with an application to traffic signal optimization for urban networks. pp. 1104-1109.

Kim, S.-J., Kim, W., Rilett, L.R., 2005. Calibration of Microsimulation Models Using Nonparametric Statistical Techniques. Transportation Research Record: Journal of the Transportation Research Board (Vol. 1935), pp 111-119.

Lee, J.-B., Ozbay, K., 2009. New Calibration Methodology for Microscopic Traffic Simulation Using Enhanced Simultaneous Perturbation Stochastic Approximation Approach. Transportation Research Record: Journal of the Transportation Research Board Vol. 2124, 233-240.

Li, L., Chen, X., Zhang, L., 2016. A global optimization algorithm for trajectory data based car-following model calibration. Transportation Research Part C: Emerging Technologies 68, 311-332.

Lin, Y., Yang, X., Jia, L., Zou, N., 2013. Development of Model-based Transit Signal Priority Control for local Arterials. Procedia - Social and Behavioral Sciences 96, pp. 2344–2353.

Lin, Y., Yang, X., Zou, N., Franz, M., 2015. Transit signal priority control at signalized intersections: A comprehensive review. Transportation Letters: the International Journal of Transportation Research 7(3), 168–180.

Ma, J., Dong, H., Zhang, H.M., 2007. Calibration of Microsimulation with Heuristic Optimization Methods. Transportation Research Record: Journal of the Transportation Research Board (Vol. 1999), pp 208-217.

Ma, T., Abdulhai, B., 2002. Genetic Algorithm-Based Optimization Approach and Generic Tool for Calibrating Traffic Microscopic Simulation Parameters. Transportation Research Record: Journal of the Transportation Research Board (Vol. 1800), p. 6-15.

Ma, W., Liu, Y., Han, B., 2013. A rule-based model for integrated operation of bus priority signal timings and traveling speed. Journal of Advanced Transportation 47(3), 369–383.

Manjunatha, P., Vortisch, P., Mathew, T.V., 2013. Methodology for the Calibration of VISSIM in Mixed Traffic, Transportation Research Board 92nd Annual Meeting. Transportation Research Board, Washington, DC, United States.

Minitab, 2016. Minitab Inc. Minitab, State College, PA.

Mirchandani, P., Lucas, D., 2004. Integrated Transit Priority and Rail/Emergency Preemption in Real-Time Traffic Adaptive Signal Control. Journal of Intelligent Transportation Systems 8(2), 101–115.

Mudigonda, S., Ozbay, K., 2015. Robust calibration of macroscopic traffic simulation models using stochastic collocation. Transportation Research Part C: Emerging Technologies 59, 358-374.

Myers, R.H., Montgomery, D.C., Anderson-Cook, C.M., 2009. Response surface methodology: Process and product optimization using designed experiments, 3rd ed. ed. Wiley, Oxford.

Osorio, C., Chong, L., 2015. A Computationally Efficient Simulation-Based Optimization Algorithm for Large-Scale Urban Transportation Problems. Transportation Science 49(3), 623-636.

Osorio, C., Flötteröd, G., Zhang, C., 2015. A Metamodel Simulation-based Optimization Approach for the Efficient Calibration of Stochastic Traffic Simulators. Transportation Research Procedia 6, 213-223.

Pande, A., Wolshon, B., 2016. Traffic engineering handbook. Institute of Transportation Engineers.

Paz, A., Molano, V., 2014. Development of a Tool for an Efficient Calibration of CORSIM Models, University of Nevada, Las Vegas,Transportation Research Center, Department of Civil and Environmental Engineering, Howard R. Hughes College of Engineering., Augost, 2014.

Paz, A., Molano, V., Martinez, E., Gaviria, C., Arteaga, C., 2015a. Calibration of traffic flow models using a memetic algorithm. Transportation Research Part C: Emerging Technologies 55, 432-443.

Paz, A., Molano, V., Sanchez-Medina, J., 2015b. Holistic Calibration of Microscopic Traffic Flow Models: Methodology and Real World Application Studies. 38, 33-52.

Schultz, G.G., Rilett, L.R., 2004. Analysis of distribution and calibration of car-following sensitivity parameters in microscopic traffic simulation models. Transportation Research Board. 41-51.

Stevanovic, A., 2010. Adaptive traffic control systems : domestic and foreign state of practice. Transportation Research Board, National Cooperative Highway Research Program (NCHRP) Synthesis 403, Washington, D.C.

Teodorović, D., Janić, M., 2017. Transportation Engineering: Theory, Practice, and Modeling. Butterworth-Heinemann.

Treiber, M., Kesting, A., 2013. Microscopic Calibration and Validation of Car-Following Models – A Systematic Approach. Procedia - Social and Behavioral Sciences 80, 922-939.

TSIS-CORSIM, 2010. Traffic Software Integrated System-Corridor Simulation 6.2. Dept. of Transportation, McTrans Center, USA.

Vasconcelos, L., Neto, L., Santos, S., Silva, A.B., Seco, Á., 2014a. Calibration of the Gipps Car-following Model Using Trajectory Data. Transportation Research Procedia 3, 952-961.

Vasconcelos, L., Seco, Á., Silva, A.B., 2014b. Hybrid Calibration of Microscopic Simulation Models. 262, 307-320.

Vaze, V.S., Antoniou, C., Wen, Y., Ben-Akiva, M.E., 2009. Calibration of Dynamic Traffic Assignment Models with Point-to-Point Traffic Surveillance. Transportation Research Record: Journal of the Transportation Research Board (Vol. 2090), pp 1-9.

Zamanipour, M., Head, L., Ding, J., 2014. Priority System for Multimodal Traffic Signal Control, Transportation Research Board 93rd Annual Meeting, p. 13p.

Zhong, R., Fu, K., Sumalee, A., Ngoduy, D., & Lam, W. , 2016. A cross-entropy method and probabilistic sensitivity analysis framework for calibrating microscopic traffic models. Transportation Research Part C: Emerging Technologies. 63, 147-169.

Zhou, G., Gan, A., 2009. Design of Transit Signal Priority at Signalized Intersections with Queue Jumper Lanes. Journal of Public Transportation 12(4), 117–132.

Zhou, G., Gan, A., Shen, L.D., 2007. Optimization of adaptive transit signal priority using parallel genetic algorithm. Tsinghua Science and Technology 12(2), 131–140.

Appendix: A Response Surface Modeling in Minitab

This section describes the steps of Response Surface Modelling design, data importing, model building for each response, and the optimization in Minitab.

A. Response Surface Modeling Design

In order to design the response surface model, the first step is defining the properties of the model, such as the type of design (Box-Behnken, Central Composite), number of factors (continuous, categorical), replications, and blocks, etc. Replicates is also defined as the multiple simulation runs with the same factor settings (levels) and these are subject to the same sources of variability, independently of one another. In response surface design, replicate measurements are taken from multiple simulation runs. Similarly, blocks in response surface design are defined as a group of experiments conducted under relatively homogeneous conditions. In this research study, there is only one block for the simulation-based model, as every measurement is taken under consistent simulated conditions changing only the input (factor settings) not the simulation environment (CORSIM).

First, the "Create Response Surface Design…" is selected from the main menu of Minitab, as Stat ➔ DOE ➔ Response Surface ➔ Create Response Surface Design shown in Figure A.1. Consequently, the "Create Response Surface Design" window opens shown in Figure A.2.

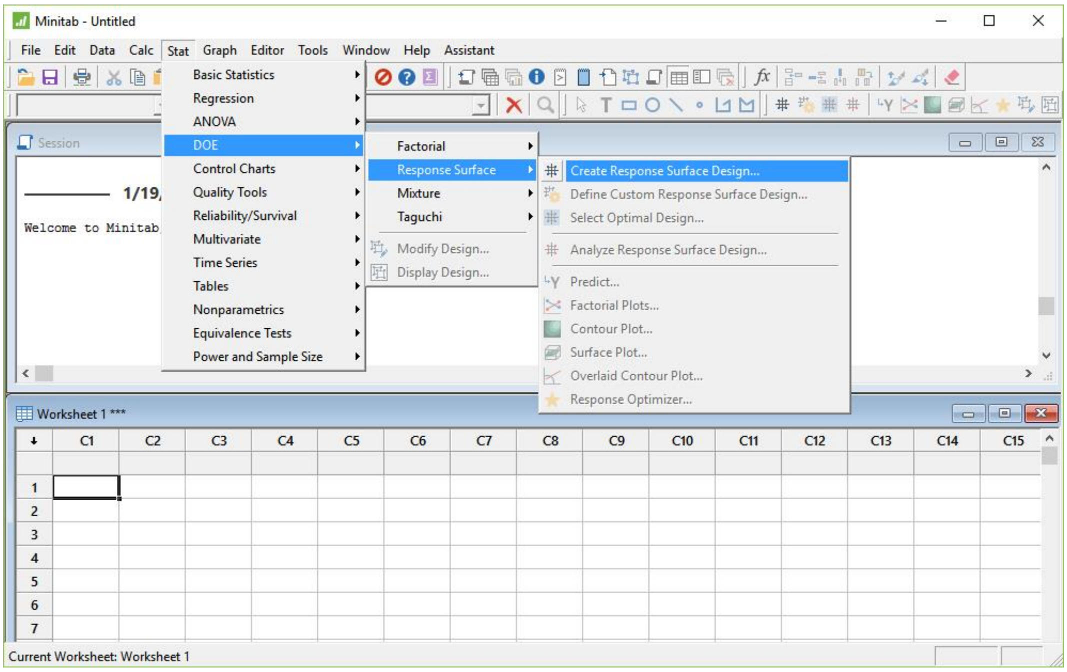

Figure A.1: Selection of “Create Response Surface Design”

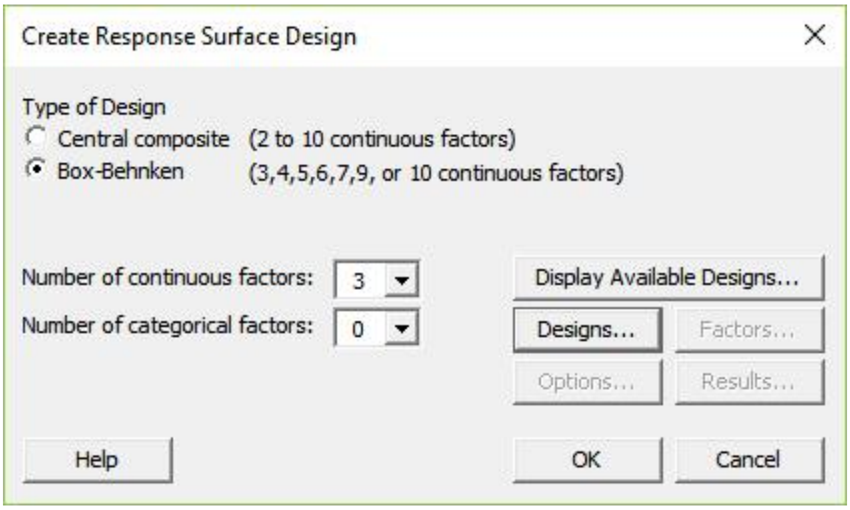

Figure A.2: Selection of “Type of Design” and number of factors

For the “Type of Design”, “Box-Behnken” is selected. For the “Number of continuous factors:”, “3” is selected, representing the various coefficients (β^V, β^bor β^p, and β^B) as shown in Figure A.2. It is to be noted that both $\beta^b$and β^p in the presented model formulation in Chapter 3 are considered equal and as such the number of factors is only three not four.

The "Designs…" tab is selected to set up the number of center points, replicates, blocks, as shown in Figure A.3.

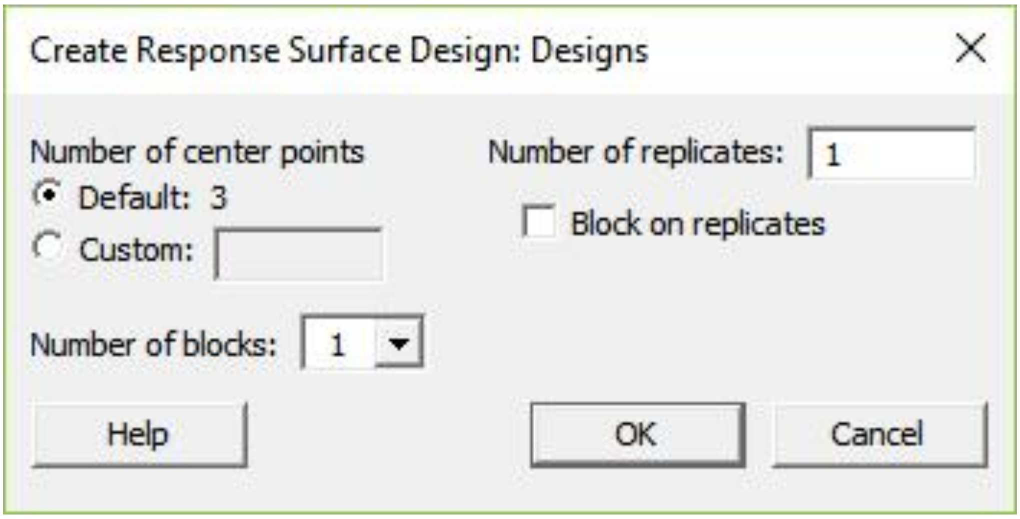

Figure A.3: Selection of number of center points, blocks, and replicates

In Figure A.3, the default "3" number of center point is selected; as well as for the "Number of replicates:" and "Number of blocks:", "1" is kept. It is to be noted that the number of replicates here is set to 1 despite the fact that 10 simulation runs are carried out for each set of factors. The replicate of 1 here represents the average values obtained from the 10 simulation runs.

To keep the settings, "OK" is clicked. Other options such as Factors, Options, and Results are activated, as shown in Figure A.4.

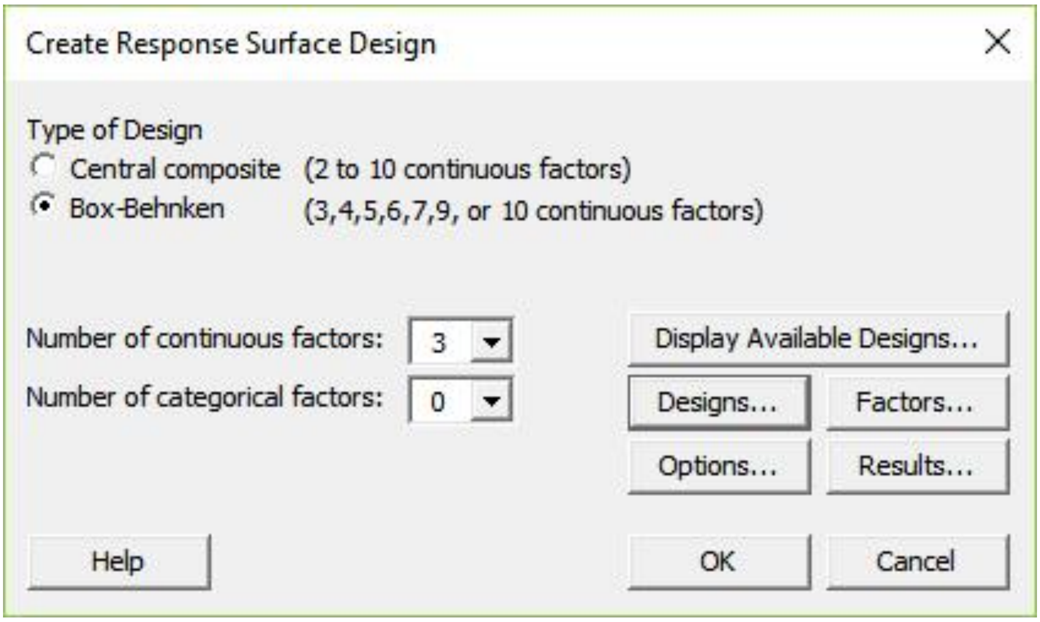

Figure A.4: RSM design after selection of design properties

To input the factors and their levels (low, high), “Factors…” is clicked to open the “Create Response Surface Design: Factors” window shown in Figure A.5.

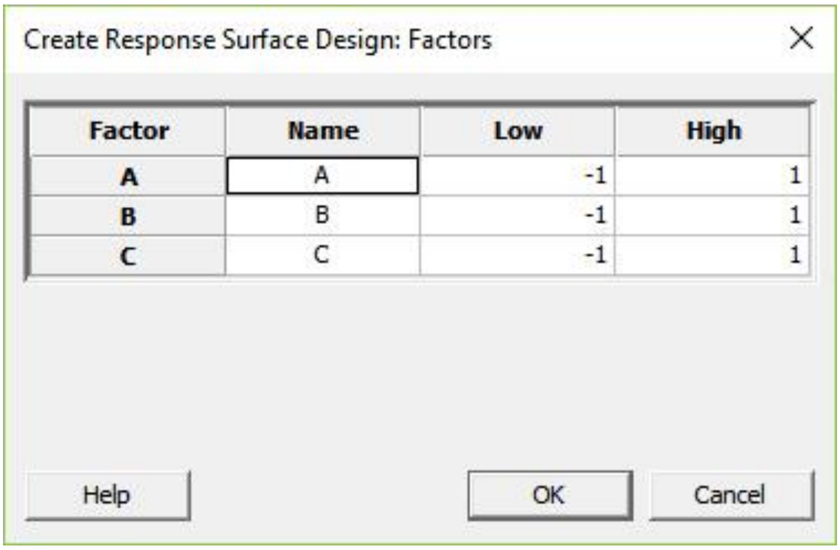

Figure A.5: Entry of the factors and their levels

The “Names” of the three factors (Coefficient for virtual queue of vehicles, β^V, Coefficient for transit priority, β^bor β^p, Downstream blockage penalty coefficient, β^B) are modified to BQL, BTP, and BDC, respectively, as shown in Figure A.6. The Low and $High$ levels of the factors shown in Table A.1 (preliminary regions of factors) are used to modify the ranges in Figure A.5, to ones shown in Figure A.6. By clicking “OK”, the dialog box shown in Figure A.4 reappears.

Table A.1: Factors and their levels for the model 1 of split actuated control for “E2” demand scenario

Factors	***“Low” Level***	***“High” Level***
Coefficient for virtual queue of vehicles, β^V	-1000	15000
Coefficient for transit priority, $\beta^b or\ \beta^p$	-2000	10000
Downstream blockage penalty coefficient, β^B	-5	25

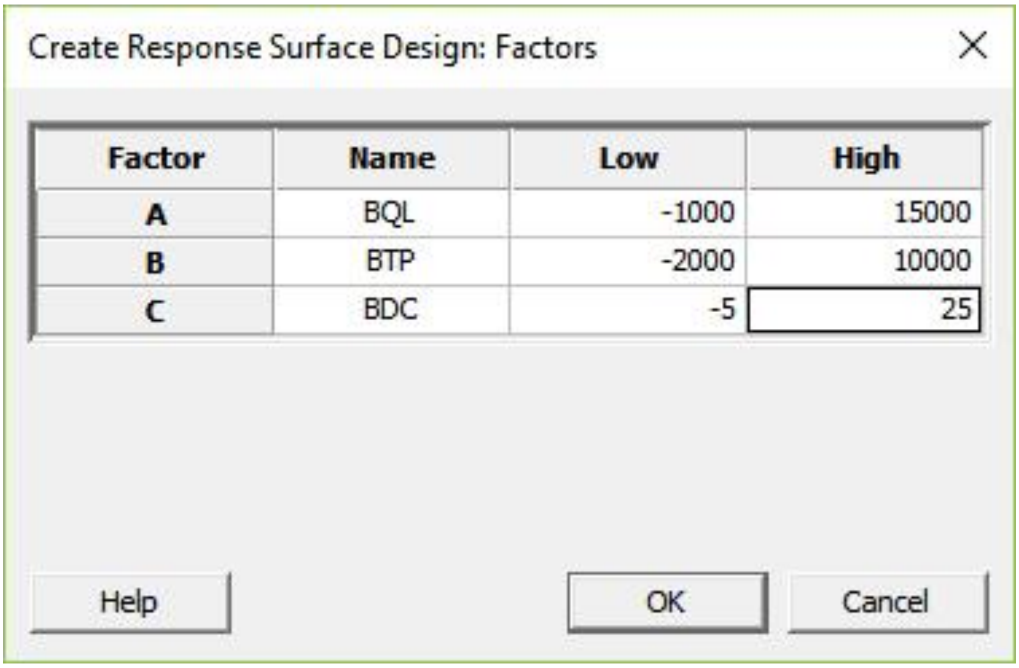

Figure A.6: Modifying the “Names” of factors and their Low and High levels

At this stage, the properties for the response surface modeling is set. By clicking “OK” in the dialog box shown in Figure A.4, the response surface design is created for the factor settings, as shown in Figure A.7.

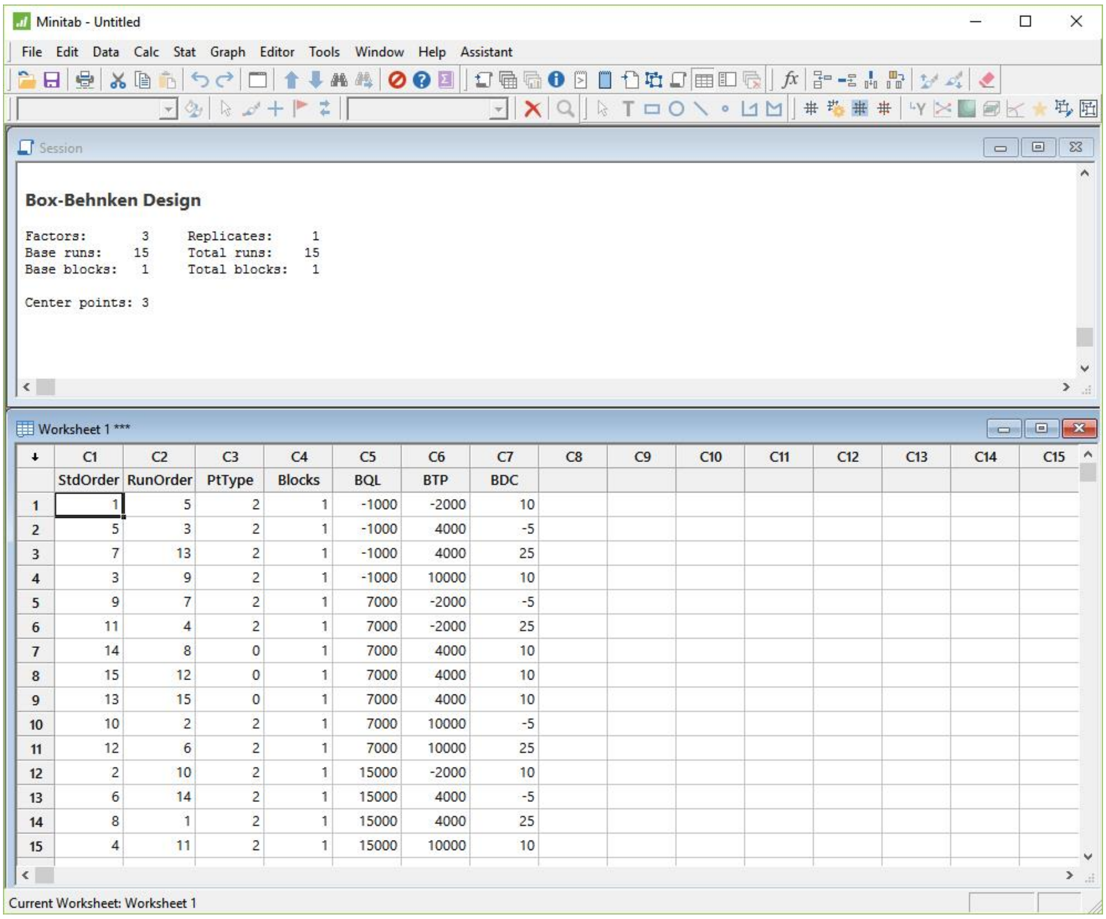

↓	C1 StdOrder	C2 RunOrder	C3 PtType	C4 Blocks	C5 BQL	C6 BTP	C7 BDC	C8	C9	C10	C11	C12	C13	C14	C15
1	1	5	2	1	-1000	-2000	10								
2	5	3	2	1	-1000	4000	-5								
3	7	13	2	1	-1000	4000	25								
4	3	9	2	1	-1000	10000	10								
5	9	7	2	1	7000	-2000	-5								
6	11	4	2	1	7000	-2000	25								
7	14	8	0	1	7000	4000	10								
8	15	12	0	1	7000	4000	10								
9	13	15	0	1	7000	4000	10								
10	10	2	2	1	7000	10000	-5								
11	12	6	2	1	7000	10000	25								
12	2	10	2	1	15000	-2000	10								
13	6	14	2	1	15000	4000	-5								
14	8	1	2	1	15000	4000	25								
15	4	11	2	1	15000	10000	10								

Figure A.7: Box-Behnken response surface design

B. Building Responses Models

Following the design of the response surface model (RSM), the CORSIM simulation is executed ten (10) times for each factor level settings (as shown in each raw of Figure A.7). Subsequently, the resulting average total number of bus trips, network total travel time, and trip’s average travel time, of the 10 simulation runs are exported to the worksheet in the Minitab to build the model for each response, as shown in Figure B.1. The variables Trips, TTT and MTT represent the average response values of the ten simulation runs using the corresponding factor settings.

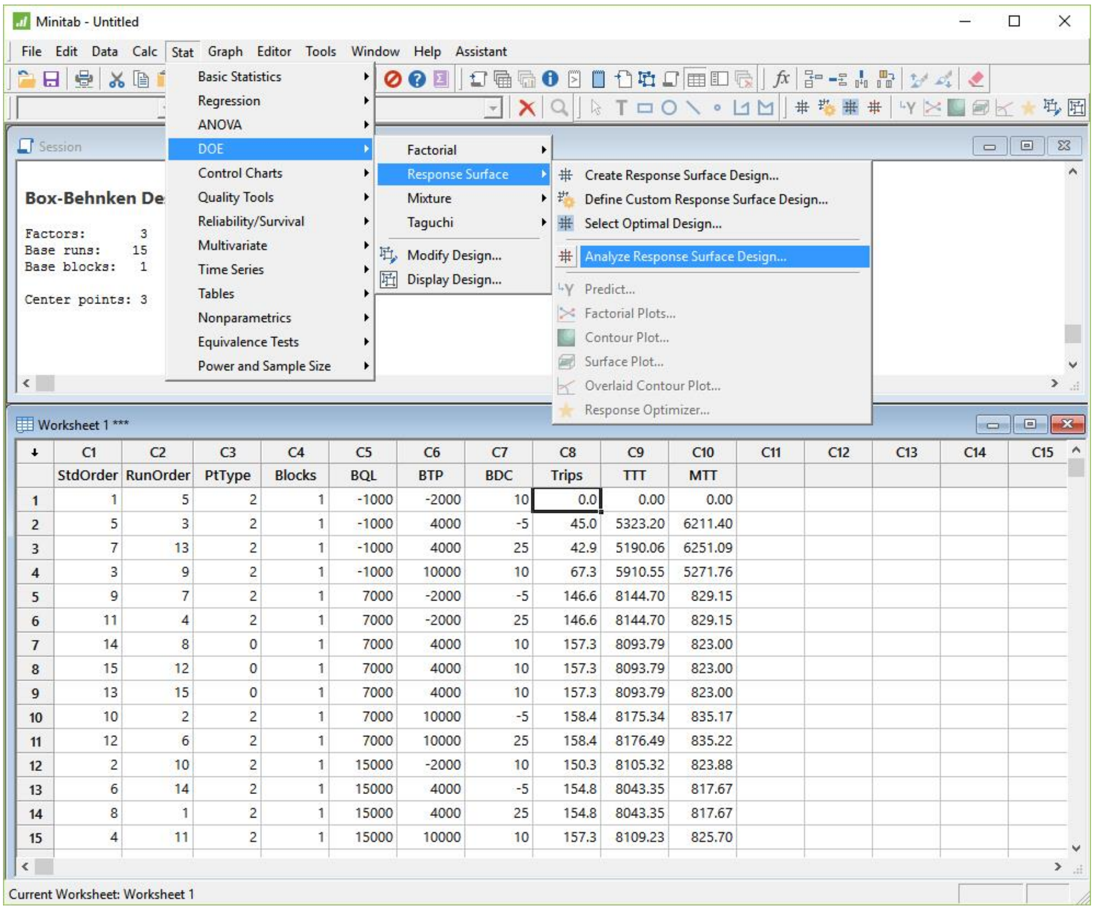

Figure B.1: Selection of “Analyze Response Surface Design”

The process of analysis starts by selecting “Analyze Response Surface Design…” from the main menu of Minitab, as Stat ➔ DOE ➔ Response Surface ➔ Analyze Response Surface Design as shown in Figure B.1. The “Analyze Response Surface Design” window opens as shown in Figure B.2.

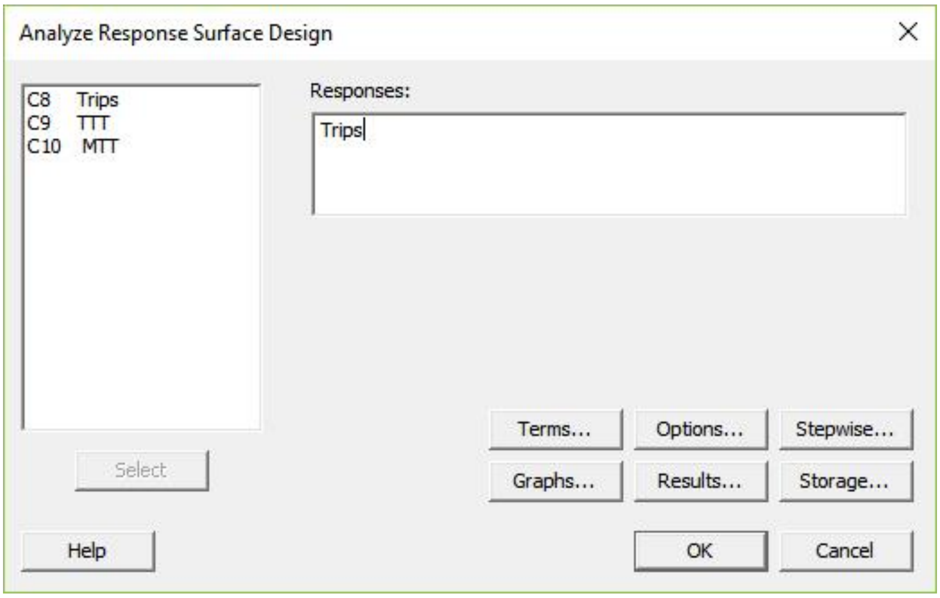

Figure B.2: Selection of the "Trips" as one response to analyze the model

As there are three responses exported from the simulation model, three response surface models are built for the responses. As an example, "Trips" is selected as a response to build the model shown in Figure B.2.

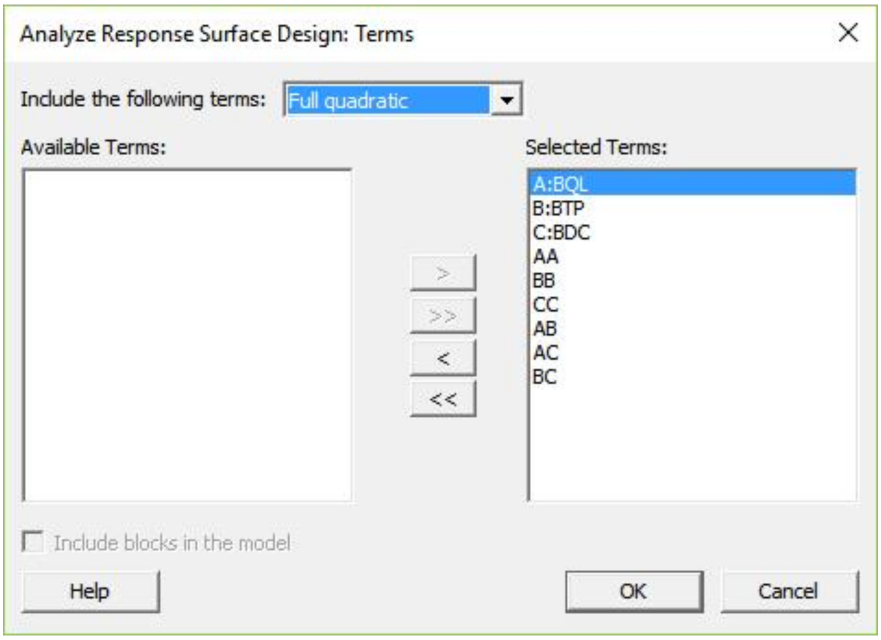

Figure B.3: Selection of the "Terms" to select the full quadratic model

The “Terms…” of a “Full quadratic” model are selected to set up the second-order model (the single factor effects, the square effects and the interaction among the factors), as shown in Figure B.3. All terms are considered in the model for the first time to identify the significant terms. By clicking “OK” in the dialog box, the output (ANOVA table) of the response surface model is shown as in Figure B.4. Subsequently, the non-significant terms are identified as shown in Figure B.5.

Analysis of Variance

Source	DF	Adj SS	Adj MS	F-Value	P-Value
Model	9	41454.6	4606.1	63.08	0.000
Linear	3	27879.1	9293.0	127.26	0.000
BQL	1	26680.5	26680.5	365.38	0.000
BTP	1	1198.1	1198.1	16.41	0.010
BDC	1	0.6	0.6	0.01	0.934
Square	3	12665.4	4221.8	57.82	0.000
BQL*BQL	1	12571.3	12571.3	172.16	0.000
BTP*BTP	1	100.8	100.8	1.38	0.293
BDC*BDC	1	0.7	0.7	0.01	0.928
2-Way Interaction	3	910.1	303.4	4.15	0.080
BQL*BTP	1	909.0	909.0	12.45	0.017
BQL*BDC	1	1.1	1.1	0.02	0.907
BTP*BDC	1	0.0	0.0	0.00	1.000
Error	5	365.1	73.0		
Lack-of-Fit	3	365.1	121.7	*	*
Pure Error	2	0.0	0.0		
Total	14	41819.7			

Figure B.4: ANOVA output for the “Trips” of full quadratic model

Analysis of Variance					
Source	DF	Adj SS	Adj MS	F-Value	P-Value
Model	9	41454.6	4606.1	63.08	0.000
Linear	3	27879.1	9293.0	127.26	0.000
BQL	1	26680.5	26680.5	365.38	0.000
BTP	1	1198.1	1198.1	16.41	0.010
BDC	1	0.6	0.6	0.01	0.934
Square	3	12665.4	4221.8	57.82	0.000
BQL*BQL	1	12571.3	12571.3	172.16	0.000
BTP*BTP	1	100.8	100.8	1.38	0.293
BDC*BDC	1	0.7	0.7	0.01	0.928
2-Way Interaction	3	910.1	303.4	4.15	0.080
BQL*BTP	1	909.0	909.0	12.45	0.017
BQL*BDC	1	1.1	1.1	0.02	0.907
BTP*BDC	1	0.0	0.0	0.00	1.000
Error	5	365.1	73.0		
Lack-of-Fit	3	365.1	121.7	*	*
Pure Error	2	0.0	0.0		
Total	14	41819.7			

Figure B.5: ANOVA output for the “Trips” of full quadratic model (the non-significant terms are highlighted)

The next step is to eliminate the non-significant terms, one at a time, commencing with the term with the highest P-value. The model is reanalyzed following each elimination. For example, for the “Trips” response, the interaction effect between the downstream blockage penalty coefficient, β^B (BDC) with both coefficient for virtual queue of vehicles, β^V (BQL) and coefficient for transit priority, β^p(BTP), and the square effect term of β^p are all eliminated at a time for simplicity; since their P-value is near to 1, as shown in Figure B.5. The output (ANOVA table) of the response surface model following the elimination of the non-significant terms is illustrated in Figure B.6 and Figure B.7.

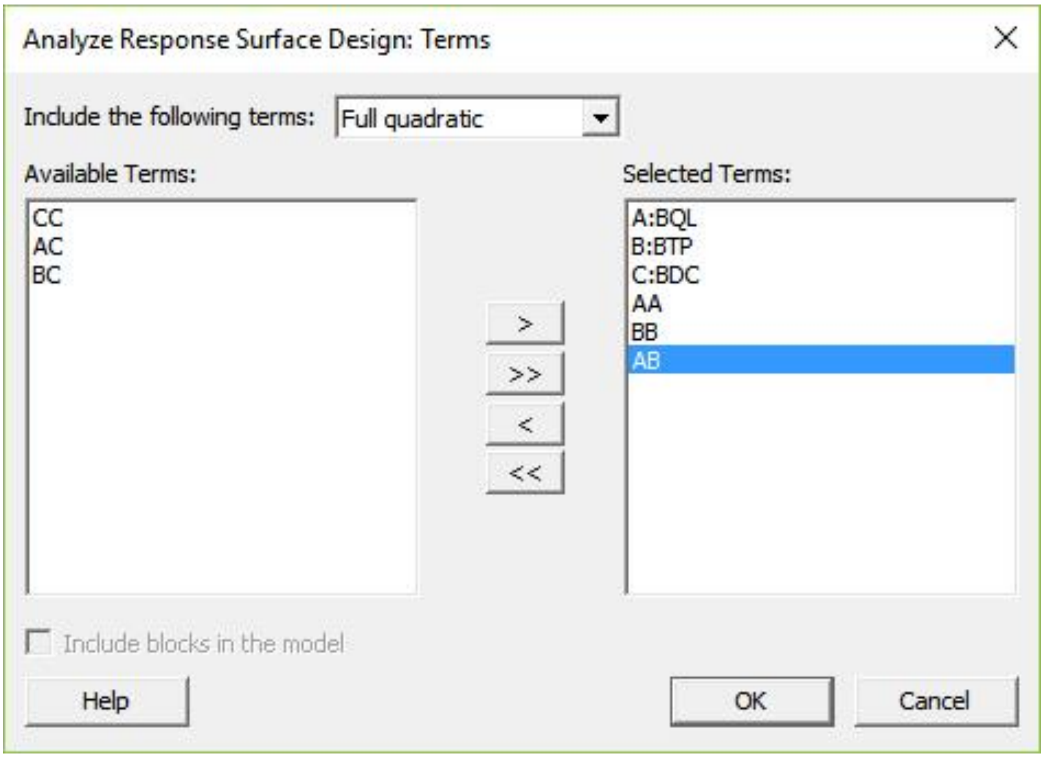

Figure B.6: Selection of “Trips” response for reanalysis, keeping the significant terms to develop the model

Analysis of Variance

Source	DF	Adj SS	Adj MS	F-Value	P-Value
Model	6	41452.8	6908.8	150.65	0.000
Linear	3	27879.1	9293.0	202.64	0.000
BQL	1	26680.5	26680.5	581.79	0.000
BTP	1	1198.1	1198.1	26.12	0.001
BDC	1	0.6	0.6	0.01	0.915
Square	2	12664.7	6332.4	138.08	0.000
BQL*BQL	1	12660.3	12660.3	276.07	0.000
BTP*BTP	1	102.7	102.7	2.24	0.173
2-Way Interaction	1	909.0	909.0	19.82	0.002
BQL*BTP	1	909.0	909.0	19.82	0.002
Error	8	366.9	45.9		
Lack-of-Fit	6	366.9	61.1	*	*
Pure Error	2	0.0	0.0		
Total	14	41819.7			

Figure B.7: ANOVA output for the “Trips” following the elimination of the non-significant terms

When the terms of significant effect on the “Trips” response are identified, the models for the other two responses (TTT and MTT) are constructed similarly. Afterward, given the developed models for all the responses, the optimization is executed as described in the following section.

C. Responses Optimization

Following the construct of the response surface models for Trips, TTT and MTT (including only the significant terms), the next step is to determine the optimal combination of factors for specific objective functions (such as minimizing TTT and MTT while maximizing Trips).

To carry on the optimization, the “Response Optimizer…” is selected from the main menu of Minitab, (Stat ➔ DOE ➔ Response Surface ➔ Response Optimizer) as shown in Figure C.1. The “Response Optimizer” window opens as shown in Figure C.2 to set the optimization goals of each response individually.

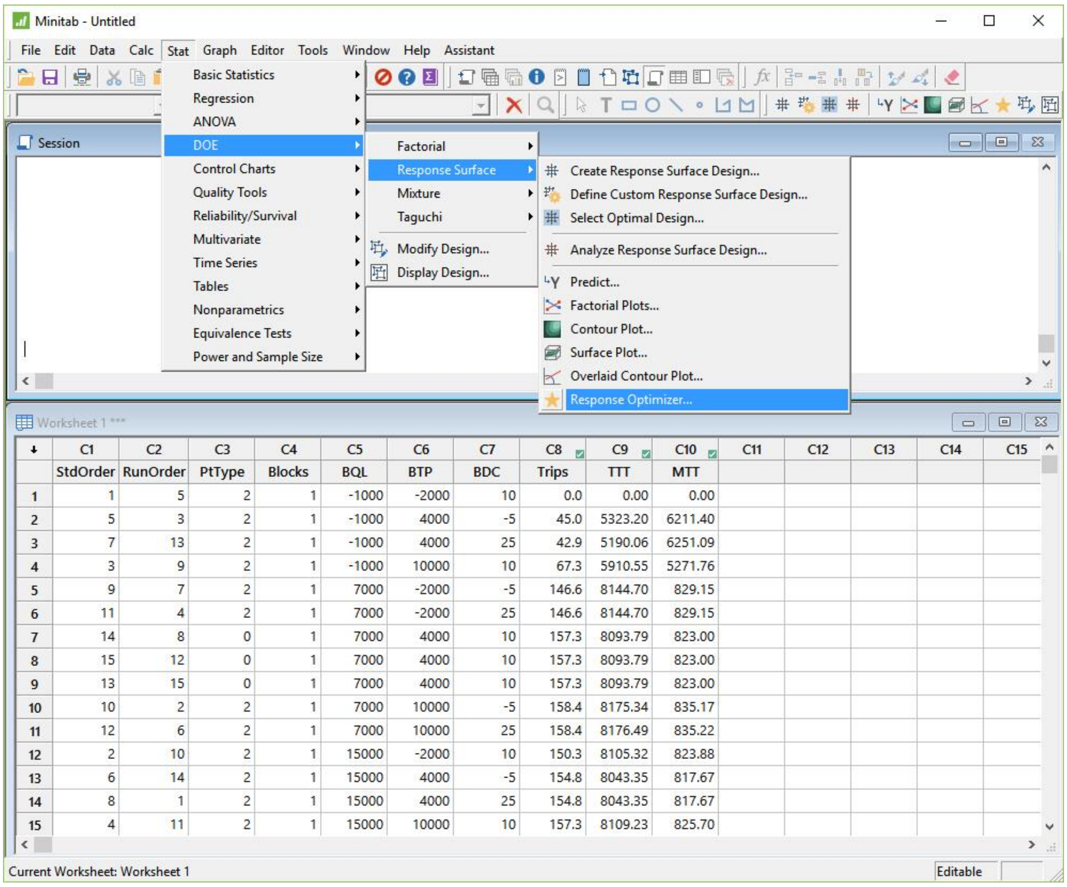

Figure C.1: Selection of “Response Optimizer”

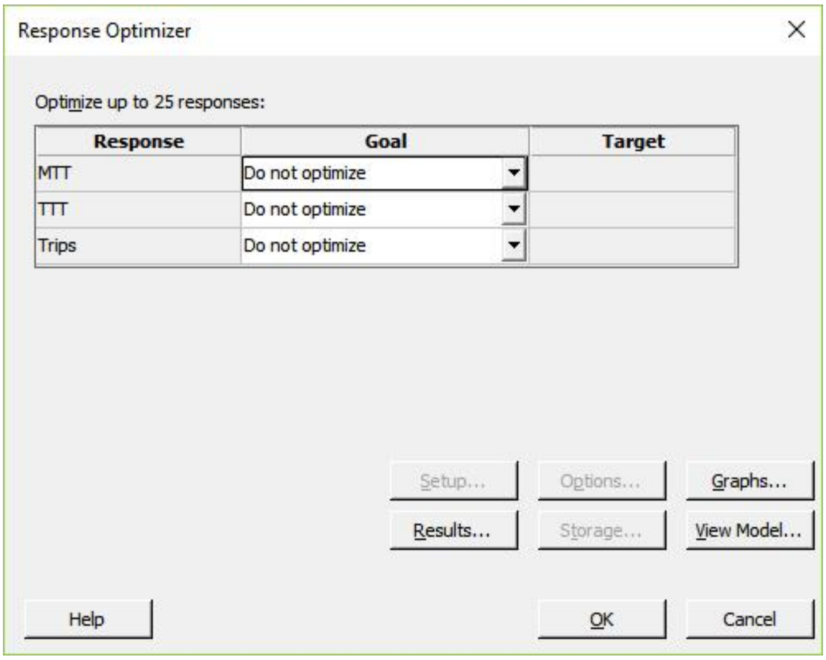

Figure C.2: Setting the “Goals” of the various responses

The goal (objective) of each response is selected as shown in Figure C.3. Herein, both TTT and MTT are to be minimized, and the Trips is to be maximized. Subsequently, the “OK” in the dialog box is clicked to execute. The output of the response optimizer is shown in Figure C.4.

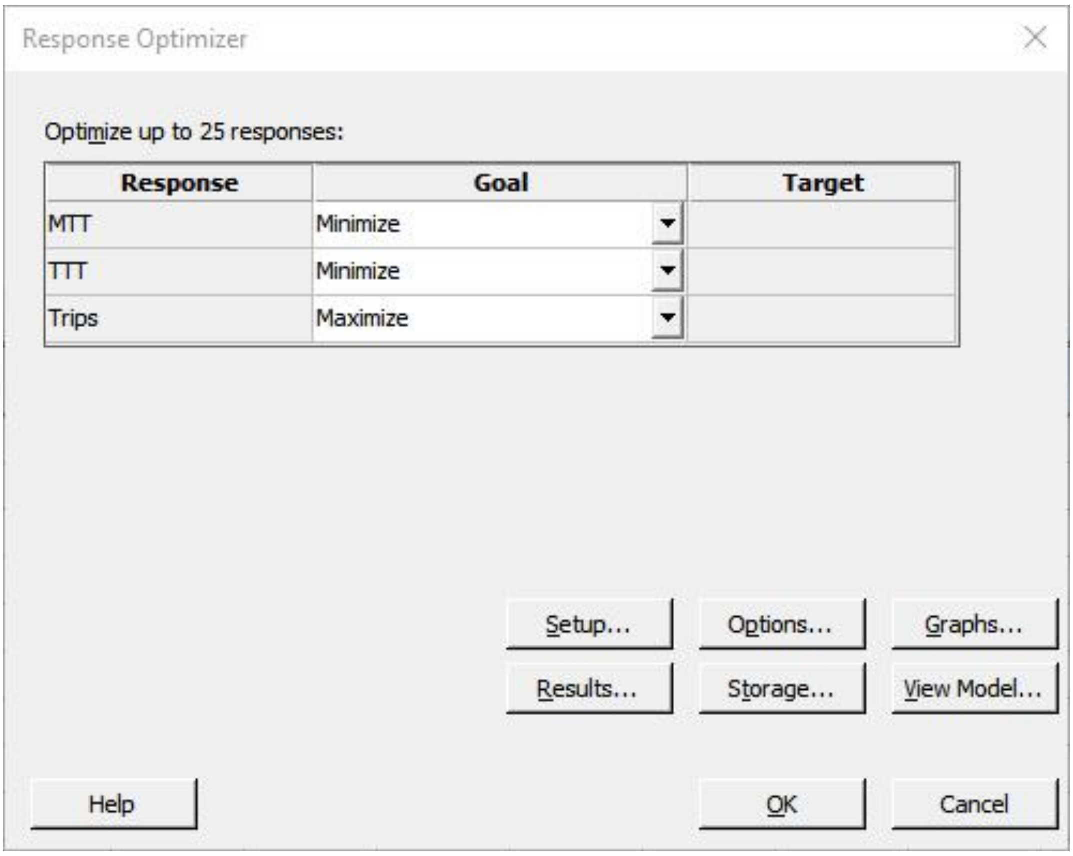

Figure C.3: Selection of triple “Goal” for three responses

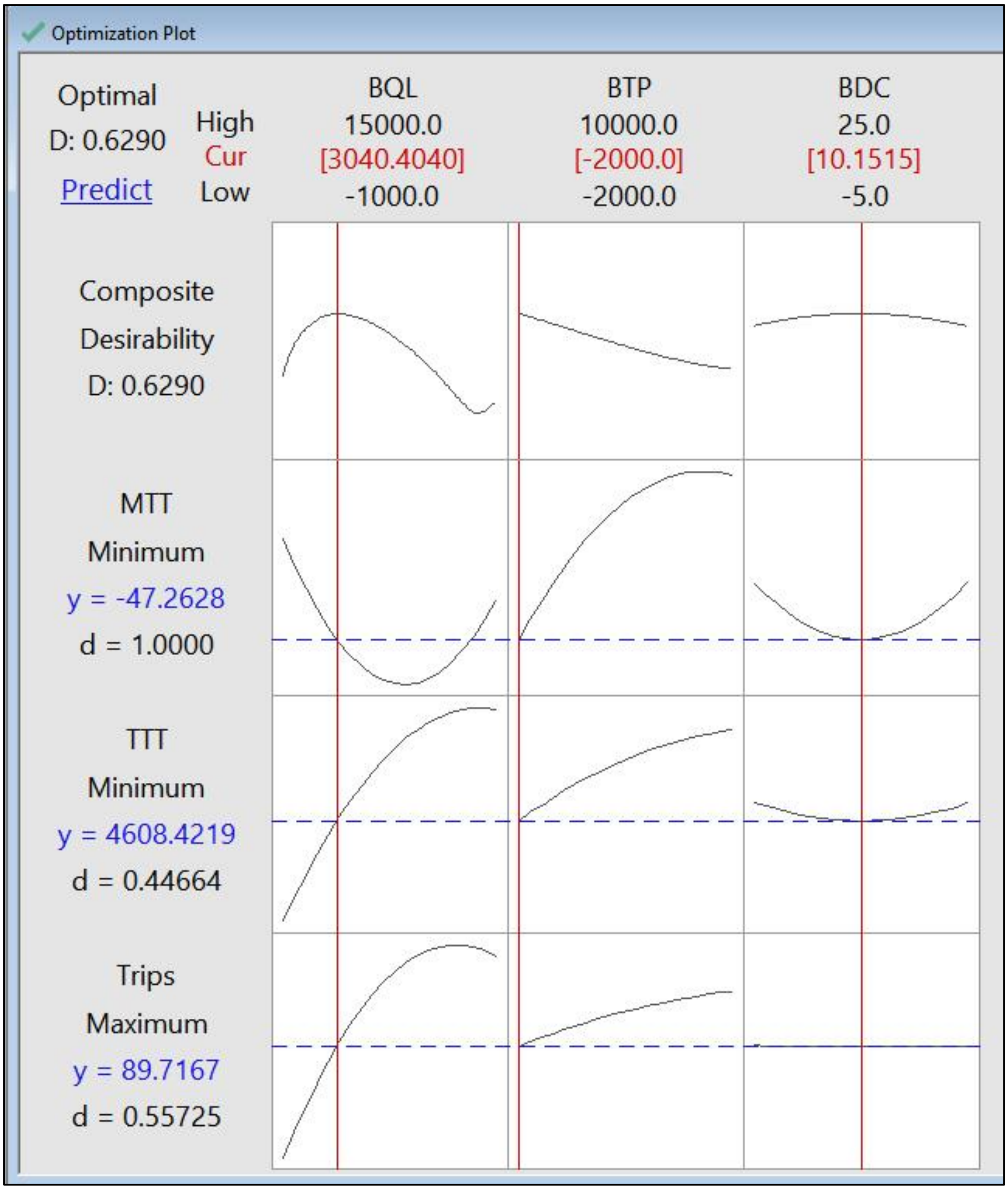

Figure C.4: Optimal solution for the selected triple objective functions

Figure C.4 shows the optimal settings of the factors of coefficient for virtual queue of vehicles, β^V (BQL), coefficient for transit priority, β^b or β^p (BTP), and downstream blockage penalty coefficient, β^B (BDC), for the three objective functions (minimizing TTT and MTT and maximizing Trips). The optimal setting; one with the highest composite desirability of 0.629 is 3040.4 for the β^V (BQL), -2000 for the β^b or β^p (BTP) and 10.15 for the β^B(BDC). The following step is to maybe change the penalty coefficient ranges and repeat the whole process again to test different models. For instance, given that the optimal BTP value is identified to be the border (minimal) value (-2000) of the initially specified range, a new range can be specified for this factor and then the processes of model design, building, and optimization are repeated as described above.

Alternatively, one may seek different optimization arrangements, by considering only two response optimization (two goals instead of three), as shown in Figure C.5.

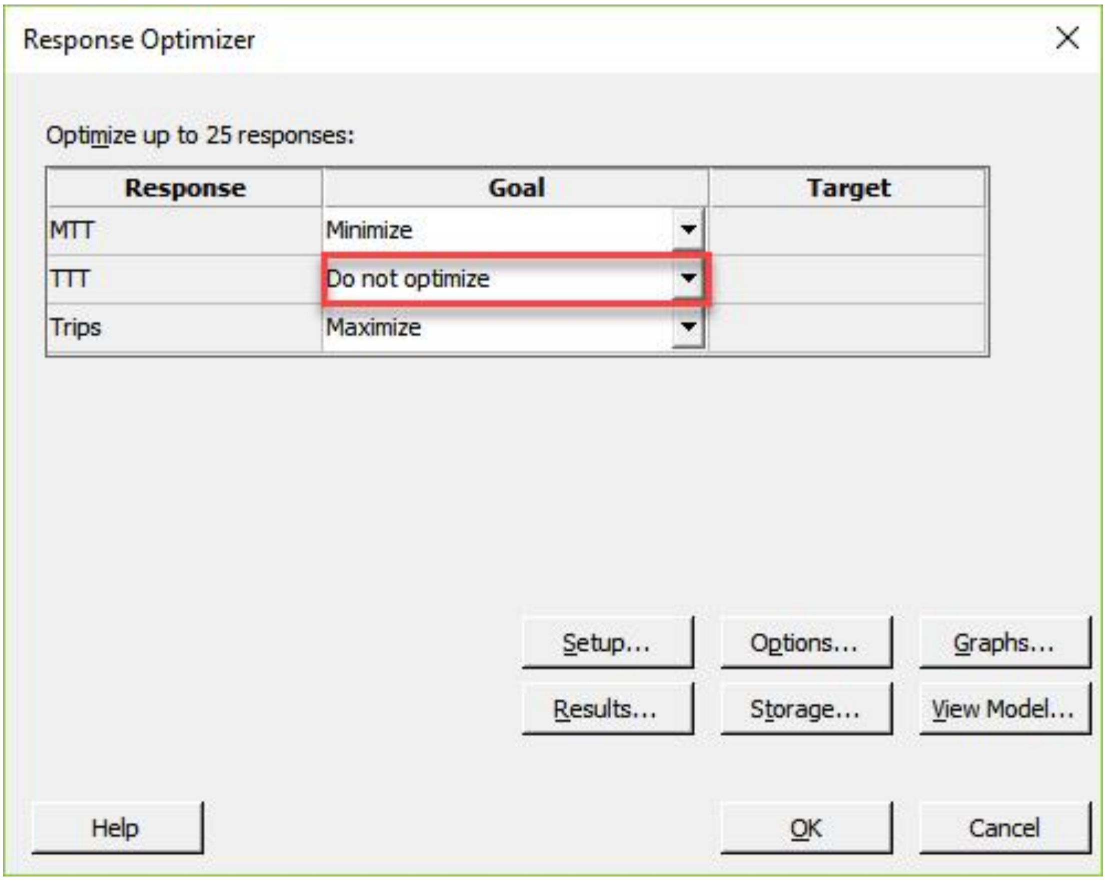

Figure C.5: Reselection of two "Goals" for the responses

Herein, the goals are restated as (minimizing MTT and maximizing Trips), as shown in Figure C.5. That is, the TTT response is not considered for optimization. Following the reapplication of the surface optimizer on only two responses, the output of the response optimizer is obtained as shown in Figure C.6. In this case, the optimal factor setting (with the highest composite desirability of 1.0) is 12898.9 for β^V (BQL), 10000 for β^bor β^p (BTP), and -3.45 for β^B (BDC). One can also seek optimization of one goal and obtain the corresponding optimal factor settings in the same way.

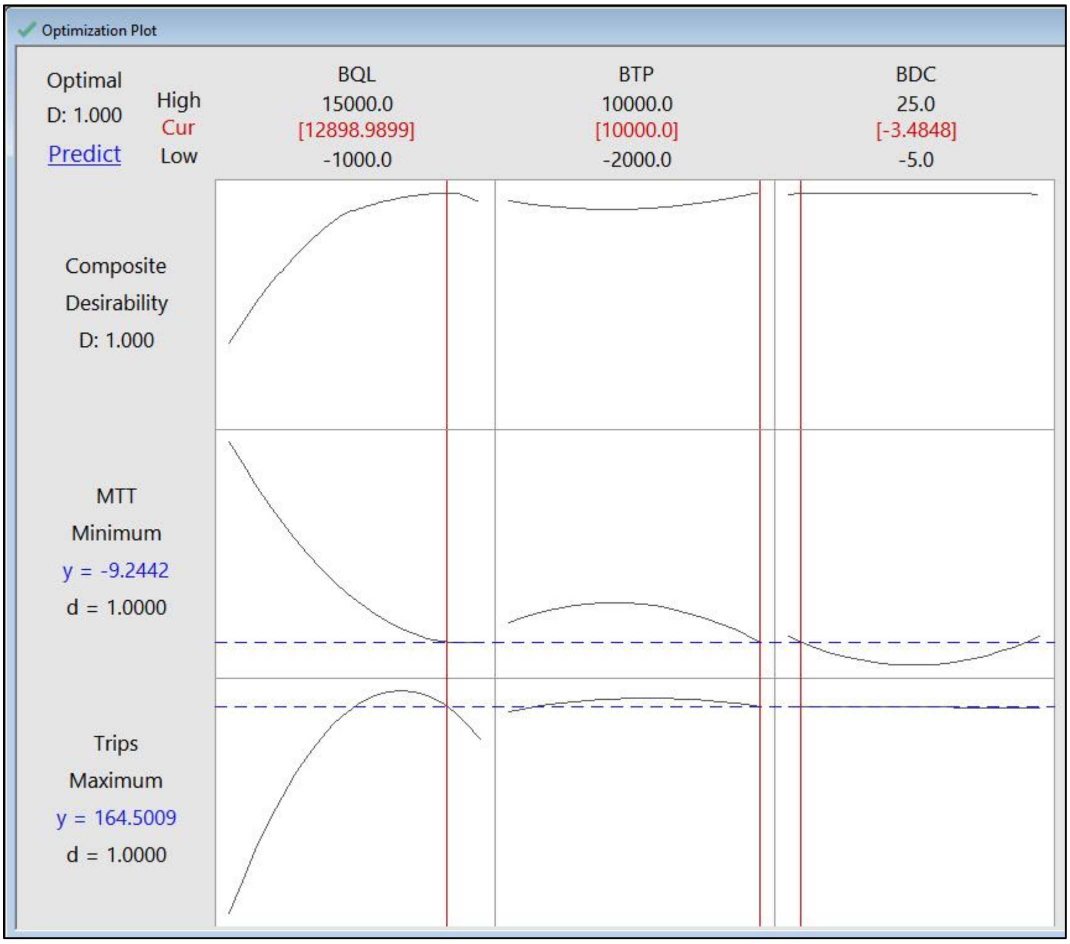

Figure C.6: Optimal solution for only two objective functions